Cellulose oligomers preparation by depolymerisation for the synthesis of new bio-based amphiphilic compounds

Elise Billes

université de BORDEAUX

THÈSE PRÉSENTÉE
POUR OBTENIR LE GRADE DE

DOCTEUR DE L'UNIVERSITÉ DE BORDEAUX

École doctorale des Sciences Chimiques
Spécialité : Polymères

Par Elise BILLES

Préparation d'oligomères de cellulose par dépolymérisation pour la synthèse de nouveaux composés amphiphiles bio-sourcés

Sous la direction de Dr. Véronique Coma, Pr. Stéphane Grelier et Dr. Frédéric Péruch

Soutenue le 20 novembre 2015

Membres du jury :

Mme SAVE, Maud	IPREM, Pau	Présidente
M. FORT, Sébastien	CERMAV, Grenoble	Rapporteur
M. JEROME, François	IC2MP, Poitiers	Rapporteur
Mme COMA, Véronique	LCPO, Bordeaux	Directeur de thèse
M. GRELIER, Stéphane	LCPO, Bordeaux	Directeur de thèse
M. PERUCH, Frédéric	LCPO, Bordeaux	Directeur de thèse

Préparation d'oligomères de cellulose par dépolymérisation pour la synthèse de nouveaux composés amphiphiles bio-sourcés

Le but de cette thèse est de produire des oligomères de cellulose de dispersité faible. Pour ce faire, deux méthodes ont été imaginées :

- La méthode « fishing » où des oligomères de cellulose sont obtenus par hydrolyse acide puis sont séparés par solubilisation sélective dans une phase organique à l'aide d'un polymère synthétique. Le ratio des tailles du polymère synthétique et des oligomères de cellulose sera responsable de la sélectivité.
- La méthode « masking » où des portions de cellulose de la taille des futurs oligomères sont protégées par un polymère synthétique lors d'une hydrolyse enzymatique.

Dans les deux cas, les polymères synthétiques contiennent des acides boroniques qui permettent une interaction réversible avec les sucres.

Malgré de nombreuses tentatives, ces deux méthodes n'ont pas été couronnées de succès. Pour la première, le procédé n'était pas sélectif. Pour la seconde, le polymère permettant une interaction tout au long de la chaine de cellulose n'a pas pu être synthétisé. La dispersité des oligomères obtenus par hydrolyse acide (degrés de polymérisation (DP) de 1 à 12) a cependant pu être réduite de façon satisfaisante en solubilisant les DP les plus faibles dans le méthanol.

Enfin, la fraction insoluble dans le méthanol, après fonctionnalisation de l'extrémité réductrice par un groupement azide, a été couplée à un acide stéarique fonctionnalisé alcyne par chimie « click ». L'auto-assemblage de ce nouveau composé amphiphile a été étudié dans l'eau, la CMC a été mesurée à 100 $mg.L^{-1}$. Les objets observés sont sphériques, de taille homogène avec un diamètre moyen de 140 nm ce qui indique une morphologie en vésicule.

Mots-clés : Cellulose, hydrolyse acide, chimie « click », composé amphiphile, RAFT, acide boronique, bio-sourcé

Cellulose oligomers preparation by depolymerisation for the synthesis of new bio-based amphiphilic compounds

The purpose of this study is to produce uniform cellulose oligomers. In this frame, two methods were considered:

- For the "fishing" method, the oligomers obtained by acidic hydrolysis of cellulose are separated by selective solubilisation in an organic phase thanks to a synthetic polymer. The size ratio between the synthetic polymer and the cellulose oligomer would be responsible for the selectivity.
- For the "masking" method, parts of cellulose backbone having the size of the future oligomers are protected with a synthetic polymer during an enzymatic hydrolysis.

In both cases, the synthetic polymers contain boronic acid groups that interact reversibly with saccharides.

Despite various attempts, these two methods were not crowned with success. The first one was eventually not selective. For the second one, the polymer allowing an interaction all along the cellulose backbone could not be synthesised. The dispersity of the oligomers obtained by acidic hydrolysis (polymerisation degree (DP) from 1 to 12) was satisfactorily decreased by solubilising the smaller DP in methanol.

To finish, the methanol-insoluble fraction was functionalised at the reducing end with an azide group. It was then coupled to an alkyne-functionalised stearic acid by click chemistry. The self-assembly of this new amphiphilic compound was studied in water, the CMC was measured at 100 $mg.L^{-1}$. The particles formed were spherical, homogeneous and had an average diameter of 140 nm, which indicate a vesicle morphology.

Key words: Cellulose, acidic hydrolysis, click chemistry, amphiphilic compounds, RAFT, boronic acid, bio-based

Laboratoire de Chimie des Polymères Organiques
LCPO, UMR 5629
16 av. Pey Berland
F-33607 Pessac

« On ne fait jamais attention à ce qui a été fait ; on ne voit que ce qui reste à faire. », Marie Curie

« En essayant continuellement, on finit par réussir, donc : plus ça rate, plus on a de chances que ça marche » (Citation Shadok)

Remerciements

Je souhaiterai commencer par remercier l'Université de Bordeaux pour le financement de cette thèse.

Je voudrais en suite remercier le jury qui a bien voulu l'évaluer.

Merci au directeur du LCPO, Mr Cramail, pour m'avoir accueilli dans son laboratoire où il fait très bon travailler.

Mes plus gros remerciements iront ensuite à mes trois directeurs qui m'ont d'abord fait confiance pour m'occuper de ce sujet et qui m'ont aussi énormément aidé durant ces trois années : Mr Péruch pour sa disponibilité (tout au long mais en particulier durant la rédaction), Mr Grelier pour ses idées originales et Mme Coma pour ses avis. Vous avez toujours été là quand j'en ai eu besoin et pour ça je vous en remercie.

Deux gros mercis vont aussi aux deux stagiaires de Master qui ont participé à ces travaux : Jérémie Grange pour la partie sur le « fishing » et Kelechukwu Nnabuike Onwukamike pour la partie auto-assemblage. Vous m'avez fait gagner beaucoup de temps et je n'aurais pas pu arriver aussi loin dans le sujet sans votre aide précieuse.

J'ai aussi une très forte pensée pour toutes les équipes techniques et administratives du LCPO qui nous simplifient la vie au quotidien et qui sont tous très agréables à côtoyer : Anne-Laure Wirotius (experte RMN, merci beaucoup pour toute ton aide sur les attributions et sur les analyses que tu as faites), Mélanie Bousquet (SEC dans le chloroforme, merci beaucoup pour ta disponibilité et ta rigueur scientifique), Eric Virol (SEC dans l'eau et HPLC entre autre, merci énormément pour ton aide, ta disponibilité et ta gentillesse), Nicolas Guidolin et Amélie Vax (SEC dans le THF, merci beaucoup pour votre aide), Patricia Castel (MALDI), Pierre Bertho (TEM, merci pour les images), Cédric Le Coz et Gérard Dimier qui ont bien aidé Kenny et que j'ai adoré croiser dans les couloirs. Et pour le coté administratif : merci à Catherine Roulinat, à Dominique Richard, Bernadette Guillabert, Corinne Goncalves-de-Carvalho, Claude Le Pierres et sans oublier Loïc Petrault sans qui il serait très difficile de travailler. Merci à vous pour votre gentillesse, votre disponibilité, c'est vraiment très agréable.

Pour les remerciements plus personnels (je vais faire sobre sinon je vais pas y arriver), je voulais dire un grand merci à mes triplettes Blandine et Estelle, on a commencé ensemble, on a fini ensemble, on a galéré ensemble et c'est sûr que ça rapproche. Merci à Estelle de m'avoir fait apprécier le footing, c'était pas gagné mais tu l'as fait !! Un grand merci à celles qui se sont rajoutées à notre petit groupe : Julie, Amélie (la castraise) et Dounia, ça m'a fait super plaisir de faire votre connaissance et j'espère vraiment qu'on

gardera contact. Nos débats pendant les repas de midi vont beaucoup me manquer !!! Et encore félicitations à Amélie pour la naissance de son petit Léo.

Je pense aussi aux autres qui ont commencé leurs thèses en même temps et dont j'ai eu le plaisir de faire la connaissance au long de ces trois ans: Edgar, Kevin (nos discussions du soir dans ton labo vont me manquer !), Olivia (dommage qu'on n'ait pas discuté plus souvent au long de la thèse) et Déborah (j'espère vraiment qu'on gardera contact).

Un merci spécial à la team IP'15 avec qui j'ai vraiment passé de super moments, ça a été une expérience géniale et merci à M. Carlotti de m'avoir permis de la vivre. Un merci doublement spécial à Kevin, Mickael, Océane et Benji pour ce super flash mob pendant le gala #MenInBlack #StayingAlive, je l'oublierai jamais.

Merci à Benji et à Jérémie B. pour la conférence en Pologne, je me suis vraiment amusée (un peu trop même …).

Merci à tous ceux avec qui j'ai échangé des sourires dans les couloirs, ça réchauffe le cœur.

Merci à tous ceux avec qui j'ai partagé un bureau ou un labo, ça a été un plaisir de passer tout ce temps avec vous, en particulier Karine, Yannick, Christian, Matthieu, Julie, Dounia.

Merci à Bastien pour son soutien au quotidien, à mes amies Adeline et Marlène qui ont fait le déplacement pour ma soutenance et qui sont toujours là après tant d'années, à ma famille qui s'est aussi déplacée, merci pour votre soutien.

Merci à mes amis de l'école d'ingé qui sont toujours là et avec qui je passe toujours de super moments. J'ai passé un super week-end post-soutenance avec vous, merci encore !

Merci à la famille LCPO anciens, présents et futurs (un grand bon courage aux nouveaux mais ne vous inquiétez pas trop, vous êtes entre de bonnes mains).

Résumé long

La cellulose est un polymère naturel et abondant mais dont le potentiel n'est pas entièrement exploité car sa cristallinité empêche sa solubilisation dans la plupart des solvants usuels. Seuls des solvants peu courants, et donc parfois chers, y parviennent mais les solutions souvent très visqueuses pouvant entrainer des dégradations. Une fonctionnalisation améliore grandement la solubilité de la cellulose mais sa structure de départ ainsi que certaines propriétés sont altérées.

Les oligomères de cellulose ont la même structure que cette dernière mais avec un degré de polymérisation réduit qui leur permet d'être solubles dans l'eau. Ils sont obtenus par synthèse chimique ou enzymatique ou par hydrolyse de la cellulose par voie acide ou enzymatique ainsi que par d'autres moyens moins étudiés. Par la suite et selon les applications, il est aussi intéressant de les séparer selon leur taille. Pour ce faire, la méthode la plus courante est la chromatographie. Cependant, les faibles rendements en font une technique utilisée par manque d'alternative.

L'objectif de cette thèse est donc de produire des oligomères de cellulose les plus uniformes possible sans utiliser de méthode chromatographique. Deux méthodes ont donc été envisagées (**Figure 1**):

- La première, appelée « masking », consiste à protéger des portions de cellulose de la taille des futurs oligomères avec un polymère synthétique pendant que les parties non-protégées sont hydrolysées par voie enzymatique.
- La deuxième, dite « fishing », doit permettre de solubiliser sélectivement des oligomères de cellulose dans une phase organique à l'aide d'un copolymère. La sélectivité viendrait du ratio entre la taille du polymère et celle de l'oligomère récupéré. Plus long sera le polymère, plus long sera l'oligomère solubilisé.

Ces deux méthodes nécessitant une interaction réversible avec la cellulose, les acides boroniques ont été choisis car ils permettent une complexation réversible sur les diols présents sur les sucres.

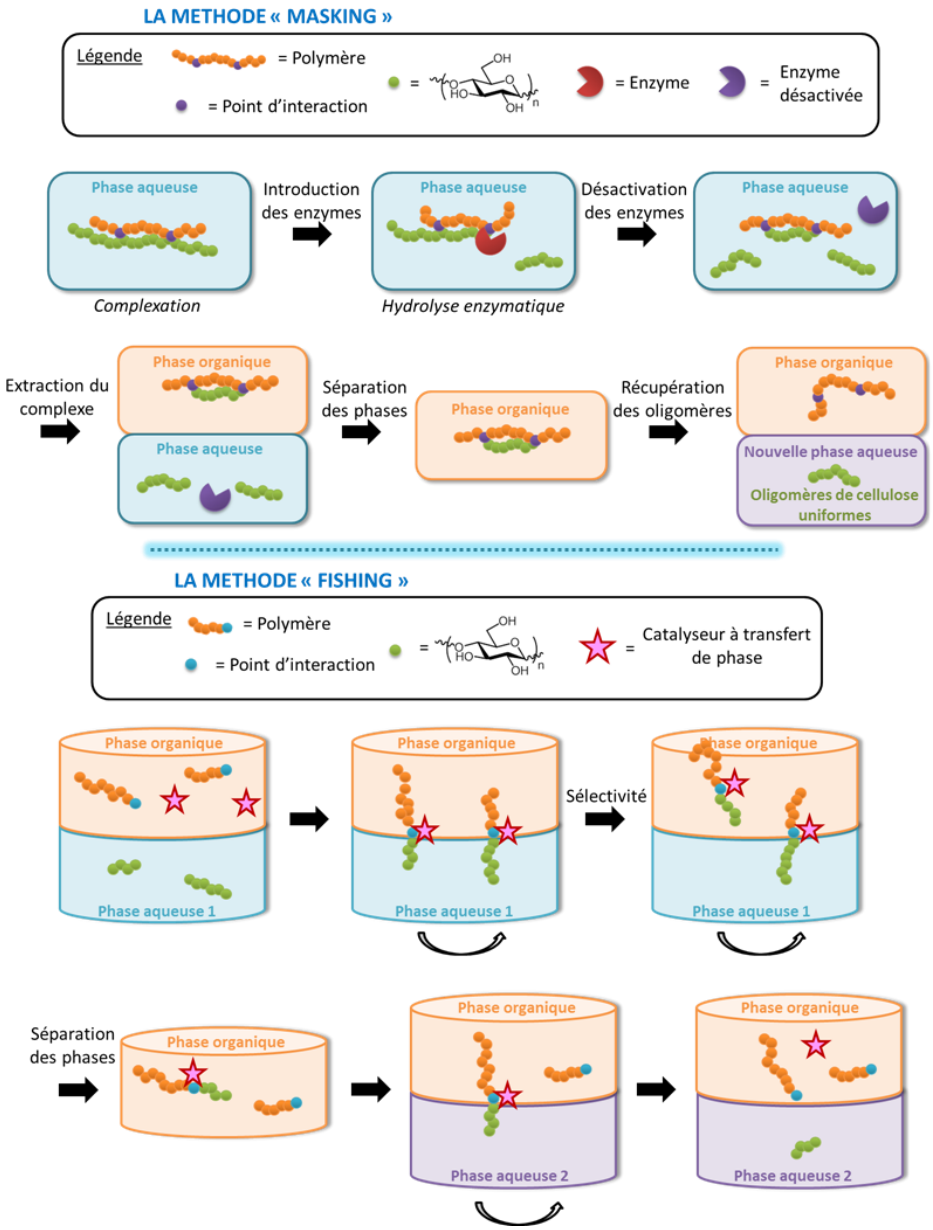

Figure 1. Schéma des méthodes "masking" et "fishing"

Pour vérifier la faisabilité de ces méthodes, une étude préliminaire sur des composés modèles a permis de mieux comprendre et mettre en évidence l'interaction entre les acides boroniques et les sucres. Le méthylglucoside et le glucose ont servi de modèle pour la cellulose et le polymère a été remplacé par l'acide phénylboronique. Il a été montré que l'acide boronique se complexait préférentiellement en position 4,6 sur le methylglucoside et en position 1,2 et 3,5 sur la forme α-furanose du glucose. Il a aussi été observé que l'anhydride boronique pouvait se complexer sur les positions 2,3 du méthylglucoside.

L'étude préliminaire sur la complexation entre les acides boroniques et les sucres a également été effectuée sur d'autres monosaccharides que ceux trouvés dans la cellulose pour élargir le champ des applications de ces méthodes à d'autres polysaccharides comme les hémicelluloses. Les résultats sont répertoriés dans le **Tableau 1**.

Tableau 1. Structures des complexes déterminées lors de l'étude préliminaire avec l'acide phénylboronique selon le sucre étudié et le solvant de complexation

Sucre étudié	Complexation dans $CDCl_3$		Complexation dans DMSO-d_6	
	Forme du sucre	Position de(s) acide(s) boronique(s)	Forme du sucre	Position de(s) acide(s) boronique(s)
Xylose	α-furanose	1,2 & 3,5	α-furanose	1,2 & 3,5
Mannose	Furanose ou pyranose	2,3 & 5,6 ou 4,6	Non étudié	
Arabinose	α-furanose	1,2 & 3,4	α-furanose	1,2 & 3,4
Galactose	Non déterminé		Pyranose Pyranose α-pyranose	4,6 3,4,6 1,2 & 3,4,6
Cellobiose	Pas de complexation		-	1,2 et/ou 4',6'

Sachant que les positions 1 et 4 ne sont pas libres sur la chaîne de cellulose, cette étude a permis de définir le type de polymère le plus approprié à chaque méthode :

- Pour la méthode « masking », un copolymère statistique de styrène et d'acide 4-vinylphénylboronique (AVB) sous forme d'anhydride avec l'acide phénylboronique (APB) (**Figure 2**) devrait permettre une interaction tout au long de la chaîne de cellulose afin de protéger de nombreuses liaisons osidiques lors de la dépolymérisation enzymatique. La nécessité d'avoir un polymère comportant des anhydrides boroniques et le besoin d'éviter la formation d'un réseau d'anhydride exigent l'utilisation de ces deux composés.
- Pour la méthode « fishing », un copolymère à blocs polystyrène-poly(acide 4-vinylphénylboronique) (**Figure 2**) semble préférable afin d'éviter la formation d'un réseau car deux acides boroniques pourraient se complexer sur le même oligomère. Cependant, la taille du bloc contenant les acides boroniques doit être ajustée pour éviter la formation de réseau et que la méthode ne soit pas compromise par la possible formation d'anhydrides.

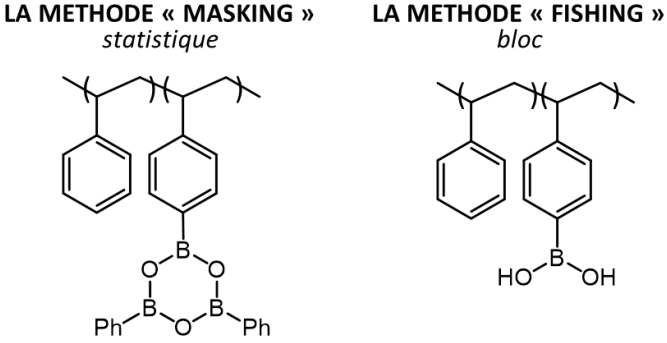

Figure 2. Structure d'un copolymère statistique de styrène et d'AVB sous forme d'anhydride avec l'APB et d'un copolymère à blocs polystyrène-poly(AVB)

La synthèse des deux polymères définis en **Figure 2** a ensuite été étudiée. Tout d'abord, comme la dispersité des polymères doit être la plus uniforme possible, la polymérisation anionique a été envisagée. Cependant, l'AVB, protégé ou non, désactive les anions et la fonctionnalisation post-polymérisation a conduit à des polymères insolubles. Pour pallier à ces difficultés, nous nous sommes tournés vers la polymérisation radicalaire de type RAFT. Différents paramètres comme la nature du monomère, de l'agent de transfert ou du solvant ont été étudiés pour optimiser les conditions de polymérisation.

Pour le copolymère choisi pour la méthode « masking », deux voies de synthèse ont été imaginées :

- Les anhydrides sont introduits sur un polymère statistique déjà synthétisé. Toutefois, des expériences par RMN DOSY (RMN 2D ^{1}H *versus* coefficient de diffusion, utilisation d'acide tolylboronique) ont permis de montrer que les anhydrides n'ont pas pu être formés quelles que soient les conditions utilisées.
- Le monomère d'AVB sous forme d'anhydride avec l'APB est polymérisé. De l'AVB est introduit dans un excès d'APB en milieu hydrophobe pour favoriser la formation des anhydrides. L'ensemble est ensuite polymérisé en présence de styrène. Dans ce cas, des problèmes de solubilité ont empêché une bonne polymérisation.

Malgré ces essais, le copolymère statistique de styrène et d'AVB sous forme d'anhydride avec l'APB n'a donc pas pu être synthétisé avec succès et la méthode de « masking » a dû être abandonnée.

Pour la méthode de « fishing », en revanche, quatre polymères ont pu être synthétisés : trois copolymères à blocs avec un bloc de quelques unités d'AVB et un bloc styrène de tailles variables. Pour comparaison un polymère statistique ayant la même taille et les mêmes proportions de styrène et d'AVB que le plus petit des copolymères à blocs a aussi été synthétisé.

Parallèlement, des oligomères de cellulose ont pu être obtenus. En effet, l'acide phosphorique a été utilisé pour hydrolyser la cellulose et former des oligomères avec un bon rendement. Ce procédé a, de plus, été optimisé par rapport à ceux décrits dans la littérature. Juste après l'hydrolyse acide, la cellulose a une masse molaire moyenne réduite et les fractions solubles et insolubles dans l'eau sont séparées par solubilisation. Cependant, une analyse en SEC après acétylation montre un recouvrement des deux distributions en masse molaire indiquant que des oligomères solubles dans l'eau sont encore présents dans la fraction insoluble. L'extraction n'a cependant pas pu être poussée davantage probablement à cause d'une mauvaise dispersion de la fraction insoluble. Les oligomères ont ensuite été caractérisés par différentes techniques. La spectrométrie de masse et la SEC à éluant eau ont

démontré la présence d'oligomères de DP de 1 à 12. Leurs ratios ont pu être déterminés par HPLC, cependant les DP supérieurs à 6 avaient une concentration trop faible pour être détectés. Les oligomères obtenus étaient principalement composés de cellotetraose à 29%. Les ratios de glucose, cellobiose, cellotriose et cellopentaose étaient équivalents et compris entre 17 et 19%. Le cellohexaose représentait seulement 3% car la solubilité dans l'eau diminue avec l'augmentation du DP.

La méthode « fishing » a ensuite été appliquée. Un « blanc » a d'abord été réalisé et a confirmé que les oligomères de cellulose ne sont pas extraits quand la phase organique ne contient pas de polymère. Puis les quatre polymères précédents ont été comparés et les copolymères à blocs ont bien permis une extraction, toutefois sans aucune sélectivité. Il semblerait cependant que ces copolymères aient permis de récupérer la quantité maximale d'oligomères. Le copolymère statistique n'a cependant permis l'extraction d'aucun oligomère probablement à cause de la formation d'un réseau emprisonnant les oligomères dans la phase aqueuse.

Une autre méthode permettant de séparer les oligomères selon leur taille a donc été recherchée. Les alcools étant connus pour solubiliser les oligomères de cellulose, trois alcools différents (méthanol, éthanol et isopropanol) ont été utilisés pour séparer les oligomères par solubilisation sélective. La séparation la plus intéressante a été obtenue par solubilisation dans le méthanol car les deux autres ne solubilisaient que partiellement du cellobiose. Ainsi, la fraction soluble dans le méthanol était composée de cellotriose (28%), de cellobiose (27%) et de glucose (27%) et la fraction insoluble dans le méthanol contenait 42% de cellotetraose et 36% de cellopentaose ainsi que tous les DP les plus élevés.

Dans un deuxième temps, nous avons étudié la synthèse de composés amphiphiles basés sur ces oligomères insolubles dans le méthanol et leur auto-assemblage. Afin de conserver la structure et les propriétés des oligomères, seule l'extrémité de chaîne a été fonctionnalisée par amination réductrice pour introduire un groupement azide terminal. L'acide stéarique a été choisi pour le bloc hydrophobe à cause de sa linéarité et de sa disponibilité en grande quantité. Il s'agit de plus d'un composé bio-sourcé présent dans les graisses animales ou végétales. Une fonction alcyne terminale a été introduite sur l'acide gras et les deux blocs ont été couplés par chimie « click » grâce à la cycloaddition d'Huisgen. Le catalyseur au cuivre n'a pas pu être complétement éliminé. En effet, le procédé de purification usuel est la dialyse, or dans notre cas, trop de produit aurait été perdu à cause de leur petite taille. La même réaction a été appliquée à la cellobiose pour comparaison.

Les équilibres hydrophile/lipophile (HLB) de ces composés ont été calculées et il semblerait qu'ils soient plutôt hydrophiles. Cependant, le composé à base de cellobiose

s'agrégeait après 24h dans l'eau (**Figure 3**) probablement à cause d'un ratio longueur de bloc hydrophile sur hydrophobe défavorable. Le composé était toutefois soluble dans le DMSO qui, étant un bon solvant des deux blocs, n'induisait pas d'auto-assemblage.

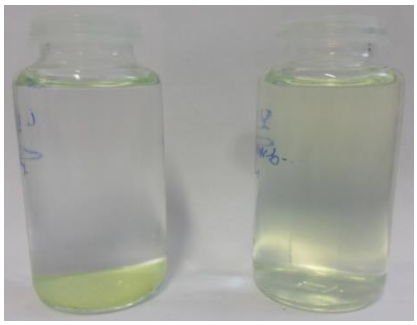

Figure 3. Photos représentant des solutions de composes amphiphiles à base d'acide stéarique et de cellobiose (à gauche) ou d'oligomères de cellulose (à droite) après 24h dans l'eau à 100 mg.L^{-1}

En revanche, le composé à base d'oligomères s'auto-assemblait dans l'eau sans agrégation et a pu être étudié dans ce solvant. La concentration micellaire critique (CMC) a été mesurée à 100 mg.L^{-1} ce qui est plutôt faible pour de tels composés. La taille moyenne des particules observée à 200 mg.L^{-1} était de 140 nm avec un PDI de 0,21 et reste plutôt stable dans le temps. La **Figure 4** présente les images de microscopie électronique en transmission (MET) des objets observés à 200 mg.L^{-1} dans l'eau. Les particules sont plus ou moins sphériques et assez homogènes. Elles sont probablement des vésicules compte tenu de leur grande taille en milieu aqueux. L'homogénéité de la distribution des tailles de particules indique une bonne dispersion des différentes tailles d'oligomères.

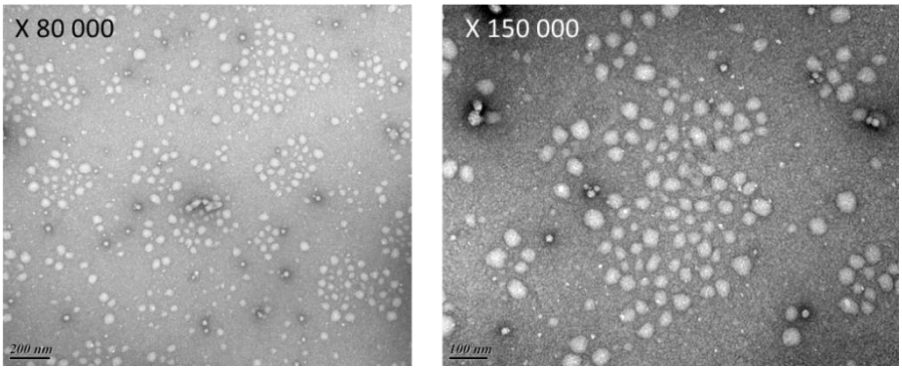

Figure 4. Images de MET observées avec des composés amphiphiles à base d'oligomères de cellulose et d'acide stéarique à 200 mg.L^{-1} dans l'eau

Les perspectives de ce travail sont de produire les oligomères de cellulose par voie enzymatique qui est plus en phase avec la chimie verte que l'hydrolyse acide. Pour cela, une hydrolyse fractionnée semblerait être la meilleure solution, cependant, un gros travail d'optimisation est à prévoir. La méthode de « fishing » devra aussi être plus étudiée pour

essayer d'obtenir une sélectivité. La méthode de « masking » pourrait aussi être testée avec un copolymère à bloc qui protégerait les futurs oligomères par encombrement stérique ou par enroulement autour de la chaîne cellulose. Pour cela, un bloc autre que le styrène pourrait être choisi pour favoriser une interaction par liaison hydrogène par exemple. La séparation par solubilité pourrait aussi être améliorée par une précipitation sélective. En effet, les oligomères seraient solubilisés dans l'eau et l'ajout graduel d'un anti-solvant les feraient précipiter au fur et à mesure. Pour finir, l'impact sur l'auto-assemblage de la longueur et de la nature du bloc hydrophobe des composés amphiphiles à base d'oligomères de cellulose pourrait être étudié. Ces composés pourraient être étudiés pour la libération contrôlée de principe actif.

Table of Contents

Abbreviations

2D	Two dimensional

A

AFM	Atomic force microscopy
AIBN	Azobisisobutyronitrile
[Amim]Cl	1-allyl-3-methylimidazolium chloride
APBA	3-acrylamidophenylboronic acid
ARS	Alizarin red S
ATRP	Atom transfer radical polymerisation

B

[Bmim]Cl	1-butyl-3-methylimidazolium chloride
BSPA	3-(benzylthiocarbonothioylthio)propanoic acid
BTTCP	2-(butylthiocarbonothioylthio)propanoic acid

C

CAS	Chemical abstracts service
CAZy	Carbohydrate-active enzymes
CB-SA	Amphiphilic compound based on cellobiose and stearic acid
CBH	Cellobiohydrolase
CESA	Cellulose synthase
CMC	Critical micelle concentration
CPADB	4-cyanopentanoic acid dithiobenzoate
CO-SA	Amphiphilic compound based on cellulose oligomers and stearic acid
COSY	Correlation spectroscopy (^{1}H-^{1}H)
CTA	Chain transfer agent
Cuam	Cuprammonium hydroxide
CuAAC	Copper-catalysed azide-alkyne cycloaddition
Cuen	Cupriethylenediamine hydroxide
Cuoxam	Cuprammonium hydroxide

D

Đ	Dispersity
DBTTC	Dibenzyl trithiocarbonate

DLS	Dynamic light scattering
DMAc	Dimethylacetamide
DMF	Dimethylformamide
DMSO	Dimethyl sulfoxide
DMP	2-dodecylsulfanylthiocarbonylsulfanyl-2-methyl-propionic acid
DOSY	Diffusion-ordered spectroscopy
DP	Polymerisation degree
DP_{th}	Theoretical polymerisation degree
DS	Substitution degree
DSC	Differential scanning calorimetry

E-F

EA	Ethyl acetate
EG	Endoglucanase
ELSD	Evaporating light scattering detector
[Emim]Ac	1-ethyl-3-methylimidazolium acetate
FT-IR	Fourier transformation infra-red

H

ΔH_c	Crystallisation enthalpy
ΔH_m	Melting enthalpy
HEMA	Tris-(2-hydroxyethyl)-methylammonium methylsulfate
HEPES	4-(2-hydroxyethyl)-1-piperazineethanesulfonic acid
HCW	Hot compressed water
HLB	Hydrophilic-lipophilic balance
HPILC	High performance “ionic liquid” chromatography
HPLC	High performance liquid chromatography
HSQC	Heteronuclear single quantum correlation (^{1}H-^{13}C)

I-J

IR	Infra-red
$J_{C\text{-}C}$	Carbon-carbon coupling constant
$J_{H\text{-}H}$	Proton-proton coupling constant
JMOD	J-modulated spin-echo

L

LAMA	2-lactobionamidoethylmethacrylate
LCST	Lower critical solution temperature
LPMO	Lytic polysaccharide monooxygenases

M

MALDI	Matrix-assisted laser desorption/ionisation
MBSP	Methyl 3-benzylsulfanylthiocarbonylsulfanylpropionate
MeOH	Methanol
M_n	Number average molar mass
M_{th}	Theoretical molar mass
M_w	Mass average molar mass
MW	Microwave

N

N2B	Naphthalene-2-boronic acid
NMMO	*N*-methylmorpholine-*N*-oxide
NMR	Nuclear magnetic resonance

P

PAPBA	Poly(3-acrylamidophenylboronic acid)
PBA	Phenylboronic acid
PBS	Phosphate buffered saline
PBLG	Poly(γ-benzyl-L-glutamate)
PDI	Polydispersity index
PDMA	Poly(N,N-dimethylacrylamide)
PEG	Poly(ethylene glycol)
PLAMA	Poly(2-lactobionamidoethylmethacrylate)
PNIPAM	Poly(*N*-isopropylacrylamide)
PS	Polystyrene
PTMSS	Poly(4-trimethylsilylstyrene)
PVBA	Poly(4-vinylphenylboronic acid)

R-S

RAFT	Reversible addition-fragmentation chain transfer

RI	Refractive index
RT	Room temperature
SEC	Size exclusion chromatography
SEM	Scanning electron microscopy

T

T_b	Boiling point
TBAF	Tetrabutylammonium fluoride
T_c	Crystallisation temperature
$T_{d\ 5\%}$	Degradation at 5% temperature
TEM	Transmission electron microscopy
T_g	Glass transition temperature
TGA	Thermogravimetric analysis
THF	Tetrahydrofuran
T_m	Melting temperature

U

UDP	Uridine diphosphate
UV	Ultraviolet

V-W

VBA	4-vinylphenylboronic acid
V-70	2,2'-azobis(4-methoxy-2.4-dimethyl valeronitrile)
WIF	Water insoluble fraction

X

XOS-Ol	Amphiphilic compound based on xylo-oligomer and oleic acid
XOS-Ric	Amphiphilic compound based on xylo-oligomer and ricinoleic acid

General introduction

The European Association for Chemical and Molecular Sciences listed six intertwined problems that humanity will be facing soon but that cannot be easily solved on the basis of our current technology: Energy, Raw materials, Water, Food, Health and Air[1].

Nowadays, the chemists are mainly focused on the "Raw materials" problem as they are delving into greener alternatives to the materials currently used at large scale[2,3] (production of polymers in 2012: 265 millions of tons[4]). Their work is starting to pay even though the production of bio-based plastics in 2013 represented less than 1% of the global production of plastics. In the same period, bio-based plastics only involved 0.01% of the worldwide agricultural area of 5 billion hectares[4] and are consequently not in competition with the "Food" issue. Regrettably, only 37.6% of the bio-based plastics possibly produced are biodegradable (**Figure 5**).

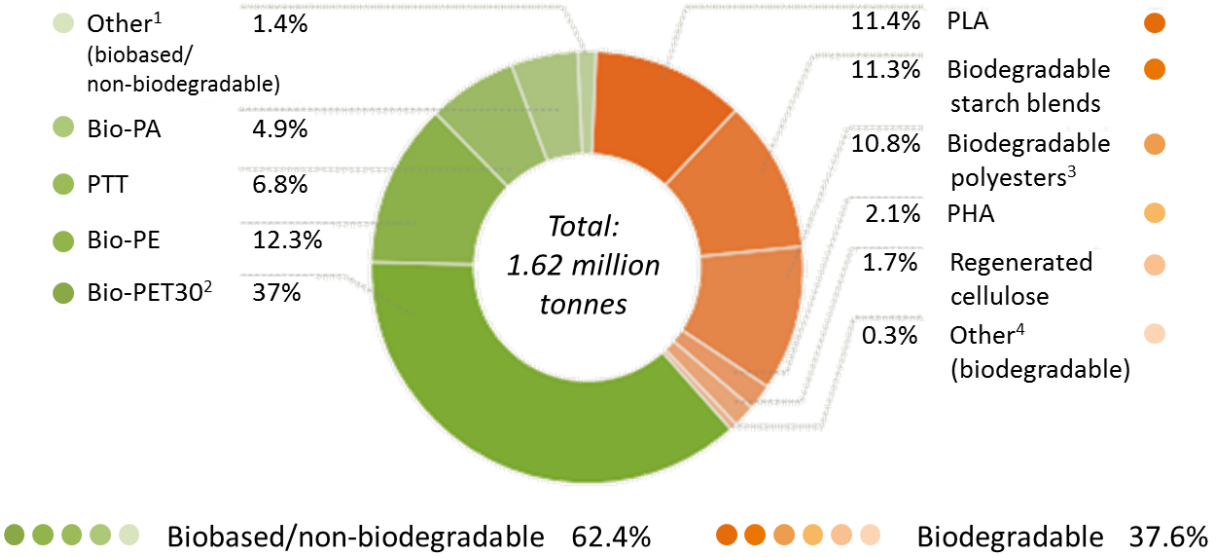

Figure 5. Global production capacities of bio-based plastics in 2013 (by material)[4] – [1] Contains durable starch blends, Bio-PC, Bio-TPE, Bio-PUR (except thermosets), [2] Bio-based content amounts to 30 %, [3] Contains PBAT, PBS, PCL, [4] Biodegradable cellulose ester

PA: polyamide, PTT: polytrimethylene terephthalate, PE: polyethylene, PET30: polyethylene terephthalate 30% glass reinforced, PLA: polylactic acid, PHA: polyhydroxyalkanoates, PC: polycarbonate, TPE: thermoplastic elastomer, PUR: polyurethane, PBAT: polybutyrate, PBS: polybutylene succinate, PCL: polycaprolactone.

The bio-based and biodegradable "regenerated cellulose"[5] only represents 1.7% of the total production capacities of bio-based plastics in 2013 (**Figure 5**) while cellulose is one of the most abundant natural polymers on the planet. Moreover, cellulose is renewable in a short time frame compared to oil, which is currently indispensable (≤ 50 years *versus*

millions of years). This small percentage is the result of great difficulties for transformation and process. The chemists' society is however aware of its exceptional potential as the number of publications on the subject exceeds a thousand per year (**Figure 6**).

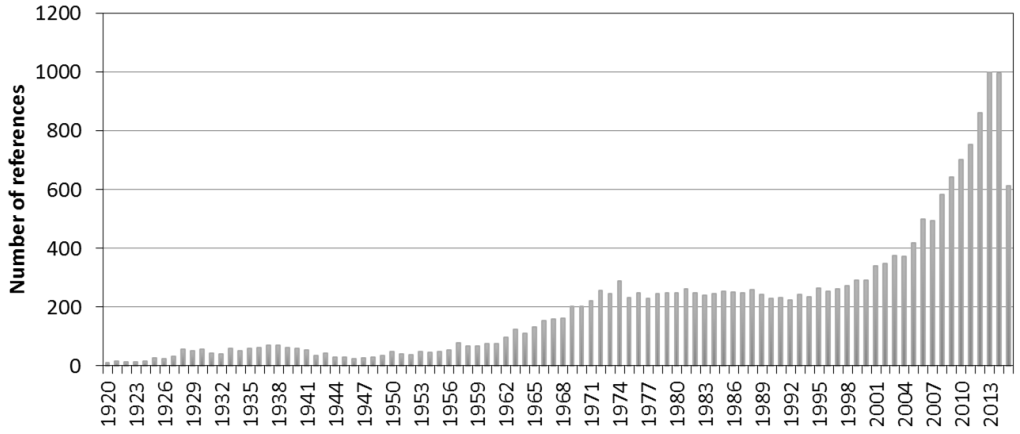

Figure 6. Number of references about cellulose per year from 1920 to mid-August 2015 (references containing the appellation as entered, data from SciFinder)

Cellulose oligomers are materials with the same structure as cellulose but with a smaller molar mass that grants them water-solubility. The currently commercialised cellobiose does not have the same properties as cellulose because its reactivity is drastically influenced by the reducing end group. Cellulose oligomers of higher polymerisation degree (DP) are seldom commercially available and at very high prices. Moreover, no more than a few hundreds of milligrams are purchasable at once because of their time-consuming production.

The processes currently proposed in the literature are difficult to put in place or only allow small oligomer sizes (DP 3-4). Some protocols allow the production of oligomers in good yield but the separation according to their size (necessary for some applications) is achieved by affinity chromatography, which is a low yields method.

The goal of this work is to produce low dispersed cellulose oligomers with an easily accessible production and separation technique. In this frame, two new and innovative strategies were probed. They both involve the use of a synthetic polymer to either protect parts of the cellulose during a hydrolysis or to enable a selective solubilisation.

The first chapter establishes a state of the art on the structure, solubility and characterisation of cellulose and on the cellulose oligomers production and separation methods currently available.

As the synthetic polymers employed in the considered strategies are required to have a reversible interaction with cellulose, boronic acids will be utilised. The second chapter thus deals with a preliminary study about the complexation of boronic acids on sugars to determine the synthetic polymer structure best suited for both of the strategies put in place.

In the third chapter, the syntheses of the boronic acid containing polymers will be investigated.

In the fourth chapter, the strategies to produce and separate the cellulose oligomers will be tested.

To finish, in the fifth chapter, an application of the cellulose oligomers will be investigated. Amphiphilic compounds based on the cellulose oligomers produced will be synthesised and their self-assembly studied.

---

[1] E. Keinan, *Angew. Chem. Int. Ed.* **2013**, *52*, 2667–2672.

[2] R. Mülhaupt, *Macromol. Chem. Phys.* **2013**, *214*, 159–174.

[3] T. Iwata, *Angew. Chem. Int. Ed.* **2015**, *54*, 3210–3215.

[4] European Bioplastics, *Bioplastics: Facts and Figures*, **2012**.

[5] S. Wang, A. Lu, L. Zhang, *Prog. Polym. Sci.* **2015**, in press, DOI 10.1016/j.progpolymsci.2015.07.003

Chapter I. State of the art

Table of Contents

I. 1. Generality on cellulose

Anselme Payen, a French chemist, discovered cellulose in 1838 when he treated various plants with acids and ammonia followed by extractions[1]. Cellulose constituted the remaining fibrous product that could not be treated. The name “cellulose” comes from “cell” that refers to the plant cells where the production occurs and “ose” the French suffix referring to saccharides. Nowadays, cellulose represents $1.5x10^{12}$ tons of the total annual biomass production and is thus considered as almost inexhaustible[2]. Most of it ends up in the paper industry but its numerous and fascinating properties are the reason why various fields like electrical displays[3], nanotechnology[4] or biomedical applications[5] made use of it under the native form or chemically modified form.

I. 1. A) Biosynthesis

The main production source of cellulose is annual plants like tree or cereal straw but some algae and bacteria[6–9] also produce it.

Cellulose is synthesised in the plants cell walls among with lignin and hemicelluloses[10] (**Figure I-1a and b**) in different ratio depending on the source of the lignocellulosic biomass (**Table I-1**). Each of them is playing a specific role in the cell:

- Lignin[11] is a natural aromatic polymer that acts like glue to maintain all the components of the cell together. Its antioxidant and hydrophobic properties also shield the plant cell. Its structure is complex with three different monomers (*p*-coumaryl alcohol, coniferyl alcohol and sinapyl alcohol) bound by ether or carbon-carbon bonds. The ratio between the three monomers depends on the lignin origin.
- Hemicelluloses[12] are branched polysaccharides that act as bridges between the cellulose microfibrils. The branching prevents any crystallinity and confers solubility in water. The hemicelluloses chains are composed of several monosaccharides like xylose, mannose and galactose among other, and contain 500 to 3 000 sugars.
- Cellulose microfibrils are the main component of the cell wall (**Table I-1**) and contribute, with lignin, to the rigidity of the assembly. They are composed of 36 cellulose chains[13] coming from 6 rosette subunits[14] (**Figure I-1c**).

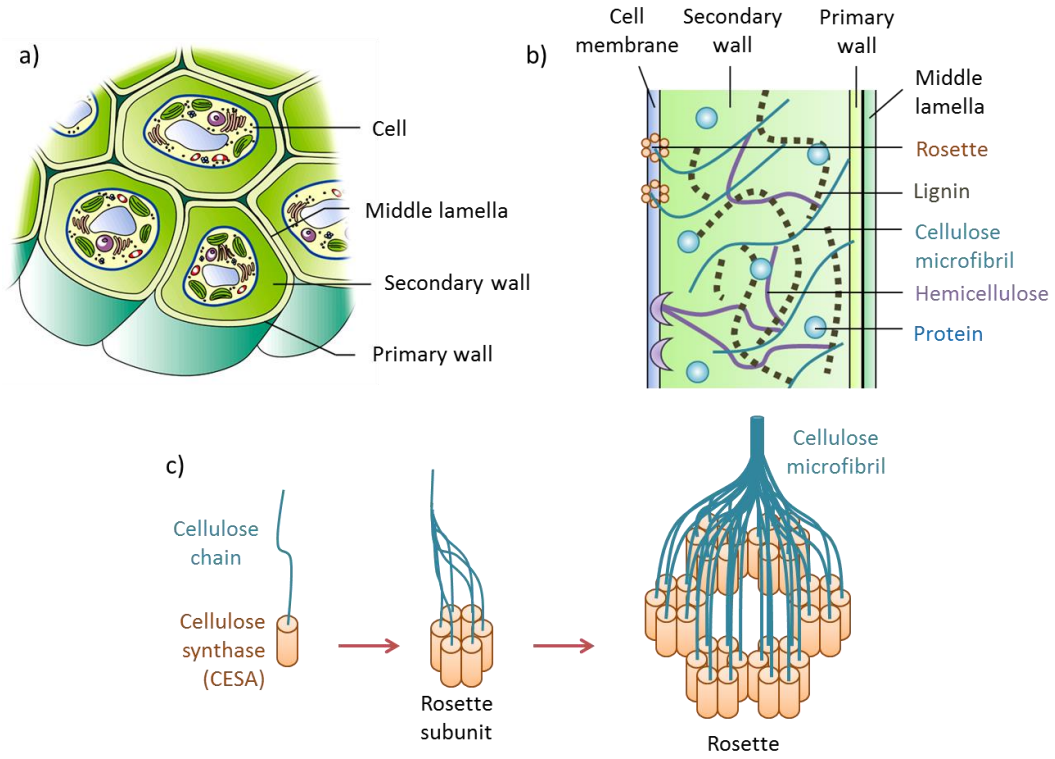

Figure I-1. Composition of a) cells in plants, b) cell walls (adapted from Sticklen[10]) and c) rosette (adapted from Doblin *et al.*[14])

Table I-1. Chemical composition of several types of lignocellulosic biomass (from Becer and coll.[15])

	Cellulose (%)	Hemicellulose (%)	Lignin (%)
Hardwood	40.4 – 54.1	18.4 – 35.9	15.5 – 24.1
Softwood	42.0 – 50.0	11.0 – 27.0	20.0 – 27.9
Agricultural waste	25.0 – 47.0	12.0 – 36.0	6.1 – 25.0
Grasses	25.0 – 40.0	25.0 – 50.0	10.0 – 30.0

Cellulose is synthesised by a large complex of cellulose synthases[16] (CESA), which are organised in rosettes (**Figure I-1c**). CESA complexes use uridine diphosphate (UDP)-α-glucose (**Figure I-2a**) as the substrate for the cellulose synthesis[10,17]. Every other monomer is turned by the enzymes at 180° as represented in **Figure I-2b**. The chains are then associated in microfibrils[18] by enzymes called the "terminal complex"[19]. As the cellulose chains have a high affinity toward themselves due to hydrogen bonding, a high crystallinity is induced. But from time to time, they are disordered causing amorphous-like areas[20].

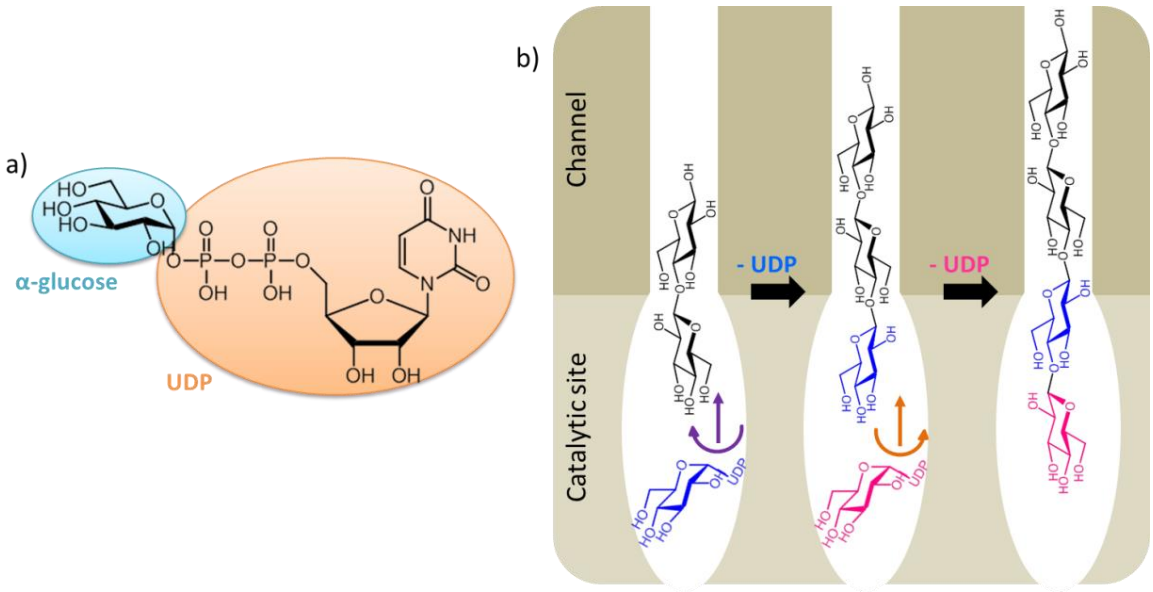

Figure I-2. a) Structure of UDP-α-glucose and b) Proposed model for the synthesis and translocation of cellulose (adapted from Zimmer and coll.[21])

I. 1. B) Structure and properties

Cellulose chains are linear and consist of anhydroglucose units linked together by β-1,4 bonds (**Figure I-3a**). 1 and 4 are the positions of the glycosidic bonds on the glucose. The numbering starts at the anomeric proton as represented in **Figure I-3b**. The β notation indicates that the substituent on the 1-position is in equatorial conformation (**Figure I-3c**). The other configuration where this substituent is in axial conformation is called α and is found in other polysaccharide. Each anhydroglucose unit has a length of 0.515 nm and every other is turned at 180° to form the real repeating unit that is cellobiose (**Figure I-3a**).

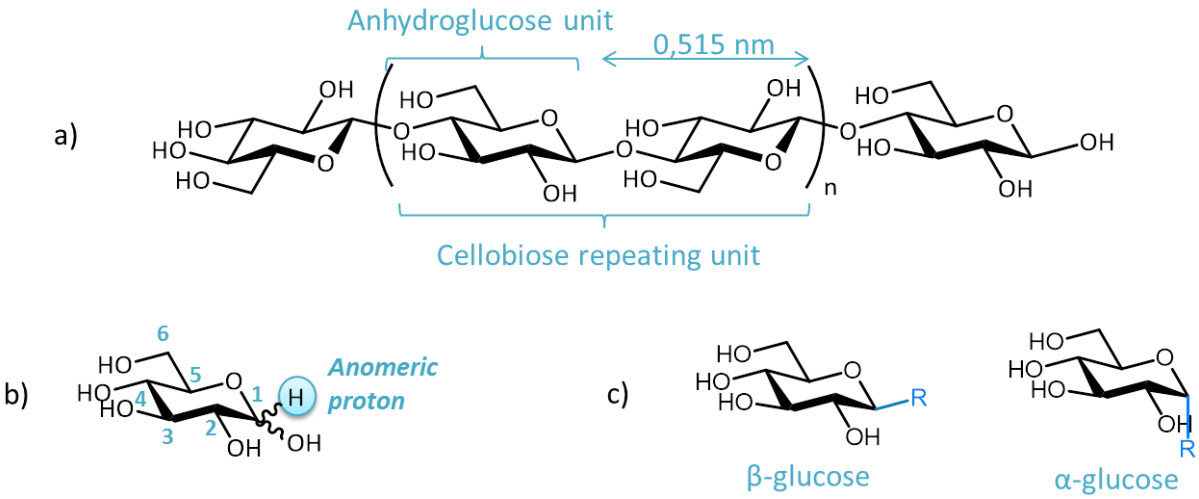

Figure I-3. a) Cellulose structure (polymerisation degree, DP = 2n+2), b) Numbering of saccharides carbons (example of glucose), c) Definition of an α- or a β-bond

I. 1. B) i) Open form

The propensity of saccharides to present an "open" form explains the equilibrium between the α- and β-form and is present on all the mono- and polysaccharides. The saccharide can "open" and form an alcohol and an aldehyde as represented **Figure I-4**. For cellulose, the only glucose per chain that has this property is the one at the extremity called the reducing end. The other extremity is called the non-reducing end.

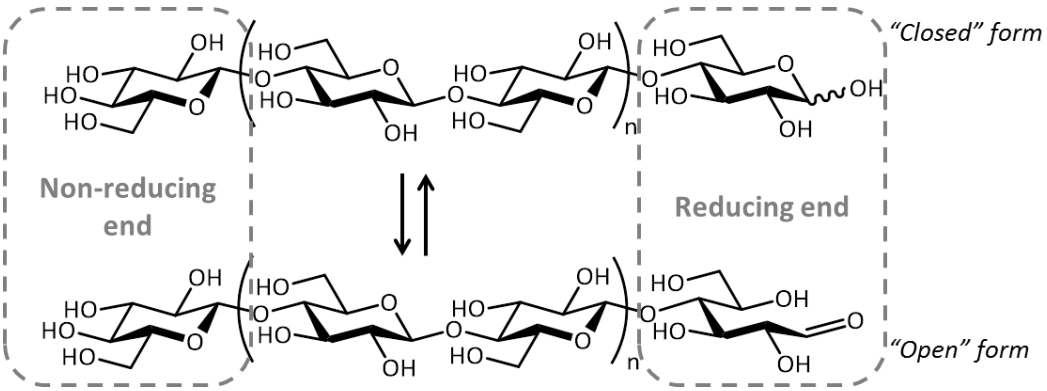

Figure I-4. Definition of the reducing and non-reducing end of cellulose

For saccharides in solvents such as water, the α- and β- forms are in equilibrium. When the sugar "closes", the bond can be created again on both sides of the alcohol leading to either the α- or the β-form of the saccharide. For the glucose, this interconversion has a half-life time of 5 minutes at 37°C in water[22]. In water at 27°C, aqueous D-glucose usually contains 37% of the α-form and 63% of the β-form, the ratio becomes 43.5%/56.5% in dimethyl sulfoxide (DMSO) at 27°C[23].

This equilibrium is often used to functionalise this particular position in the view of click-chemistry for example. It is the most reactive position of all the cellulose backbone.

I. 1. B) ii) Pyranose/Furanose equilibrium

Because of the "open"/"closed" equilibrium, the pyranose/furanose equilibrium also occurs. The glucose form presented until now is called pyranose and has a 6-bonds cycle. But when the "open" form closes, the hydroxyl group on the 4-position may also react and the sugar has then a 5-bonds cycle (**Figure I-5**). This form, called furanose, is thermodynamically less stable than pyranose[24] and is present at less than 0.05% in aqueous D-glucose[25].

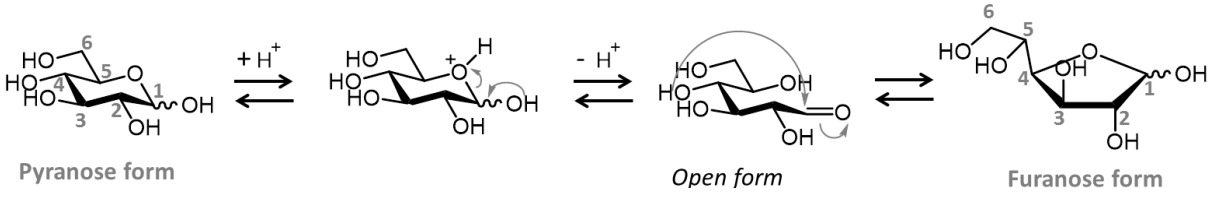

Figure I-5. Equilibrium between the pyranose and furanose forms (adapted from Isbell and Wade[26])

These four forms of glucose are differentiable by NMR (**Table I-2**). The α- and β-forms have different chemical shifts (**Appendix I.I**, p 49) and pyranose and furanose forms have different coupling constants.

Table I-2. Possible forms of glucose and how to differentiate them by NMR

	Pyranose form	**Furanose form**	Difference
α-form	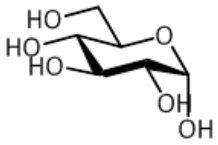	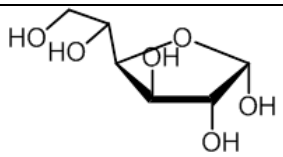	^{1}H and ^{13}C NMR chemical shifts
β-form	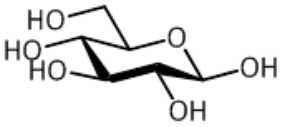	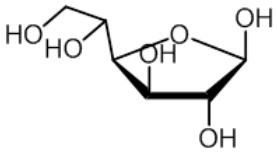	
Difference	$J_{H\text{-}H}$ or $J_{C\text{-}C}$ coupling constants[27]		

I. 1. B) iii) Crystallinity/Morphology

Another major property coming from the cellulose structure is its crystallinity. The numerous hydroxyl groups present on its backbone induce intra- and inter-chains hydrogen bonding (**Figure I-6**).

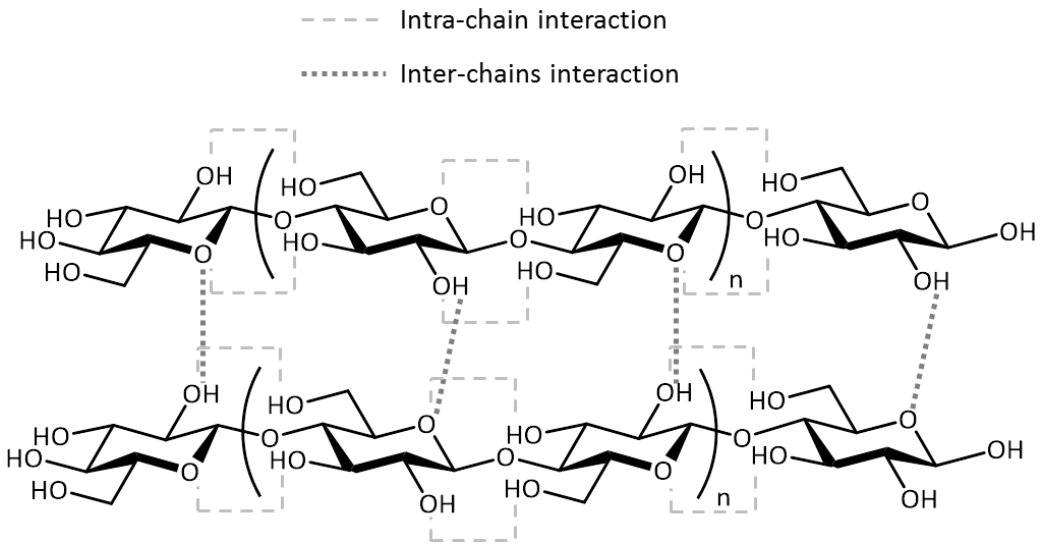

Figure I-6. Representation of the different hydrogen bonding responsible of the cellulose crystallinity (adapted from Kadokawa[28])

Cellulose crystallinity and morphology depend on its origin as observed in **Figure I-7**. Cellulose from cotton is one of the most crystalline. Cellulose from wood pulp has a polymerisation degree (DP) between 300 and 1 700 but cellulose from cotton or other plant fibres have a DP between 800 and 10 000.

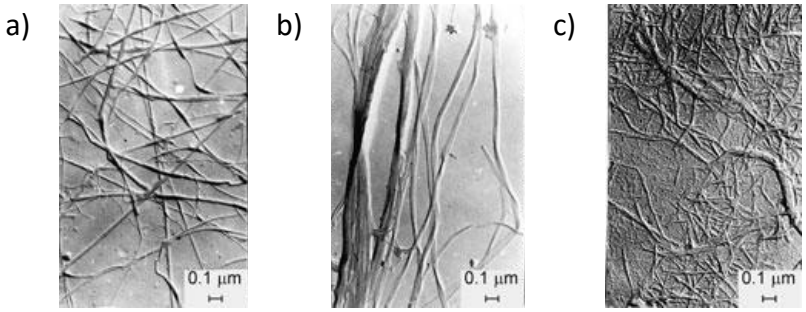

Figure I-7. Electron micrographs of cellulosic microfibrils of varying origins: a) algae (*Valonia* spp.), b) cotton linters and c) spruce sulphite pulps (from Klemm *et al.*[2])

Cellulose also exists in several polymorphs, identified in 1996 by Kroon-Batenburg and coll. in 1996[29] and summarised in **Figure I-8a**. Native cellulose is only found under the polymorph I and is invariably transformed into polymorph II after any regeneration treatment. If the regeneration occurs at high temperatures, cellulose IV can be produced[30]. Cellulose III is obtained after a treatment with ammonia.

Considering the structures (**Appendix I.II**, p 50), the I_α polymorph consists in a one-chain triclinic P1 structure whereas I_β corresponds to two chains organised along a $P2_1$ monoclinic space group[31]. Cellulose I has a parallel orientation and cellulose II has an antiparallel orientation (**Figure I-8b**). It is a fact established by the literature but the mechanism of the transformation from one to the other is still debated[2,29]. The conformation of the chain in cellulose III has features similar to cellulose II but with parallel chains like in cellulose I[32]. And cellulose IV has a two chain P1 structure with parallel orientation for IV_I and antiparallel for IV_{II}[33].

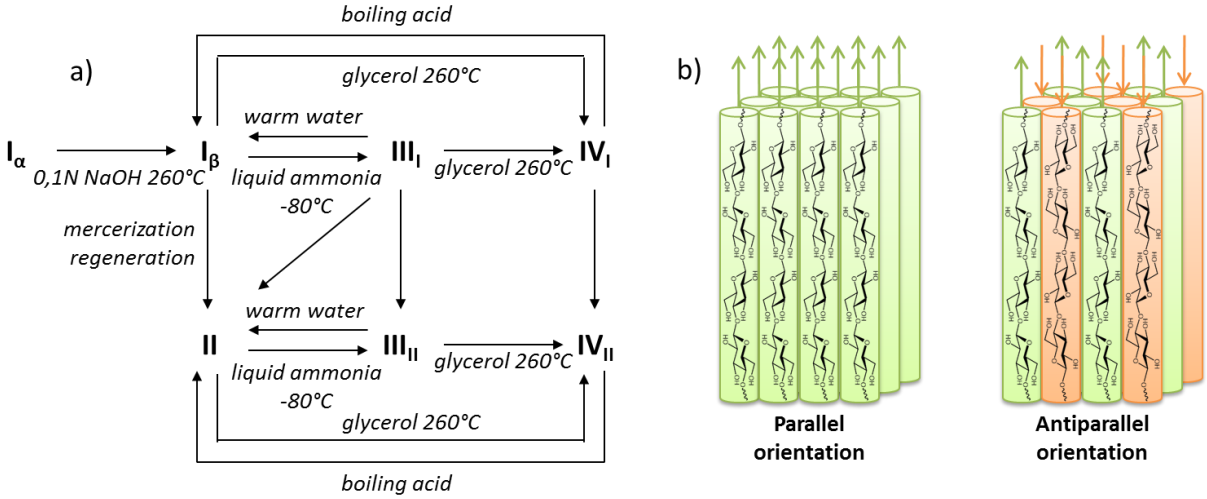

Figure I-8. a) Polymorphs of cellulose (adapted from Kroon-Batenburg *et al.*[29]) and b) Representation of a parallel and antiparallel orientation of cellulose chains (adapted from Kadokawa[28])

I. 1. C) Cellulose solubility

To solubilise cellulose, the solvent has to break the hydrogen bonding network in place and prevent it from occurring again[34,35] by creating interactions with cellulose that have an energy above 25.0 kJ.mol^{-1} [36]. No common solvents meet this requirement but some mixtures or unusual solvents do, as described below. Cellulose solvents are categorised between derivatizing/non-derivatizing and aqueous/non-aqueous (**Figure I-9**). A non-derivatizing solvent procures a physical solubilisation whereas a derivatizing solvent functionalise some hydroxyl groups of the cellulose thus changing its solubility.

Another reason to the cellulose insolubility could be its amphiphilic character[37]. The hydrophobic sides tend to stick together in aqueous solvents creating insoluble hydrophobic "pockets". Consequently, solubility would be facilitated in amphiphilic solvents, as ionic liquids, or in the presence of cosolutes.

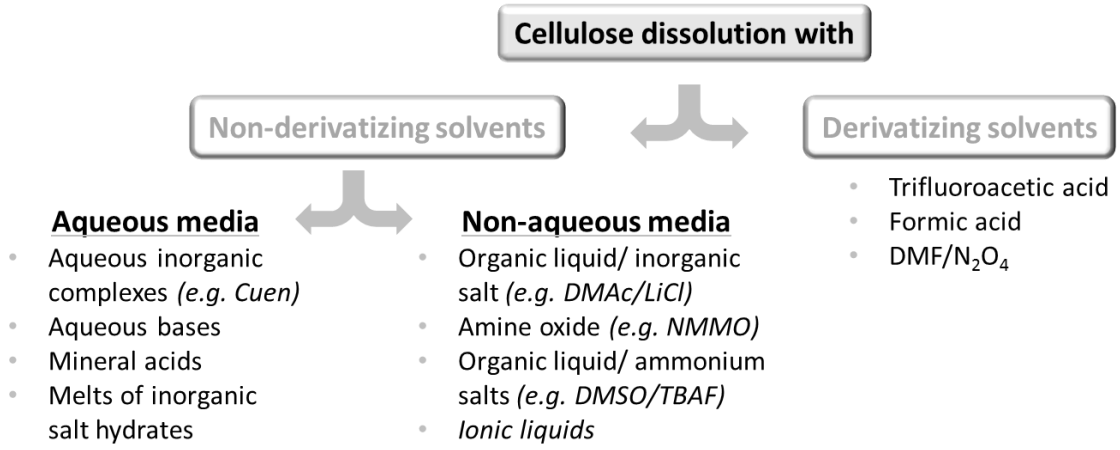

Figure I-9. Classification of cellulose solvents and examples (adapted from Heinze and Koschella[38])

I. 1. C) i) Inorganic metal complexes

The forces that take place to solubilise cellulose in inorganic metal complexes solutions are complex coordination with the cellulose anionic oxygen and Coulomb interaction[39]. Even at low cellulose content, these solutions usually have a high viscosity[40] that prevents the incorporation of more material.

The most used of these types of solutions are cupriethylenediamine hydroxide (Cuen, $[Cu(H_2N–(CH_2)_2–NH_2)_2](OH)_2$) and cuprammonium hydroxide (Cuam or Cuoxam, $[Cu(NH_3)_4](OH)_2$). Cuen solutions main application is to determine the cellulose polymerisation degree depending on the solution viscosity[41]. This method was principally used in the pulp and paper industry. The concentration of cellulose in 0.5 M of Cuen can reach 8 g.L^{-1} [41].

A French chemist Louis-Henri Despeissis patented in 1890 an industrial process to produce textile fibres using cellulose dissolved in Cuam[42]. This process is still used

nowadays notably in Asahi (Japan) but the high cost coming from the need of using cellulose cotton and copper salts prevents it from reaching larger scale[43].

I. 1. C) ii) Aqueous bases and additives

Mercerization which consists in soaking cellulose in a strong aqueous base is one of the most technically relevant processes in cellulose technology and is used to change the crystal structure from cellulose I to cellulose II[44] (**Figure I-8a**, p 22).

At low temperature, hydrates of NaOH are able to form hydrogen bonds with the cellulose chains[34]. However, above a certain concentration the cellulose forms aggregates in the NaOH solution and a suspension is obtained[45]. Only 2% w/v of cellulose could be totally dissolved in 5% w/v NaOH solution[44].

The addition of urea increases the solubility by helping the introduction of the molecules into the cellulose network and by screening the hydrophobic effect that would create cellulose aggregation[46,47]. The ratio 6 wt% NaOH/ 4 wt% urea was found to be one of the best to dissolve cellulose I with around 5 wt% of cellulose of bagasse solubilised[48].

The disadvantage of these systems is that the solubility greatly depends on the cellulose morphology[49], crystallinity, molar mass and on the temperature[50]. Nevertheless, films, membranes, microspheres, hydrogels and fibres can be produced from this solvent system[51]. This process was patented by Jiangsu Long-Ma Green Chemical Fiber Co. Ltd[52] with a cellulose concentration of 3 to 8 wt% in NaOH at 7.0-7.5 wt% and urea at 11.0-12.0 wt% at low temperature (-12°C).

Other bases can be used with urea[53], lithium hydroxide is more efficient but less used because of health and environmental considerations; potassium hydroxide is really less efficient than sodium hydroxide.

One of the most important industrial processes for cellulose is based on its dissolution in sodium hydroxide. The viscose process was invented by a French scientist Hilaire de Chardonnet. After solubilisation, cellulose xanthate (**Figure I-10**) is produced by reaction with carbon disulphide. The cellulose fibres are then regenerated by defunctionalisation using mineral acids.

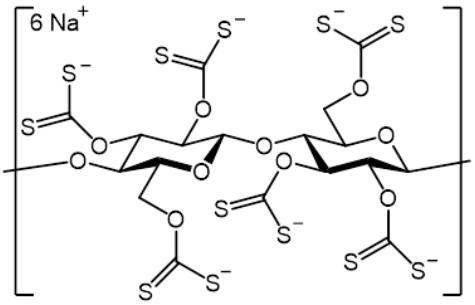

Figure I-10. Cellulose xanthate structure

I. 1. C) iii) Molten salts hydrates

Molten salts hydrates, like $LiClO_4 \cdot 3H_2O$ or $ZnCl_2 \cdot 4H_2O$, were first employed to solubilise cellulose in the early 20th century because of their low cost and low toxicity[54]. Cellulose can be precipitated from these solutions by a simple addition of water and the salt

recovered after evaporation. The nature of the salt tunes the crystallinity, the surface area and the morphology of the cellulose obtained after precipitation[55]. For instance, cellulose I is obtained after regeneration from $LiCl{\cdot}5H_2O$ as it is a weak swelling agent whereas $LiCl{\cdot}2H_2O$, inducing a greater swelling, produces cellulose II.

Interaction between cellobiose, as cellulose model, and Li^+ cation was investigated by ^7Li NMR[56]. Cellobiose was found to be part of the first coordination sphere of the lithium cation replacing the water molecules. The hydroxyl groups thus form direct coordination bonds with the Li^+ cation which explains the good solvation of cellulose in such solvents. The same conclusions were drawn with the Ca^+ cation after dissolution of cellulose in $Ca(SCN)_2$ and analysis by IR spectroscopy[57].

Only low concentrations can be reached with these solutions[55], for instance, $LiCl{\cdot}2ZnCl_2{\cdot}8H_2O$, one of the most promising systems, could only dissolve 5 wt% of cellulose because of the high viscosity of the solution.

These solvents have no industrial applications probably due to the fact that their effectiveness greatly depends on the water content and that their inherent acidity unavoidably depolymerise the cellulose yielding to lower molar masses[54,55]. The acidic hydrolysis is also favoured by the high temperature needed (up to 100°C) to solubilise the cellulose.

I. 1. C) iv) Dimethylacetamide (DMAc)/Lithium chloride

DMAc/LiCl mixture was first patented for the solubilisation of cellulose by McCormick in 1981[58]. The dissolution mechanism represented in **Figure I-11** was determined by several NMR studies[59]. This interaction is put in jeopardy by the presence of water that induces aggregation[60]. This is why no industrial application uses this type of solvent. In addition, it takes more than three weeks at 25°C to solubilise cellulose at 20 wt% [60].

This system is mostly known for its good compatibility with SEC columns which allows direct measurement of the cellulose molar mass[61]. Unfortunately, the hydrodynamic volume of the cellulose and the elution behaviour is deformed by polymer-polymer and/or polymer-solvent interactions[62].

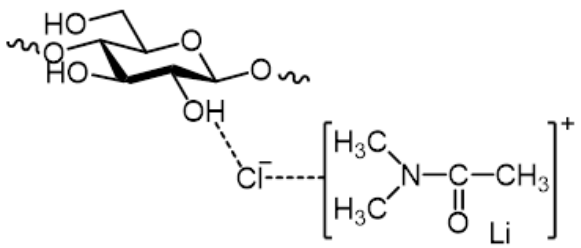

Figure I-11. Mechanism of the dissolution of cellulose in DMAc/LiCl (from McCormick *et al.*[59])

I. 1. C) v) N-methylmorpholine-N-oxide (NMMO)

N-methylmorpholine-*N*-oxide (NMMO, **Figure I-12**) is the most industrially successful of all non-derivatizing solvents. It is used in the Lyocell process to produce cellulose fibres such as the commercial Courtaulds' Tencel[63]. However some side-reaction may occur during this process, especially in the presence of water, like NMMO decomposition, cellulose depolymerisation, rheological inconstancies or temporary or permanent discoloration[64]. Some stabilisers like propyl gallate may be added to the solution to avoid them.

Cellulose concentrations can reach up to 23 wt% in this solvent[35]. As the N–O bond is highly dipolar (**Figure I-12**), the oxygen creates hydrogen bonds with the hydroxyl groups of the cellulose thus cleaving intermolecular interaction[35].

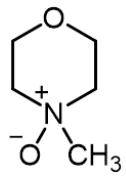

Melting point: 180-184°C

Soluble in water

Figure I-12. Structure and some properties of NMMO

I. 1. C) vi) DMSO/tetrabutylammonium fluoride (TBAF)

DMSO/TBAF solutions are able to dissolve cellulose with a DP up to 1 200 at 16 $g.L^{-1}$ in fifteen minutes at room temperature[65]. The dissolution occurs thanks to the fluoride that is able to break intermolecular hydrogen bonding in the cellulose. In the presence of water, the cations are withdrawn from the chains and gelation occurs if the H_2O/F^- ratio exceeds 2/1[66].

These systems have no industrial application but allow the analysis of cellulose in solution by NMR spectroscopy[67].

I. 1. C) vii) Ionic liquids

An ionic liquid is a salt with a melting point below 100°C. They have many interesting properties like chemical and thermal stability, non-flammability and very low vapour pressure. Due to these properties, they are sometimes considered as "green" solvents as they can also be recycled[68] even though their inner toxicity is undeniable[69,70]. But more and more research are oriented toward the design of environmentally friendly ionic liquids[71].

They were first used to solubilise cellulose in 2002 by Rogers and coll.[72]. The most promising at that time was 1-butyl-3-methylimidazolium chloride ([Bmim]Cl) with a cellulose concentration of 10 wt% at 100°C. The interaction between the chloride anions and the cellulose hydroxyls was found to occur with a 1:1 stoichiometry[73]. An addition of water

breaks these interactions and makes the cellulose precipitate. The precipitated cellulose structure had evolved from cellulose I to cellulose II while losing crystallinity. This process may cause some depolymerisation[74]. Many other ionic liquids were tested later on for their efficacy to solubilise cellulose[75] and the better results were observed for [Bmim]Cl, 1-ethyl-3-methylimidazolium acetate ([Emim]Ac) and 1-allyl-3-methylimidazolium chloride ([Amim]Cl) as represented in **Table I-3**. For now, [Emim]Ac is the only one to be found at industrial scale, TITK (Thüringisches Institut für Textil) adapted a dry-wet spinning process especially for this solvent[76]. Industrial applications of ionic liquids will probably increase over the years as, for now, this technology is still quite recent and their prices are still high.

Table I-3. Characteristics of three ionic liquids

Name	1-butyl-3-methyl imidazolium chloride	1-ethyl-3-methyl imidazolium acetate	1-allyl-3-methyl imidazolium chloride
Abreviation	[Bmim]Cl	[Emim]Ac	[Amim]Cl
Structure	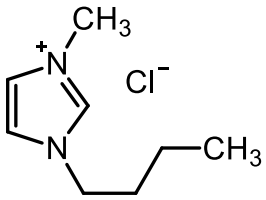	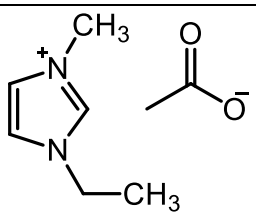	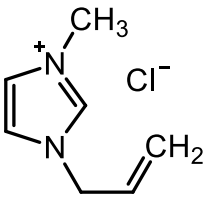
Melting point	73°C	- 20°C	49-51°C
Max cellulose concentration [a]	25 wt% (microwave, 100°C)[72]	15 wt% (110°C)[77]	14.5 wt% (80°C)[78]
Price (€/g) [b]	1.19	2.67	5.41

[a] The time allowed for the dissolution was not mentioned in the publication cited, [b] For the larger packaging from Sigma-Aldrich in May 2015

Recently, Jérôme and coll.[79] proposed a new enzyme-compatible, biodegradable and inexpensive ionic liquid that could solubilise cellulose up to 6 wt% in 10 minutes at 110°C: choline acetate in association with 15 wt% of tributylmethylammonium chloride. This dissolution rate is really small compared to [Bmim]Cl that requires 30 min under microwave for a 8 wt% concentration[80] or [Emim]Ac that necessitates 2h for a 5 wt% concentration[81].

I. 1. D) Characterisation

A characterisation by direct dissolution may cause some degradation or too viscous solutions, as seen previously, which could influence the analysis. To prevent this issue, the solubility of cellulose can be tuned by functionalisation.

I. 1. D) i) Cellulose functionalisation

Cellulose functionalisation is possible in all of the solvents cited in §I. 1. C) as the chains are well dispersed and accessible[82]. Ionic liquids have several advantages like a better control, mild conditions, low excess of reagent, short reaction time and recycling of the solvent[83]. But the ionic liquid has to be chosen carefully otherwise unwanted reaction may occur. For example, a tosylation in [Emim]Ac produced cellulose acetate, instead of tosylate, as the toluenesulfonyl chloride activated the acetate ions of the solvent[84].

The substitution degree (DS) is employed to determine the extent of a functionalisation and is defined as the average number of substituted hydroxyl groups per glucose unit. The theoretical maximal value is thus 3.0. The determination is usually done by NMR analysis after perpropionylation of the remaining hydroxyls groups (**Figure I-13**). The DS is then calculated thanks to the integration of specific peaks following a method introduced by Goodlett *et al*. in 1971[85] and further developed later on[86] (**Appendix I.III**, p 51). Some other methods exist to calculate the DS like sulphur analysis for tosylation[87], elemental analysis[83], HPLC after complete depolymerisation[88], from the weight loss in thermogravimetric analysis (TGA) after a functionalisation with an isocyanate as its elimination causes a step in the TGA curve[89] or fluorescence if the substituents are fluorescence active[90].

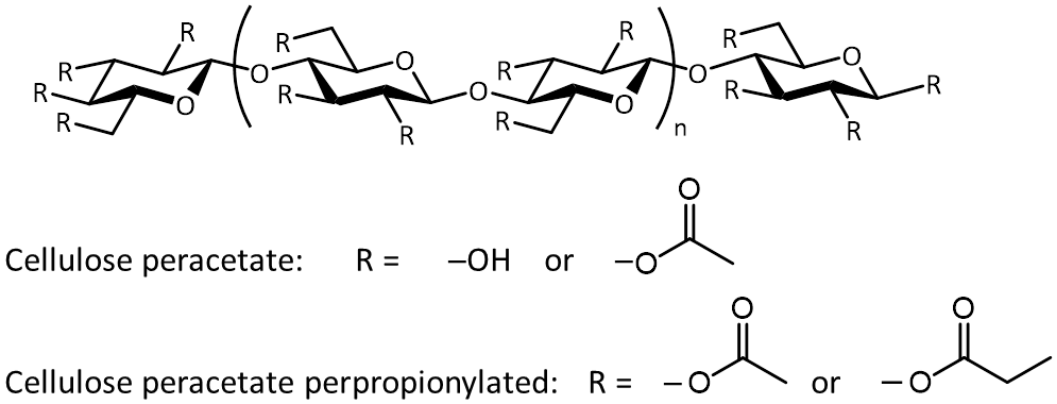

Figure I-13. Representation of cellulose peracetate and cellulose peracetate perpropionylated

The solubility in a targeted solvent depends on the kind of functionalisation and on the substitution degree. For example, cellulose triacetate is soluble in chloroform but cellulose acetate with a DS between 0.6 and 0.9 is soluble in water[82].

Other characterisation methods can be applied on functionalised cellulose compared to the natural one like size exclusion chromatography (SEC) in tetrahydrofuran (THF) for cellulose tricarbanilate[91] or NMR analysis in $CDCl_3$ of cellulose acetate[92]. **Figure I-14** represents some examples of functionalisation.

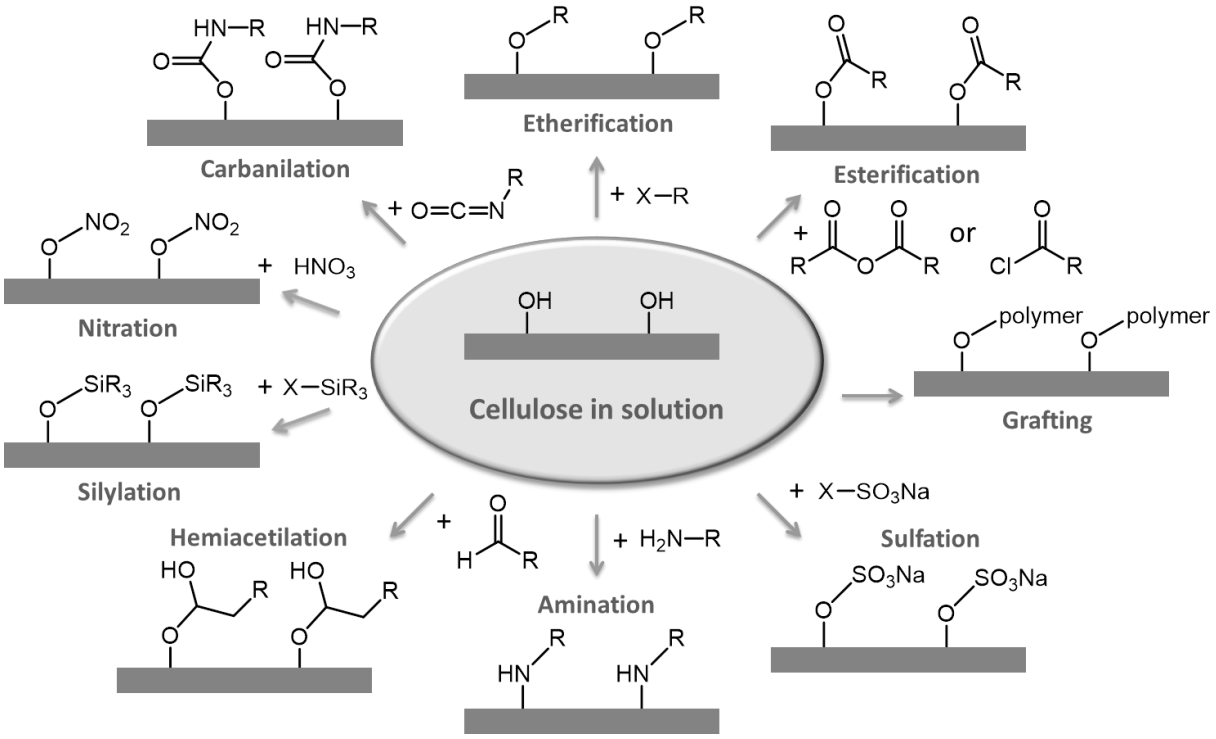

Figure I-14. Examples of cellulose functionalisation (adapted from Mecerreyes and coll.[93]) with examples of reactants (X is any halogen and for grafting many methods exist)

Functionalisation also tunes the material properties. For example, cellulose acetate that is used in paper industry and textiles but also in pharmaceuticals, plastics and coatings[94]. Cellulose diacetate is a component of cigarette filters. Celluloid, a material considered as the first thermoplastic[95], was created by Parkesine in 1856 as an ivory replacement and is composed of cellulose nitrate and camphor. Because of a high flammability, this material has been gradually replaced since then. Functionalised cellulose are produced industrially. Cellulose acetate represented 900 000 tons per year in 2001 and cellulose xanthate (**Figure I-10**, p 24) that composes cellophane or the viscose fabric, was produced at 3 200 000 tons per year[82].

I. 1. D) ii) Molar mass determination

Over the years, several ways of measuring the molar mass of cellulose were developed as it is critical information for its characterisation.

By viscosity

As seen previously in §I. 1. C) i) (p 23), the molar mass can be determined by measuring the viscosity of a solution of cellulose in Cuen[96], thanks to the Kuhn–Mark–Houwink relations[40] (**Equation I-1**).

$$[\eta] = K\, {M_w}^{a}$$ **Equation I-1**

*With $[\eta]$: the intrinsic viscosity measured based on the flowing time of a cellulose solution in Cuen in a capillary viscometer at 25°C[96] and K and a the Mark–Houwink parameters that depends on the solvent and on the temperature (**Table I-4**).*

Other solvents can also be used like *N*-methylmorpholine-*N*-oxide (NMMO), DMAc/LiCl or NaOH/urea (**Table I-4**).

Table I-4. Some examples of Mark–Houwink parameters for cellulose in solution

Solvent	Temperature	Molar mass range (kg.mol^{-1})	K	a	Reference
Cuen	25°C	50 – 1360	6.531 x 10^{-2}	0.735	Ref [40]
NMMO·H_2O	80°C	50 – 1360	3.428 x 10^{-2}	0.735	Ref [40]
DMAc + 0.5% LiCl	80°C	27 – 180 42 – 330	7.9 x 10^{-6} 1.0 x 10^{-4}	1.0 0.7	Ref [97]
DMAc + 9% LiCl	30°C	125 – 700	1.278 x 10^{-4}	1.19	Ref [59]
6 wt% NaOH + 4 wt% urea	25°C	32 – 129	2.45 x 10^{-2}	0.815	Ref [98]

By Size Exclusion Chromatography (SEC)

Cellulose tricarbanilate can be analysed by SEC in THF[91,99]. The main drawbacks of this method are the lack of cellulose tricarbanilate standards for the calibration and the necessity to accurately measure the DS, which influences the molar mass.

The functionalisation step could be avoided by adapting the solvent of the SEC to cellulose. For example, Spiess *et al.*[100] characterised their products directly by a SEC in dimethylformamide (DMF) containing 10% v/v of [Emim]Ac. The celluloses employed had an average molar mass from 28 to 109 kg.mol^{-1}. Ohno and coll. even developed a High Performance "Ionic Liquid" Chromatography (HPILC)[101] with 1-ethyl-3-methylimidazolium methylphosphonate as the eluent. The system was thermostated so the ionic liquid viscosity allowed a constant flow. The flow rate had to be really slow (0.01 mL.min^{-1}) to stay below the operating pressure. Pullulan standards with a molar mass from 112 to 5.9 kg.mol^{-1} were used to calibrate the apparatus.

By Light Scattering

Light scattering allows determining the cellulose molar mass but a solubilisation step is necessary. This method has many limitations and is not much employed.

The relationship between the Rayleigh factor R_θ and the molar mass M_w is represented in **Equation I-2**[59]. This equation validity domain is with a low angle photometer used for quasi-elastic light scattering measurement, at a small forward scattering angle and low sample concentration.

$$\frac{Kc}{R_\theta} = \frac{1}{M_w} + 2A_2c \qquad \textbf{Equation I-2}$$

*With c the sample concentration in g.mL^{-1}, A_2 the second viral coefficient and K the polymer optical constant (**Equation I-3**).*

$$K = \frac{2\pi^2 n^2}{\lambda^4 N_A}\left(\frac{dn}{dc}\right)^2(1 + cos^2\theta) \qquad \textbf{Equation I-3}$$

With n the refractive index of the solution, λ the incident beam wavelength, N_A the Avogadro number, $\frac{dn}{dc}$ the specific refractive index increment that can be found in the literature and θ the angle of the scattered light collection.

Then $\frac{Kc}{R_\theta}$ is plotted depending on the concentration of the sample and the average molar mass is calculated from the intercept and A_2 from the slope[59]. This method does not give any indication over the dispersity of the sample.

By calculation of the reducing end concentration

Another method to determine the average DP is to calculate the ratio between the glycosyl monomer concentration and the reducing end concentration[102].

The glycosyl monomer concentration can be calculated by the phenol-sulphuric acid method[103] and the reducing end concentration via the 2,2'-bicinchoninate method[104]. This method only gives an average of the molar mass with no indication of the initial dispersity.

I. 2. Cellulose oligomers

Cellulose oligomers (**Appendix I.IV**, p 52) are cellulose chains with a low DP that grant them the property of being water-soluble (**Figure I-15**). This property makes them easier to process and characterise compared to native cellulose. They serve as cellulose models[105,106] as they conserve their inherent structure unlike functionalised cellulose. The commercial cellobiose does not have the same properties as cellulose because its reactivity is drastically influenced by the reducing end group, this is why a higher DP is needed.

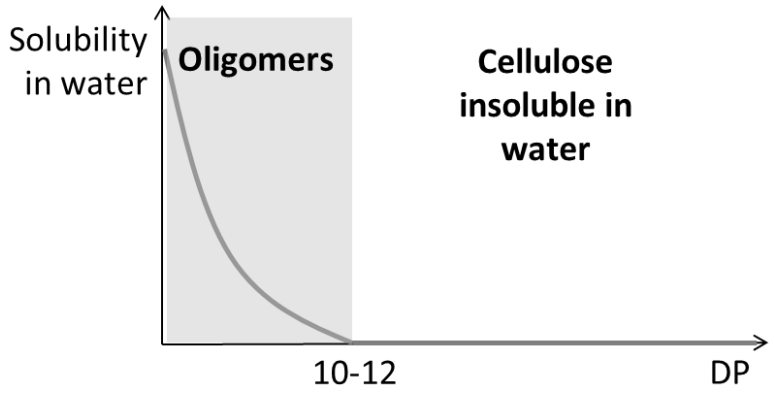

Figure I-15. Schematic representation of the water solubility depending on cellulose DP

They have other applications like substrate for the measurement of cellulase activity[107]. Besides, as they are not digested by the human organism that does not possess the necessary enzymes[108,109], they thus could be used for their prebiotic status[110] as dietary fiber, sweetener or weight controlling agent[111]. Cellulose oligomers were patented for their help in the prevention or improvement of lifestyle-related diseases in the field of food and medicines as they decrease neutral fat and total cholesterol concentrations in the liver by oral intake[112]. All these specific applications explain the growing interest they arise, limited by their difficult production in large scale (**Figure I-16**). Notwithstanding, BASF deposited a patent on their production by enzymatic depolymerisation very recently[113].

Several pathways were developed to obtain these oligomers over the years. The four main ones are by chemical synthesis, enzymatic synthesis, enzymatic depolymerisation and acidic depolymerisation.

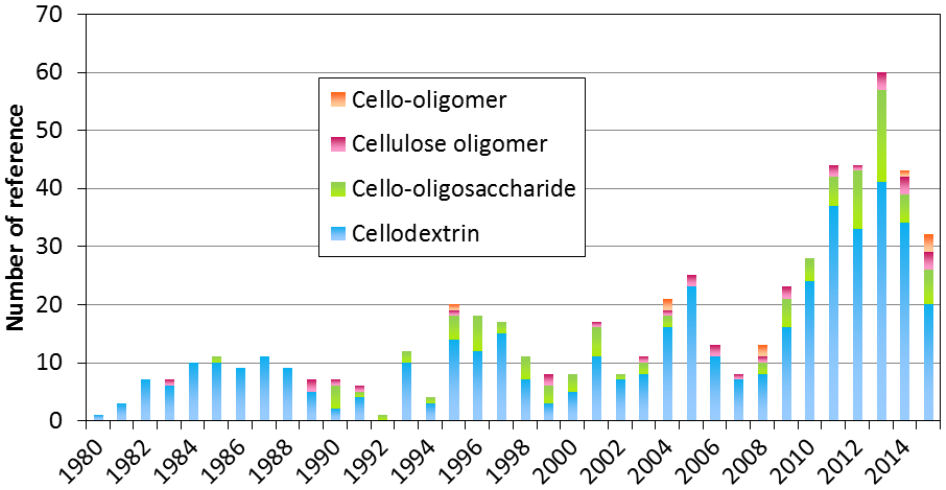

Figure I-16. Number of references per year depending on the appellation from 1980 to mid-August 2015 (references containing the appellation as entered, data from SciFinder)

I. 2. A) Chemical synthesis

The pathway that chemists would consider first is chemical synthesis. The first team to succeed such a challenge was Nakastubo et al. in 1996[114]. It was done by cationic ring opening polymerisation of 3-O-benzyl-6-O-pivaloyl-α-glucopyranose (**Figure I-17**). The starting monomer is synthesised from commercially available 1,2:5,6-di-O-isopropylidene-α-D-glucopyranose via an eight step reaction pathway with a final yield of around 60%[115]. The specific positions of the protecting groups allow a great stereoselectivity[116–118]. The polymerisation occurred in dichloromethane with triphenylcarbenium tetrafluoroborate at 20°C and after 2h a DP around 20 was obtained with a yield of 62%[114]. The benzylated cellulose is soluble in THF and was analysed by SEC with a polystyrene calibration. If the initial monomer concentration is divided by two, a DP of around 10 with a yield of 93% is obtained after a 14h polymerisation at 20°C. After that, the protecting groups have to be removed to obtain un-functionalised cellulose.

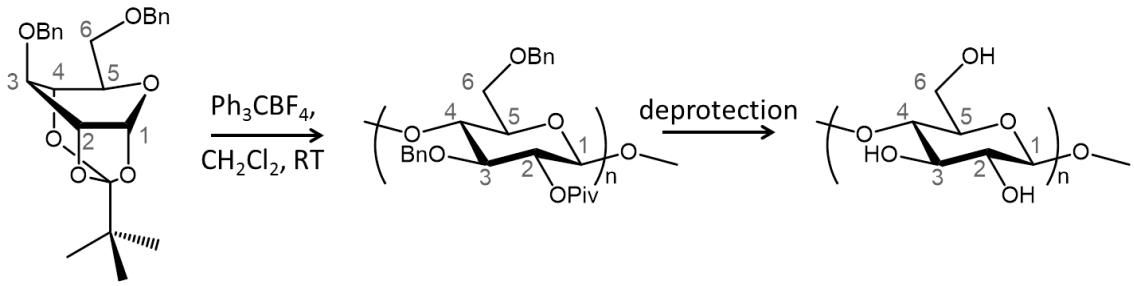

Figure I-17. Cationic ring opening polymerisation of 3-*O*-benzyl-6-*O*-pivaloyl-α-glucopyranose (Bn = benzyl $–C_6H_5$, Piv = pivaloyl $–C(O)C(CH_3)_3$)

Smaller cellulose oligomers can also be obtained by long chemical synthesis involving the use of a glycosyl acceptor and a glycosyl donor[119,120]. The glycosyl acceptor bears a good leaving group, as tosyls[121,122] or halogens[123], at the position where the bound is to be formed. For the glycosyl donor, the relative reactivity of the positions is of great importance: if a more reactive position than the one where the bound is to be formed is available, it has to be protected. The protection is usually done either by functionalisation with acetate or benzyl groups, or by the use of protecting agents like boronic acids[123,124]. But in the end, the higher the DP, the more numerous the chemical steps. For example, cellooctaose could be obtained either starting from 3-O-benzyl-6-O-pivaloyl-α-glucopyranose (structure represented in **Figure I-17**) and cellobiose after more than 15 steps[125] or starting from a functionalised glucose after 11 steps[126].

I. 2. B) Enzymatic synthesis

To mimic the nature, enzymatic synthesis can also be considered[127–129]. The enzymes used are hydrolases, phosphorylases, glycosyltransferases or sucrase-type[28]. Hydrolases are the enzymes that catalyse the *in vivo* depolymerisation of their corresponding substrate. *In vitro* however, they catalyse a glycosylation to produce saccharidic chains (**Figure I-18a**). Phosphorylase breaks glycosylic linkage in the presence of inorganic phosphate to produce monosaccharidic phosphate. But as the bond energy of the produced compound is comparable with a glycosylic bond, the reaction is reversible (**Figure I-18b**). Leloir glycosyltransferase are the enzymes that catalyse the synthesis of saccharidic chains *in vivo* (**Figure I-18c**). Sucrase-type, which is specific to glucans and fructans (**Figure I-18d** representing the case of glucans), break sucrose to produce either glucan chains and fructose or fructan chains and glucose.

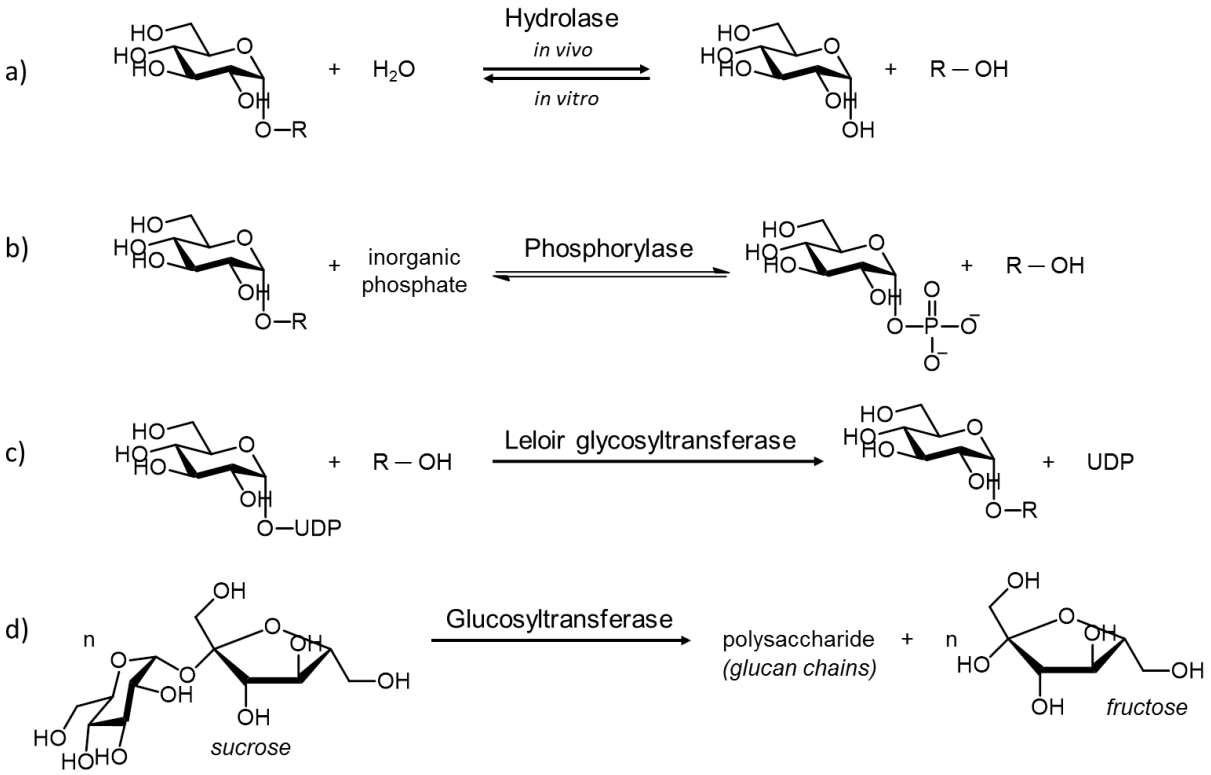

Figure I-18. Typical enzymes involved in the synthesis of polysaccharide (adapted from Kadokawa[28])

An example of *in vitro* enzymatic synthesis of cellulose catalysed by hydrolases is the work of Kobayashi and his team in the 80's. β-cellobiosyl fluoride (**Figure I-19**) was used as substrate in a mixed solvent of acetonitrile and acetate buffer (pH 5) (5/1)[130,131] [for the mechanism, **Appendix I.V**, p 53]. This substrate is well recognised by the enzymes and is obtained from 1,2,4,6-tetra-*O*-acetyl-3-*O*-(2,3,4,6-tetra-*O*-acetyl-β-D-glucopyranosyl)-α-D-glycopyranose (itself obtained from controlled acid-catalysed acetolysis of Actigum CS6 containing scleroglucan) by a three steps synthesis with a total yield of 71%[132]. The polymerisation is stopped by adding methanol so the anomeric position of the cellulose obtained is methylated[133,134]. A polymerisation degree of around 22 is reached but by changing the reaction conditions oligomers with a DP of 8 can be produced predominantly[130].

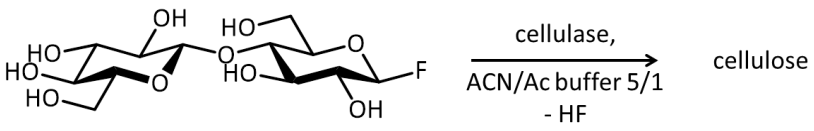

Figure I-19. β-D-cellobiosyl fluoride enzymatic polymerisation

Another example[135] employed a mutant glycosynthase on tetrahydropyranyl-cellobiosyl fluoride and the β-methyl form of glucose, for example, to obtain methyl β-cellotriose. Other β-methylated substrate could also be used. The yields obtained were

78% for the production of methyl β-cellotriose, 90% for methyl β-cellotetraose, 83% for methyl β-cellopentaose and 60% for methyl β-cellohexaose.

Reactions catalysed by phosphorylase allows to reach a wide range of carbohydrate structures[136]. Svensson and coll.[137] used α-D-glucose 1-phosphate as donor with glucose and cellobiose as acceptor and succeeded to produce cellulose oligomers with DP from 3 to 9 with a 48% yield. Their respective ratio was dependent on the reaction time. In a more recent work[138], the distribution of the cellulose oligomers produced was found to be dependent on the cellobiose concentration. A cellobiose concentration of 10, 5, 1 or 0.2 mM gave an average DP of 7, 9, 11 or 13, respectively, with a low dispersity. The α-D-glucose 1-phosphate concentration was 20 times higher than the cellobiose concentration and no cellobiose was found in the oligomers obtained. The reaction was thus complete.

Another type of reaction studied was the transglycosylation of cellobiose or cellotriose by cellulolytic enzyme *endo*-acting endoglucanase I[139]. The reaction took place in acetate buffer (pH 4.0) at 50°C for 1 hour. The oligomer formation is observed by an increase of the turbidity which decreases if the reaction lasts more than 1h. Cellobiose gave a DP of up to 7 while cellotriose gave oligomers with DP from 4 to 16 with a 30% yield.

I. 2. C) Enzymatic depolymerisation

The enzymatic depolymerisation of extracted cellulose[140,141] can also be a good alternative to obtain cellulose oligomers. However, in the literature, enzymatic depolymerisation was mainly studied for the production of bio-ethanol from glucose without any by-products that would decrease the fermentation yield[142–152].

I. 2. C) i) Mechanism

The enzymatic depolymerisation mechanism involves three different kinds of cellulases (**Figure I-20**)[141,153]: the endoglucanases[154] (EC 3.2.1.4) are the only one to attack high molecular weight cellulose, they break β-bond randomly and thus increase the concentration of reducing end in the medium. The exoglucanases (EC 3.2.1.91), also called cellobiohydrolases[155], break shorter cellulose chain (DP 30-60[153]) from both reducing and non-reducing ends releasing cellobiose which is then broken down into glucose by β-glucosidases[156]. The cellulase system produced by the most common cellulose fungi producers, *Trichoderma reesei*, is made up of two exoglucanases Cel7A (CBH I) and Cel6A (CBH II), and at least five endoglucanases Cel7B (EG I), Cel5A (EG II), Cel12A (EG III), Cel61A (EG IV), and Cel45A (EG V)[157] (**Appendix I.VI**, p 54). Cel7A, Cel7B, Cel5A and Cel12A hydrolyse cellulose according to a conformation retaining mechanism whereas Cel6A and

Cel45A produce a substrate this an inversion of its conformation[158,159] [for the representation of the mechanisms, **Appendix I.VII**, p 56].

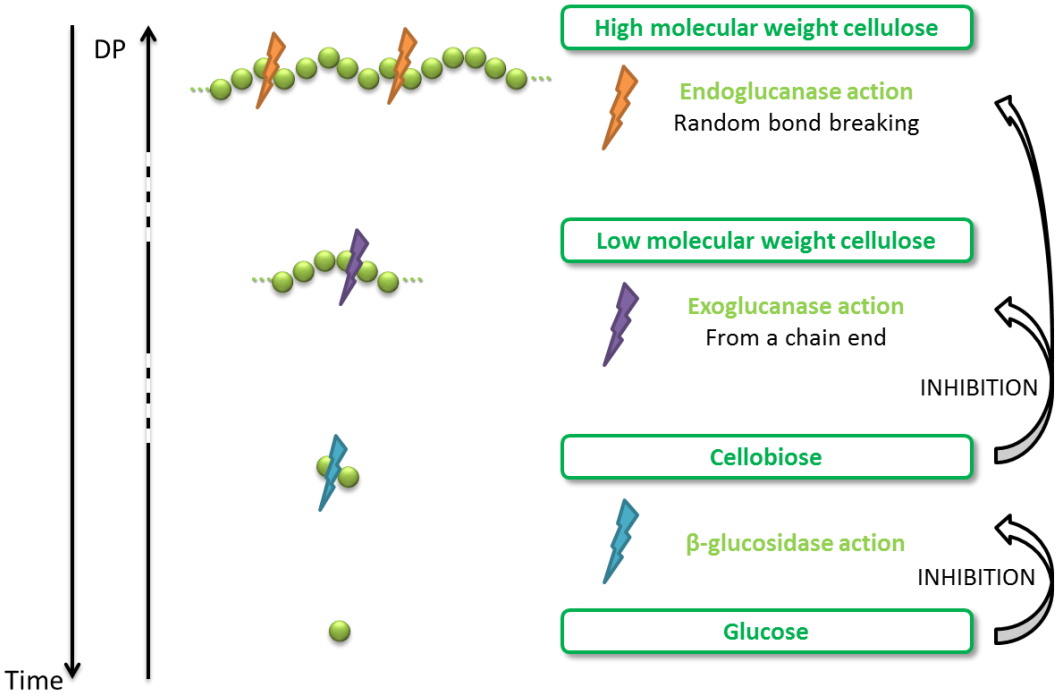

Figure I-20. Schematic process of the enzymatic hydrolysis of cellulose

Their actual structure was described by Davies and Henrissat in 1995[160]:

- Endoglucanases have a cleft structure (**Figure I-21a**) that favours the random binding
- Exoglucanases have a tunnel structure (**Figure I-21b**) which allows them to move progressively and release the hydrolysis product while staying bonded to the substrate
- β-glucosidases have a pocket structure (**Figure I-21c**) granting them a good recognition of the non-reducing end

On **Figure I-21**, the red part corresponds to the catalytic centre which is composed of aspartic acid that donate the proton necessary to the hydrolysis (**Appendix I.VII**, p 56)[159].

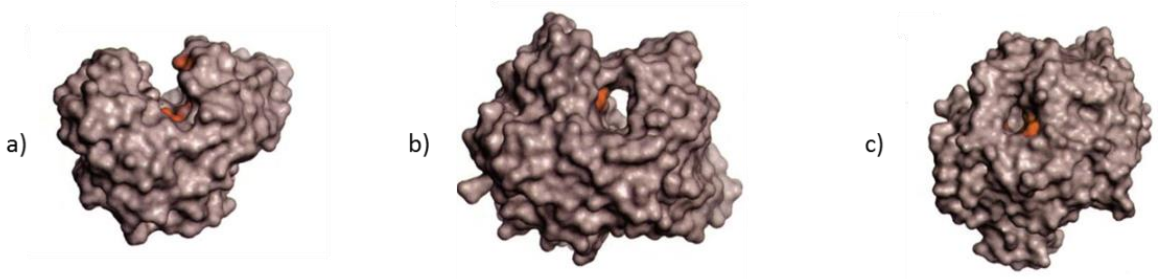

Figure I-21. Structure of a) endoglucanase, b) exoglucanase and c) β-glucosidase (adapted from Davies and Henrissat[160]); the red part is the catalytic centre

Lytic polysaccharide monooxygenases (LPMO) also have the propensity of hydrolysing cellulose by an oxidative mechanism. These enzymes degrade crystalline

substrate[161] as well as cellulose oligomers[162]. They can also be used in combination with other enzymes to increase the hydrolysis efficiency[163].

To increase the enzyme accessibility to the cellulose chains, there is usually a pre-treatment before the actual hydrolysis[164,165]. One of the most studied nowadays is the use of ionic liquids[166–170]. They were introduced previously in §I. 1. C) vii) (p 26) for the cellulose solubility but it was found that after introducing an anti-solvent, the cellulose precipitates with a cellulose II morphology and thus a decreased crystallinity[171]. However, some traces of ionic liquids stay bound to the cellulose and have an impact on the activity of the enzymes. For example, [Bmim]Cl was found to totally deactivate the enzymes[172] because of the harmful effect of the chloride anion. On the other hand, ionic liquids could be specially designed to simultaneously solubilise cellulose and be compatible with the enzymes. Zhao *et al*.[77] tested many ionic liquids, some of them especially designed for the purpose, and found out that the acetate anion was the most suited for such applications and that oxygen-containing cations and low cation bulkiness were beneficial to the cellulose solubilisation. Choline acetate is enzyme-compatible[79]. Tris-(2-hydroxyethyl)-methylammonium methylsulfate (HEMA) also presented great result as endoglucanase had the same activity after 2 h in citrate buffer at 45°C or in HEMA at 75°C[173].

The other kind of pre-treatments are acidic (but it produces by-product that inhibit further fermentation)[174], alkaline[175–177], biological[178], mechanical[179,180], by irradiation[181], by ammonia expansion[182] or by chemical modification[183]. They are currently less studied but all serve to decrease the cellulose crystallinity.

I. 2. C) ii) Cellulose oligomers

The production of cellulose oligomers by enzymatic depolymerisation induces many challenges as they are produced in the early stage of the hydrolysis[184] and are also hydrolysed by the enzymes[153,185]. The exoglucanase CBH II was found to degrade the oligomers with different rate depending on their size as following[186]:

Cellohexaose > cellotetraose > cellopentaose > cellotriose

After the enzymatic depolymerisation, the main product is cellobiose as highlighted in **Table I-5**. Cellobiose is an enzyme inhibitor[157,187] (**Figure I-20**, p 37) and the inhibition extant depends on the enzyme concentration, the cellulose surface area accessible to the enzyme, the substrate concentration, and β-glucosidase activity (as it is the only enzyme to reduce the cellobiose concentration)[188]. Nevertheless, 100% of conversion can still be reached depending, mainly, on the enzymes, substrate and pre-treatment[189].

Table I-5. Molar percentages of products formed by the action of CBH I on cellulose oligomers of different polymerisation degree[190] (in bold is the higher percentage per row)

Substrate DP	Products (%)		
	DP 1	DP 2	DP 3
4	17	**68**	15
5	26	**56**	17
6	26	**47**	25
7	19	**71**	8
8	20	**64**	17

Consequently, the hydrolysis has to be stopped before the oligomers of interest are hydrolysed. The most effective pathway to do so is probably by a multi-stage hydrolysis where the substrate is removed from the reaction media, washed, and hydrolysed again with fresh buffer and enzymes (**Figure I-22**). The buffer retrieved contains the water-soluble fraction. This optimises the rate and yield of enzymatic hydrolysis reactions as the substrate is regularly washed from all the inactive enzymes irreversibly adsorbed that prevent the intervention of new active ones[191]. For the washing, the substrate was flushed repeatedly with sodium acetate buffer and deionized water, and freeze-dried. Yong and coll.[184] compared a two stages and three stages hydrolysis with several stage durations using an enzyme cocktail without β-glucosidases. The higher cellulose oligomer yield (52%) was obtained after a three stage hydrolysis of 6h/6h/12h. The DP distribution was not studied. For comparison, in the same conditions, a single stage hydrolysis of 24h gave a 25% yield.

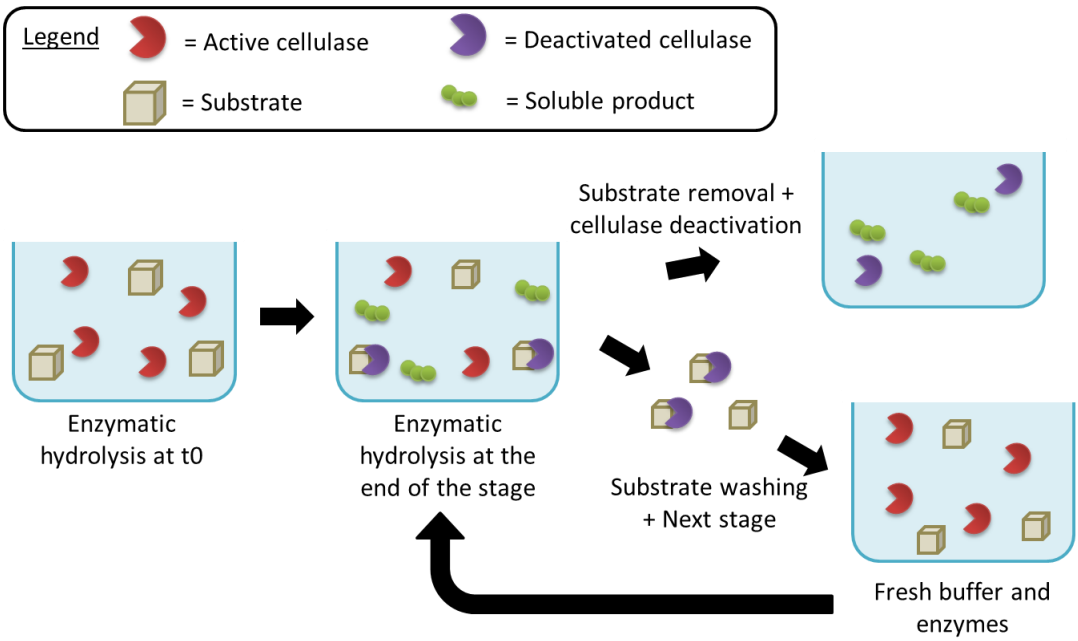

Figure I-22. Principle of a multi-stage enzymatic hydrolysis

Moreover, when the cellulose is methylated uniformly on the 6-position all along the backbone, only endoglucanase attacks it and the main product is cellulose oligomers with an average DP of around 8[192]. No more than 10% of the initial product was hydrolysed even after 96h of reaction; the reason could be the decrease of the substrate DP as the enzymes predominantly acting on such substrate are the endoglucanases. When the 2- and 3-positions of a cellulose chain are methylated, the β-1,4 bonds are covered by the methyl groups and were not reached by the enzymes unless an unsubstituted glucose unit was nearby. The effect of the defunctionalisation was not studied.

I. 2. D) Acidic depolymerisation

Compared to enzymatic hydrolysis, acidic depolymerisation requires harsher conditions thus producing unwanted by-products but the kinetic is faster and has a higher yield in producing cellulose oligomers.

Acidic hydrolysis of cellulose is usually used to produce cellulose nanocrystals[193] by breaking only the amorphous zones. Nevertheless, the hydrolysis pushed further also degrade the crystalline parts and decrease the average molar mass [see **Appendix I.VIII** for the mechanism, p 58]. The main drawback is the formation of furanic by-product due to the acidic dehydration of glucose (**Appendix I.IX**, p 58).

Several types of acids were used to produce water soluble cellulose oligomers as listed on **Table I-6**. An important factor influencing the DP obtained is the precipitation solvent (Entry 1a to 1d). The acid influences greatly the yield, the best one was obtained with phosphoric acid (Entry 1 and 2) or hydrochloric acid but at high temperature (Entry 9i). A mixture of 80/20 HCl/H_2SO_4 was tested at room temperature (Entry 8) and seemed to increase the yield compared to the corresponding pure acids (Entry 3 to 7). HF/SbF_5 and trifluoroacetic acid also give good yields (Entry 9 and 10) but their cost and corrosive aspect make them second-rate candidates.

Table I-6. Parameters and result of several acidic hydrolysis of cellulose to produce water soluble oligomers (the yields in bold are above 65%)

Entry	Cellulose	Acid	Conditions	Precipitation in	DP (PDI)	Yield	Reference
1a	Avicel	H_3PO_4 at 85%	20 h at 55°C	Ethanol	5.7 (1.3)	47%	Ref [194]
1b				Isopropanol	14.6 (1.9)	56%	
1c				Acetone	19.1 (4.0)	53%	
1d				THF	14.6 (2.1)	**68%**	
2	Fibrous cellulose	H_3PO_4 at 85%	6 weeks at RT	Water	8 to 15 (2.0)	52%	Ref [195]
3	Whatman cellulose	Fuming HCl	Time to warm from 0°C to RT	Water	3 to 7	≈5%	Ref [196]
4	Cellulose APX	Fuming HCl	2 to 3 h at 25°C	Isopropanol	1 to 12	5%	Ref [197]
5	Whatman cellulose	Fuming HCl	2 h at 25°C	Water	1 to 7	?	Ref [198]
6	Fibrous cellulose	Concentrated HCl	15-20 min at -30°C + 2-3 h at 25°C	Isopropanol	1 to 6	3%	Ref [199]
7	Avicel	H_2SO_4 at 80% then diluted	7 min at 4°C + 14 min at 70°C (after dilution)	Water	1 to 8	1.8%	Ref [200]
8	Avicel	80% HCl at 37% 20% H_2SO_4 at 98%	4 to 5.5 h at RT	Acetone	1 to 8	45%	Ref [201]
9a	Avicel	HF	50 min at 0°C	-	1 to 13	2%	Ref [202]
9b		SbF_5	50 min at 20°C	-		2%	
9c		HF / SbF_5 (1.9%)	50 min at 20°C	-		**89%**	
9d		HF / SbF_5 (3.8%)	50 min at 20°C	-		**75%**	
9e		HF / SbF_5 (8.4%)	50 min at 20°C	-		48%	
9f		HF / SbF_5 (13.6%)	50 min at 20°C	-		57%	
9g		HF / SbF_5 (21.6%)	50 min at 20°C	-		**78%**	
9h		HCl	50 min at 20°C	-		4%	
9i		HCl	50 min at 130°C	-		**68%**	
9j		H_3PO_4	50 min at 20°C	-		4%	
9k		CF_3SO_3H	50 min at 20°C	-		3%	
9l		CF_3SO_3H / SbF_5	50 min at 20°C	-		none	
10	Whatman cellulose	Diluted $C_2HF_3O_2$	24 h at 72°C	Water	1 to 6	59%	Ref [203]

Some teams were also interested in keeping the water insoluble part after the acidic hydrolysis as the polymerisation degree was also decreased. Dilute HCl, H_3PO_4 at room temperature or H_3PO_4 at 8°C produced hydrolysed cellulose with an average DP, determined by SEC in DMAc/LiCl, of around 50, 35 and 70 respectively[204]. Schütz *et al*.[205] used Amberlyst 15, an acidic resin, in [Bmim]Cl so the purification step was really simplified. They obtained hydrolysed cellulose with an average DP of around 30 with a yield of 81%. The DP was determined by SEC in THF after tricarbanilation with a polystyrene calibration. More recently, betaïne hydrochloride in tributylmethylammonium chloride produced cellulose with a polymerisation degree of 65 ± 5 with a 75% yield after 10 minutes or 40 ± 5 with a 40% yield after 20 minutes at 150°C[206]. The DP was determined by viscosity in a Cuen solution. Both ionic liquid and acid could be almost entirely recovered after the hydrolysis.

I. 2. E) **Other pathways**

I. 2. E) i) Pivaloylysis

Pivaloylysis is a degradation of cellulose triacetate to produce acetylated cellulose oligomers[207,208]. The protocol involves pivalic anhydride and boron trifluoride diethyl etherate in dichloromethane. The oligomers obtained were functionalised at both extremities with a pivalic group. They were then separated by a chromatographic method and the yields obtained are listed in **Table I-7**.

Table I-7. Yield of the pivaloylysis reaction depending on the reaction time (reaction at 40°C)[207]

DP	1	2	3	4	5	6	7	8
Reaction time	> 200h	200h	95h	60h	45h	36h	24h	24h
Yield	100%	44%	23%	25%	17%	7%	3.7%	3.7%

I. 2. E) ii) Mechanical depolymerisation

Cellulose, impregnated with sulphuric acid, was milled in a planetary ball mill at 300 rpm for 15 minutes which produced cellulose oligomers with an average DP of around 7[209]. However, ramifications were formed during the treatment and changed the cellulose properties and particularly its solubility[209,210]. The ramification increased the water-solubility for oligomers of DP > 10.

I. 2. E) iii) Pyrolysis

The pyrolysis of cellulose at high temperature (400 to 600°C) leads to the competition of two degradation mechanisms: the “unzipping” mode[211] and the random chain cleavage.

The latter occurs at short reaction time and induces the production of most of the oligomers[212]. Oligomers from DP 2 to 7 were obtained with a yield of up to 20% depending on the reaction parameters[212] while oligomers with DP from 1 to 10 were also produced at lower temperature 100-350°C for 30 minutes but with a lower yield (3%)[213]. No change of structure was mentioned.

I. 2. E) iv) Hot compressed water (HCW)/Supercritical water

Hot compressed water acts as solvent as well as reactant. When the hydrolysis occurs at 280°C and 20 MPa, oligomers with polymerisation degrees from 1 to 25 are recovered but only oligomers with a DP from 1 to 5 stay soluble in water even at ambient conditions, the oligomers with higher DP precipitate[214]. Another study presented 40% yield of cellulose oligomers with a DP from 1 to 5 after a treatment at 380°C for 16 seconds[215]. More recently, cellulose oligomers with a DP from 2 to 9 were obtained with a yield of 42% after a treatment with supercritical water at 380°C and 250 bar for 0.4 seconds[216].

I. 2. E) i) Plasma irradiation

A partial depolymerisation was also observed after non-thermal atmospheric plasma irradiation due to the formation of hydroxyl radicals[217]. The DP of α-cellulose was decreased from 1000 to 160 after a 3 hours irradiation. The procedure also formed 22 wt% of glucose so it is possible that oligomers were also formed but in too low quantity to be observed.

I. 2. F) **Summary**

All of the approaches to produce cellulose oligomers mentioned in §I. 2. are summarised in **Figure I-23**. From all these methods, the ones that give the higher yield in water soluble cellulose oligomers are acidic hydrolysis, enzymatic depolymerisation, supercritical water treatment and enzymatic synthesis. The last two require either specific and expensive equipment or substrates with time-consuming preparations.

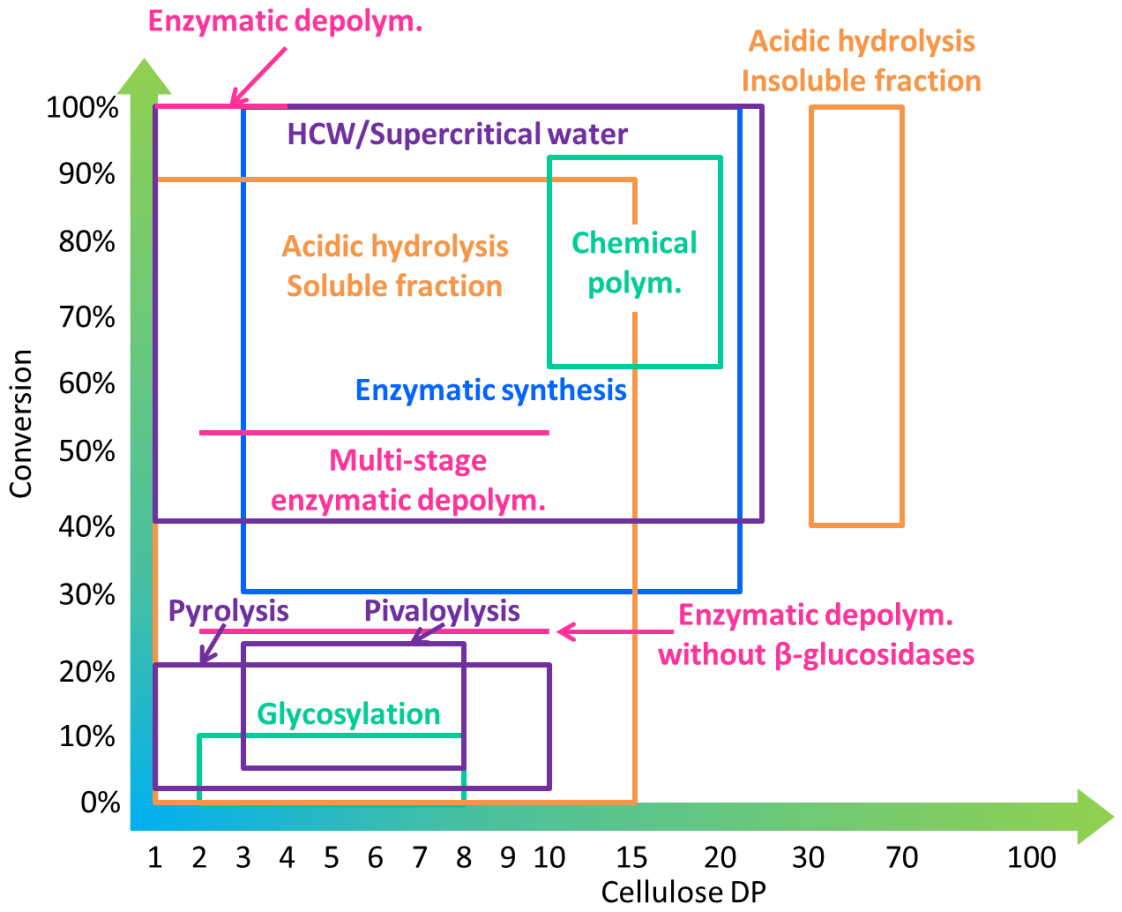

Figure I-23. Summary of the cellulose oligomer production methods seen in §I. 2. depending on the cellulose conversion and DP obtained

I. 3. Cellulose oligomers separation

I. 3. A) Currently used separation

After the cellulose oligomers are produced, their separation is sometimes necessary for specific applications such as biological ones. The usual method employed is chromatography. After acidic hydrolysis, a column based on activated charcoal and celite using a gradient of water/ethanol as eluent was able to produce oligomers ranging from 700 mg of cellotriose to 200 mg of celloheptaose from 10 g of native cellulose over five days[218]. More recently, after acidic hydrolysis with a mixture of HCl and H_2SO_4 (**Table I-6**, Entry 8, p 41), a two-column system based on Bio-Gel P-4 (fine polyacrylamide beads) and Bio-Rad AG 50W-X4 resin (cation exchange resin) had been used to obtain oligomer preparations at 240 mg/day for cellotriose, 330 mg/day for cellotetraose, 260 mg/day for cellopentaose, and 130 mg/day for cellohexaose, with purity >99% for DP from 3 to 5 and >95% for DP 6[201].

Cation exchange resins are really efficient to separate oligosaccharides. Because of the many hydroxyl groups present on their backbone, the oligomers are well adsorbed on

the column. The eluent then breaks these interactions and desorb them in order of decreasing molar mass. Even sugars of the same molecular weight (as glucose and mannose) are separated with this method as the separation also depends on ion exclusion, steric exclusion, electrostatic attraction or repulsion and Van der Walls forces among other[219]. The most commonly used column is based on calcium cation, Ca^{2+}, as it can be eluted with water alone[220] which prevents the use of co-solvent that could precipitate the oligomers of higher DP. Other examples are silver based column that provides an increased retention and resolution than the calcium ones[221] or diethylaminoethyl derivatives of Spheron® using borate buffer as the eluent[222].

Nevertheless, the chromatographic separation low yield explains the high prices of the cellulose oligomers seldom commercially available as highlighted in **Table I-8**.

Table I-8. Price of cellulose oligomers in €/mg depending on the supplier (data from the corresponding supplier website seen in May 2015)

Supplier	Elicityl (FR)	Megazyme (IR)	Dextra (UK)	Carbosynth (UK)	TCI
DP 3	6.10	2.63	7.97	3.74	10.00
DP 4	9.70	2.63	7.97	3.74	22.30
DP 5	14.50	2.67	6.18	11.52	10.06
DP 6	21.80	8.15	-	24.00	-
DP 7	42.60	-	-	37.44	-

Cellulose oligomers may also be separated according to their solubility in different solvent. For example, DP 5 and 6 are not soluble when the ratio of ethanol in an ethanol/water solution exceeds 80%[199]. This method was also represented in **Table I-6**, Entry 1a to 1d (p 41) as the precipitation solvent influences the range of cellulose DP that are obtained[194]. In another study[223], several successive solubilisations were applied to separate cellulose oligomers according to their sizes (**Table I-9**).

Table I-9. Solubility of cellulose oligomers according to their DP in several solvent (adapted from Claisse[223])

Solvent	Water	Methanol	Methanol/Ethyl acetate 50/50 v/v
DP 1-2	Soluble	Soluble	Soluble
DP 3-4	Soluble	Soluble	Insoluble
DP 5-9	Soluble	Insoluble	Insoluble
DP ≥ 10	Insoluble	Insoluble	Insoluble

I. 3. B) Looking for alternatives

The purpose of this project was to find alternative pathways to obtain low dispersed cellulose oligomers. Two procedures, detailed below, were considered: the "masking" method, based on enzymatic depolymerisation, and the "fishing" method, based on acidic hydrolysis.

I. 3. B) i) Masking method

The principle, represented in **Figure I-24**, was to "protect" parts of the cellulose from the attack of enzymes with a polymer containing boronic acid groups that act as interaction points (see Chapter II). The length between two interaction points would determine the length of the oligomers obtained. The polymer/oligosaccharide complex would then be extracted using an organic phase and finally the low dispersed cellulose oligomers would be recovered after breaking the complex with another aqueous phase.

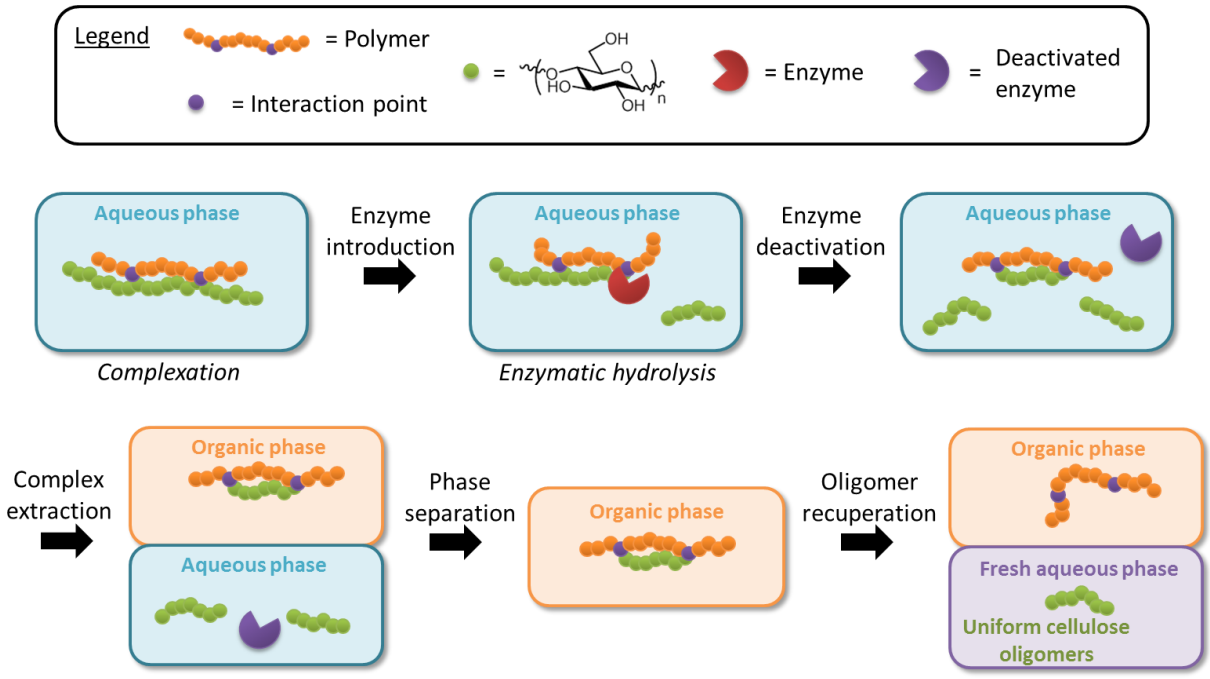

Figure I-24. Principle of the "masking" method

I. 3. B) ii) Fishing method

The "fishing" method principle is to use boronic acid containing polymers to selectively extract cellulose oligomer into an organic phase. First, they would be produced by acidic hydrolysis to obtain a mixture of different DP. Then, the extraction selectivity would result from the length of the polymer used and, more specifically, its ratio compared to the cellulose oligomer "caught". The longer the polymer, the longer the DP solubilised in the organic phase (**Figure I-25**). The process will be helped by a phase transfer catalyst.

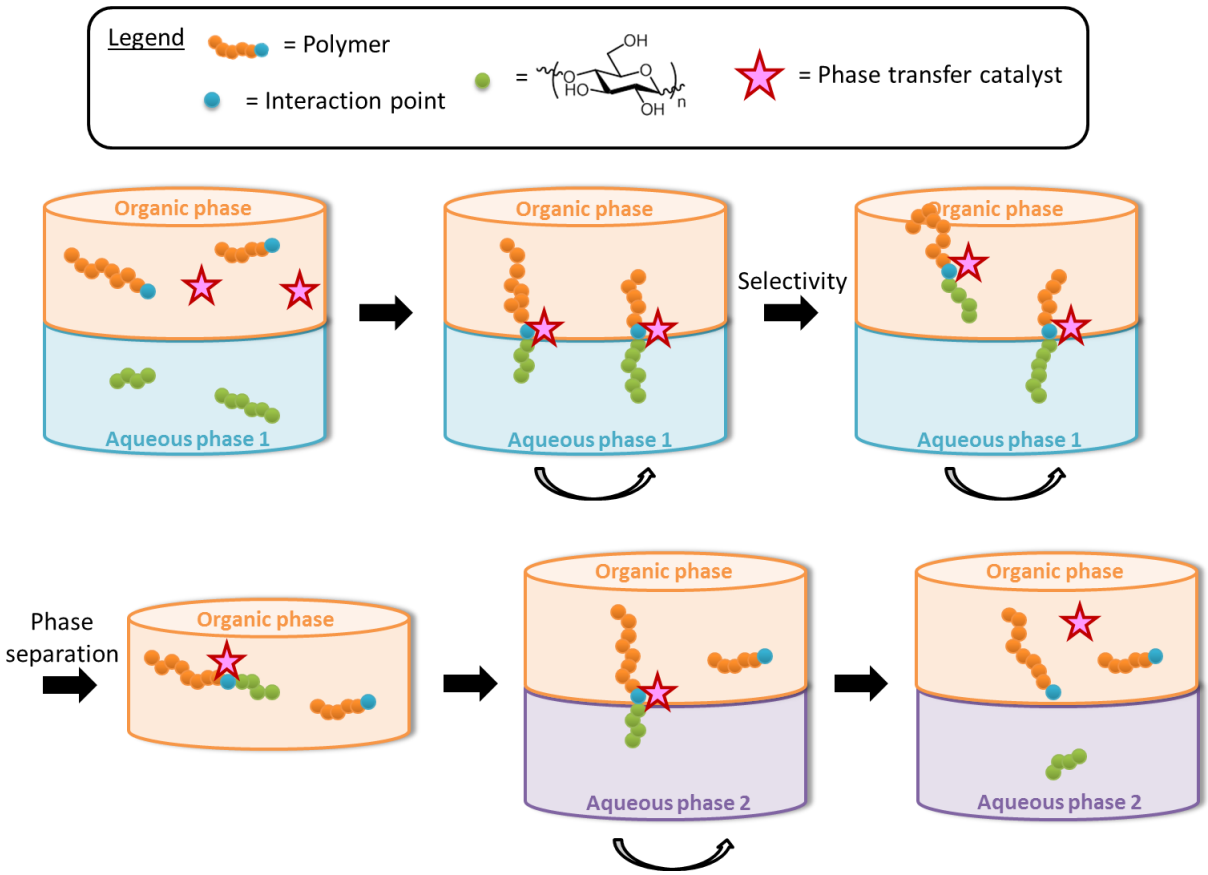

Figure I-25. Principle of the "fishing" method

Chapter conclusion

Cellulose is an abundant natural polymer with many valuable properties. Unfortunately, its poor solubility in common solvents reduces its application range and functionalisation alters its inherent structure and features.

Cellulose oligomers are really interesting products that have the structure of cellulose but are soluble in water. They can be produced by several pathways like chemical synthesis, enzymatic synthesis, enzymatic depolymerisation or acidic hydrolysis among other.

As the goal of this study was to produce uniform cellulose oligomers without using chromatography, two pathways were considered: the “masking” method based on enzymatic depolymerisation and the “fishing” method using acidic hydrolysis. Both methods employ the sugar/boronic acid interaction, the first one to control the cellulose oligomer length and the second one to selectively solubilise oligomers in an organic solvent.

A preliminary study on the interaction of boronic acid with sugars is thus necessary to determine the polymer structure the most suited for each method.

Appendix

Appendix I.I: Attributed ^{1}H NMR spectra of glucose in DMSO-d_6

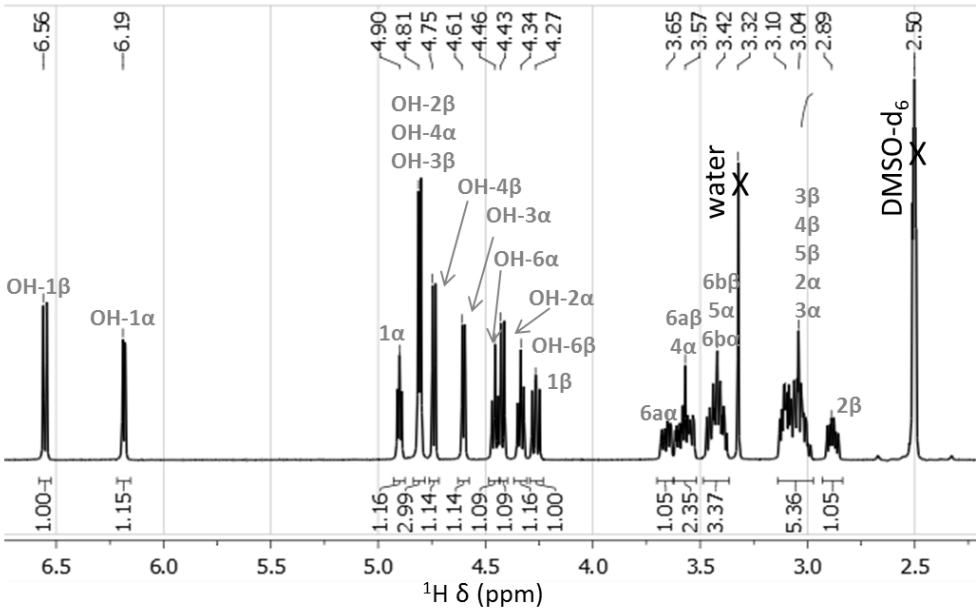

^{1}H δ (ppm)	Hydroxyl groups					Backbone protons						
Position	1	2	3	4	6	1	2	3	4	5	6a	6b
α-glucose 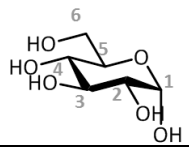	6.19	4.43	4.61	4.81	4.46	4.90	3.10 - 3.04	3.10 - 3.04	3.57	3.42	3.65	3.42
β-glucose 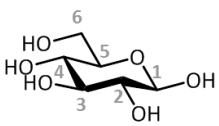	6.56	4.81	4.81	4.75	4.34	4.27	2.89	3.10 - 3.04	3.10 - 3.04	3.10 - 3.04	3.57	3.42

Appendix I.II: Structure of cellulose polymorphs[159]

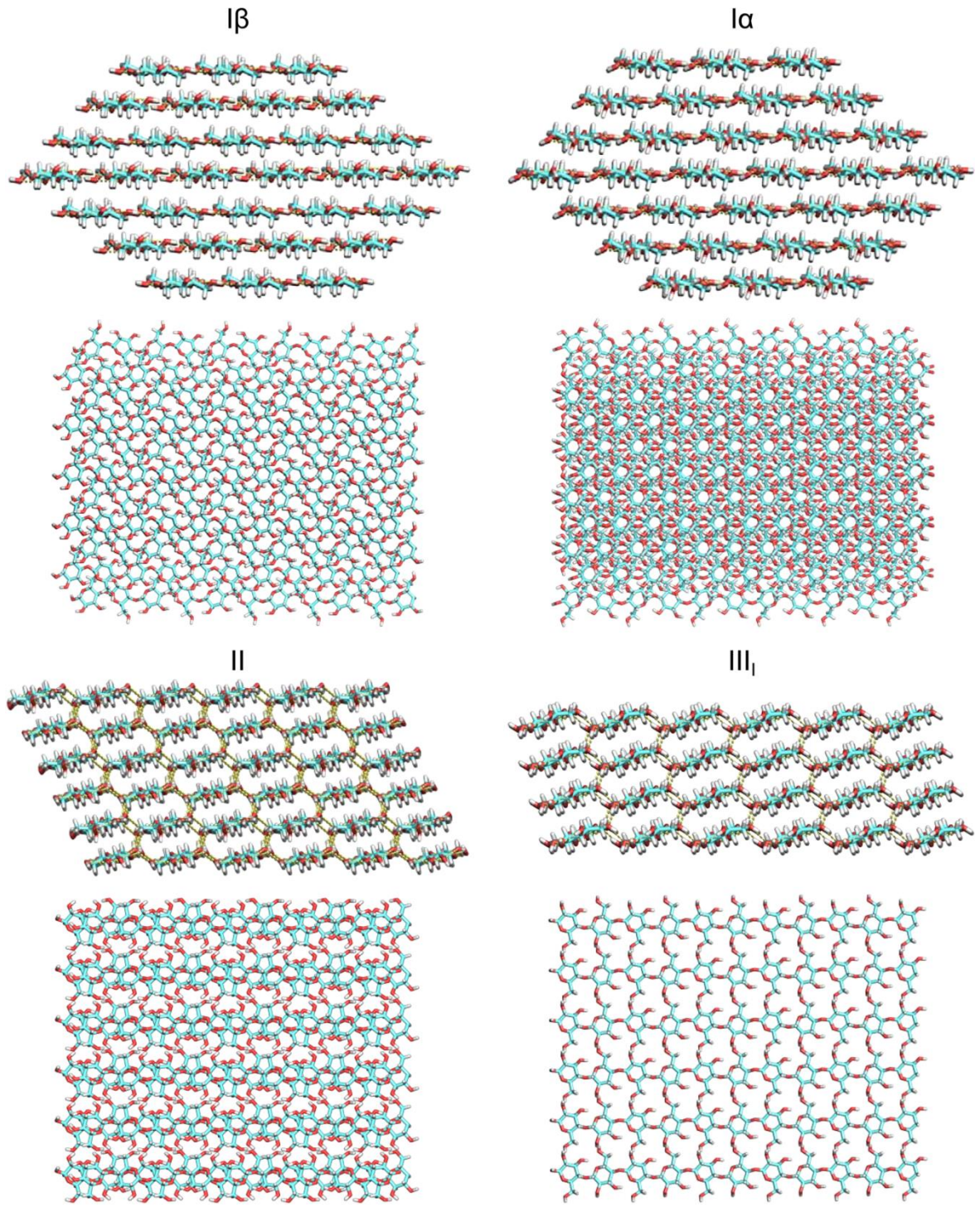

Appendix I.III: DS calculation method[87]

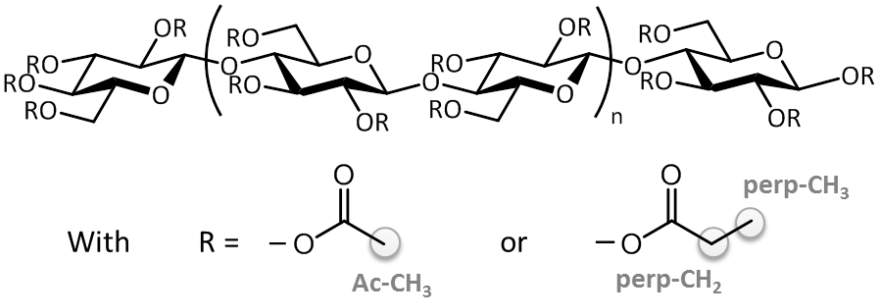

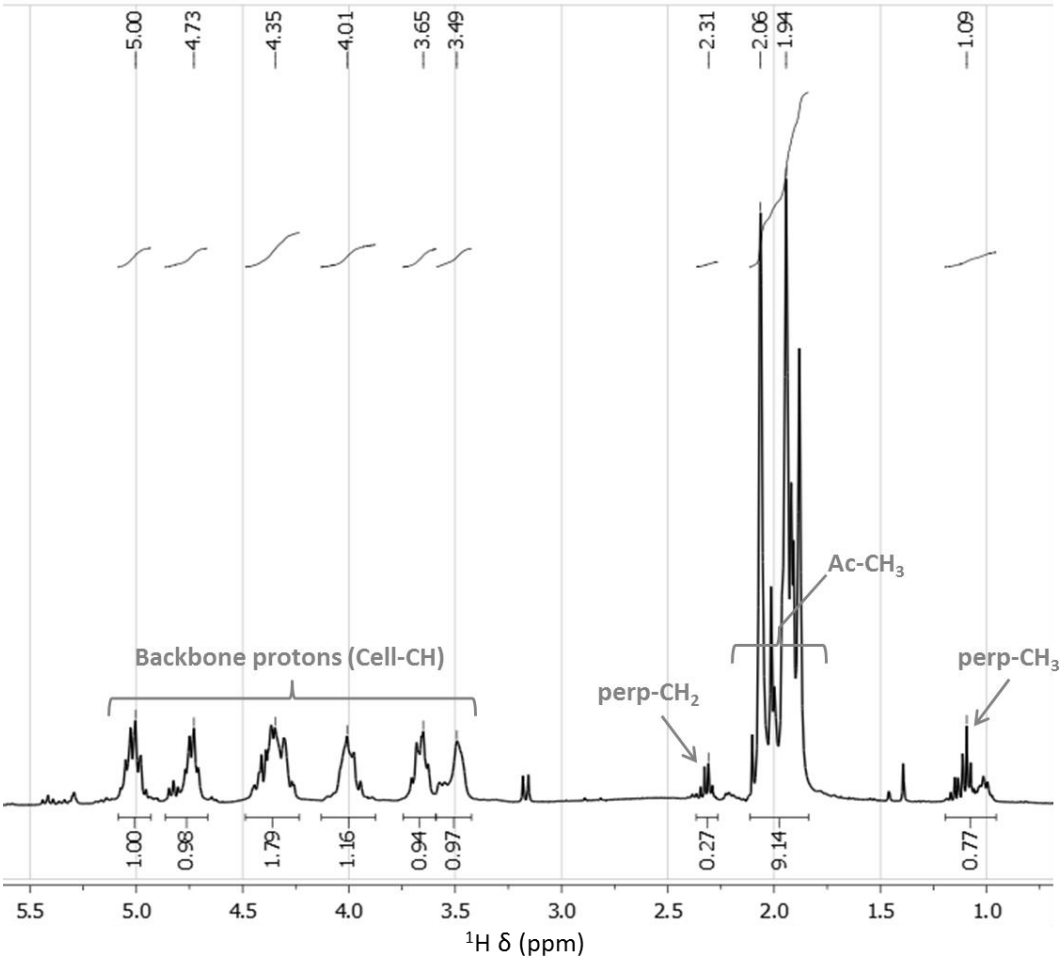

^{1}H NMR spectra in $CDCl_3$ of cellulose acetate perpropionylated

$$DS = 3 - \frac{7 \times I_{perp-CH2}}{2 \times I_{Cell-CH}}$$

With $I_{perp-CH2}$: Peak integral of ethyl protons of propionoyl moieties (perp-CH_2)

I_{Cel-CH}: Peak integral of all protons of anhydroglucose unit (Cell-CH)

Here, DS = 2.86

Appendix I.IV: Cellulose oligomer characteristics

DP	Name	Structure	Molar mass ($g.mol^{-1}$)	Melting point (°C) [198]	Molecular dimensions (Å) [198]		CAS number
					Length	Diameter	
1	**Glucose**	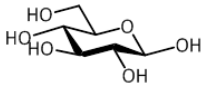	180.16	(α) 146 (β) 150	-	-	50-99-7
2	**Cellobiose**	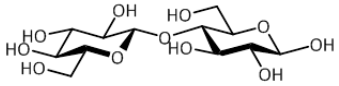	342.29	225	14.6	6.42	528-50-7
3	**Cellotriose**	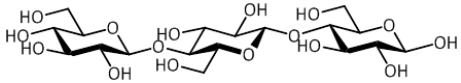	504.43	206-209	20.2	6.56	33404-34-1
4	**Cellotetraose**	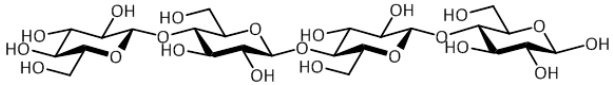	666.57	252-253	26.2	6.60	38819-01-1
5	**Cellopentaose**	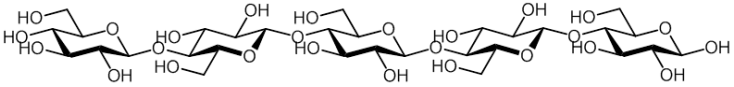	828.71	266-268	31.8	6.66	2240-27-9
6	**Cellohexaose**	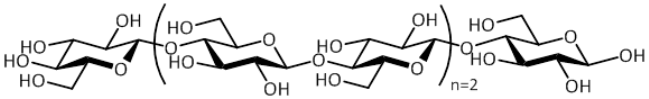	990.85	275-278	37.6	6.68	2478-35-5
7	**Celloheptaose**	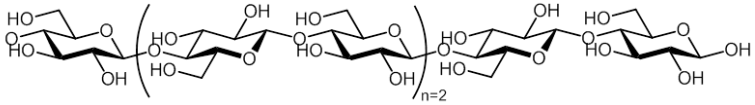	1152.99	283-286	-	-	52646-27-2
8	**Cellooctaose**	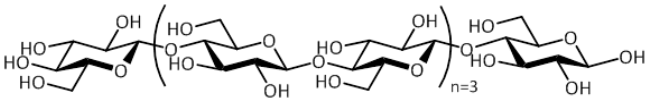	1315.14	-	-	-	-

Appendix I.V: Enzymatic polymerisation mechanism[224]

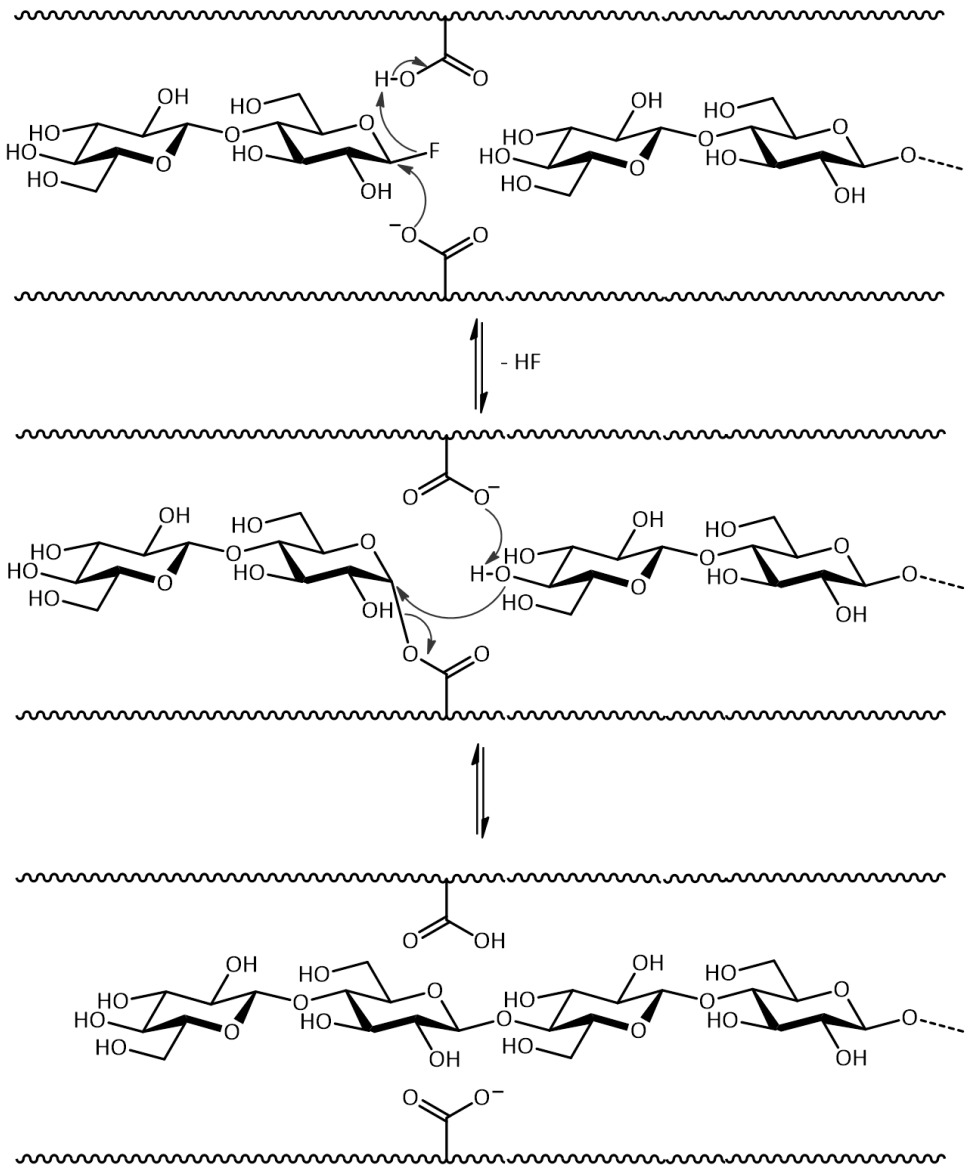

Appendix I.VI: *T. reesei* QM9414 and QM6a cellulases reported in CAZy[159]

Classical name	CAZy[225] name	Common name	Product configuration	Substrate specificity
Bgl2 EC3.2.1.21	GH1 Cel1A	β-glucosidase 2	retaining	p-nitrophenyl-β-D-glucoside, p-nitrophenyl-β-D-cellobioside, methylumbelliferyl-β-Dglucoside, 5-bromo-4-chloro-3-indolyl-β-D-glucoside
EC3.2.1.21	GH1 Cel1B	β-glucosidase	retaining	predicted β-glucosidase activity
Bg1 EC3.2.1.21	GH3 Cel3A	β-glucosidase 1	retaining	Glc_2/Glc_3/Glc_4/Glc_5/Glc_6, gentiobiose, laminaribiose, laminaritriose, sophorose, 2-chloro-4-nitrophenyl-β-D-glucopyranoside, p-nitrophenyl-β-D-glucopyranoside, CMC, laminarin, β-glucan
EC3.2.1.21	GH3 Cel3B	β-glucosidase	retaining	predicted β-glucosidase activity
EC3.2.1.21	GH3 Cel3C	β-glucosidase	retaining	predicted β-glucosidase activity
EC3.2.1.21	GH3 Cel3D	β-glucosidase	retaining	predicted β-glucosidase activity
EC3.2.1.21	GH3 Cel3E	β-glucosidase	retaining	predicted β-glucosidase activity
EGII (formerly EGIII) / EC3.2.1.4	GH5 Cel5A	Engoglucanase II	retaining	CMC-Na, Avicel, ball-milled cellulose, PASC
EC3.2.1.4	GH5 Cel5B	Engoglucanase	retaining	predicted endoglucanase activity
CBHII / EC3.2.1.91	GH6 Cel6A	Cellobiohydrolase II	inverting	Avicel, CMC, Glc_3/Glc_4/Glc_5/Glc_6, PASC

Glc_x: Cellulose oligomer of DP x, CMC: carboxymethyl cellulose, CMC-Na: sodium carboxymethyl cellulose, PASC: phosphoric acid swollen cellulose

Appendix I.VI (following): *T. reesei* QM9414 and QM6a cellulases reported in CAZy[159]

Classical name	CAZy[225] name	Common name	Product configuration	Substrate specificity
CBHI / EC3.2.1.176 / EC3.2.1.91	GH7 Cel7A	Cellobiohydrolase I	retaining	4-methylumbelliferyl-β-D-lactoside, 2-chloro-4-nitrophenol-β-D-lactoside, 3,4-dinitrophenyl-β-D-cellobioside, 3,4-dinitrophenyl-β-D-lactoside, BMCC
EGI EC3.2.1.4	GH7 Cel7B	Endoglucananse I	retaining	Glc_3/Glc_4/Glc_5/Glc_6, pNPC, pNPL, PASC, Avicel, BC, pretreated corn stover, CMC, xyloglucan, xylan, arabinoxylan, mannan, galactomannan, barley β-glucan, hydroxyethylcellulose
EGIII / EC3.2.1.151 / EC3.2.1.4	GH12 Cel12A	Endoglucananse III	retaining	CMC, PASC, Avicel, Glc_4/Glc_5, barley β-glucan, glucomannan, filter paper
EGV EC3.2.1.4	GH45 Cel45A	Endoglucananse V	inverting	CMC, PASC, Avicel, Glc_3/Glc_4/Glc_5, barley β-glucan, glucomannan, filter paper
Egl6 EC3.2.1.151	GH74 Cel74A	Endoglucananse and xyloglucanase	inverting	xyloglucan, hydroxyethylcellulose
EG7	AA9 (formerly GH61) Cel61B	LPMO	oxidative	cellulose

BMCC: bacterial microcrystalline cellulose, Glc_x: Cellulose oligomer of DP x, pNPC: p-nitrophenyl-ß-D-cellobioside, pNPL: p-nitrophenyl-ß-D-lactoside, PASC: phosphoric acid swollen cellulose, CMC: carboxymethyl cellulose, LPMO: lytic polysaccharide monooxygenases

Appendix I.VII: Enzymatic hydrolysis mechanism with retention or inversion of the anomeric conformation[158,159]

Anomeric retaining conformation

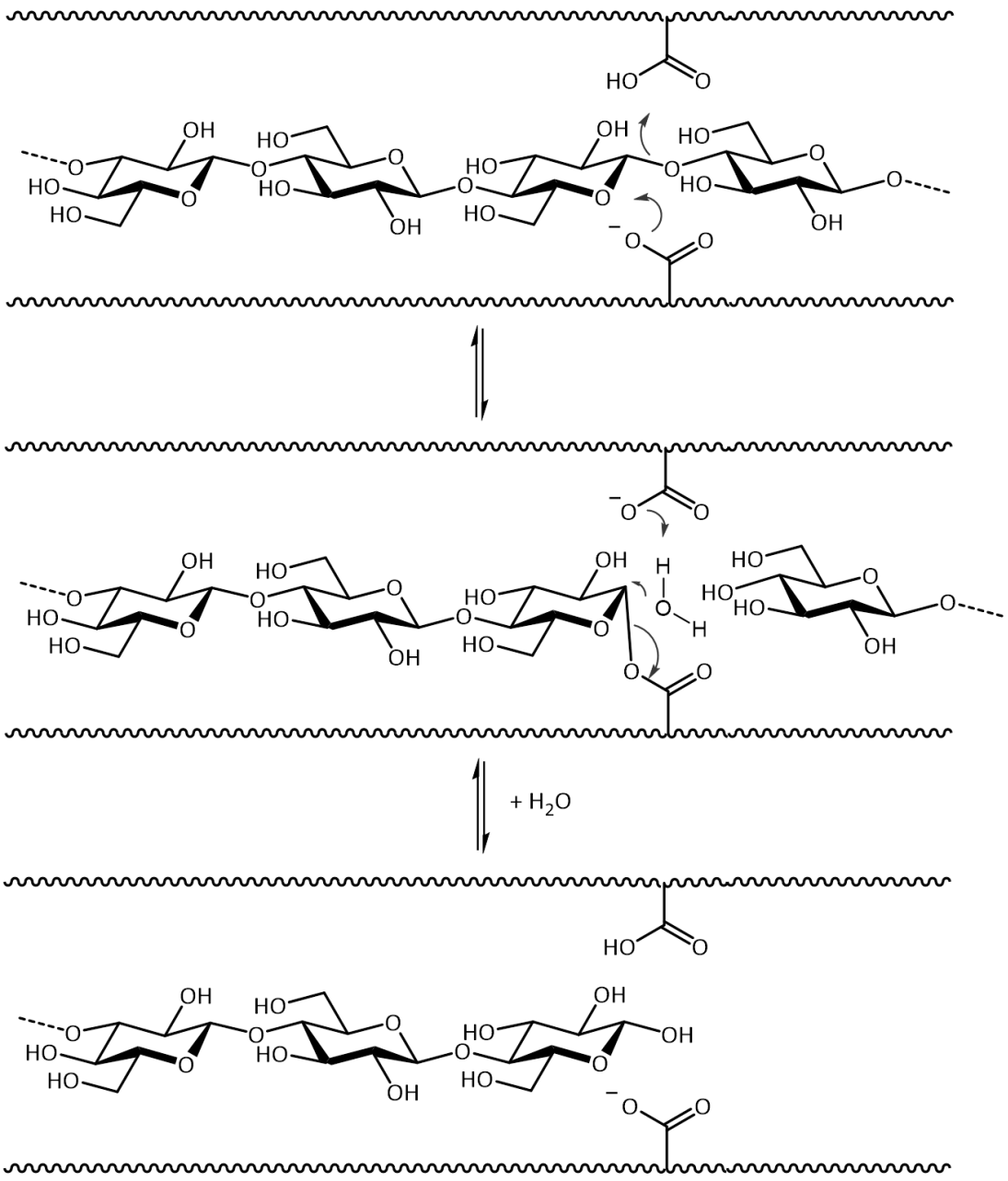

Appendix I.VII (following): Enzymatic hydrolysis mechanism with preservation or inversion of the anomeric conformation[158,159]

Anomeric conformation inversion

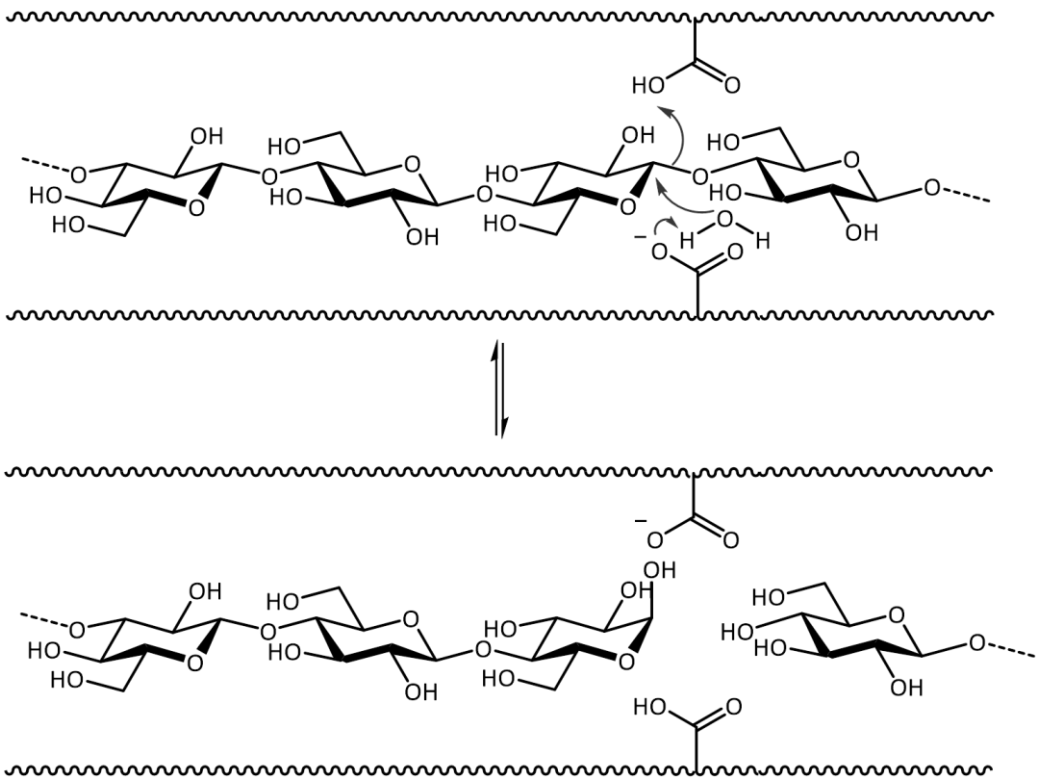

Appendix I.VIII: Mechanism of the cellulose acidic hydrolysis[226]

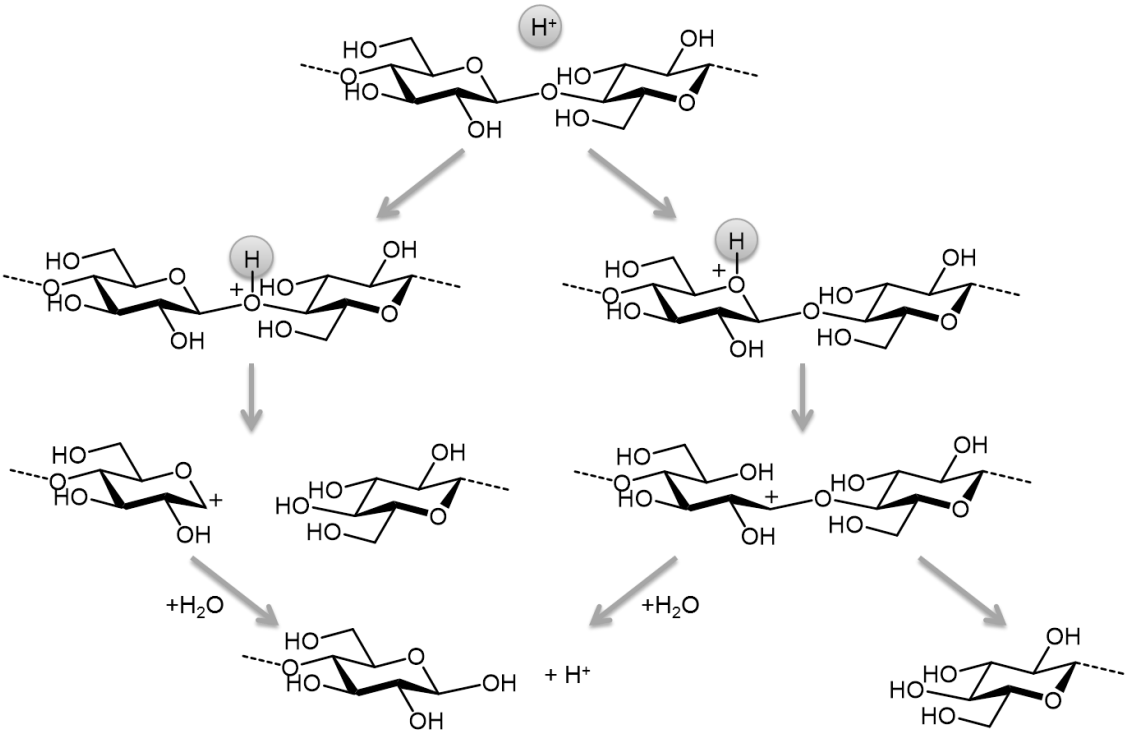

Appendix I.IX: Mechanism of the formation of hydroxymethylfurfural from glucose in acidic conditions[227,228]

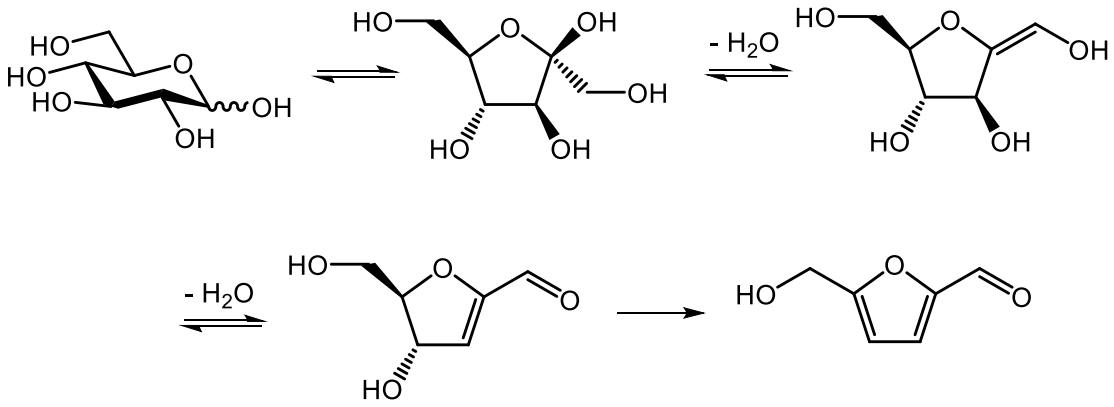

References

[1] A. Payen, *CR Hebd. Seances Acad. Sci.* **1838**, *7*, 1052–1056.

[2] D. Klemm, B. Heublein, H. P. Fink, A. Bohn, *Angew. Chem. Int. Ed.* **2005**, *44*, 3358–3393.

[3] J. Kim, S. Yun, Z. Ounaies, *Macromolecules* **2006**, *39*, 4202–4206.

[4] X. Han, Y. Zheng, C. J. Munro, Y. Ji, A. B. Braunschweig, *Curr. Opin. Biotechnol.* **2015**, *34*, 41–47.

[5] S. Dong, H. J. Cho, Y. W. Lee, M. Roman, *Biomacromolecules* **2014**, *15*, 1560–1567.

[6] S.-P. Lin, I. Loira Calvar, J. Catchmark, J.-R. Liu, A. Demirci, K.-C. Cheng, *Cellulose* **2013**, *20*, 2191–2219.

[7] U. Römling, *Res. Microbiol.* **2002**, *153*, 205–212.

[8] Y. Huang, C. Zhu, J. Yang, Y. Nie, C. Chen, D. Sun, *Cellulose* **2014**, *21*, 1–30.

[9] P. Ross, R. Mayer, M. Benziman, *Microbiol. Mol. Biol. Rev.* **1991**, *55*, 35–58.

[10] M. B. Sticklen, *Nat. Rev. Genet.* **2008**, *9*, 433–443.

[11] W. Boerjan, J. Ralph, M. Baucher, *Annu. Rev. Plant Biol.* **2003**, *54*, 519–546.

[12] B. C. Saha, *J. Ind. Microbiol. Biotechnol.* **2003**, *30*, 279–291.

[13] C. Somerville, S. Bauer, G. Brininstool, M. Facette, T. Hamann, J. Milne, E. Osborne, A. Paredez, S. Persson, T. Raab, et al., *Science* **2004**, *306*, 2206–2211.

[14] M. S. Doblin, I. Kurek, D. Jacob-Wilk, D. P. Delmer, *Plant Cell Physiol.* **2002**, *43*, 1407–1420.

[15] F. H. Isikgor, C. R. Becer, *Polym. Chem.* **2015**, *6*, 4497–4559.

[16] M. Mutwil, S. Debolt, S. Persson, *Curr. Opin. Plant Biol.* **2008**, *11*, 252–257.

[17] I. M. Saxena, R. M. Brown, *Ann. Bot.* **2005**, *96*, 9–21.

[18] D. P. Delmer, Y. Amor, *Plant Cell* **1995**, *7*, 987–1000.

[19] R. M. Brown Jr., I. Saxena, K. Kudlicka, *Trends Plant Sci.* **1996**, *1*, 149–156.

[20] R. J. Moon, A. Martini, J. Nairn, J. Simonsen, J. Youngblood, *Chem. Soc. Rev.* **2011**, *40*, 3941–3994.

[21] J. L. W. Morgan, J. Strumillo, J. Zimmer, *Nature* **2013**, *493*, 181–186.

[22] W. J. Malaisse, I. Verbruggen, M. Biesemans, R. Willem, *Int. J. Mol. Med.* **2004**, *13*, 855–857.

[23] S. J. Angyal, *Carbohydr. Res.* **1994**, *263*, 1–11.

[24] B. Ma, H. F. Schaefer III, N. L. Allinger, *J. Am. Chem. Soc.* **1998**, *120*, 3411–3422.

[25] C. Williams, A. Allerhand, *Carbohydr. Res.* **1977**, *56*, 173–179.

[26] H. S. Isbell, C. W. R. Wade, *J. Res. NBS A Phys. Chem.* **1967**, *71A*, 137–148.

[27] M. Bielecki, H. Eggert, J. C. Norrild, *J. Chem. Soc., Perkin Trans. 2* **1999**, 449–455.

[28] J. Kadokawa, *Chem. Rev.* **2011**, *111*, 4308–4345.

[29] L. M. J. Kroon-Batenburg, B. Bouma, J. Kroon, *Macromolecules* **1996**, *29*, 5695–5699.

[30] R. L. Dudley, C. A. Fyfe, P. J. Stephenson, Y. Deslandes, G. K. Hamer, R. H. Marchessault, *J. Am. Chem. Soc.* **1983**, *105*, 2469–2472.

[31] H. Chanzy, *Cellulose* **2011**, *18*, 853–856.

[32] M. Wada, H. Chanzy, Y. Nishiyama, P. Langan, *Macromolecules* **2004**, *37*, 8548–8555.

[33] E. S. Gardiner, A. Sarko, *Can. J. Chem.* **1985**, *63*, 173–180.

[34] C. Olsson, G. Wesman, in *Cellul. - Fundam. Asp.*, InTech, **2013**, pp. 143–178.

[35] B. Medronho, B. Lindman, *Curr. Opin. Colloid Interface Sci.* **2014**, *19*, 32–40.

[36] A. M. Bochek, *Russ. J. Appl. Chem.* **2003**, *76*, 1711–1719.

[37] B. Lindman, G. Karlström, L. Stigsson, *J. Mol. Liq.* **2010**, *156*, 76–81.

[38] T. Heinze, A. Koschella, *Polímeros Ciência e Tecnol.* **2005**, *15*, 84–90.

[39] K. Saalwächter, W. Burchard, P. Klüfers, G. Kettenbach, P. Mayer, D. Klemm, S. Dugarmaa, *Macromolecules* **2000**, *33*, 4094–4107.

[40] J. Eckelt, A. Knopf, T. Röder, H. K. Weber, H. Sixta, B. A. Wolf, *J. Appl. Polym. Sci.* **2011**, *119*, 670–676.

[41] M. Kes, B. E. Christensen, *J. Chromatogr. A* **2013**, *1281*, 32–37.

[42] G. B. Kauffman, *J. Chem. Educ.* **1993**, *70*, 887–893.

[43] C. Woodings, in *Regen. Cellul. Fibres*, Elsevier, **2001**, pp. 1–21.

[44] A. Isogai, R. H. Atalla, *Cellulose* **1998**, *5*, 309–319.

[45] C. Roy, T. Budtova, P. Navard, *Biomacromolecules* **2003**, *4*, 259–264.

[46] N. Isobe, K. Noguchi, Y. Nishiyama, S. Kimura, M. Wada, S. Kuga, *Cellulose* **2013**, *20*, 97–103.

[47] E. Wernersson, B. Stenqvist, M. Lund, *Cellulose* **2015**, *22*, 991–1001.

[48] J. Zhou, L. Zhang, *Polym. J.* **2000**, *32*, 866–870.

[49] X. Chen, J. Chen, T. You, K. Wang, F. Xu, *Carbohydr. Polym.* **2015**, *125*, 85–91.

[50] H. Qi, C. Chang, L. Zhang, *Cellulose* **2008**, *15*, 779–787.

[51] X. Luo, L. Zhang, *Food Res. Int.* **2013**, *52*, 387–400.

[52] J. Cai, C. Li, Y. Mao, H. Qi, L. Zhang, J. Zhou, *Method for Preparing Regenerated Cellulose Fibre by Two-Step Coagulating Bath Process*, **2010**, EP 1900860 B1.

[53] J. Cai, L. Zhang, *Macromol. Biosci.* **2005**, *5*, 539–548.

[54] S. Sen, J. D. Martin, D. S. Argyropoulos, *ACS Sustainable Chem. Eng.* **2013**, *1*, 858–870.

[55] H. Leipner, S. Fischer, E. Brendler, W. Voigt, *Macromol. Chem. Phys.* **2000**, *201*, 2041–2049.

[56] E. Brendler, S. Fischer, H. Leipner, *Cellulose* **2001**, *8*, 283–288.

[57] M. Hattori, T. Koga, Y. Shimaya, M. Saito, *Polym. J.* **1998**, *30*, 43–48.

[58] C. L. McCormick, *Novel Cellulose Solutions*, **1981**, US 4278790 A.

[59] C. L. McCormick, P. A. Callais, B. H. Hutchinson, *Macromolecules* **1985**, *18*, 2394–2401.

[60] A. Potthast, T. Rosenau, R. Buchner, T. Röder, G. Ebner, H. Bruglachner, H. Sixta, P. Kosma, *Cellulose* **2002**, *9*, 41–53.

[61] A. M. Emsley, M. Ali, R. J. Heywood, *Polymer* **2000**, *41*, 8513–8521.

[62] T. Bikova, A. Treimanis, *Carbohydr. Polym.* **2002**, *48*, 23–28.

[63] É. Borbély, *Acta Polytech. Hungarica* **2008**, *5*, 11–18.

[64] T. Rosenau, A. Potthast, H. Sixta, P. Kosma, *Prog. Polym. Sci.* **2001**, *26*, 1763–1837.

[65] S. Köhler, T. Heinze, *Macromol. Biosci.* **2007**, *7*, 307–314.

[66] Å. Östlund, D. Lundberg, L. Nordstierna, K. Holmberg, M. Nydén, *Biomacromolecules* **2009**, *10*, 2401–2407.

[67] G. T. Ciacco, T. F. Liebert, E. Frollini, T. J. Heinze, *Cellulose* **2003**, *10*, 125–132.

[68] N. L. Mai, K. Ahn, Y.-M. Koo, *Process Biochem.* **2014**, *49*, 872–881.

[69] D. Zhao, Y. Liao, Z. Zhang, *CLEAN – Soil, Air, Water* **2007**, *35*, 42–48.

[70] A. Jordan, N. Gathergood, *Chem. Soc. Rev.* **2015**, *44*, 8200–8237.

[71] A. Sosnowska, M. Barycki, M. Zaborowska, A. Rybinska, T. Puzyn, *Green Chem.* **2014**, *16*, 4749–4757.

[72] R. P. Swatloski, S. K. Spear, J. D. Holbrey, R. D. Rogers, *J. Am. Chem. Soc.* **2002**, *124*, 4974–4975.

[73] R. C. Remsing, R. P. Swatloski, R. D. Rogers, G. Moyna, *Chem. Commun.* **2006**, 1271–1273.

[74] R. De Silva, K. Vongsanga, X. Wang, N. Byrne, *Cellulose* **2015**, *22*, 2845–2849.

[75] A. Pinkert, K. N. Marsh, S. Pang, M. P. Staiger, *Chem. Rev.* **2009**, *109*, 6712–6728.

[76] F. Hermanutz, F. Gähr, E. Uerdingen, F. Meister, B. Kosan, *Macromol. Symp.* **2008**, *262*, 23–27.

[77] H. Zhao, G. A. Baker, Z. Song, O. Olubajo, T. Crittle, D. Peters, *Green Chem.* **2008**, *10*, 696–705.

[78] H. Zhang, J. Wu, J. Zhang, J. He, *Macromolecules* **2005**, *38*, 8272–8277.

[79] Q. Zhang, M. Benoit, K. De Oliveira Vigier, J. Barrault, F. Jérôme, *Chem. – A Eur. J.* **2012**, *18*, 1043–1046.

[80] J. Vitz, T. Erdmenger, C. Haensch, U. S. Schubert, *Green Chem.* **2009**, *11*, 417–424.

[81] A. Sant'Ana da Silva, S.-H. Lee, T. Endo, E. P. S. Bon, *Bioresour. Technol.* **2011**, *102*, 10505–10509.

[82] T. Heinze, T. Liebert, *Prog. Polym. Sci.* **2001**, *26*, 1689–1762.

[83] S. Barthel, T. Heinze, *Green Chem.* **2006**, *8*, 301–306.

[84] M. Schöbitz, F. Meister, T. Heinze, *Macromol. Symp.* **2009**, *280*, 102–111.

[85] V. W. Goodlett, J. T. Dougherty, H. W. Patton, *J. Polym. Sci., Part A-1: Polym. Chem.* **1971**, *9*, 155–161.

[86] T. Liebert, M. A. Hussain, T. Heinze, *Macromol. Symp.* **2005**, *223*, 79–91.

[87] T. Heinze, R. Dicke, A. Koschella, A. H. Kull, E.-A. Klohr, W. Koch, *Macromol. Chem. Phys.* **2000**, *201*, 627–631.

[88] T. Heinze, T. Liebert, P. Klüfers, F. Meister, *Cellulose* **1999**, *6*, 153–165.

[89] W. Mormann, U. Michel, *Carbohydr. Polym.* **2002**, *50*, 201–208.

[90] U. Henniges, E. Kloser, A. Patel, A. Potthast, P. Kosma, M. Fischer, K. Fischer, T. Rosenau, *Cellulose* **2007**, *14*, 497–511.

[91] R. Evans, R. H. Wearne, A. F. A. Wallis, *J. Appl. Polym. Sci.* **1989**, *37*, 3291–3303.

[92] H. Kono, H. Hashimoto, Y. Shimizu, *Carbohydr. Polym.* **2015**, *118*, 91–100.

[93] M. Isik, H. Sardon, D. Mecerreyes, *Int. J. Mol. Sci.* **2014**, *15*, 11922–11940.

[94] W. G. Glasser, *Macromol. Symp.* **2004**, *208*, 371–394.

[95] C. P. McCord, *J. Occup. Environ. Med.* **1964**, *6*, 452–457.

[96] ISO 5351:2010, *Pulps-Determination of Limiting Viscosity Number in Cuper-Ethylenediamine (CED) Solution*, **2010**.

[97] A. M. Striegel, J. D. Timpa, *Carbohydr. Res.* **1995**, *267*, 271–290.

[98] J. Zhou, L. Zhang, J. Cai, *J. Polym. Sci., Part B: Polym. Phys.* **2004**, *42*, 347–353.

[99] H. Pala, M. Mota, F. M. Gama, *Carbohydr. Polym.* **2007**, *68*, 101–108.

[100] P. Engel, L. Hein, A. Spiess, *Biotechnol. Biofuels* **2012**, *5:77*.

[101] Y. Fukaya, A. Tsukamoto, K. Kuroda, H. Ohno, *Chem. Commun.* **2011**, *47*, 1994–1996.

[102] Y. H. P. Zhang, L. R. Lynd, *Biomacromolecules* **2005**, *6*, 1510–1515.

[103] M. DuBois, K. A. Gilles, J. K. Hamilton, P. A. Rebers, F. Smith, *Anal. Chem.* **1956**, *28*, 350–356.

[104] L. W. Doner, P. L. Irwin, *Anal. Biochem.* **1992**, *202*, 50–53.

[105] H. Liu, K. L. Sale, B. M. Holmes, B. A. Simmons, S. Singh, *J. Phys. Chem. B* **2010**, *114*, 4293–4301.

[106] K. Gessler, N. Krauss, T. Steiner, C. Betzel, A. Sarko, W. Saenger, *J. Am. Chem. Soc.* **1995**, *117*, 11397–11406.

[107] B. V. McCleary, D. Mangan, R. Daly, S. Fort, R. Ivory, N. McCormack, *Carbohydr. Res.* **2014**, *385*, 9–17.

[108] H. J. Flint, E. A. Bayer, M. T. Rincon, R. Lamed, B. A. White, *Nat. Rev. Microbiol.* **2008**, *6*, 121–131.

[109] S. Nakamura, T. Oku, M. Ichinose, *Nutrition* **2004**, *20*, 979–983.

[110] W. Sybesma, R. Kort, Y.-K. Lee, *Trends Biotechnol.* **2015**, *33*, 197–200.

[111] S. Patel, A. Goyal, *World J. Microbiol. Biotechnol.* **2011**, *27*, 1119–1128.

[112] N. Yamasaki, I. Ibuki, Y. Yaginuma, Y. Tamura, *Cellooligosaccharide-Containing Composition*, **2008**, EP 1930012 A1.

[113] M. Granström, A. Kindler, A. Spiess, S. Kluge, B. Bonhage, *Endoglucanase-Induced Production of Cellulose Oligomers*, **2014**, WO2015000858 A2.

[114] F. Nakatsubo, H. Kamitakahara, M. Hori, *J. Am. Chem. Soc.* **1996**, *118*, 1677–1681.

[115] M. Karakawa, F. Nakatsubo, *Carbohydr. Res.* **2002**, *337*, 951–954.

[116] H. Kamitakahara, F. Nakatsubo, *Macromolecules* **1996**, *29*, 1119–1122.

[117] H. Kamitakahara, M. Hori, F. Nakatsubo, *Macromolecules* **1996**, *29*, 6126–6131.

[118] H. Kamitakahara, F. Nakatsubo, K. Murakami, *Macromolecules* **1994**, *27*, 5937–5942.

[119] M. C. Galan, R. A. Jones, A.-T. Tran, *Carbohydr. Res.* **2013**, *375*, 35–46.

[120] X. Zhu, R. R. Schmidt, *Angew. Chem. Int. Ed.* **2009**, *48*, 1900–1934.

[121] T. K. Ritter, K.-K. T. Mong, H. Liu, T. Nakatani, C.-H. Wong, *Angew. Chem. Int. Ed.* **2003**, *42*, 4657–4660.

[122] P. Peng, D.-C. Xiong, X.-S. Ye, *Carbohydr. Res.* **2014**, *384*, 1–8.

[123] E. Kaji, D. Yamamoto, Y. Shirai, K. Ishige, Y. Arai, T. Shirahata, K. Makino, T. Nishino, *Eur. J. Org. Chem.* **2014**, *17*, 3536–3539.

[124] E. Kaji, T. Nishino, K. Ishige, Y. Ohya, Y. Shirai, *Tetrahedron Lett.* **2010**, *51*, 1570–1573.

[125] H. Kamitakahara, F. Nakatsubo, D. Klemm, *Cellulose* **2006**, *13*, 375–392.

[126] T. Nishimura, F. Nakatsubo, *Carbohydr. Res.* **1996**, *294*, 53–64.

[127] P. Monsan, F. Paul, *FEMS Microbiol. Rev.* **1995**, *16*, 187–192.

[128] K. G. I. Nilsson, *Trends Biotechnol.* **1988**, *6*, 256–264.

[129] S. Kobayashi, *J. Polym. Sci., Part A: Polym. Chem.* **2005**, *43*, 693–710.

[130] S. Kobayashi, K. Kashiwa, T. Kawasaki, S. Shoda, *J. Am. Chem. Soc.* **1991**, *113*, 3079–3084.

[131] H. Tanaka, S. Koizumi, T. Hashimoto, K. Kurosaki, S. Kobayashi, *Macromolecules* **2007**, *40*, 6304–6315.

[132] J.-L. Viladot, V. Moreau, A. Planas, H. Driguez, *J. Chem. Soc., Perkin Trans. 1* **1997**, 2383–2387.

[133] S. Kobayashi, S. Shoda, *Int. J. Biol. Macromol.* **1995**, *17*, 373–379.

[134] S. Kobayashi, T. Kawasaki, K. Obata, S. Shoda, *Chem. Lett.* **1993**, 685–686.

[135] S. Fort, L. Christiansen, M. Schülein, S. Cottaz, H. Drigueza, *Isr. J. Chem.* **2000**, *40*, 217–221.

[136] E. C. O'Neill, R. A. Field, *Carbohydr. Res.* **2015**, *403*, 23–37.

[137] H. Nakai, M. A. Hachem, B. O. Petersen, Y. Westphal, K. Mannerstedt, M. J. Baumann, A. Dilokpimol, H. A. Schols, J. Ø. Duus, B. Svensson, *Biochimie* **2010**, *92*, 1818–1826.

[138] D. M. Petrović, I. Kok, A. J. J. Woortman, J. Ćirić, K. Loos, *Anal. Chem.* **2015**, *87*, 9639–9646.

[139] T. Hattori, M. Ogata, Y. Kameshima, K. Totani, M. Nikaido, T. Nakamura, H. Koshino, T. Usui, *Carbohydr. Res.* **2012**, *353*, 22–26.

[140] J. S. Van Dyk, B. I. Pletschke, *Biotechnol. Adv.* **2012**, *30*, 1458–1480.

[141] Y.-H. P. Zhang, L. R. Lynd, *Biotechnol. Bioeng.* **2004**, *88*, 797–824.

[142] D. H. Fockink, M. A. C. Maceno, L. P. Ramos, *Bioresour. Technol.* **2015**, *187*, 91–96.

[143] R. K. Sukumaran, R. R. Singhania, G. M. Mathew, A. Pandey, *Renew. Energy* **2009**, *34*, 421–424.

[144] R. N. Maeda, C. A. Barcelos, L. M. Anna, N. Pereira Jr., *J. Biotechnol.* **2013**, *163*, 38–44.

[145] Y. Sun, J. Cheng, *Bioresour. Technol.* **2002**, *83*, 1–11.

[146] A. R. Rigdon, A. Jumpponen, P. V Vadlani, D. E. Maier, *Bioresour. Technol.* **2013**, *132*, 269–275.

[147] A. Jeihanipour, K. Karimi, M. J. Taherzadeh, *Biotechnol. Bioeng.* **2010**, *105*, 469–476.

[148] P. Alvira, E. Tomás-Pejó, M. Ballesteros, M. J. Negro, *Bioresour. Technol.* **2010**, *101*, 4851–4861.

[149] J. Plácido, T. Imam, S. Capareda, *Bioresour. Technol.* **2013**, *139*, 203–208.

[150] S. J. Horn, G. Vaaje-Kolstad, B. Westereng, V. G. H. Eijsink, *Biotechnol. Biofuels* **2012**, *5:45*, DOI 10.1186/1754-6834-5-45.

[151] M. J. Taherzadeh, K. Karimi, *BioResources* **2007**, *2*, 707–738.

[152] B. E. Dale, *Biofuels, Bioprod. Biorefining* **2015**, *9*, 1–3.

[153] R. Gupta, Y. Y. Lee, *Biotechnol. Bioeng.* **2009**, *102*, 1570–1581.

[154] L. E. R. Berghem, L. G. Pettersson, U.-B. Axiö-Fredriksson, *Eur. J. Biochem.* **1976**, *61*, 621–630.

[155] L. E. R. Berghem, L. G. Pettersson, U.-B. Axiö-Fredriksson, *Eur. J. Biochem.* **1975**, *53*, 55–62.

[156] L. E. R. Berghem, L. G. Pettersson, *Eur. J. Biochem.* **1974**, *46*, 295–305.

[157] R. M. F. Bezerra, A. A. Dias, *Appl. Biochem. Biotechnol.* **2005**, *126*, 49–59.

[158] B. Henrissat, *Cellulose* **1994**, *1*, 169–196.

[159] C. M. Payne, B. C. Knott, H. B. Mayes, H. Hansson, M. E. Himmel, M. Sandgren, J. Ståhlberg, G. T. Beckham, *Chem. Rev.* **2015**, *115*, 1308–1448.

[160] G. Davies, B. Henrissat, *Structure* **1995**, *3*, 853–859.

[161] C. Bennati-Granier, S. Garajova, C. Champion, S. Grisel, M. Haon, S. Zhou, M. Fanuel, D. Ropartz, H. Rogniaux, I. Gimbert, et al., *Biotechnol. Biofuels* **2015**, *8:90*, DOI 10.1186/s13068-015-0274-3.

[162] J. V Vermaas, M. F. Crowley, G. T. Beckham, C. M. Payne, *J. Phys. Chem. B* **2015**, *119*, 6129–6143.

[163] O. V Proskurina, O. G. Korotkova, A. M. Rozhkova, E. G. Kondrat'eva, V. Y. Matys, I. N. Zorov, A. V Koshelev, O. N. Okunev, V. A. Nemashkalov, T. V Bubnova, et al., *Appl. Biochem. Microbiol.* **2015**, *51*, 667–673.

[164] R. P. Chandra, R. Bura, W. E. Mabee, A. Berlin, X. Pan, J. N. Saddler, in *Biofuels* (Ed.: L. Olsson), Springer Berlin Heidelberg, **2007**, pp. 67–93.

[165] L. da Costa Sousa, S. P. S. Chundawat, V. Balan, B. E. Dale, *Curr. Opin. Biotechnol.* **2009**, *20*, 339–347.

[166] A. Brandt, J. Grasvik, J. P. Hallett, T. Welton, *Green Chem.* **2013**, *15*, 550–583.

[167] H. Zhao, C. L. Jones, G. A. Baker, S. Xia, O. Olubajo, V. N. Person, *J. Biotechnol.* **2009**, *139*, 47–54.

[168] H. Tadesse, R. Luque, *Energy Environ. Sci.* **2011**, *4*, 3913–3929.

[169] Y.-C. Sun, J.-K. Xu, F. Xu, R.-C. Sun, *Process Biochem.* **2013**, *48*, 844–852.

[170] I. P. Samayam, B. L. Hanson, P. Langan, C. A. Schall, *Biomacromolecules* **2011**, *12*, 3091–3098.

[171] Z. Liu, X. Sun, M. Hao, C. Huang, Z. Xue, T. Mu, *Carbohydr. Polym.* **2015**, *117*, 99–105.

[172] M. B. Turner, S. K. Spear, J. G. Huddleston, J. D. Holbrey, R. D. Rogers, *Green Chem.*

2003, *5*, 443–447.

[173] S. Bose, C. A. Barnes, J. W. Petrich, *Biotechnol. Bioeng.* **2012**, *109*, 434–443.

[174] B. Satari Baboukani, M. Vossoughi, I. Alemzadeh, *Biosyst. Eng.* **2012**, *111*, 166–174.

[175] Z. Hu, Z. Wen, *Biochem. Eng. J.* **2008**, *38*, 369–378.

[176] Y. Zhao, Y. Wang, J. Y. Zhu, A. Ragauskas, Y. Deng, *Biotechnol. Bioeng.* **2008**, *99*, 1320–1328.

[177] S. Kim, M. T. Holtzapple, *Bioresour. Technol.* **2005**, *96*, 1994–2006.

[178] M. Hall, P. Bansal, J. H. Lee, M. J. Realff, A. S. Bommarius, *Bioresour. Technol.* **2011**, *102*, 2910–2915.

[179] H. Peng, H. Li, H. Luo, J. Xu, *Bioresour. Technol.* **2013**, *130*, 81–87.

[180] A. Barakat, C. Mayer, A. Solhy, R. A. Arancon, H. De Vries, R. Luque, *RSC Adv.* **2014**, *4*, 48109–48127.

[181] J. S. Bak, J. K. Ko, Y. H. Han, B. C. Lee, I.-G. Choi, K. H. Kim, *Bioresour. Technol.* **2009**, *100*, 1285–1290.

[182] C. Zhang, F. Pang, B. Li, S. Xue, Y. Kang, *Bioresour. Technol.* **2013**, *138*, 314–320.

[183] H. M. Shaikh, M. G. Adsul, D. V Gokhale, A. J. Varma, *Carbohydr. Polym.* **2011**, *86*, 962–968.

[184] Q. Chu, X. Li, Y. Xu, Z. Wang, J. Huang, S. Yu, Q. Yong, *Process Biochem.* **2014**, *49*, 1217–1222.

[185] K. Tsukimoto, R. Takada, Y. Araki, K. Suzuki, S. Karita, T. Wakagi, H. Shoun, T. Watanabe, S. Fushinobu, *FEBS Lett.* **2010**, *584*, 1205–1211.

[186] V. Harjunpää, A. Teleman, A. Koivula, L. Ruohonen, T. T. Teeri, O. Teleman, T. Drakenberg, *Eur. J. Biochem.* **1996**, *240*, 584–591.

[187] Z. Xiao, X. Zhang, D. J. Gregg, J. N. Saddler, *Appl. Biochem. Biotechnol.* **2004**, *113-116*, 1115–1126.

[188] A. V Gusakov, A. P. Sinitsyn, *Biotechnol. Bioeng.* **1992**, *40*, 663–671.

[189] S. K. Khare, A. Pandey, C. Larroche, *Biochem. Eng. J.* **2015**, *102*, 38–44.

[190] B. Nidetzky, W. Zachariae, G. Gercken, M. Hayn, W. Steiner, *Enzyme Microb. Technol.* **1994**, *16*, 43–52.

[191] Z. Yu, H. Jameel, H. Chang, R. Philips, S. Park, *Biotechnol. Bioeng.* **2012**, *109*, 1131–1139.

[192] M. Nojiri, T. Kondo, *Macromolecules* **1996**, *29*, 2392–2395.

[193] Y. Habibi, L. A. Lucia, O. J. Rojas, *Chem. Rev.* **2010**, *110*, 3479–3500.

[194] T. Liebert, M. Seifert, T. Heinze, *Macromol. Symp.* **2008**, *262*, 140–149.

[195] N. Kasuya, Y. Kusaka, N. Habu, A. Ohnishi, *Cellulose* **2002**, *9*, 263–269.

[196] W. Brown, *J. Chromatogr. A* **1970**, *52*, 273–284.

[197] K. Hamacher, G. Schmid, H. Sahm, C. Wandrey, *J. Chromatogr. A* **1985**, *319*, 311–318.

[198] A. Huebner, M. R. Ladisch, G. T. Tsao, *Biotechnol. Bioeng.* **1978**, *20*, 1669–1677.

[199] O. Akpinar, R. J. McGorrin, M. H. Penner, *J. Agric. Food Chem.* **2004**, *52*, 4144–4148.

[200] M. Voloch, M. R. Ladisch, M. Cantarella, G. T. Tsao, *Biotechnol. Bioeng.* **1984**, *26*, 557–559.

[201] Y.-H. P. Zhang, L. R. Lynd, *Anal. Biochem.* **2003**, *322*, 225–232.

[202] A. Martin-Mingot, K. De Oliveira Vigier, F. Jérôme, S. Thibaudeau, *Org. Biomol. Chem.* **2012**, *10*, 2521–2524.

[203] R. E. Wing, S. N. Freer, *Carbohydr. Polym.* **1984**, *4*, 323–333.

[204] M. Meiland, T. Liebert, T. Heinze, *Macromol. Mater. Eng.* **2011**, *296*, 802–809.

[205] R. Rinaldi, R. Palkovits, F. Schüth, *Angew. Chem. Int. Ed.* **2008**, *47*, 8047–8050.

[206] F. Boissou, K. De Oliveira Vigier, B. Estrine, S. Marinkovic, F. Jérôme, *ACS Sustainable Chem. Eng.* **2014**, *2*, 2683–2689.

[207] P. Arndt, K. Bockholt, R. Gerdes, S. Huschens, J. Pyplo, H. Redlich, K. Samm, *Cellulose* **2003**, *10*, 75–83.

[208] P. Arndt, R. Gerdes, S. Huschens, J. Pyplo-Schnieders, H. Redlich, *Cellulose* **2005**, *12*, 317–326.

[209] A. Shrotri, L. K. Lambert, A. Tanksale, J. Beltramini, *Green Chem.* **2013**, *15*, 2761–2768.

[210] P. Dornath, H. J. Cho, A. D. Paulsen, P. J. Dauenhauer, W. Fan, *Green Chem.* **2015**, *17*, 769–775.

[211] F. Shafizadeh, R. H. Furneaux, T. G. Cochran, J. P. Scholl, Y. Sakai, *J. Appl. Polym. Sci.* **1979**, *23*, 3525–3539.

[212] J. Piskorz, P. Majerski, D. Radlein, A. Vladars-Usas, D. S. Scott, *J. Anal. Appl. Pyrolysis* **2000**, *56*, 145–166.

[213] Y. Yu, D. Liu, H. Wu, *Energy & Fuels* **2012**, *26*, 7331–7339.

[214] Y. Yu, H. Wu, *Ind. Eng. Chem. Res.* **2009**, *48*, 10682–10690.

[215] Y. Zhao, W.-J. Lu, H.-T. Wang, *Chem. Eng. J.* **2009**, *150*, 411–417.

[216] L. K. Tolonen, M. Juvonen, K. Niemelä, A. Mikkelson, M. Tenkanen, H. Sixta, *Carbohydr. Res.* **2015**, *401*, 16–23.

[217] M. Benoit, A. Rodrigues, Q. Zhang, E. Fourré, K. De Oliveira Vigier, J.-M. Tatibouët, F. Jérôme, *Angew. Chem. Int. Ed.* **2011**, *50*, 8964–8967.

[218] L. A. Flugge, J. T. Blank, P. A. Petillo, *J. Am. Chem. Soc.* **1999**, *121*, 7228–7238.

[219] S. Chilamkurthi, J.-H. Willemsen, L. A. M. van der Wielen, E. Poiesz, M. Ottens, *J. Chromatogr. A* **2012**, *1239*, 22–34.

[220] J. Schmidt, M. John, C. Wandrey, *J. Chromatogr. A* **1981**, *213*, 151–155.

[221] H. D. Scobell, K. M. Brobst, *J. Chromatogr. A* **1981**, *212*, 51–64.

[222] Z. Hostomská-Chytilová, O. Mikeš, P. Vrátný, M. Smrž, *J. Chromatogr. A* **1982**, *235*, 229–236.

[223] N. Claisse, Préparation et Modification D'oligosaccharides de Cellulose Par Chimie Douce Bio-Inspirée, Université de Grenoble, **2012**.

[224] M. Ohmae, A. Makino, S. Kobayashi, *Macromol. Chem. Phys.* **2007**, *208*, 1447–1457.

[225] B. L. Cantarel, P. M. Coutinho, C. Rancurel, T. Bernard, V. Lombard, B. Henrissat, *Nucleic Acids Res.* **2009**, *37*, D233–D238.

[226] Q. Xiang, Y. Y. Lee, P. O. Pettersson, R. W. Torget, *Appl. Biochem. Biotechnol.* **2003**, *107*, 505–514.

[227] R. S. Assary, T. Kim, J. J. Low, J. Greeley, L. A. Curtiss, *Phys. Chem. Chem. Phys.* **2012**, *14*, 16603–16611.

[228] Y. Pierson, F. Bobbink, N. Yan, *Chem. Eng. Process Tech.* **2013**, *1*, 1014–1019.

Chapter II. Boronic acid/sugar interaction

Table of Contents

Chapter Purpose

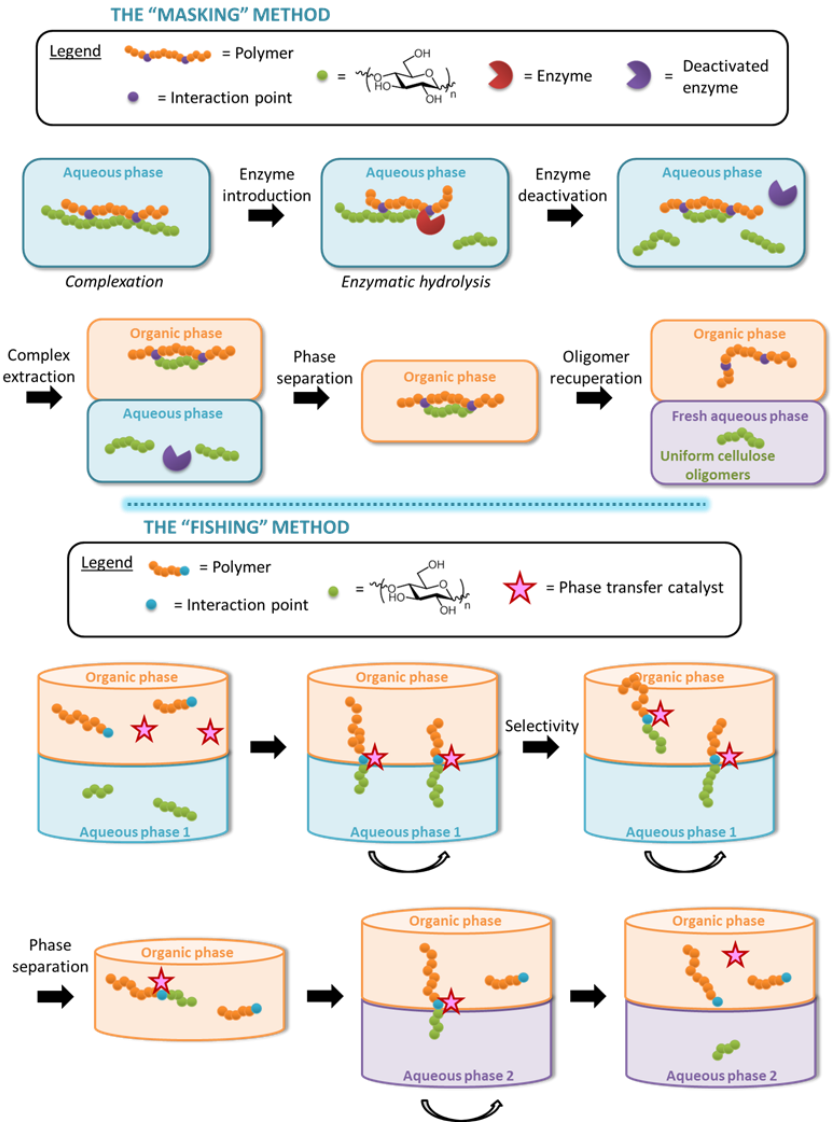

This chapter deals with the determination of boronic acids propensity to complex on sugars. Such information is essential to pick the type of polymer that will be synthesised for the "fishing" and/or the "masking" methods (block, random, other). Thus, a preliminary study was performed on analogues: glucose for the cellulose and phenylboronic acid for the polymer. Other mono-saccharides were also investigated to enlarge the application of both methods to other polysaccharides.

II. 1. Bibliography

II. 1. A) Structure of boronic acids

Boronic acids were first discovered by the English scientist Edward Frankland in 1860[1,2] by treating diethylzinc with triethyl borate. They are defined as "a trivalent boron-containing organic compounds that possess one alkyl substituent and two hydroxyl groups"[3]. They have only six valence electrons and a deficiency of two electrons. The vacant p orbital is orthogonal to the three substituents which are oriented in a trigonal planar geometry[3] (**Figure II-1**).

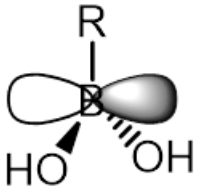

Figure II-1. Boronic acid vacant p orbital and planar structure

Boronic acids cannot be found in nature and ultimately degrade into boric acid[3] $B(OH)_3$. They usually ionise in water as represented in **Figure II-2**. The negative charge is drawn on the boron atom but is actually spread out on the three oxygen atoms[3]. The pK_a of a boronic acid can thus be calculated. The usual method is by an absorbance change at 268 nm that occurs upon conversion from the trigonal form (low pH) to the tetrahedral form (high pH)[4]. For instance, the phenylboronic acid (**Figure II-1** with R being a phenyl group) has a pK_a of 8.8.

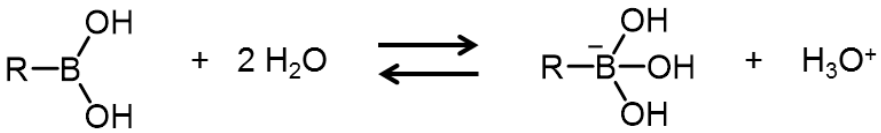

Figure II-2. Ionisation of boronic acids in water

Table II-1 lists the length and energy of some bonds found in the phenylboronic acid. B–C bonds are slightly longer, less energetic, than C–C bonds whereas B–O bonds are really more energetic thus shorter, than C–O bonds. Interestingly, the two B–O bonds do not have exactly the same length probably because of a dimer formation[5] (**Figure II-3**).

Table II-1. Length and energy of several bonds in the phenylboronic acid compared to references

	C–C (ref)	C–O (ref)	B–C	B–O[1]	B–O[2]
Length (Å)	1.54 [a]	1.43 [a]	1.568 [b]	1.378 [b]	1.362 [b]
Energy (kJ.mol^{-1}) [c]	358	384	323	519	519

[a] Average bond length, [b] Data from reference[6], [c] Data from reference[7]

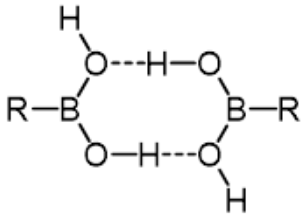

Figure II-3. Structure of a boronic acid dimer

II. 1. B) Properties and applications

In organic chemistry, boronic acids are mostly known for the Suzuki coupling reaction[8,9] that creates C–C bonds (**Figure II-4**). The reaction takes place between a boronic acid and a halide and is catalysed by a palladium catalyst and a base.

Boronic acids are also intensively studied because of their capacity to easily and reversibly bond to diols as detailed below.

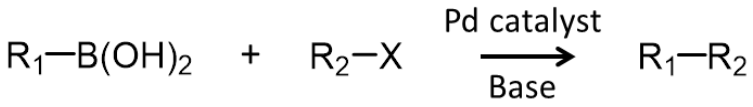

Figure II-4. General pathway for a Suzuki coupling reaction (X being a halogen)

II. 1. B) i) Complexation with diols

The complexation with diols (**Figure II-5**) is favoured at alkaline pH as demonstrated by Wang and coll.[4,10]. The determination of binding constants by the ARS method [method detailed in **Appendix II.I**, p 104] highlighted an increase with the pH. For example, with the phenylboronic acid/glucose system in phosphate buffer the constants are 0.84 M^{-1}, 4.6 M^{-1} or 11 M^{-1} at pH 6.5, 7.5, 8.5 respectively; the predicted optimal pH being 10.6[10] (definition in **Appendix II.I**, p 104). Similar results were obtained with a different binding constant calculation method based on affinity capillary electrophoresis[11].

This property opens widely the applications scope of boronic acids (**Table II-2**).

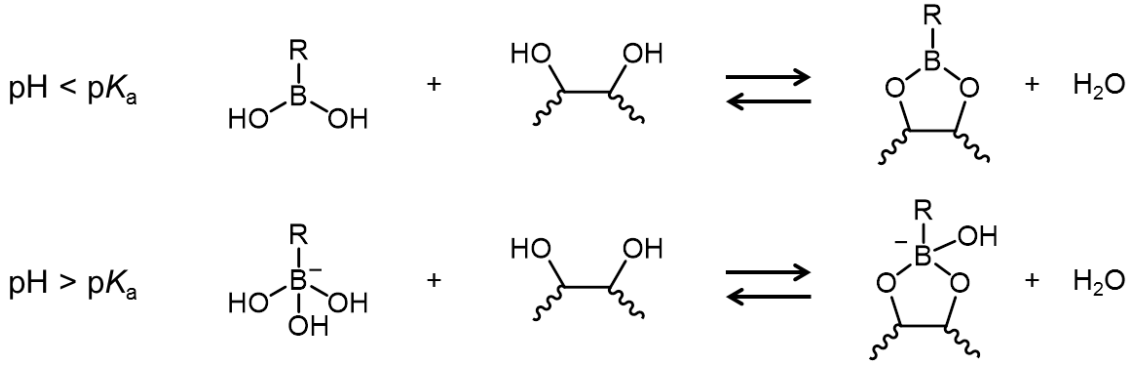

Figure II-5. Complexation of boronic acids on diol depending on the pH

Table II-2. Some applications of boronic acids in different fields

Application field	Property of interest	Reference
Biomedical	Antibacterial, antiviral	Ref [12,13]
	Glucose monitoring	Ref [14]
	Capture and release of cancer cells	Ref [15]
	Drug Velcade®	Ref [16]
	Separation and molecular recognition	Ref [17]
Organic chemistry	Protecting group	Ref [18,19]
	Diol stereoisomer differentiation	Ref [20]
	Determination of enantiomeric excess	Ref [21]
Self-assembly	Self-repairing polymers (poly(dioxaborolane)s)	Ref [22]
Chromatography	Monitoring, identification and isolation of compounds	Ref [23]
Transport	Molecular recognition and transmembrane transport	Ref [24]
Electrochemistry	Sensor for many types of analytes	Ref [25]

II. 1. B) ii) Boronic anhydride

Boronic acids are often found in equilibrium with their anhydride analogue, also called boroxines[26] (**Figure II-6**). They are produced by thermal dehydration or by exhaustive drying over phosphorus pentoxide[27].

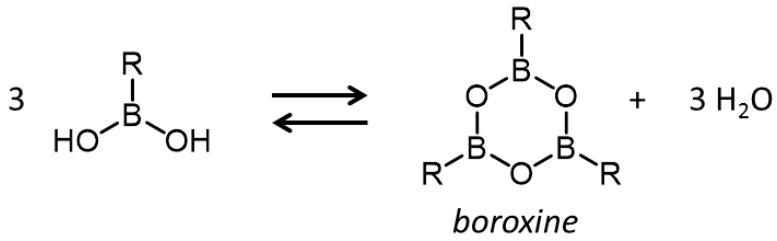

Figure II-6. Scheme of the boronic anhydride formation

Boroxines may possess an aromatic character[28] and have a planar conformation when steric hindrance does not forbid it[26]. Their applications differ from the ones of boronic acid (**Table II-3**).

Table II-3. Some applications of boronic anhydride/ boroxine

Application field	Property of interest	References
Polyelectrolyte	Enhancement of ion dissociation	Ref [29]
Materials	Covalent organic framework (zeolite analogue)	Ref [30]
	Flame retardant material (additives)	Ref [31]
	Non-linear optical materials	Ref [32]

II. 1. B) iii) Particular case of the benzoboroxoles

Benzoboroxoles (**Figure II-7**) were first studied for their ability to complex sugars by Hall and coll. in 2006[33]. Their binding constants (determined by the ARS method) with glucose and fructose at neutral pH were found to be higher than the ones obtained with phenylboronic acid (for glucose 17 M^{-1} *versus* 0 M^{-1} and for fructose 606 M^{-1} *versus* 79 M^{-1} in D_2O[33]). Moreover, this boronic acid does not have an anhydride analogue as the stable form, the 5-bond cycle, cannot rearrange into a boroxine.

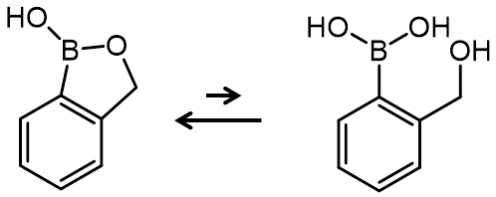

Figure II-7. Structure of benzoboroxole

II. 1. C) Sugar interaction

In the literature, some divergences, which are summarised below, were found concerning the structure of boronic acid/mono-saccharide complexes. The determination of a structure often starts with a methylated analogue on the anomeric position to avoid the pyranose/furanose equilibrium.

II. 1. C) i) Glucose

The complexed form between α- or β-methylglucoside and boric acid in water[34,35], 1-butaneboronic acid in pyridine[36], phenylboronic acid in toluene[37] or benzoboroxoles in phosphate buffer[38] have all the same structure: a complexation on the 4- and 6-positions (**Figure II-8**). However, no complexation was observed in water at pH 9.5[39] as, according to the authors, no diols are coplanar in the methylglucoside molecule.

A complexation on the 2- and 3-positions was also observed when boroxines were added in anhydrous conditions to *Structure MGlu46*[37] (**Figure II-9**).

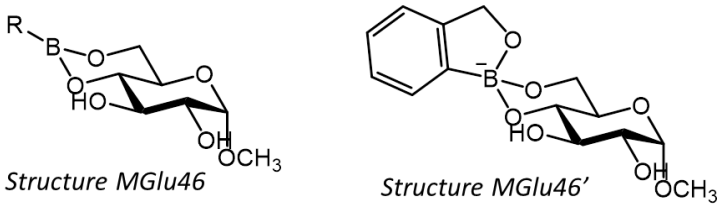

Structure MGlu46 *Structure MGlu46'*

Figure II-8. Structure of complexes on α-methylglucoside with boronic acid (*Structure MGlu46*) and benzoboroxole (*Structure MGlu46'*)

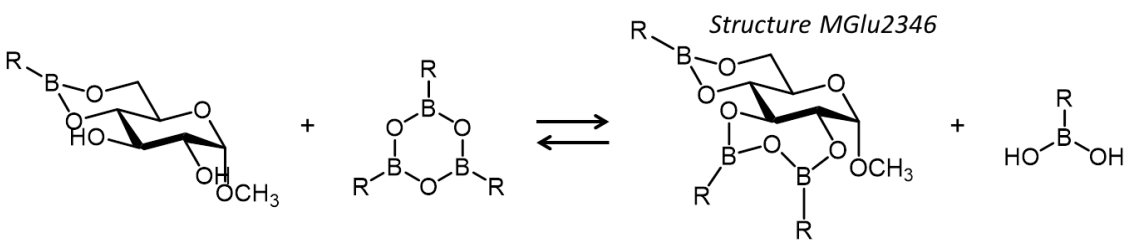

Structure MGlu2346

Figure II-9. Reaction mechanism for the formation of *Structure MGlu2346*

With glucose, two structures are proposed and confronted in the literature. For the one determined by Eggert and Norrild[40], the glucose is under an α-furanose form and two boronic acids are on the 1,2 and 3,5 positions (**Figure II-10**, *Structure Glu1235*). For the other proposed by Shinkai[41], the glucose is under an α-pyranose form and two boronic acids are on the 1,2 and 4,6 positions (**Figure II-10**, *Structure Glu1246*). Eventually, Eggert and Norrild[42] also observed *Structure Glu1246* by using anhydrous glucose in deuterated methanol in a 1:1 ratio with the boronic acid and by instantaneously recording the NMR spectrum. However, the complex rearranged with time into *Structure Glu1235*. *Structure Glu1246* was not detected when monohydrate glucose was used in the same conditions. In conclusion, this study showed that *Structure Glu1246* is only present in non-aqueous conditions and rearranges into the thermodynamically more stable *Structure Glu1235* depending on time and water content. The complexation with boronic acid thus seems to stabilise the furanose form as otherwise the pyranose form is the most stable[43].

Structure Glu1235 was also produced by complexation in deuterated DMSO[40,44,45], in pyridine[36], in water at pH 9.5[39] or in dioxane[46]. However, in D_2O at pH 11, a similar structure was observed with one of the boronic acids under a tridentate form and no free hydroxyl groups (**Figure II-10**, *Structure Glu12356*)[40].

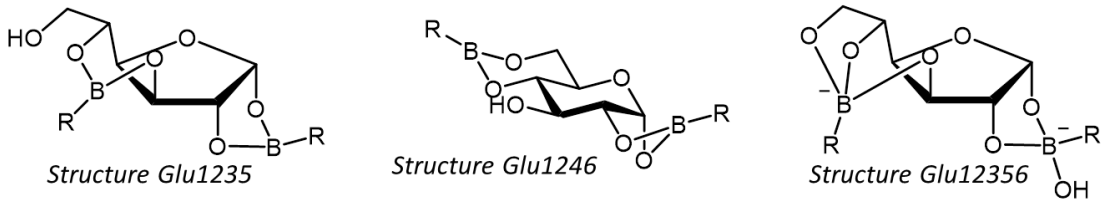

Figure II-10. Structures found in the literature for the complexation of boronic acid on glucose (*Structure Glu1235*, *Glu1246* and *Glu12356*)

II. 1. C) ii) Xylose

Xylose has the same structure as glucose without the 6-hydroxymethyl group. The complexation of xylose in D_2O at pH 9.5[39] formed two kinds of complex: *Structure Xyl12* and *Structure Xyl135* (**Figure II-11**). The authors explained that a complexation on the 3- and 5-positions on *Structure Xyl12* (**Figure II-11**, *Structure Xyl1235*) did not seem likely because of the rotational freedom of the 5-hydroxyl group[39]. This structure, the xylose analogue of *Structure Glu1235* (**Figure II-10**), was however observed while using boric acid[47].

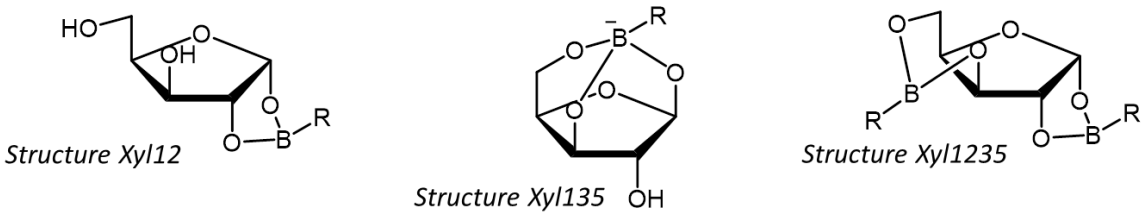

Figure II-11. Structures found in the literature for the complexation of boronic acid on xylose (*Structure Xyl12*, *Xyl135* and *Xyl1235*)

II. 1. C) iii) Galactose

Galactose has the same structure as glucose with the hydroxyl group in the 4-position in axial conformation. The complexation between boronic acid and α-methylgalactose in dry pyridine occurred on the 4- and 6-positions[36] (**Figure II-12**, *Structure MGal46*). As it was also the case with methylglucoside (**Figure II-8**, *Structure MGlu46*, p 76), the conformation of the 4-position does not influence a boronic acid complexation between the 4- and 6-positions on a sugar. With benzoboroxole, the similar complex on the 4,6 positions is less stable than the one on the 3,4 positions[38] (**Figure II-12**, *Structure MGal34'*).

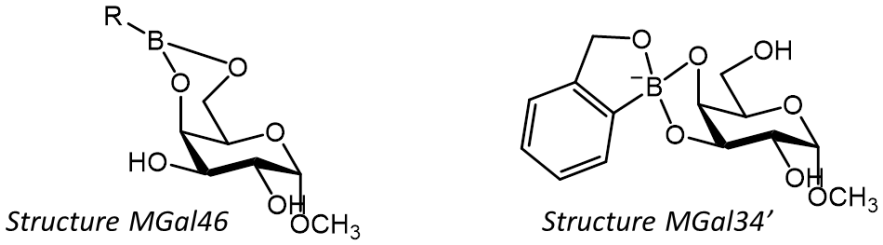

Figure II-12. Structures found in the literature for the complexation on α-methylgalactose of boronic acid (*Structure MGal46*) or benzoboroxole (*Structure MGal34'*)

For boronic acid:galactose ratios of 1:1 or 2:1 in water at pH 9.5, only a tridentate complex was formed on the α-furanose form on the 1-, 2- and 5-positions (**Figure II-13**, *Structure Gal125*)[39]. However, for a 5:1 ratio in the same pH conditions, the complexation occurred on the α-pyranose form on the 1,2 and 3,4 positions (**Figure II-13**, *Structure Gal1234*)[39]. The structure found was confirmed by modelling calculations.

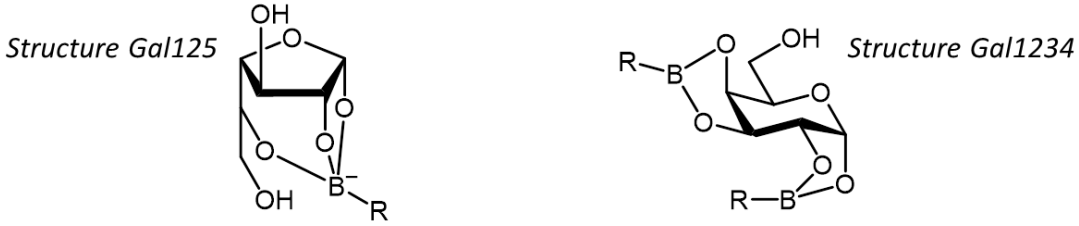

Figure II-13. Structures found in the literature for the complexation of boronic acid on galactose (*Structure Gal125* and *Gal1234*)

II. 1. C) iv) Arabinose

Arabinose has the same structure as galactose without the 6-hydroxymethyl group. The complexation on arabinose with a boronic acid:sugar 2:1 ratio in D_2O at pH 9.5[39] presented two complexes on the α-furanose form: *Structure Ara12* and the tridentate *Structure Ara125* (**Figure II-14**). Both structures are equivalents of *Structure Gal125* (**Figure II-13**). An increase in boronic acid ratio was not studied with arabinose.

Structure Ara12

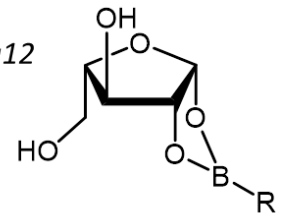

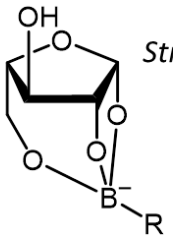

Structure Ara125

Figure II-14. Structures found in the literature for the complexation of boronic acid on arabinose (*Structure Ara12* and *Ara125*)

II. 1. C) v) Mannose

Mannose has the same structure as glucose with the hydroxyl group on the 2-position in axial conformation. With α-methylmannoside in dry pyridine, two boronic acids are complexed on one sugar on the 2,3 and 4,6 positions[36] (**Figure II-15**, *Structure MMAn2346*). The axial and equatorial conformations for 2- and 3-hydroxyl groups, respectively, allow the formation of this complex, which was not observed for α-methylglucoside (except with boronic anhydride).

With mannose, two structures were found in the literature. One of them was observed after complexation in dry pyridine, the sugar was under its α-furanose form with two boronic acids on the 2,3 and 5,6 positions (**Figure II-15**, *Structure Man2356*)[36]. The other one was observed in water at pH 9.5, the sugar is under its β-pyranose form with a tridentate boronic on the 1-, 2- and 6-positions (**Figure II-15**, *Structure Man126*)[39].

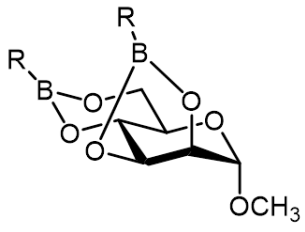

Structure MMan2346

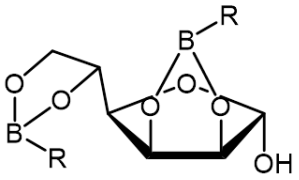

Structure Man2356

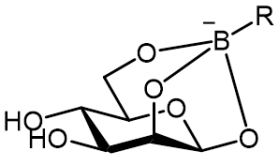

Structure Man126

Figure II-15. Structures found in the literature for the complexation of boronic acid on α-methylmannose (*Structure MMan2346*) or on mannose (*Structure Man2356* and *Man126*)

II. 1. C) vi) Cellobiose

As α-methylglucoside, β-methylcellobiose was also studied for the complexation with boronic anhydrides in toluene. In this case, two boroxines were located on the 2,3 and 2',3' positions and a boronic acid was on the 4'- and 6'-positions[48] (**Figure II-16**, *Structure MC*). Only one free hydroxyl group was left.

For cellobiose in D_2O at pH 9.5, the authors considered that β-1,4 linkage between the two anhydroglucose units prevented the rearrangement into furanose[39]. Hence, it was proposed that a boronic acid could only be located on the reducing end ring on the 1- and 2-positions of the α-form, as it supposedly is the only coplanar diol function present on the molecule (**Figure II-16**, *Structure C12*).

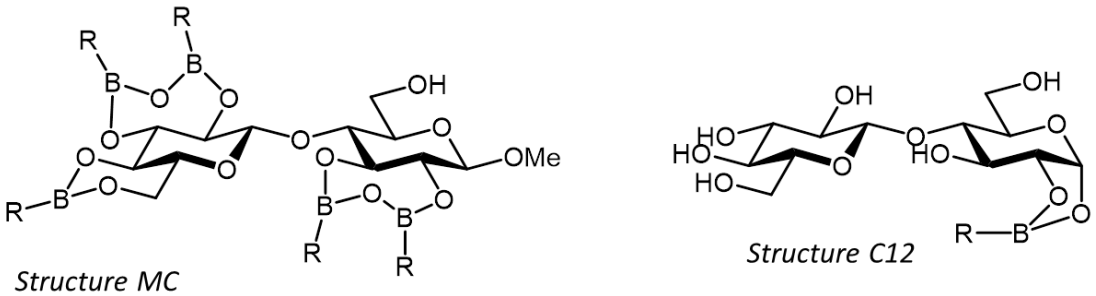

Structure MC *Structure C12*

Figure II-16. Structure of β-methylcellobiose complexed with boroxines (*Structure MC*) or the most probable structure of cellobiose complexed with boronic acid (*Structure C12*)

II. 2. Acid / Anhydride equilibrium

Before starting the study of complexation on sugars, the behaviour of phenylboronic acid (PBA) in several solvents was investigated.

PBA after a treatment at 70°C for several days and neat PBA were analysed by NMR spectroscopy in $CDCl_3$. Increasing the anhydride ratio allowed to assign the corresponding ^1H NMR signals to each compounds. The same approach was done in DMSO-d_6, a hydrophilic solvent (**Figure II-17**).

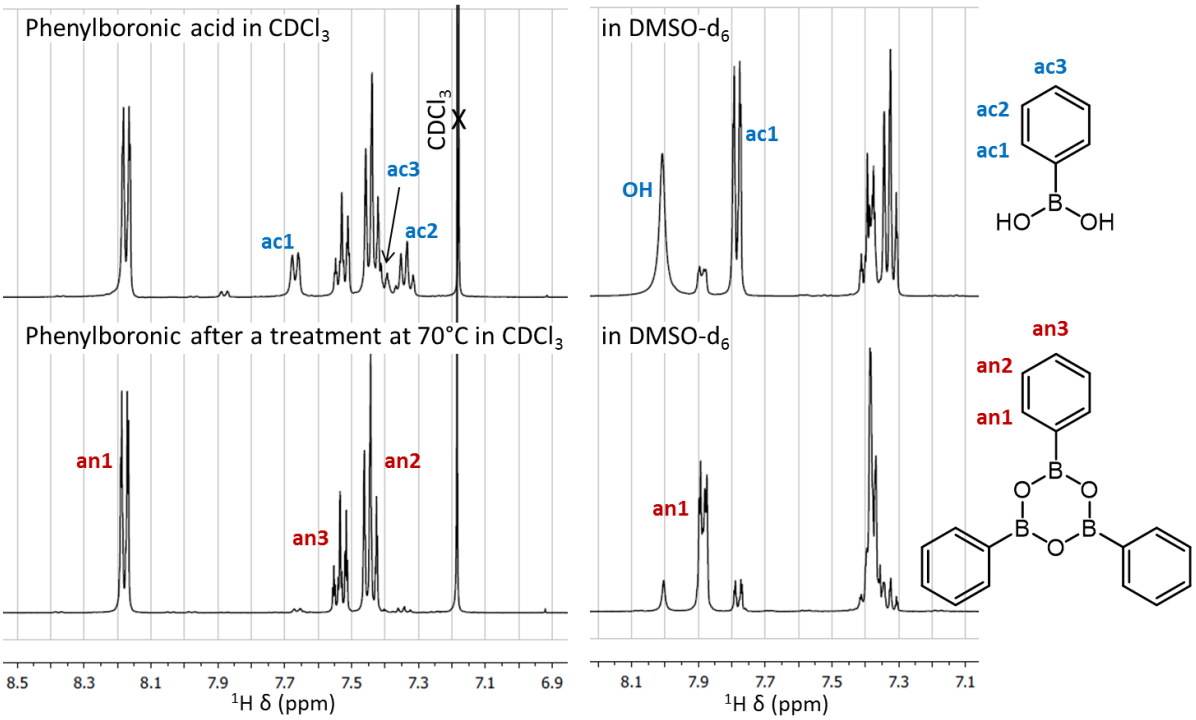

Figure II-17. Comparison of ^{1}H NMR spectra in $CDCl_3$ (left) or DMSO-d_6 (right) of neat PBA (above) or PBA after treatment at 70°C (below)

Acid and anhydride have specific NMR signals, some of which were attributed by integrations and ^{1}H-^{1}H 2D NMR analysis (COSY). The acid:anhydride ratio can then be calculated according to **Equation I-1**. The calculation is based on integrals ratio so no external reference is needed.

$$\tau_{an} = \frac{I_{an1}}{I_{an1} + 3I_{ac1}} \qquad \textbf{Equation II-1}$$

*With I_{an1} the intensity of the peak **an1** and I_{ac1} the intensity of the peak **ac1** (peaks defined in **Figure II-17**). **an1** and **ac1** correspond to 6 and 2 protons respectively.*

Then, the spectra were recorded from time to time over several days and the anhydride:acid ratio against time was plotted for different solvents (**Figure II-18**). Hydrophobic solvents, represented by circles, promoted the anhydride whereas hydrophilic solvents, represented by triangles, break them thus engendering the acid form. While DMSO-d_6, THF-d_8 and MeOD could go as far as 100% of the acid form, for toluene-d_8 and $CDCl_3$ a thermodynamic equilibrium between the two entities seems to be reached.

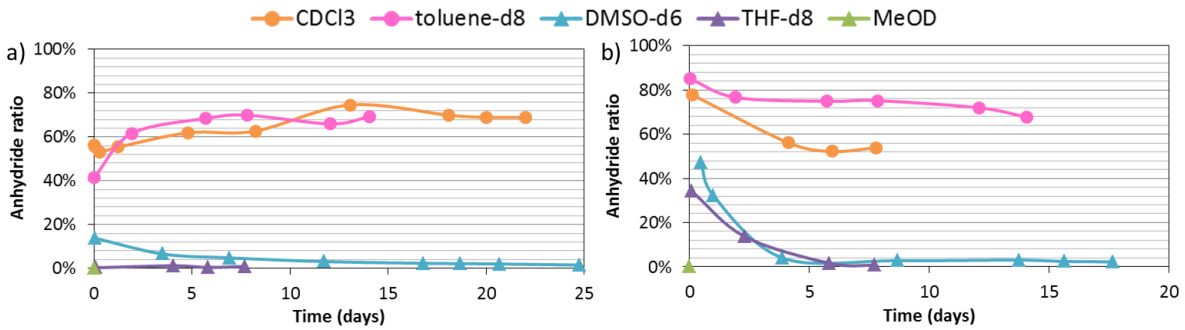

Figure II-18. Evolution of the anhydride ratio in different solvents starting from a) phenylboronic acid or b) PBA after treatment at 70°C

Then, the stability of the anhydride against complexation was investigated. An NMR tube containing phenylboronic anhydride in $CDCl_3$ was prepared and a diol was added into the tube. The three peaks corresponding to **ac1** for the acid, **an1** for the anhydride (**Figure II-17**) and **c1** for the complex (**Appendix II.II**, p 106) could be identified. The ratio of each compound could then be determined using the corresponding integrations (as explained in **Appendix II.II**, p 106).

With pinacol and 4-methylcatechol, the complexation was so fast and complete that only the complex was observed directly after introoduction. With α-methylglucoside, anhydrides were broken in less than two days but then the complex and the acid alone reached an equilibrium (**Figure II-19a**). This observation was unexpected as the acid should not be promoted in this solvent but as the experiment was done over a long period of time, some water could have disturbed the results. For glucose, both the phenylboronic acid and anhydride formed a complex after 30h (**Figure II-19b**). This experiment also indicated that, for glucosides, the equilibrium was displaced toward the complex formation in $CDCl_3$. With cellobiose, no complexation was observed meaning that it was not soluble enough in this solvent for the complexation to occur and for the equilibrium to be shifted.

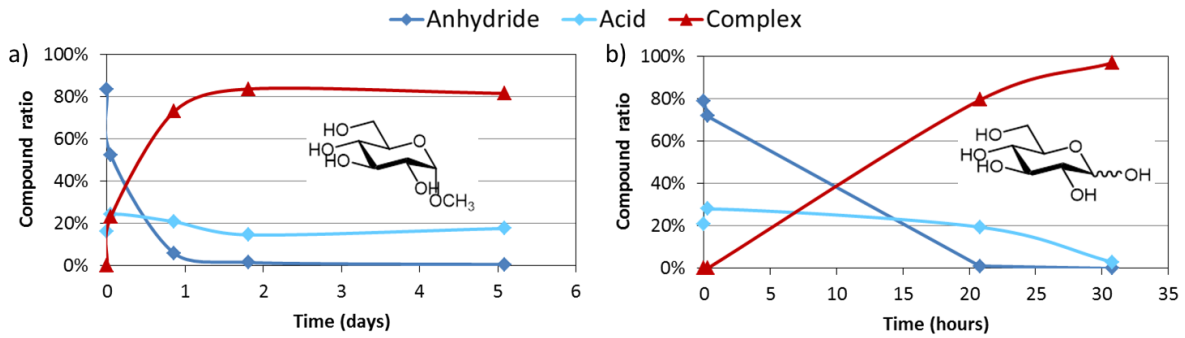

Figure II-19. Stability of the phenylboronic anhydride against complexation in $CDCl_3$ with a) α-methylglucoside and b) glucose

II. 3. Complexation on glucosides

To ascertain the structure of phenylboronic acid/sugar complexes, DMSO-d_6 was selected to record the ^{1}H NMR spectrum as the signals of the hydroxyl groups can be observed in this solvent and their positions on the sugar determined. The location of the boronic acid could then be deduced as the protons of the hydroxyl groups, involved in the complexation, are removed.

II. 3. A) Complexation of the phenylboronic acid on methylglucoside

The structure determination of the PBA:glucose complex started with the study on methylglucoside to avoid the pyranose/furanose equilibrium. Moreover, it is a model of the cellulose backbone and of the non-reducing end.

Several ratios of PBA and α-methylglucoside were prepared and directly dissolved in DMSO-d_6 (**Figure II-20**). Considering the number of signals between 7.5 and 8.0 ppm, only one complex seemed to be formed and its structure did not change with the PBA: α-methylglucoside ratio.

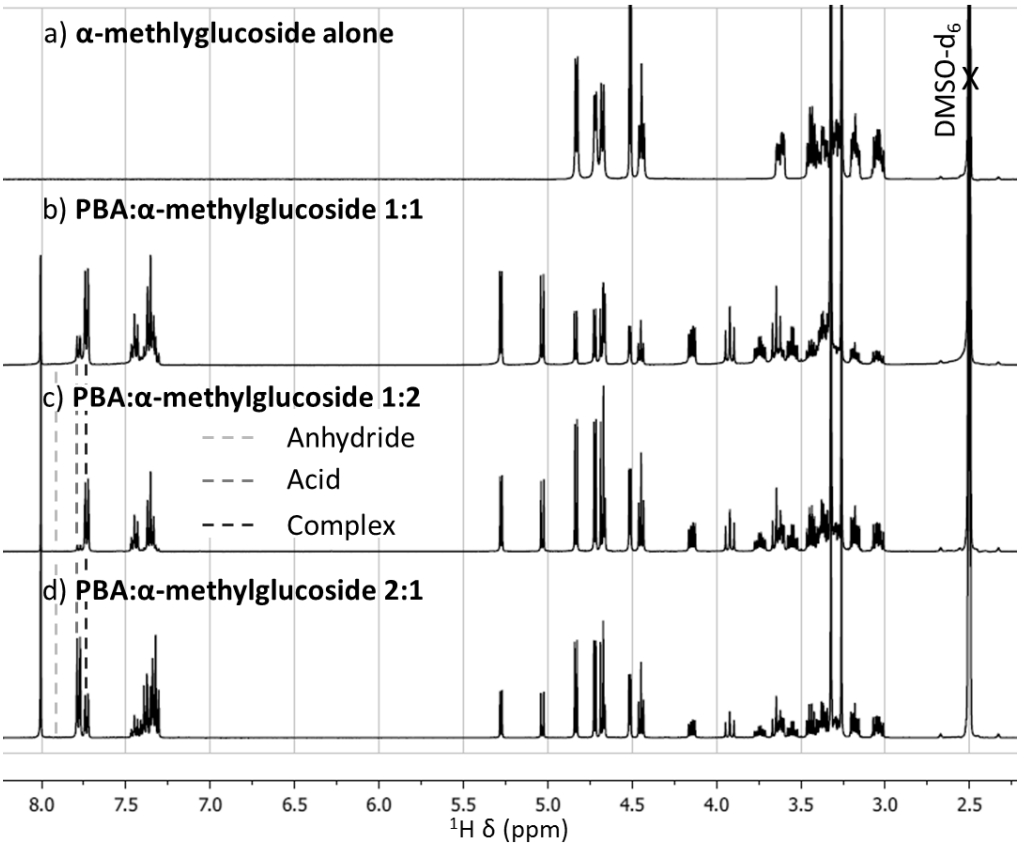

Figure II-20. ^{1}H NMR spectra of PBA and α-methylglucoside mixtures in DMSO-d_6

Further analyses were then performed on the mixture with a 2:1 ratio to avoid the overlapping of NMR signals between free α-methylglucoside and complex. The position of

the CH_2 group was deduced from the ^{1}H-^{13}C 2D NMR analysis (HSQC) as well as the signals corresponding to hydroxyl groups (**Figure II-21b**). Then, the COSY allowed to attribute the proton spectrum starting from the protons attributed to the CH_2 group on the 6-position (**Figure II-21a**) and the carbon spectrum was finally attributed *via* the HSQC (**Figure II-21b**). The remaining two free hydroxyl groups were bound to the 2- and 3-positions which corresponds to *Structure MGlu46* with a complexation on the 4- and 6-positions as represented on **Figure II-21b** and as previously observed in the literature[34–37].

The same structure was obtained with β-methylglucoside (**Appendix II.III**, p 107).

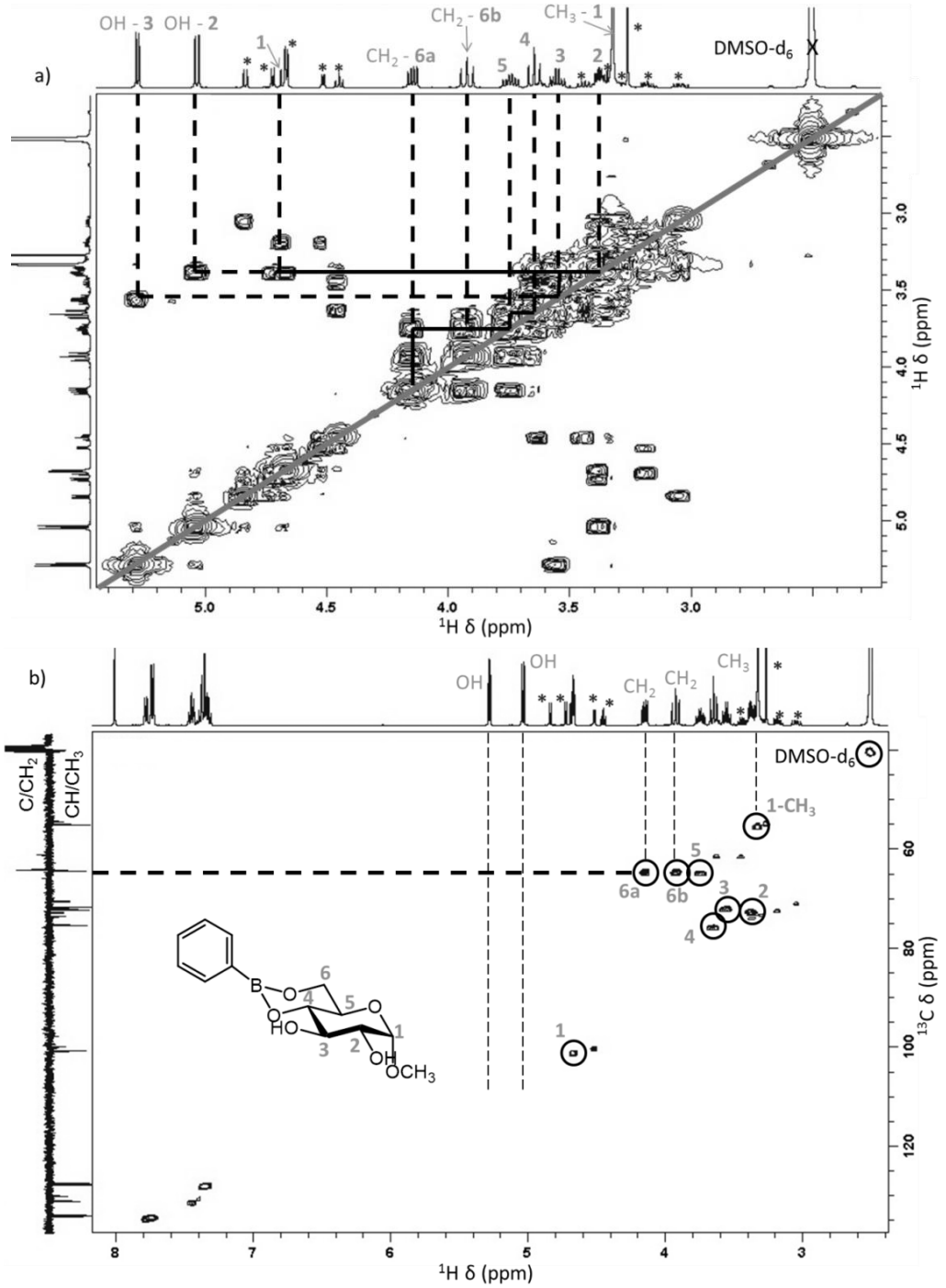

Figure II-21. a) COSY and b) HSQC of PBA:α-methylglucoside 2:1 in DMSO-d_6 – The stars correspond to free α-methylglucoside

II. 3. B) Complexation of the phenylboronic acid on glucose

As for α-methylglucoside, several ratios of PBA and glucose were prepared and the evolution of the spectrum were observed and recorded over several days. **Figure II-22** represents the ^{1}H NMR spectra of glucose alone and the three studied ratios taken at the same reaction time (10 days). The ratios PBA:glucose 1:1 and 1:2 seemed to be a mixture of several compounds whereas for the ratio 2:1 one structure was dominant because of the small number of peaks in the 3.5 - 6.5 ppm range (**Figure II-22d**).

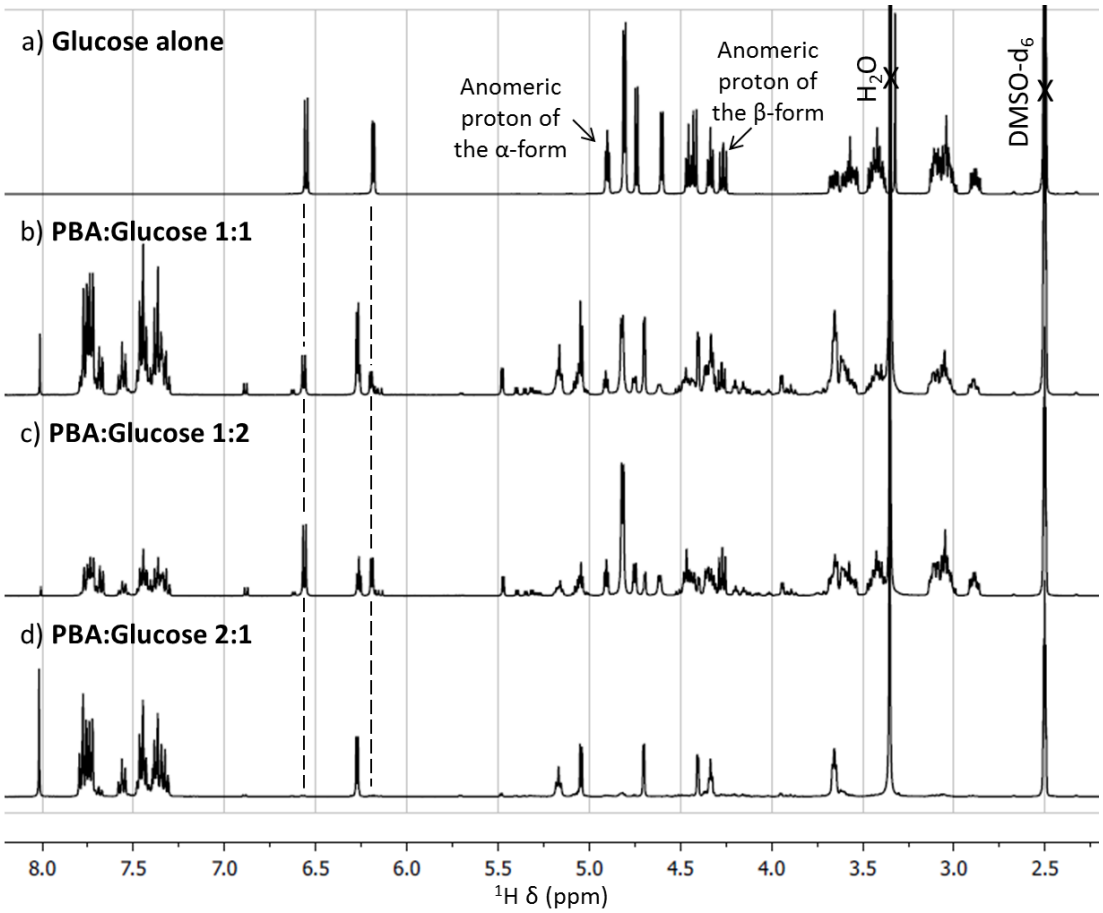

Figure II-22. ^{1}H NMR spectra of glucose alone and three PBA:glucose ratios after 10 days in deuterated DMSO

II. 3. B) i) Determination of the complexes structure

The ratio PBA:glucose 2:1 was analysed further by ^{13}C NMR, COSY and HSQC (**Appendix II.IV**, p 108). Only one free hydroxyl group was observed and the COSY analysis revealed a correlation with the peak at 3.66 ppm whose integration was consistent with the CH_2 on the 6-position. All the other positions were involved in the complexation.

To determine whether the sugar was under the pyranose or the furanose form, several criteria, listed in **Table II-4**, can be considered.

Table II-4. NMR criteria indicating a furanose form

Name	Criteria indicating a furanose form	Reference
^{1}H criterion	The anomeric proton ^{1}H chemical shift increment between the complexed and un-complexed sugar is above 0.6 ppm	Ref [39]
^{13}C criterion	All the carbons and especially the anomeric one have higher ^{13}C chemical shift (usually chemical shift of the anomeric carbon above 100 ppm)	Ref [35,40,42,49]
$J_{H\text{-}H}$ criterion	The proton-proton coupling constants $J_{2,3}$ and $J_{3,4}$ are small thus excluding the vicinal diaxial arrangement of the protons	Ref [36,40]

In this case, the anomeric proton had a ^{1}H chemical shift of 6.28 ppm, which was 1.38 ppm higher than the one of α-glucose (4.90 ppm) and 2.02 ppm higher than the one of β-glucose (4.26 ppm) (**Figure II-22a** and **20d**). Its ^{13}C chemical shift was 104.1 ppm (**Figure II-23**) and the coupling constants $J_{2,3}$ (1.8 Hz) and $J_{3,4}$ (2.5 Hz) were small (**Appendix II.IV**, p 108). All the conditions were thus fulfilled to conclude that the sugar was under the furanose form.

Finally, steric considerations implied that the furanose was in α-configuration otherwise the hydroxyl groups on the 1- and 2-positions are not coplanar and the complexation cannot take place[39].

Based on all these conclusions, the structure of the complex observed was the same as *Structure Glu1235* (**Figure II-10**, p 77) determined in the literature as the most stable one. The glucose is under the α-furanose form with two boronic acids on the 1,2 and 3,5 positions as represented on **Figure II-23**.

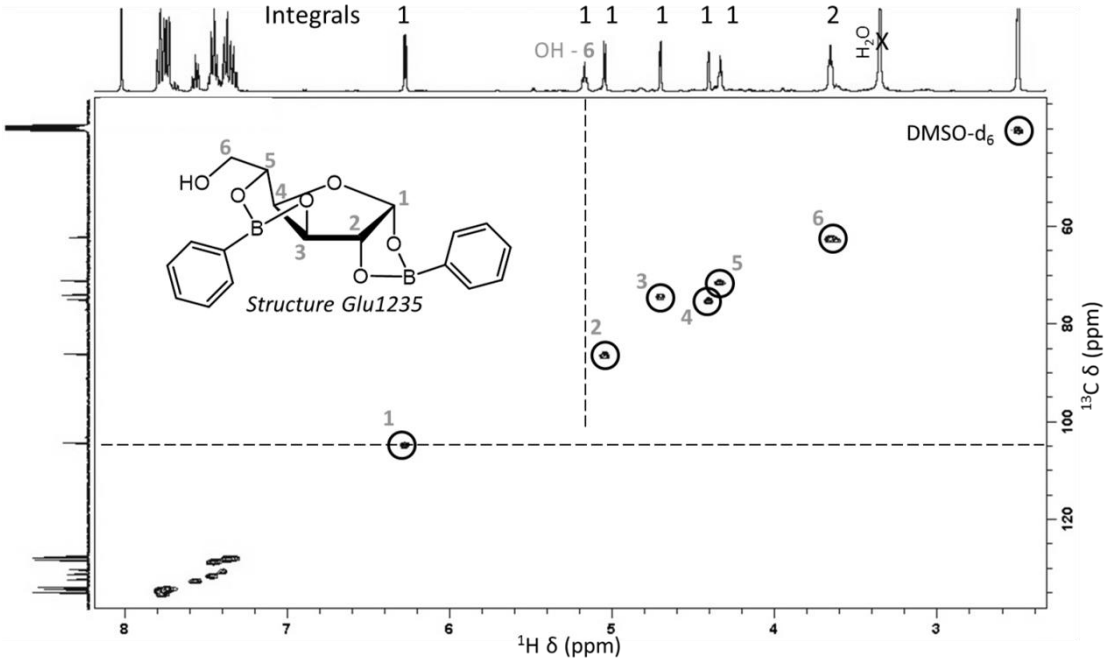

Figure II-23. Attributed HSQC for the 2:1 PBA:glucose ratio in DMSO-d$_6$

Identifying the structure of all the compounds present in the 1:1 and 1:2 ratios from the ^{1}H NMR spectra would be quite difficult because of signals overlapping. Consequently, the ^{13}C NMR spectrum was further investigated.

Two unidentified anomeric carbons with chemical shifts close to the ones of free glucose were observed by ^{13}C NMR after 8h in DMSO-d_6 (**Figure II-24**, see **Appendix II.V** for the full ^{13}C NMR spectra, p 109). The chemical shifts of the corresponding protons had an increment lower than 0.25 ppm compared to free glucose. The ^{1}H and ^{13}C criterion implied that the glucose of the undetermined complex was under a pyranose form (proton coupling constants were not calculated because of signal overlapping). The two anomeric protons might correspond to the α- and β- forms because of the closeness and likeness of the peaks so the 1-position seemed to be free.

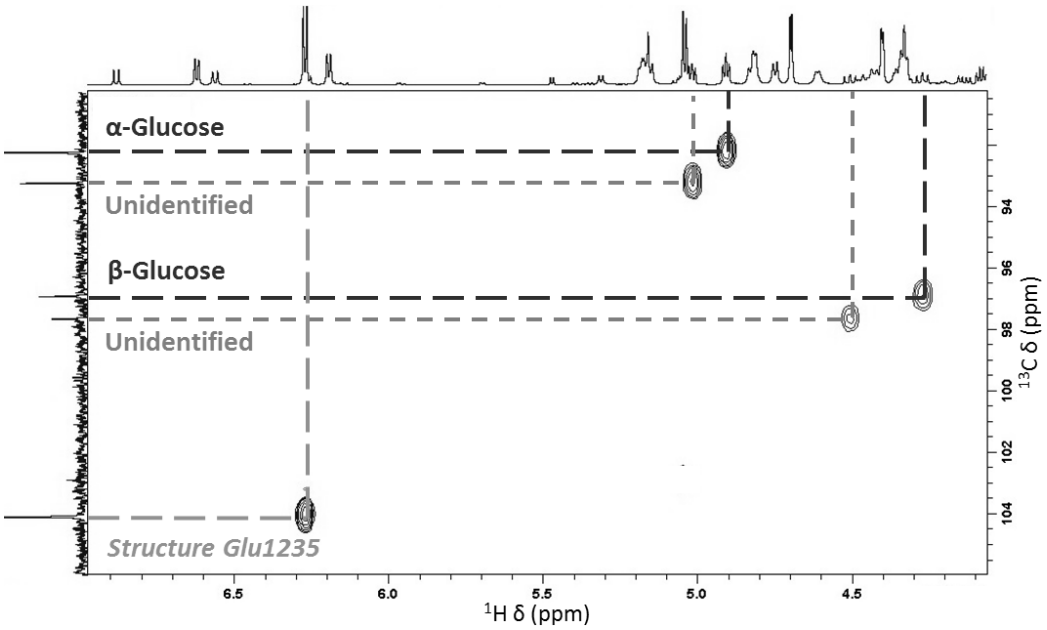

Figure II-24. HSQC in DMSO-d_6 of the 1:1 PBA:glucose ratio zoomed on the anomeric carbons – Reaction time: 8h

To try to go further in the identification of these complexes, DOSY NMR experiments were performed. The DOSY is a 2D NMR analysis that gives the plot of the ^{1}H NMR spectrum *versus* the diffusion constant. Among other parameters, this diffusion constant depends on the molar mass and a difference of around 100 g.mol^{-1} can be detected[50]. The molar mass of PBA being 122 g.mol^{-1}, this method would thus indicate whether the complex possessed one or two boronic acids (**Figure II-25**). According to the diffusion coefficient of the peaks that were attributed on **Figure II-24**, the undetermined complex seemed to bear only one boronic acid. Unexpectedly, the undetermined complex had the same diffusion coefficient as glucose.

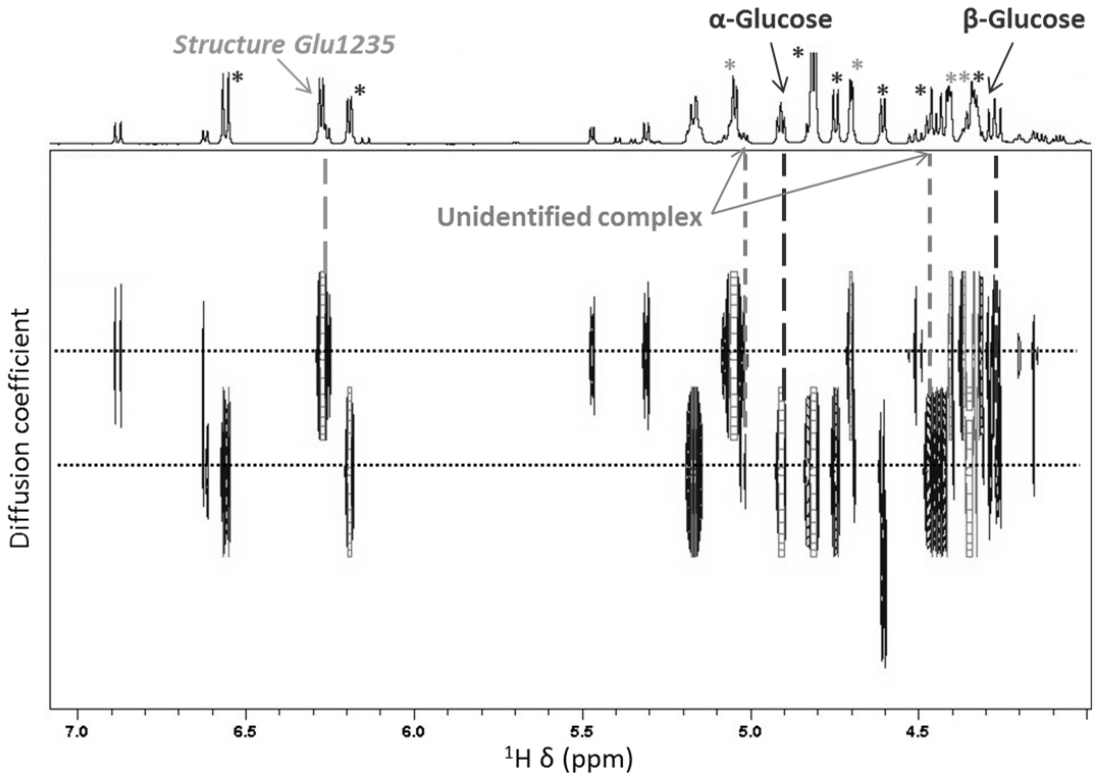

Figure II-25. DOSY in DMSO-d_6 of the 1:1 PBA:glucose ratio (light grey stars corresponds to *Structure Glu1235* and dark grey ones to free glucose)

To summarise, only one boronic acid was complexed on the pyranose form and the anomeric position seemed to be free. Based on the literature and on the study with methylglucoside, the conclusion would be that the complexation probably occurred on the 4- and 6-positions. The structure formed was thus supposedly *Structure Glu46*.

The evolution of the ratio between these complexes with time could give information about the transformation mechanism.

II. 3. B) ii) Evolution with time

Because of ^{1}H NMR signals overlapping, the ratio between the compounds could not be accurately calculated.

For the 1:1 PBA:glucose ratio (**Figure II-26**), the disappearance of the second complex was clearly observed confirming its lower stability compared to *Structure Glu1235*. With the 1:2 and 2:1 PBA:glucose ratios (**Appendix II.VI**, p 110), the conclusions were the same only the evolution rate changed.

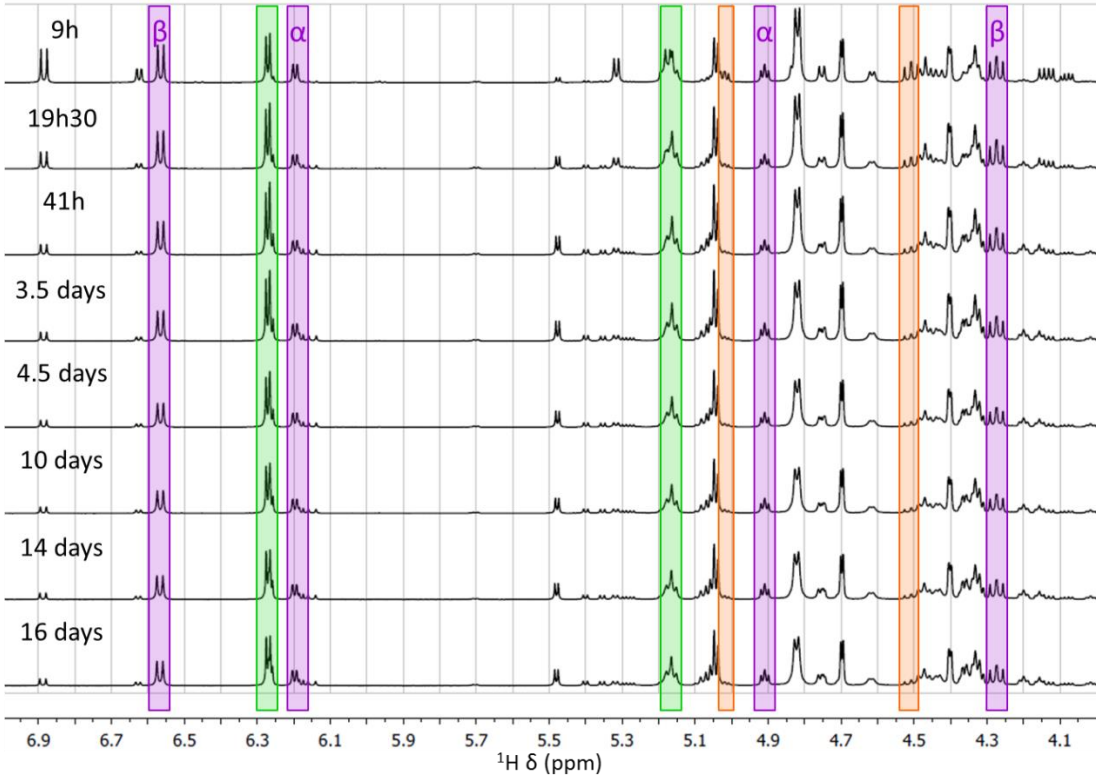

Figure II-26. Evolution with time of the 1:1 PBA:glucose ratio in DMSO-d_6 (peaks highlighted in purple correspond to free α- or β-glucose, in green to *Structure Glu1235* and in orange to the second complex)

Finally, the mechanism proposed in **Figure II-27** is in line with the one previously established by Eggert and coll.[42] except for the structure of the first complex.

First, *Structure Glu46* is formed but then evolves to the more thermodynamically stable *Structure Glu1235*. Unfortunately, the 4-position, necessary for the furanose rearrangement (**Figure I-5**, p 20), is not free leading to a likely decomplexation. Some water coming from the complexation and the hygroscopic character of DMSO allows this process. Then, the boronic acid complexes the 3,5 positions to stabilise the furanose form. As this complex is not detected, the complexation of the second boronic acid must happen quickly leading predominantly to the stable *Structure Glu1235*.

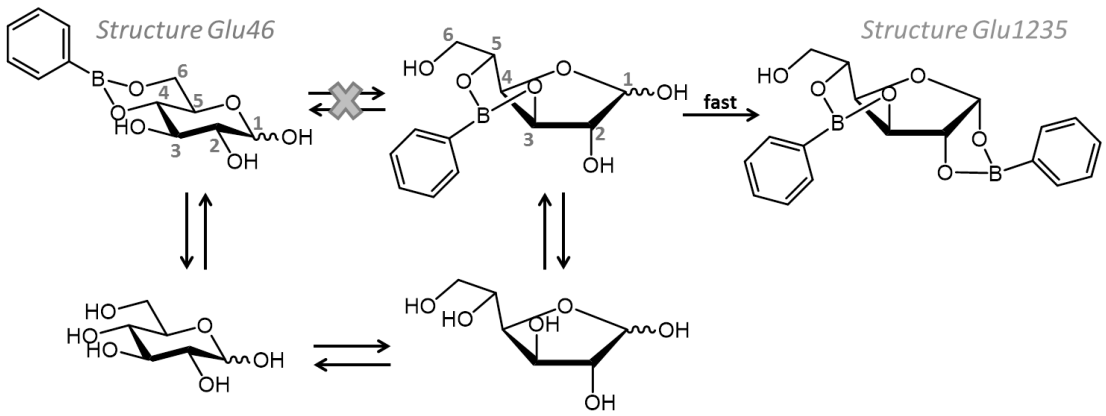

Figure II-27. Mechanism proposed for the evolution of the complexes of PBA on glucose

Both the identified structures involve either the 1- or the 4-positions which are not available along the cellulose backbone. This means that the complexation would only occur at the cellulose extremities where these positions are free.

Thankfully, a complexation on the 2- and 3-positions, available all along the cellulose backbone, was found in the literature by complexation of the boronic anhydride on the α-methylglucoside[37] (**Figure II-8**, *Structure MGlu2346*, p 76). This kind of complexation will thus be investigated.

II. 3. C) Complexation of the phenylboronic anhydride

II. 3. C) i) Methylglucoside

The same protocol performed by Liebert and coll.[37] to complex boronic anhydride on α-methylglucoside was reproduced. It involved the formation of boronic anhydride in toluene at 100°C and the addition of α-methylglucoside for the complexation. The boronic acid ratio had to be increased with respect to the 3:1 stoichiometry of the complex. After a 6h reaction, the ^{1}H NMR spectrum of the complex was recorded in DMSO-d_6 and was in accordance with the structure observed previously with α-methylglucoside except for the reduction of the two hydroxyl groups signals (**Figure II-28**). This confirmed the formation of *Structure MGlu2346*. No free α-methylglucoside was observed because of its insolubility in toluene.

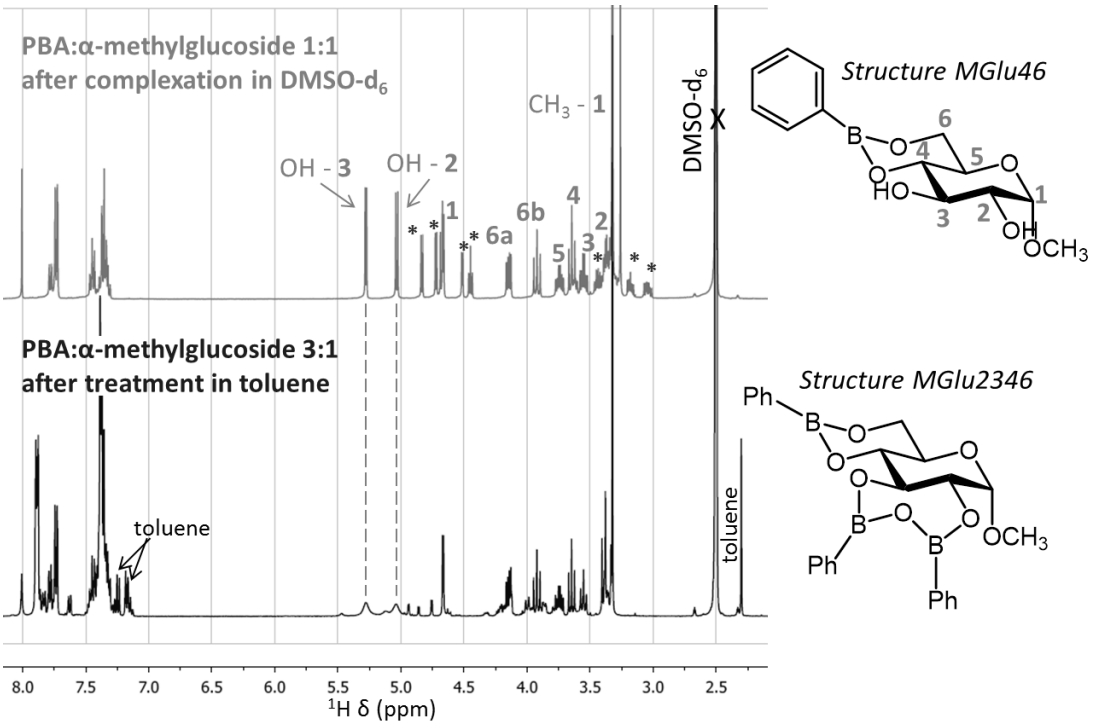

Figure II-28. Comparison of the ^{1}H NMR of the complex of PBA:α-methylglucoside obtained in DMSO-d_6 or after treatment in toluene (the stars correspond to the free α-methylglucoside)

This kind of complex could never be observed directly in DMSO-d_6 as this solvent breaks the anhydride to form the acid (**Figure II-18**, p 82). However, chloroform favoured the anhydride formation and complexation in this solvent was already observed even though the structure of the complex had not been determined (**Figure II-19a**, p 82).

A 3:1 PBA:α-methylglucoside ratio was solubilised overnight in chloroform at room temperature. The sugar not solubilised was removed by filtration before evaporating the solvent. The complex was then studied in DMSO-d_6 to observe the hydroxyl groups. The same complex as the one obtained after toluene treatment was observed with even smaller hydroxyl groups peaks (**Figure II-29**). The complexation in chloroform had several advantages over the treatment in toluene such as milder conditions and a more easily removed solvent.

The complexation in chloroform is thus the protocol chosen to obtain the complexes on different sugars but an analysis in DMSO-d_6 is still necessary to determine their structure.

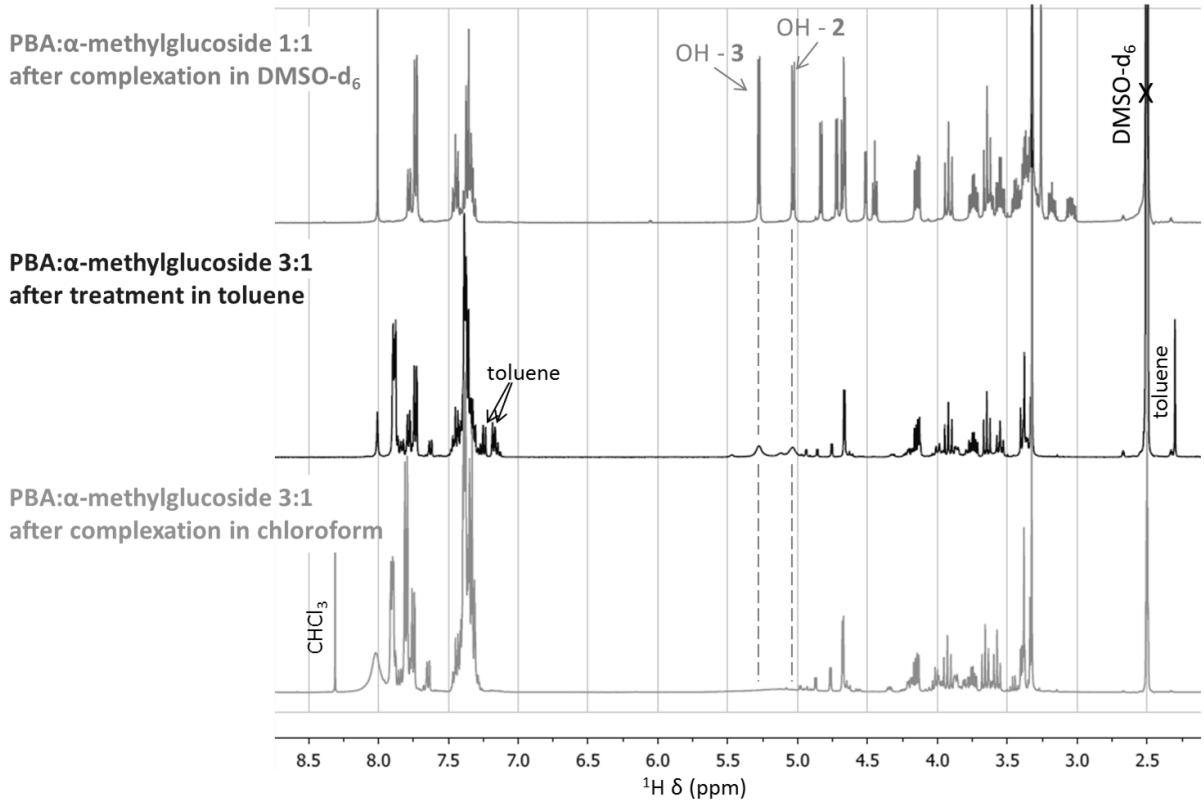

Figure II-29. Comparison of the ^{1}H NMR of the complexes of PBA:α-methylglucoside obtained in DMSO-d_6, after treatment in toluene and after complexation in chloroform

The same protocol was performed on β-methylglucoside and the same result was obtained with a complexation of the boronic anhydride on the 2,3 positions (**Figure II-30** and **Appendix II.VII**, p 111). The coupling constant $J_{2,3}$ was found to be 9.1 Hz, which is high as it is a pyranose form.

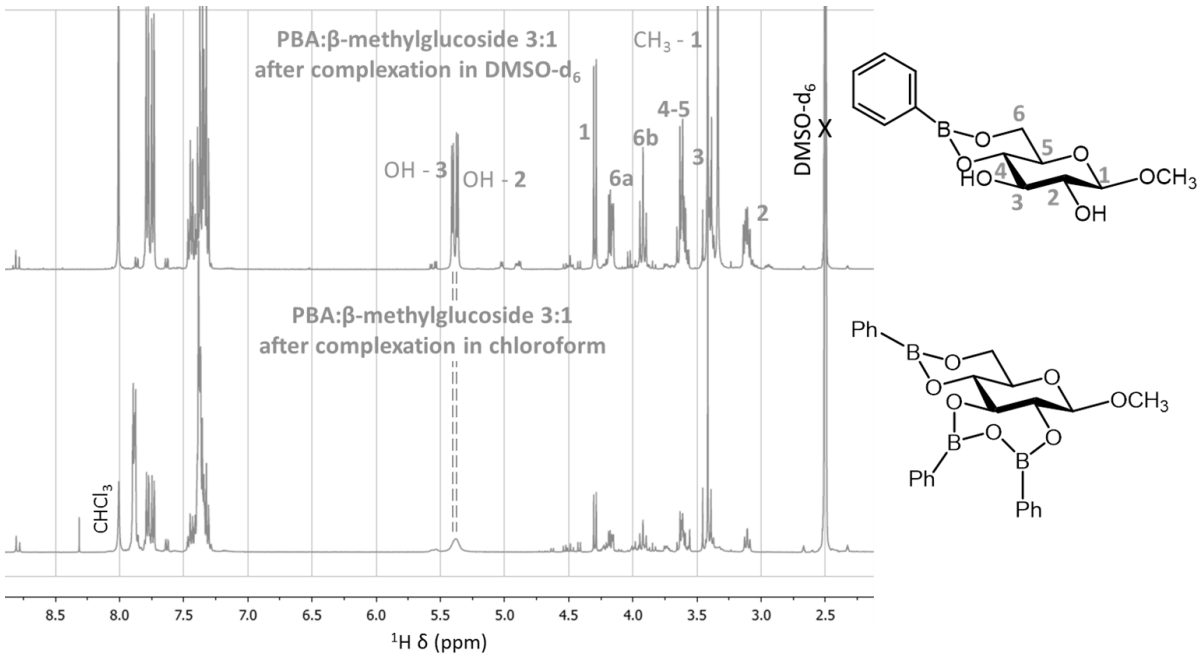

Figure II-30. Comparison of the ^{1}H NMR of the complexes of PBA:β-methylglucoside obtained in DMSO-d_6 and after complexation in chloroform

II. 3. C) ii) Glucose

Glucose and PBA complexation was also performed in chloroform. Interestingly, the resulting compound corresponded to *Structure Glu1235* (**Figure II-31**). Complexation in chloroform was thus a faster way to produce and isolate this complex. However, a complexation of the boronic anhydride on the 2- and 3-positions of glucose did not occur.

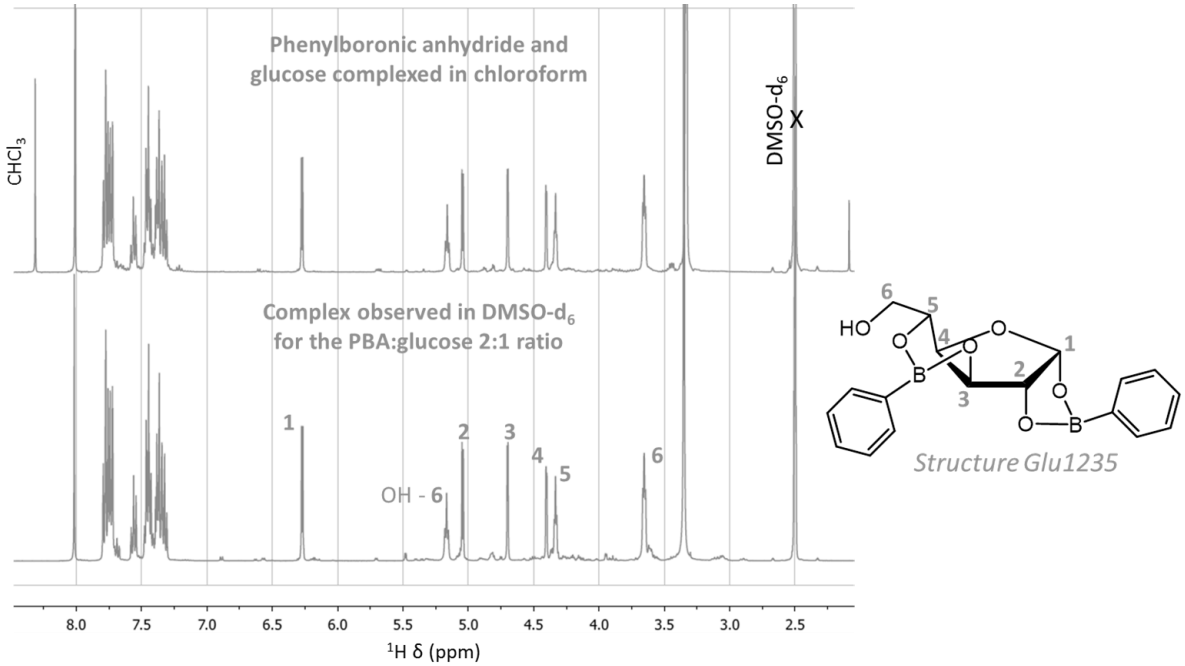

Figure II-31. Comparison of the ^{1}H NMR of the complexes of PBA:glucose obtained after complexation in chloroform or in DMSO-d_6

To the best of our knowledge, the complexation in chloroform was never studied in the literature. The structures obtained with other saccharides by this method were thus determined. But beforehand, the study of the complexation of boronic acid on glucoside will be completed with the phenylboroxole.

II. 3. D) Complexation of phenylboroxole

II. 3. D) i) In DMSO-d_6

The ^{1}H NMR spectrum in DMSO-d_6 of the 2:1 phenylboroxole:α-methylglucoside ratio corresponded to the sum of the spectra of the two entities alone even after several days (**Figure II-32**). As no shift in the NMR signals were observed, the complexation between these two entities did not occur.

The same observation was made for glucose and cellobiose (**Appendix II.VIII**, p 112).

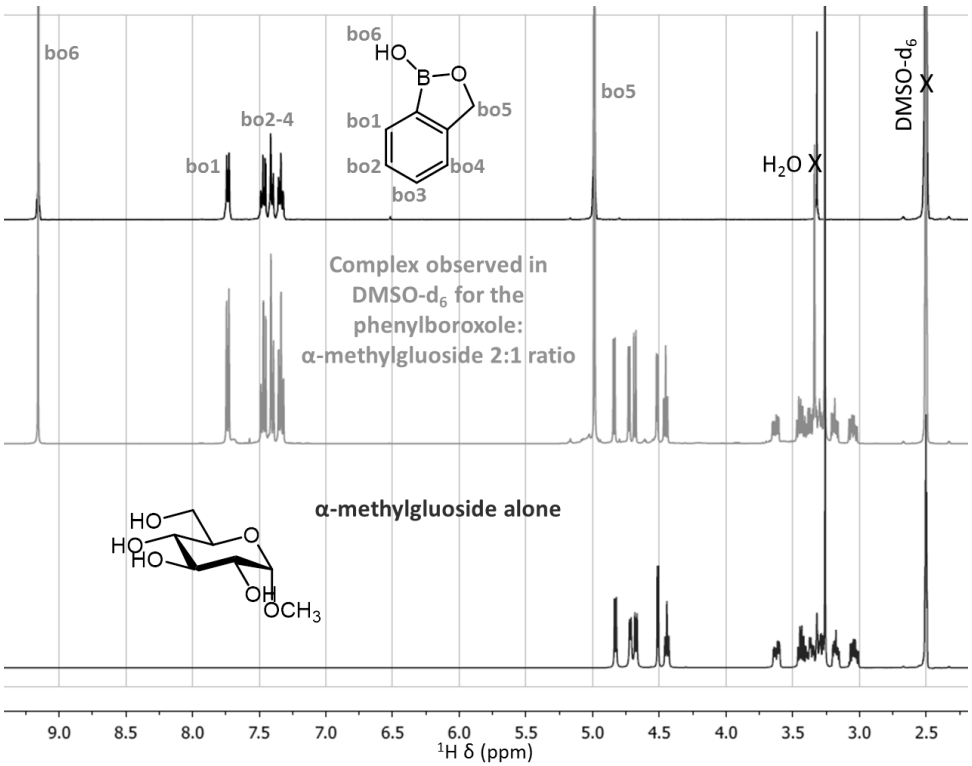

Figure II-32. ^{1}H NMR spectra of phenylboroxole alone, 2:1 phenylboroxole:α-methylglucoside ratio and α-methylglucoside alone in DMSO-d_6

II. 3. D) ii) In chloroform

As done previously in §II. 2 (p 80), glucose was added in a NMR tube containing phenylboroxole in $CDCl_3$. Even after five days, no new aromatic peaks corresponding to a complex had appeared so the complexation in chloroform also did not occur.

II. 3. D) iii) In D_2O

In the literature, the complexation between phenylboroxole and glucose occurred in water at neutral pH. These conditions were performed on a 1:1 ratio in D_2O. Unfortunately, even after 44h, no complexation was observed (**Figure II-33**). Phenylboroxole was found to be not entirely soluble in water. Even at higher pH by addition of NaOD, no complexation was observed as the spectrum of the mixture was the addition of the two spectra of the species alone. The pH did not seem to have an effect on the phenylboroxole solubility. Moreover, after a few days the glucose started to degrade.

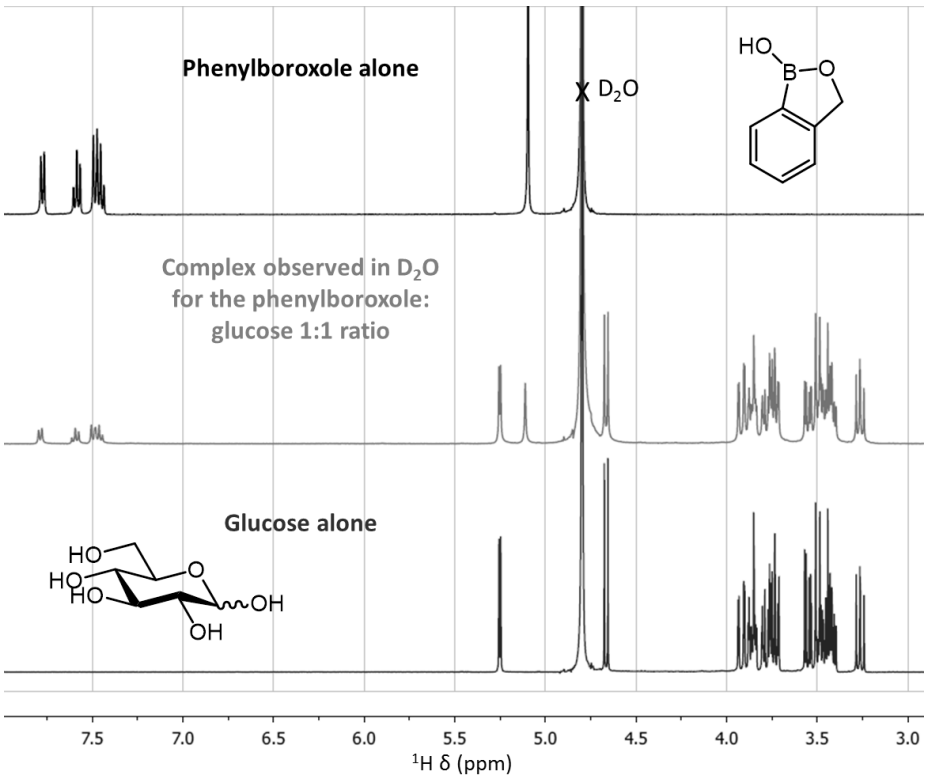

Figure II-33. ^{1}H NMR spectra of phenylboroxole alone, 1:1 phenylboroxole:glucose ratio and glucose alone in D_2O

Because of the impossibility to observe a complexation with phenylboroxole, this particular boronic acid was forsaken for the rest of the study.

II. 4. Complexation on other saccharides

As already mentioned the complexation in chloroform was not studied in the literature. Other monosaccharides were thus studied to enlarge the oligomer producing methods to polysaccharides other than cellulose.

II. 4. A) Complexation on D-xylose

After complexation in chloroform, no hydroxyl group was observed on the 2:1 PBA:xylose complex (**Appendix II.IX**, p 113) meaning that there are two boronic acids per sugar.

The anomeric proton chemical shift had an increment of 1.5 ppm (**Figure II-34a** and **b**), the anomeric carbon had a chemical shift of 104.9 ppm and the coupling constants $J_{2,3}$ (0.8 Hz) and $J_{3,4}$ (2.6 Hz) were small (**Appendix II.IX**, p 113) confirming a furanose form. In light of steric considerations, the sugar was under the α-furanose form with a complexation on the 1,2 and 3,5 positions. Obtaining *Structure Xyl1235* (**Figure II-11**, p 78) contradicts Nicholls and Paul's hypothesis[39] which was that the rotational freedom of the 5-hydroxyl prevents a complexation on this position.

The same complex was also obtained from complexation in DMSO-d_6 with a 2:1 PBA:xylose ratio (**Figure II-34c**). With the 1:1 ratio in DMSO-d_6, another complex was observed (**Figure II-34d**, orange arrows) but the structure was not determined. Our hypothesis, considering the boronic acid:xylose ratio and the chemical shifts of the peaks, was that the sugar was under the furanose form with a boronic acid either on the 1,2 or 3,5 positions.

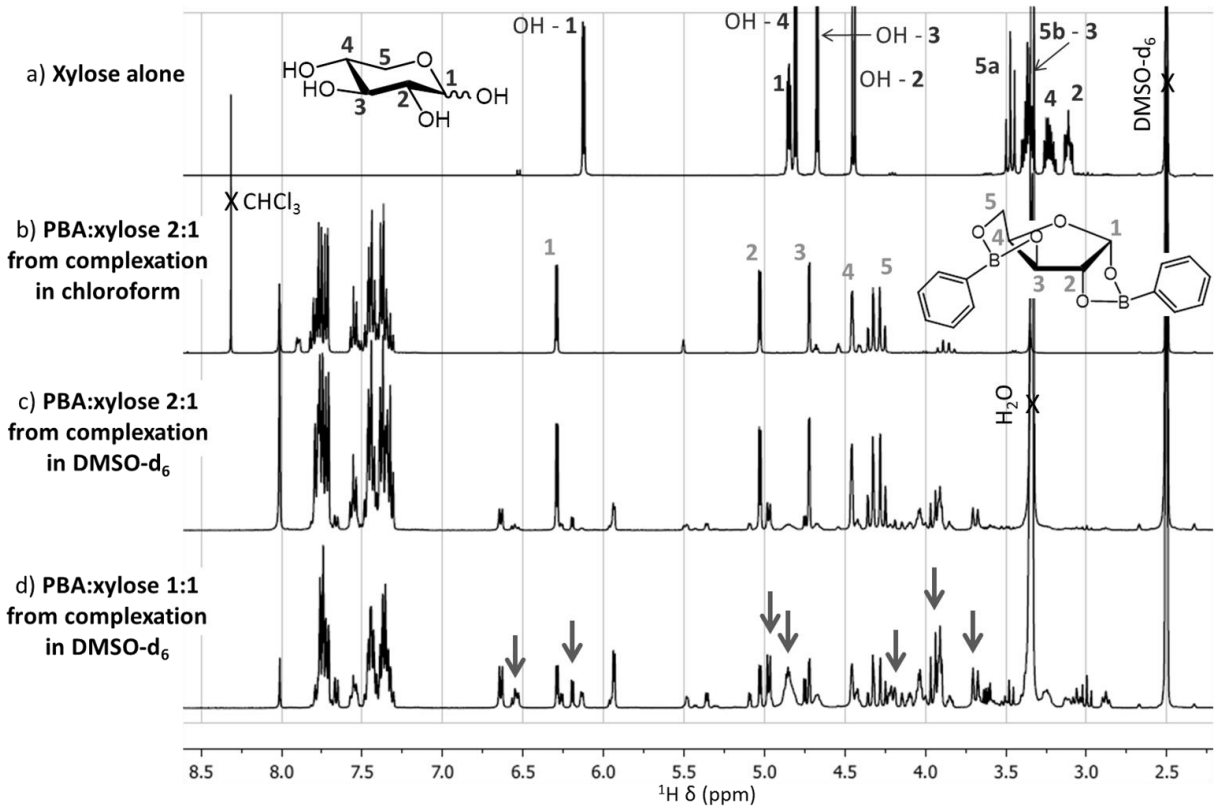

Figure II-34. Attributed ^{1}H NMR spectra of xylose and PBA:xylose complexes

II. 4. B) Complexation on D-mannose

For the mannose complex, only one hydroxyl group was observed and seemed to be located on the anomeric position (**Appendix II.X**, p 114). Hence the four other hydroxyl groups were involved in the complexation. The anomeric proton chemical shift of the complex had an increment of 0.50 ppm from the α-form and 0.83 from the β-form (**Figure II-35**) which was quite close to the 0.6 ppm limit. The anomeric carbon had a ^{13}C chemical shift of 101.0 ppm and the coupling constants $J_{2,3}$ (6.2 Hz) and $J_{3,4}$ (0.7 Hz) (**Appendix II.X**, p 114) seemed to indicate a pyranose form even though they were quite close to the limits.

In the literature, both types of complexation on the 2,3 and 4,6 positions of the α-methylmannose and on the 2,3 and 5,6 complex on the α-furanose form of mannose were observed (**Figure II-15**, *Structure MMan2346* and *Man2356*, p 79). Consequently, none of the two possibilities can be discarded.

On this report, the structure on the pyranose form is used (**Figure II-35**) but the furanose form is not firmly denied.

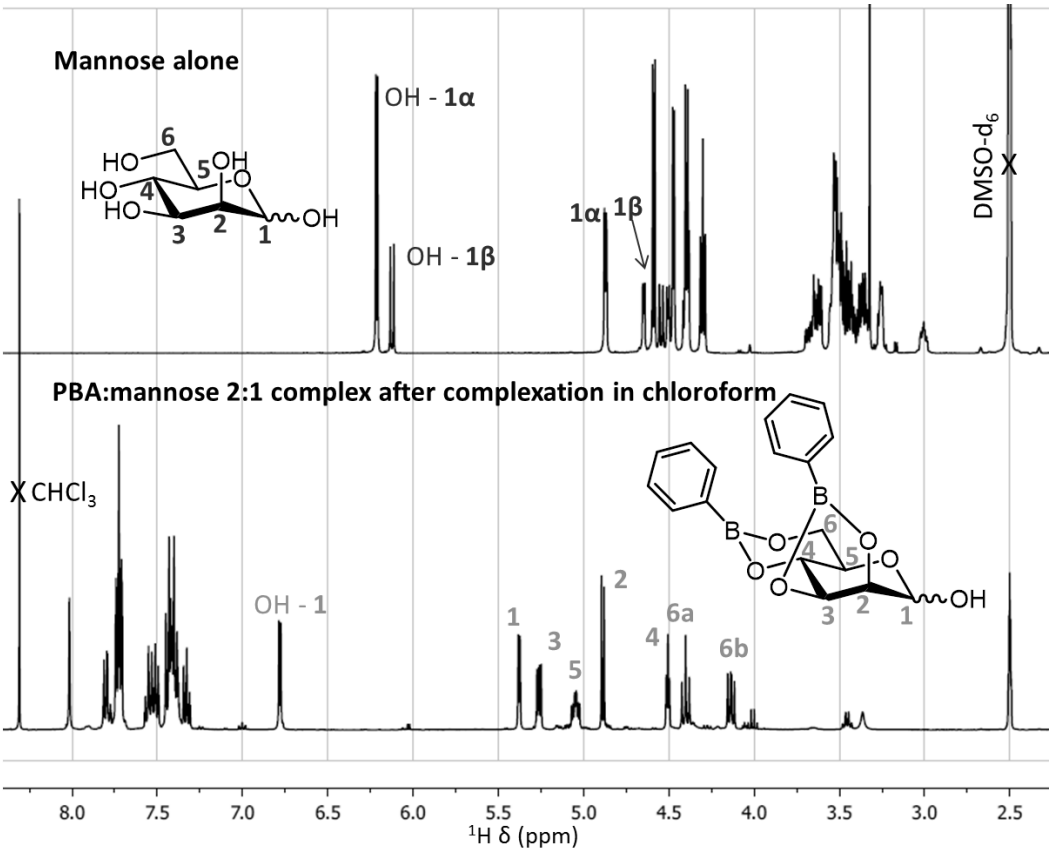

Figure II-35. Attributed ^{1}H NMR spectra of mannose and PBA:mannose complex

II. 4. C) Complexation on D-arabinose

After complexation in chloroform, the PBA:arabinose complex did not present any hydroxyl groups (**Appendix II.XI**, p 115) indicating that one sugar bore two boronic acids.

The ^{1}H chemical shift increment of the anomeric proton was 1.1 ppm (**Figure II-36a** and **b**) but the anomeric carbon had a ^{13}C chemical shift of 92.76 ppm and the coupling constants $J_{2,3}$ (2.5 Hz) and $J_{3,4}$ (8.7 Hz) were high. Even though the ^{1}H criterion was not met, we concluded that the sugar was under the pyranose form.

Because of steric considerations, the complexation was found to occur on the 1,2 and 3,4 positions of the α-pyranose form (structure represented on **Figure II-36**). The same complex was observed by complexation in DMSO-d_6 with a 2:1 PBA:arabinose ratio (**Figure II-36c**).

In the literature, complexation was only found on the furanose form on the 1,2 or, as a tridentate, on the 1,2,5 positions. Both these complexes have at least one free hydroxyl group. The complexation in chloroform thus probably allowed the formation and isolation of a new complex on arabinose.

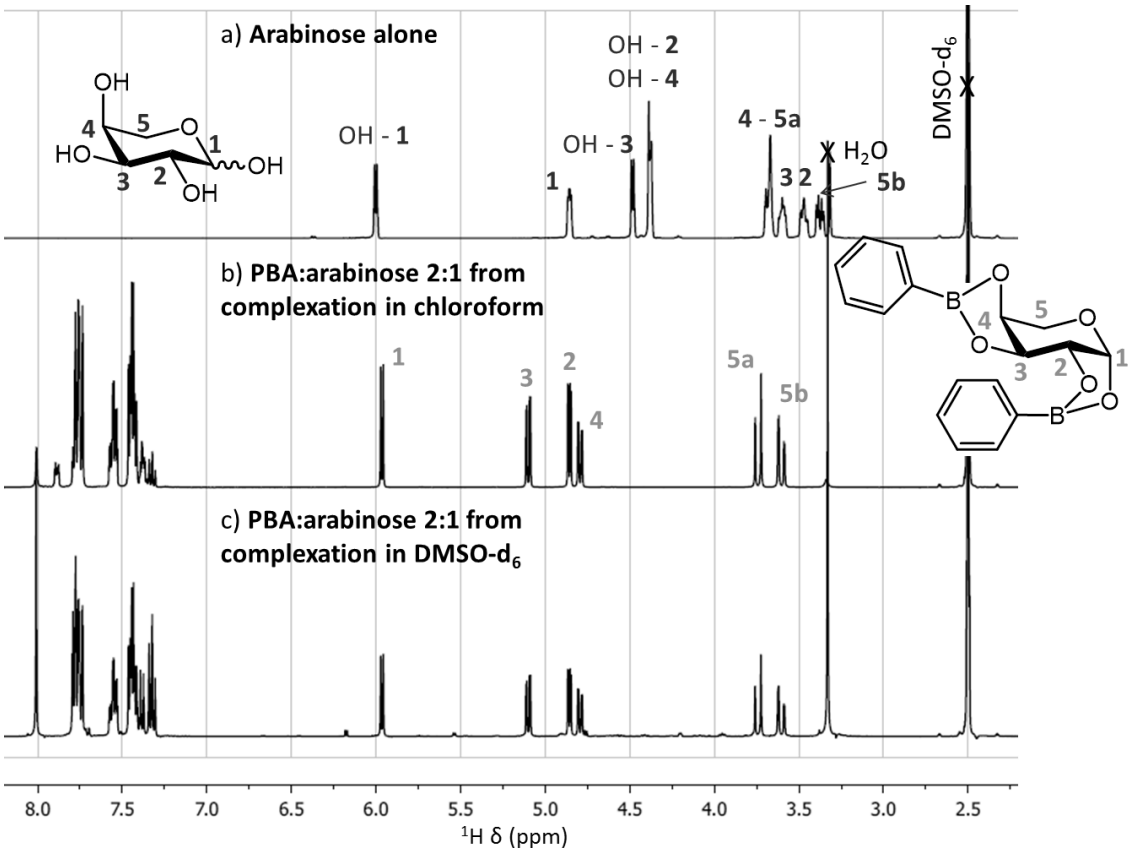

Figure II-36. Attributed ^{1}H NMR spectra of arabinose and PBA:arabinose complexes

II. 4. D) Complexation on D-galactose

The spectrum of the complex on galactose obtained after complexation in chloroform was too crowded and had a too small intensity to accurately identify all the species present (**Figure II-37**).

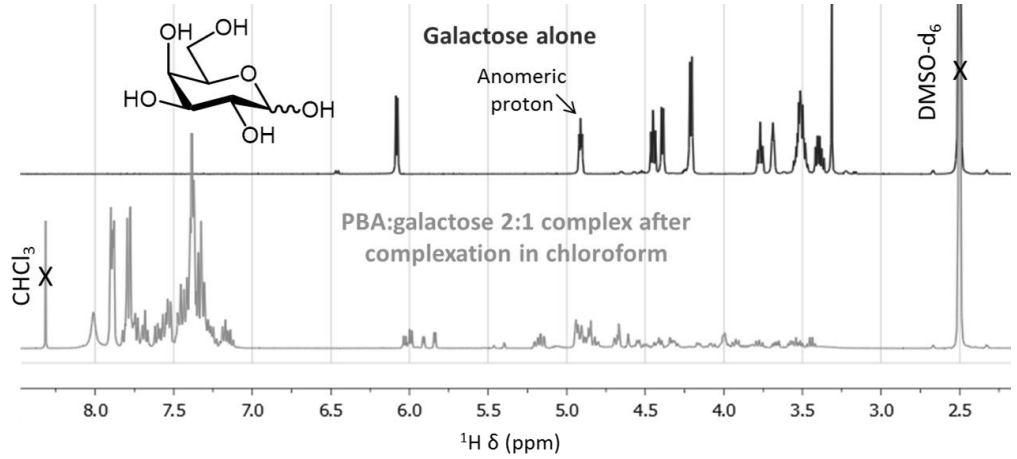

Figure II-37. ^{1}H NMR spectra in DMSO-d_6 of the galactose alone and of the PBA:galactose complex obtained after complexation in chloroform

Consequently, the complexation was only studied in DMSO-d_6. The evolution of the PBA:galactose 1:1 and 2:1 ratios was recorded over time and an evolution of the ratio between the different peaks was observed. Three complexes were identified (**Appendix II.XII**, p 116) and **Figure II-38** represents their structure as well as their evolution over time for the two ratios studied. On the PBA:galactose 1:1 ratio, a small percentage of *Structure 2/1* was detected (below 10%) and *Structure b1/1* seemed to evolve into *Structure t1/1* which is probably more thermodynamically stable. For the PBA:galactose 2:1 ratio, *Structure 2/1* seemed to rearrange into *Structure t1/1* until an equilibrium was reached where the three structures had the same proportion.

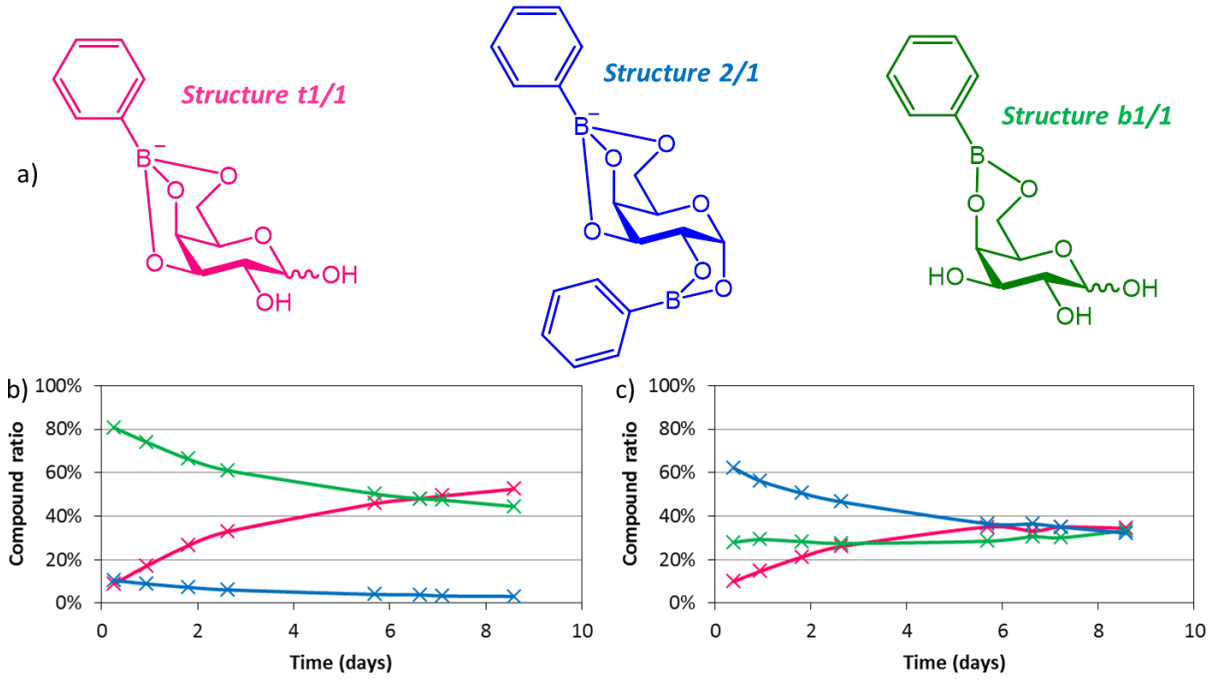

Figure II-38. a) Structure of the three complexes observed by complexation of PBA on galactose in DMSO-d_6 and evolution with time of the PBA:galactose b) 1:1 ratio and c) 2:1 ratio

II. 4. E) Complexation on cellobiose

As mentioned in §II. 2 (p 80), no complexation was observed between cellobiose and phenylboronic anhydride in chloroform. The complexation in DMSO-d_6 was thus investigated. Several ratios were studied (**Figure II-39b** to **g**) and the mixture in DMSO-d_6 was heated to displace the equilibrium toward the complex formation (**Figure II-39h** and **i**). In all of these conditions, only one complex seemed to be formed as only one new peak appeared in the 7.5-8.0 ppm region. If we consider the literature and the small changes observed for the rest of the spectra, *Structure C12* (**Figure II-16**, p 80) with a complexation on the 1- and 2- positions of the reducing end sugar, was most probably formed. However, a complexation on the 4'- and 6'-positions of the non-reducing end sugar was not excluded considering the results of the complexation on methylglucoside.

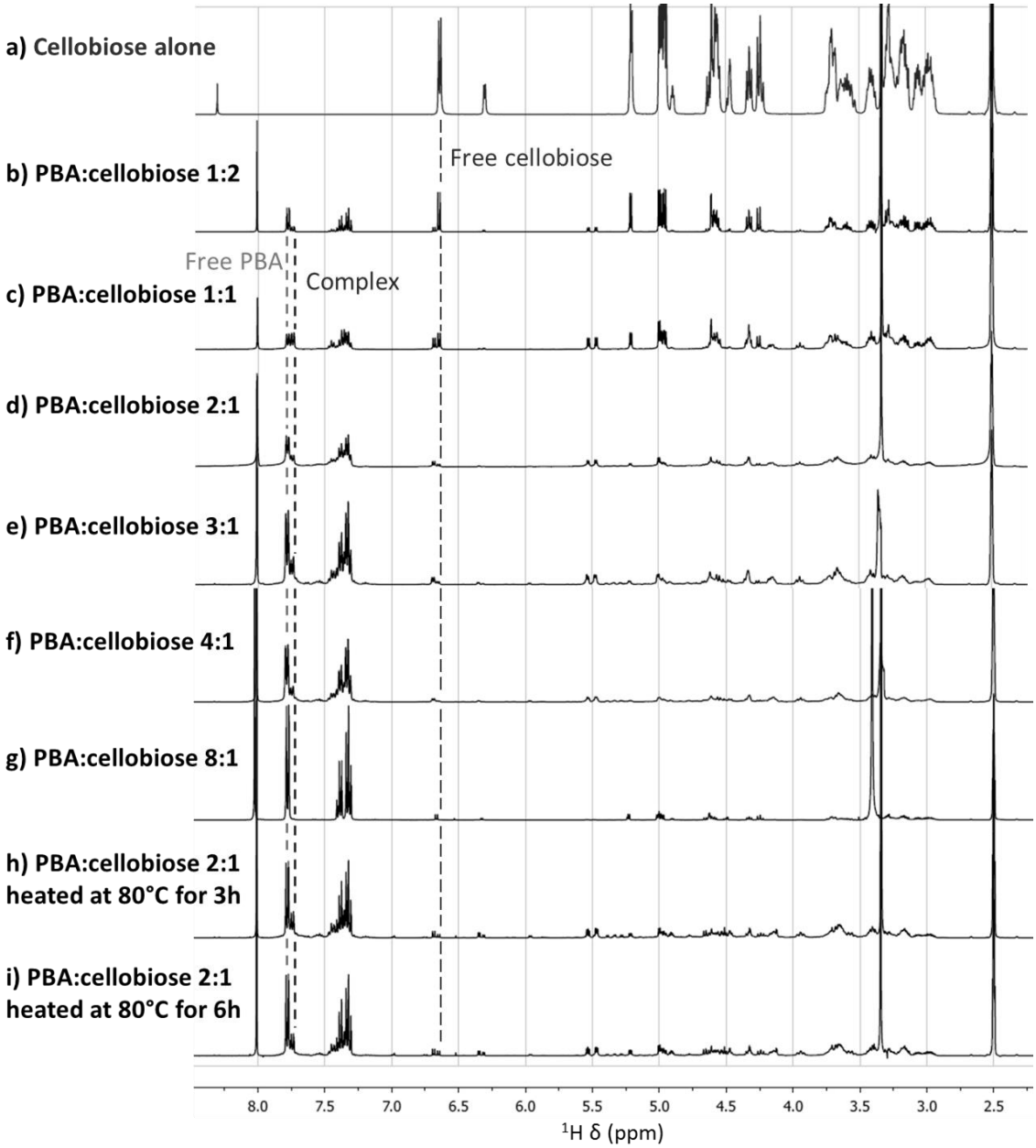

Figure II-39. ^{1}H NMR spectra of several ratios of PBA cellobiose in DMSO-d_6

II. 4. F) Summary

Table II-5 summarises the structures and **Appendix II.XIII** (p 119) and **II.XIV** (p 120) the ^{1}H and ^{13}C assignments of the complexes determined in this chapter.

For cellulose, the complexation would only occur at the extremities as the 1- and 4-positions are not available along the backbone. The boronic acid would be on the 1- and 2-positions of the reducing end as confirmed by the study on cellobiose and/or on the 4- and 6-positions on the non-reducing end as determined with β-methylglucoside. Only boronic anhydride can be located on the 2- and 3- positions.

Table II-5. Summary of all the structures determined in this chapter

Complexation in	DMSO-d_6	Chloroform
α-methylglucoside	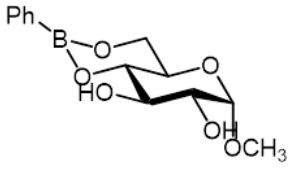	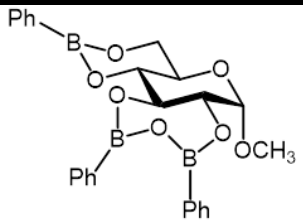
β-methylglucoside	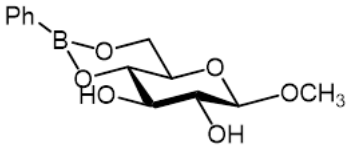	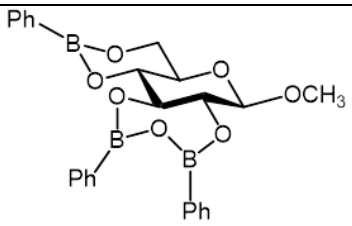
Glucose	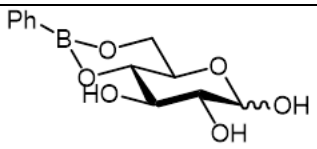 rearranging into 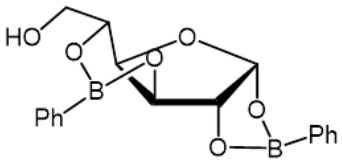	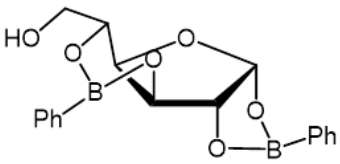
Xylose	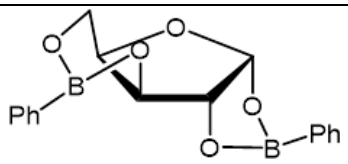 and at least another one not confirmed	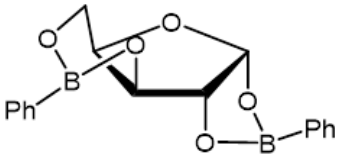

Table II-5 (following). Summary of all the structures determined in this chapter

Complexation in	DMSO-d_6	Chloroform
Mannose	Not determined	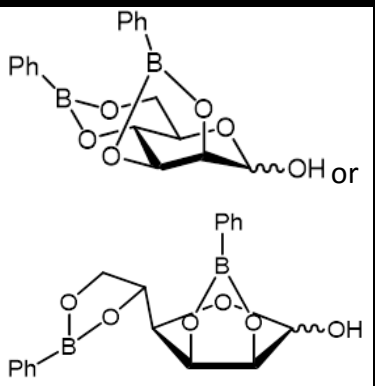
Arabinose	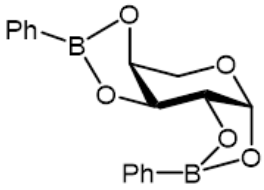	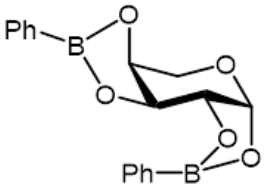
Galactose	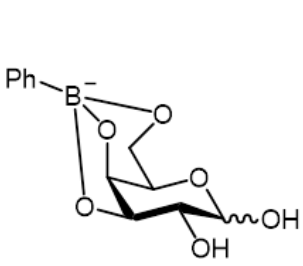 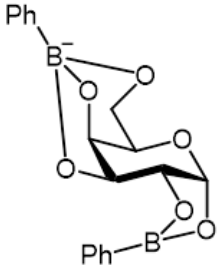 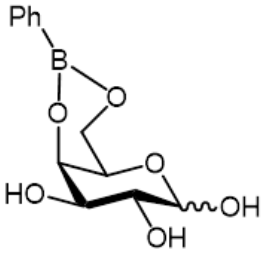 Evolving toward an equilibrium with the same ratio for the three structures	Not determined (^{1}H NMR spectrum too crowded)
Cellobiose	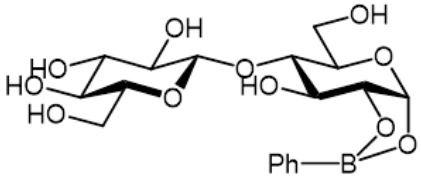 or 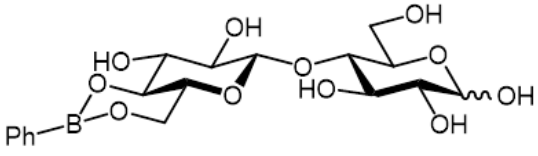	No complexation

Chapter conclusion

A bibliographic study highlighted that boronic acids complexation on sugars could occur in water and that their association constant increased with the pH.

The formation of the anhydride form was favoured in hydrophobic solvents even though an equilibrium with the acid form was observed. However, with hydrophilic solvents, 100% of acid form was reached.

After that, a complexation study on analogues suggested that the complexation of boronic acid on cellulose would only occur at the extremities. For the "fishing" method, it is not an issue but for the "masking" method several interaction points between the cellulose chain and the polymer along the backbone are needed to protect the future oligomers. Fortunately, boronic anhydrides were able to complex the 2- and 3-positions.

As a result, two polymer structures were chosen: a 4-vinylphenylboronic acid (VBA)-styrene block copolymer for the "fishing" method (**Figure II-40a**) and a random copolymer of styrene and 4-vinylphenylboronic acid under the anhydride form with phenylboronic acid for the "masking" method (**Figure II-40b**).

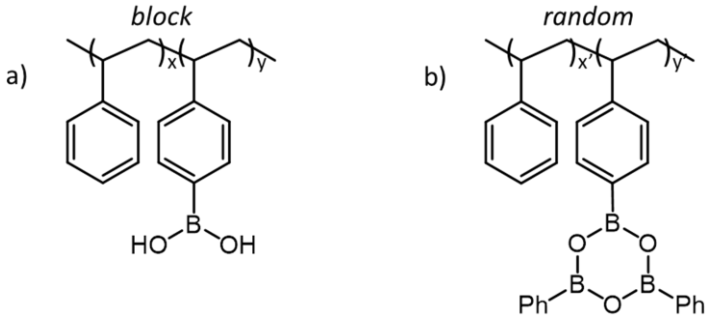

Figure II-40. Structure of a) a VBA-styrene block copolymer and b) a random copolymer of styrene and VBA under the anhydride form with PBA

For the "fishing" method, a block is necessary as two boronic acids may complex the same oligomer and a random copolymer could induce a network formation. The boronic acid block needs to be small to prevent networking and anhydride formation by steric hindrance but not too small so an anhydride formation does not jeopardise the method.

Appendix

Appendix II.I: ARS method to determine boronic acid/diol binding constants[4,10]

The Alizarin Red S (ARS) method is based on a fluorescence change after complexation with a boronic acid. However, the presence of a second diol in the mixture leads another competitive equilibrium as represented below. This new equilibrium perturbs the one between boronic acid and ARS thus quenching the fluorescence.

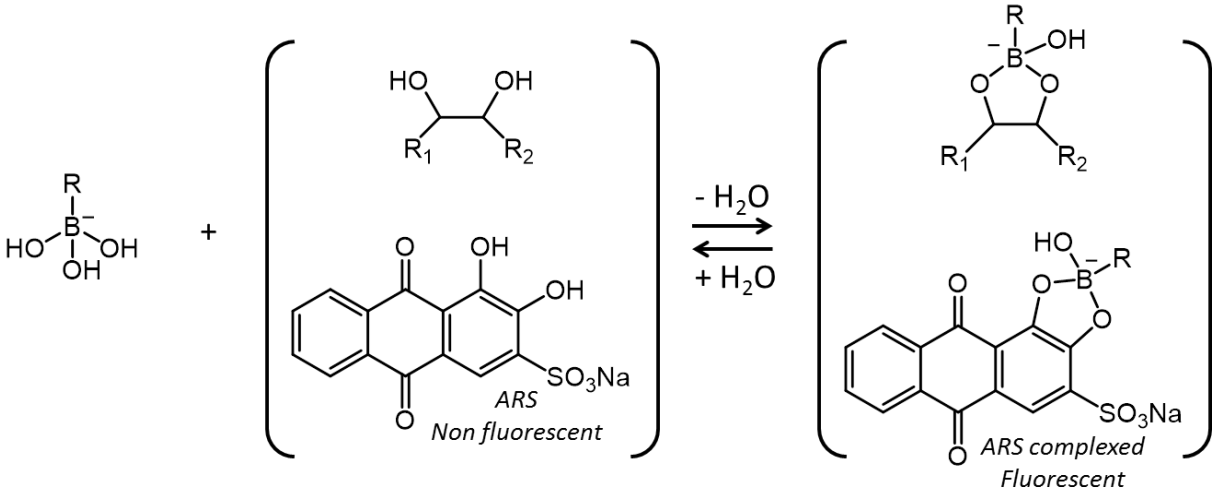

The determination of a binding constant is performed by first calculating the constant with ARS alone and then, a titration of the boronic acid/ARS solution with the target diol compound has to be carried out.

Determination of the binding constant of ARS alone[4]

The fluorescence of solutions of ARS in phosphate buffer with different equivalent of boronic acid (from 10 to 200) has to be measured. The fluorescence intensities are measured with an excitation wavelength of 468 nm and an emission wavelength of 572 nm. The equation below explicates the relationship between the fluorescence intensity changes and the equilibrium constant. The binding constant with ARS K_{eq1} is thus the quotient of the intercept over the slope of the plot of $^{1}/_{\Delta I_f}$ depending on $^{1}/_{[L]}$.

$$\Delta I_f = \frac{(\Delta k\mathrm{p}_0 K_{eq1})[L][I_0]}{1 + K_{eq1}[L]} \quad \Leftrightarrow \quad \frac{1}{\Delta I_f} = (\Delta k\mathrm{p}_0 K_{eq1}[I_0])^{-1}\frac{1}{[L]} + (\Delta k\mathrm{p}_0[I_0])^{-1}$$

With ΔI_f the fluorescence intensity change, Δkp_0 a constant derived from the intrinsic fluorescence and the laser power, K_{eq1} the association constant of the ARS/boronic acid

system, $[L]$ the ligand concentration (here, in the considered boronic acid) and $[I_0]$ the total indicator concentration (here, ARS)

Determination of the binding constant of the targeted diol[4]

The binding constant is determined by plotting $^1/_P$ depending on Q with both of those values defined as below. Q is determined by the change of fluorescence of the solution.

$$P = [L_0] - \frac{1}{QK_{eq1}} - \frac{[I_0]}{Q+1} \qquad Q = \frac{[I]}{[IL]}$$

With $[L_0]$ the total amount of boronic acid, K_{eq1} the binding constant with ARS alone determined previously, $[I_0]$ the total indicator concentration (here, ARS), $[I]$ concentration of free ARS and $[IL]$ concentration of complexed ARS

This last equation highlights the relation between the binding constant, P and Q. The binding constant K_{eq} is thus determined by dividing the slope of the plot of $^1/_P$ depending on Q by the constant K_{eq1} determined previously.

$$\frac{[S_0]}{P} = \frac{K_{eq1}}{K_{eq}}Q + 1$$

With $[S_0]$ the total amount of targeted diol, K_{eq1} the binding constant with ARS alone determined previously and K_{eq} the binding constant with the targeted diol

Determination of the predicted optimal pH

The predicted optimal pH is defined as the average between the pK_a of the considered boronic acid and the pK_a of the targeted diol.

Appendix II.II: Calculation of the acid/anhydride/complex ratios

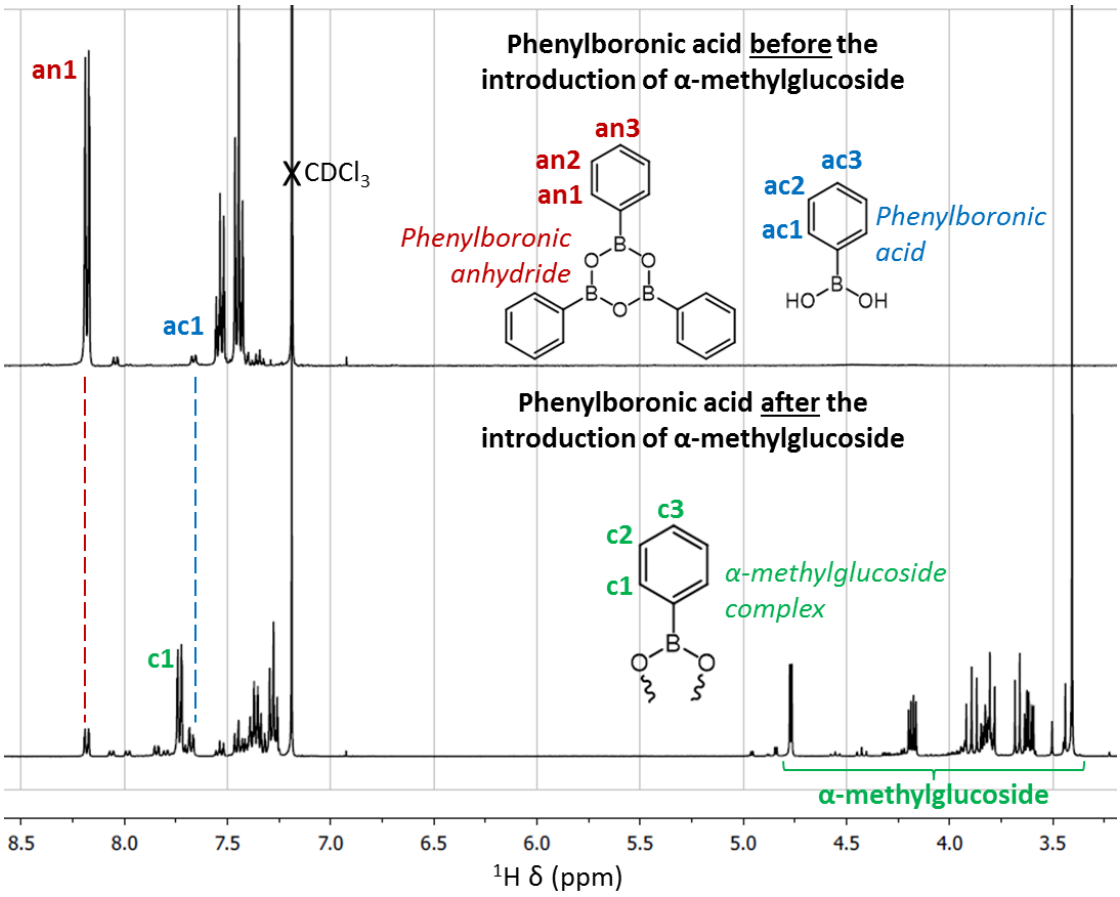

^{1}H NMR spectra in $CDCl_3$

As **an1** corresponds to 6 protons when **ac1** and **c1** correspond to only 2, the ratios of each compound were calculated as follow:

$$\tau_{acid} = \frac{I_{ac1}}{I_{ac1} + {}^{I_{an1}}/_{3} + I_{c1}} \qquad \tau_{anhydride} = \frac{{}^{I_{an1}}/_{3}}{I_{ac1} + {}^{I_{an1}}/_{3} + I_{c1}}$$

$$\tau_{complex} = \frac{I_{c1}}{I_{ac1} + {}^{I_{an1}}/_{3} + I_{c1}}$$

With τ_x the ratio of the compound x and I_p the integration of the peak p defined on the figure above

The calculation is based on the ratio of integrals so no external reference is needed.

Appendix II.III: Phenylboronic acid:β-methylglucoside complex in DMSO-d_6

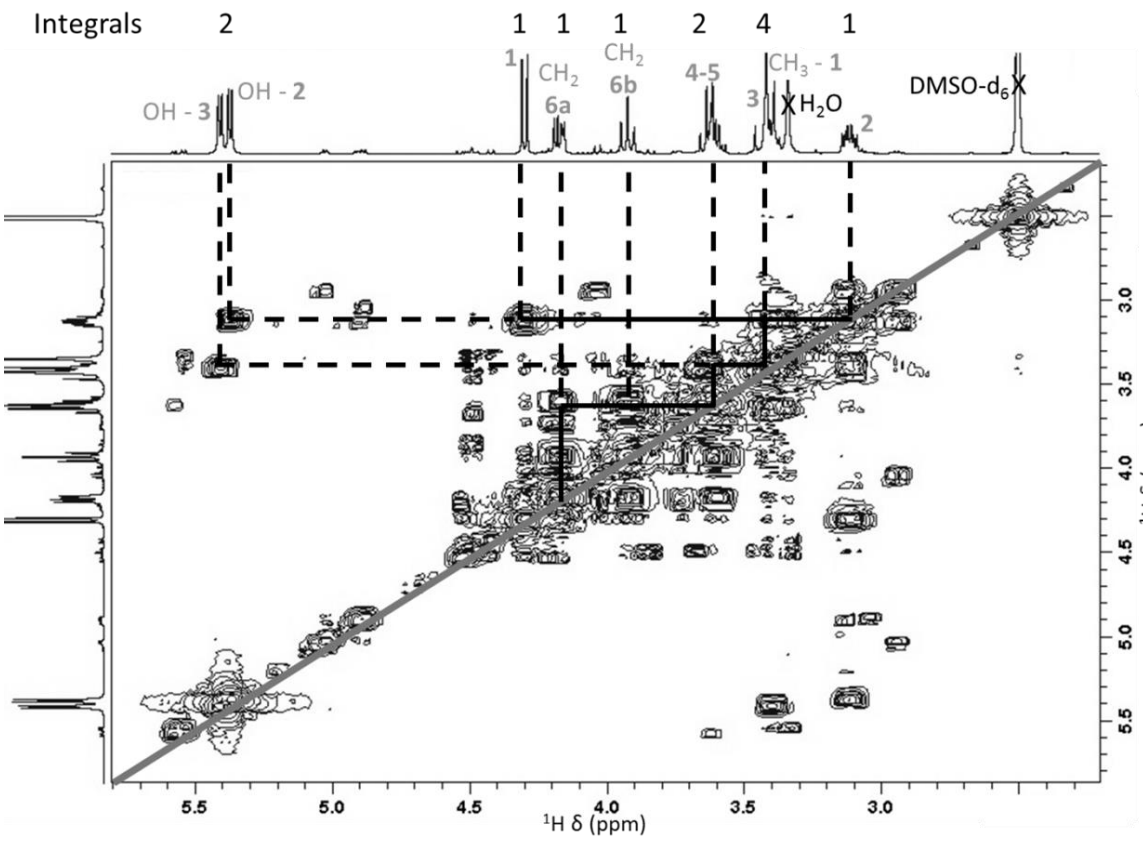

COSY in DMSO-d_6 of the phenylboronic acid:β-methylglucoside complex

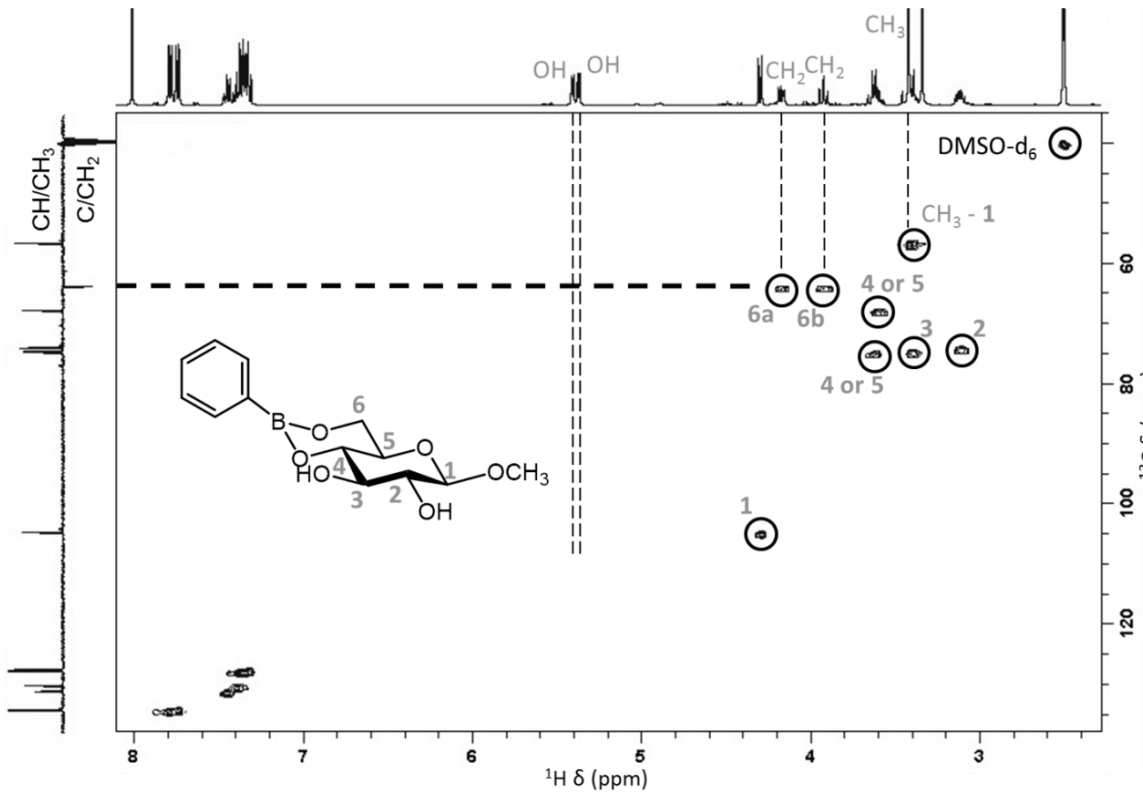

HSQC in DMSO-d_6 of the phenylboronic acid:β-methylglucoside complex

Appendix II.IV: Phenylboronic acid:glucose 2:1 ratio in DMSO-d_6

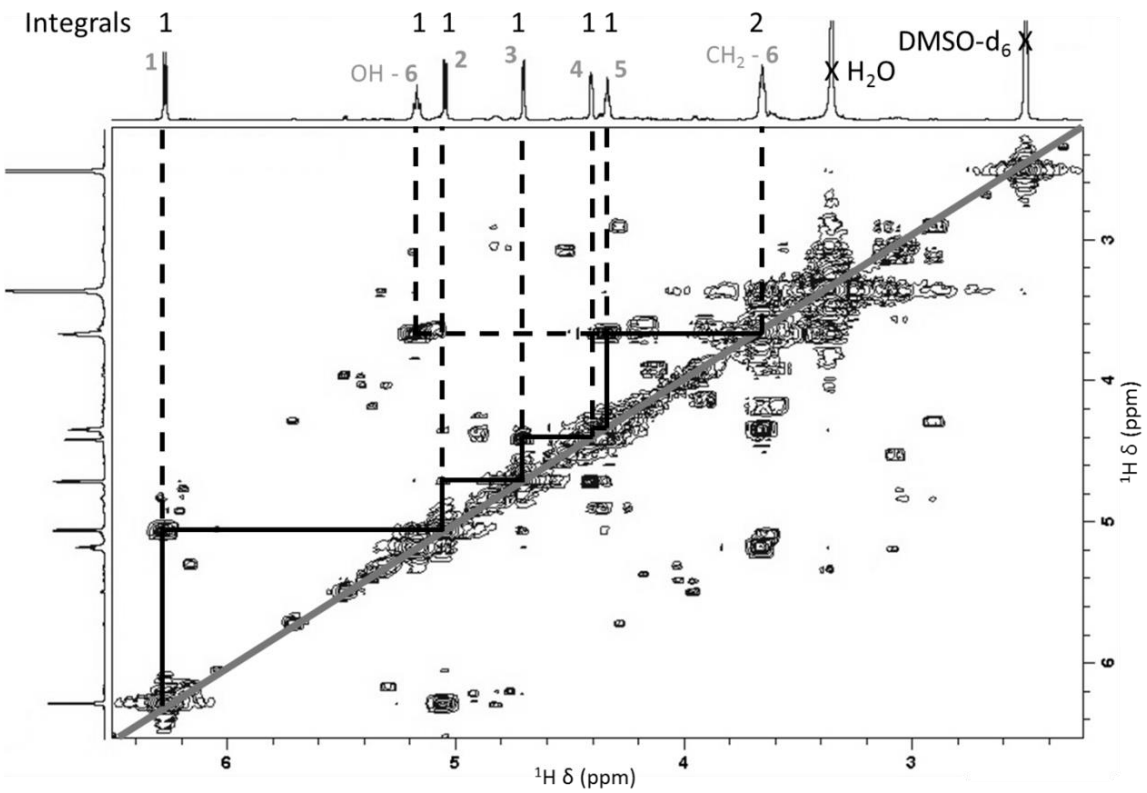

COSY in DMSO-d_6 of phenylboronic acid:glucose 2:1 ratio

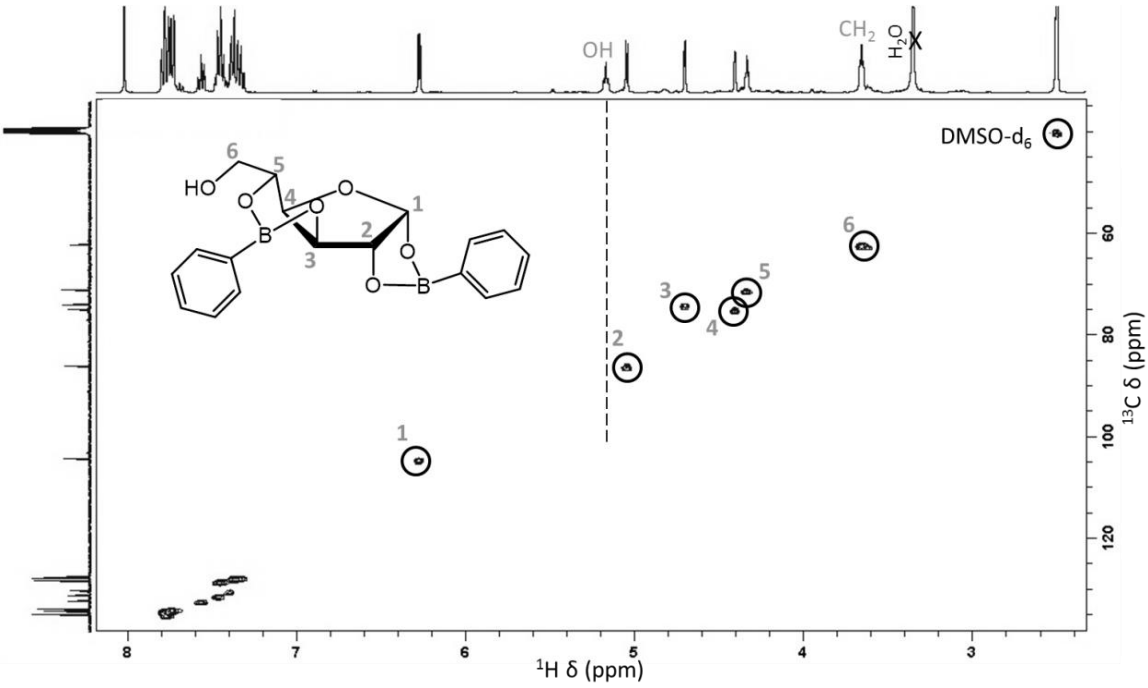

HSQC in DMSO-d_6 of phenylboronic acid:glucose 2:1 ratio

$J_{H\text{-}H}$ coupling constants of the sugar part of the PBA:glucose 2:1 complex

$J_{1,2}$	$J_{2,3}$	$J_{3,4}$	$J_{4,5}$	$J_{5,6a}$	$J_{5,6b}$	$J_{6a,6b}$
4.3 Hz	1.8 Hz	2.5 Hz	Not measured			

Appendix II.V: Phenylboronic acid:glucose 1:1 ratio in DMSO-d_6 (^{13}C NMR)

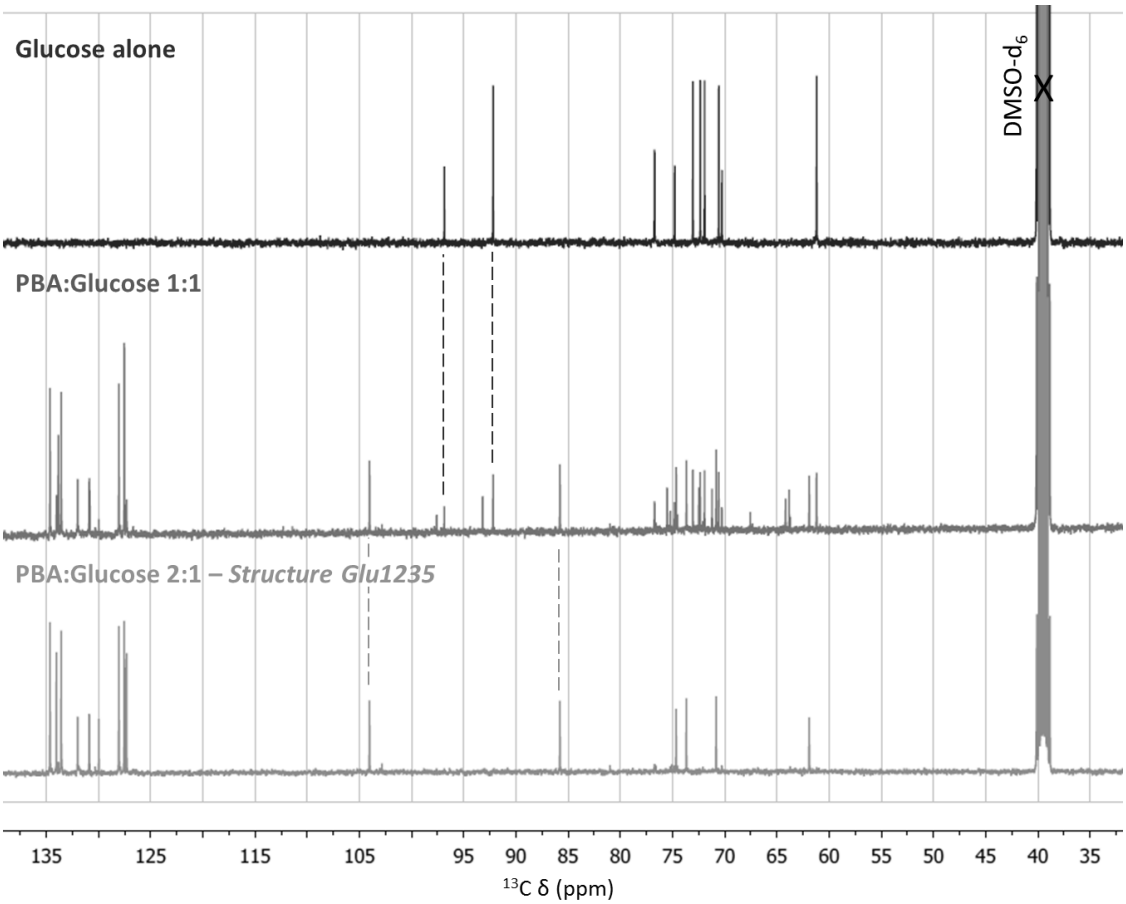

^{13}C NMR in DMSO-d_6 of free glucose, phenylboronic acid:glucose 1:1 ratio and 2:1 ratio

Appendix II.VI: Evolution with time of the 1:2 and 2:1 PBA:glucose ratios in DMSO-d_6

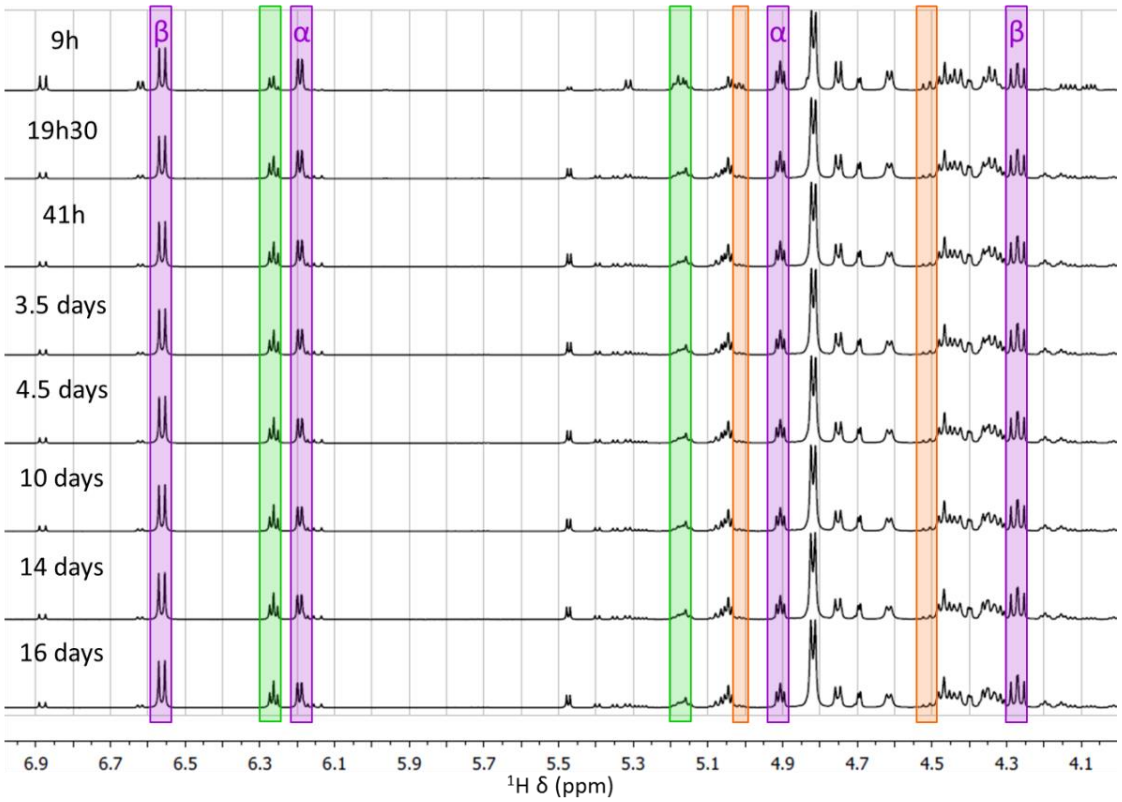

Evolution with time of the 1:2 PBA:glucose ratio in DMSO-d_6 (peaks highlighted in purple correspond to free α- or β-glucose, in green to *Structure Glu1235* and in orange to the second complex)

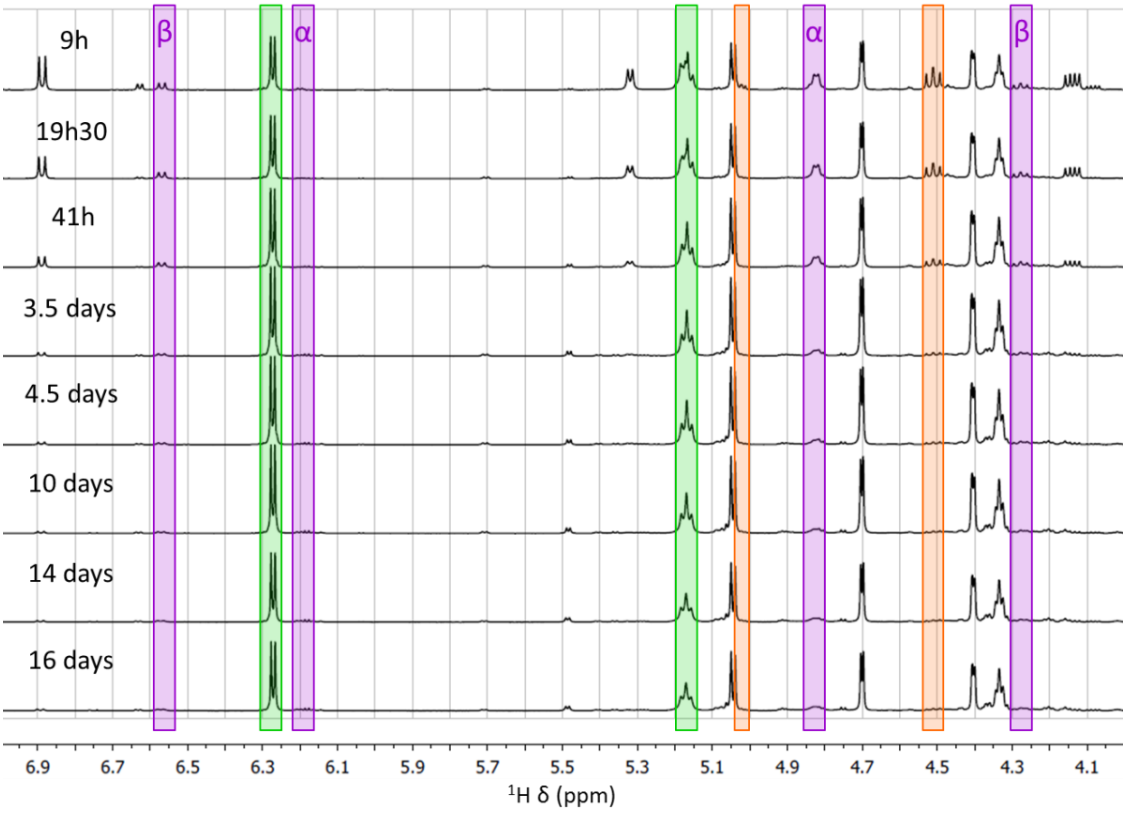

Evolution with time of the 2:1 PBA:glucose ratio in DMSO-d_6 (same colour code as above)

Appendix II.VII: Complex PBA:β-methylglucoside after complexation in chloroform

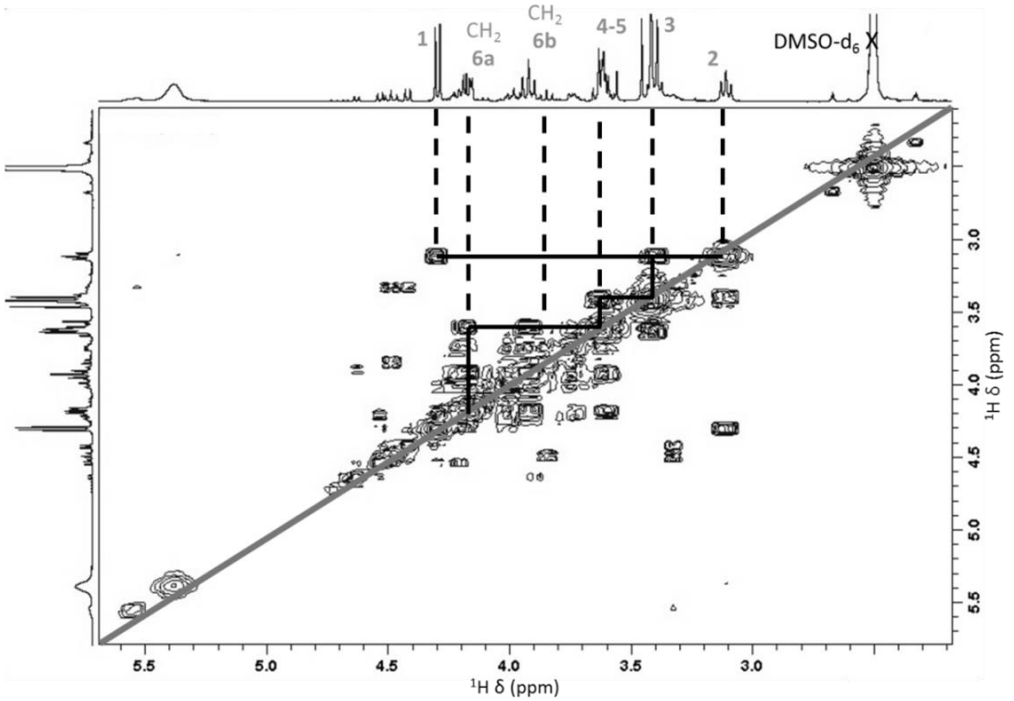

COSY in DMSO-d_6 of the phenylboronic acid:β-methylglucoside complex obtained after complexation in chloroform

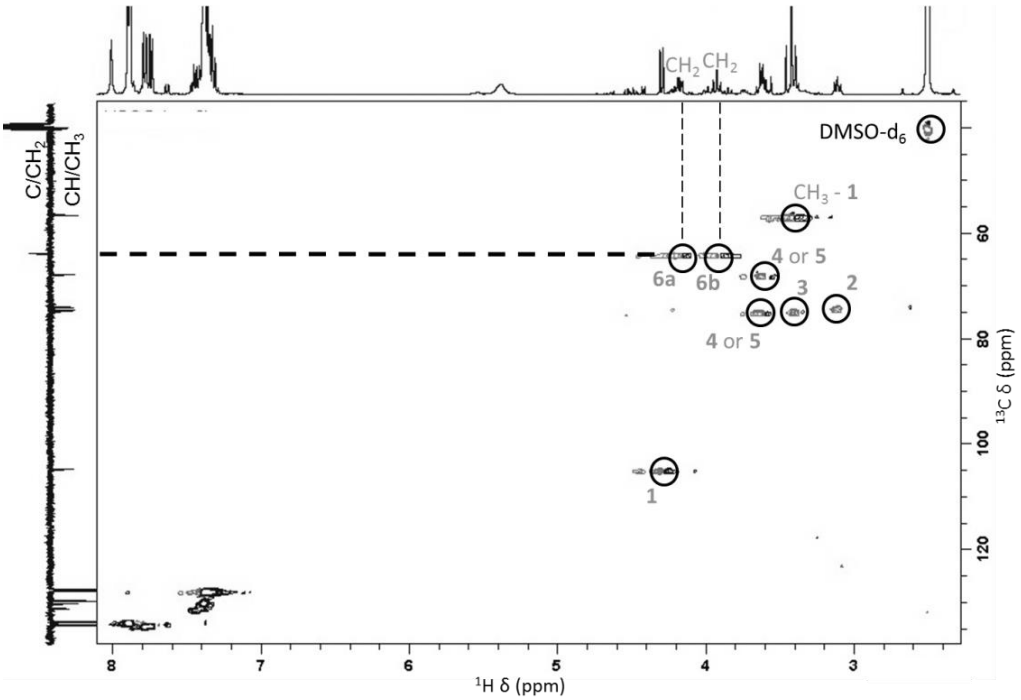

HSQC in DMSO-d_6 of the phenylboronic acid:β-methylglucoside complex obtained after complexation in chloroform

$J_{H\text{-}H}$ coupling constants of the sugar part of the PBA:β-methylglucoside complex

$J_{1,2}$	$J_{2,3}$	$J_{3,4}$	$J_{4,5}$	$J_{5,6a}$	$J_{5,6b}$	$J_{6a,6b}$
7.7 Hz	9.1 Hz	Not measured				

Appendix II.VIII: Complexation of phenylboroxole on glucose and on cellobiose

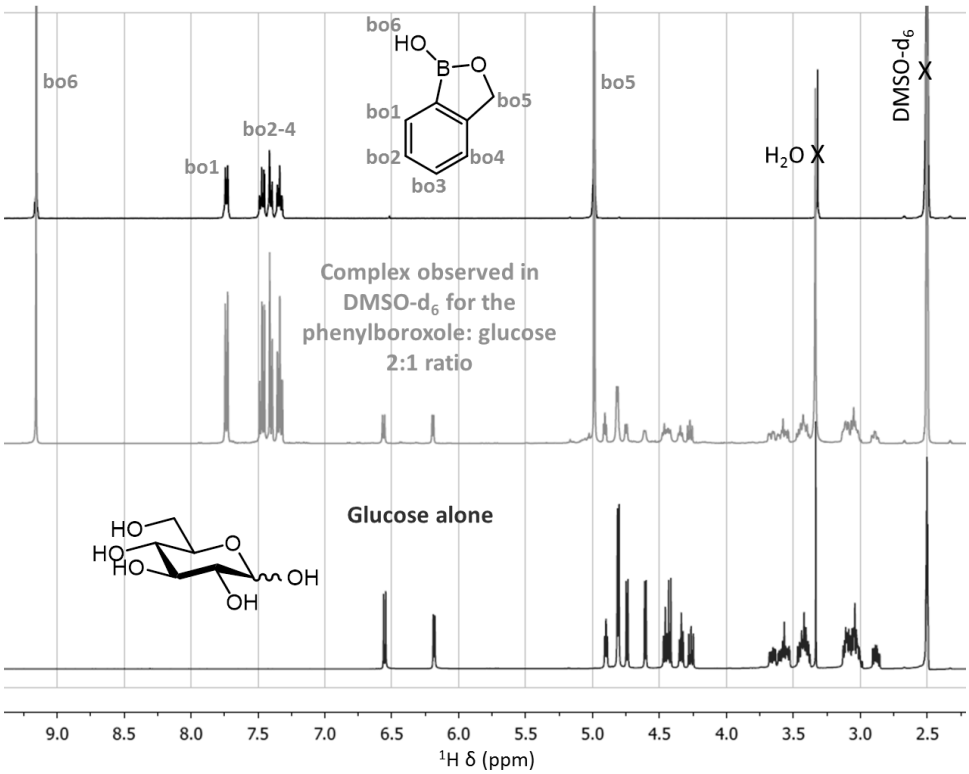

^{1}H NMR spectra of phenylboroxole alone, 2:1 phenylboroxole:glucose ratio and glucose alone in DMSO-d_6

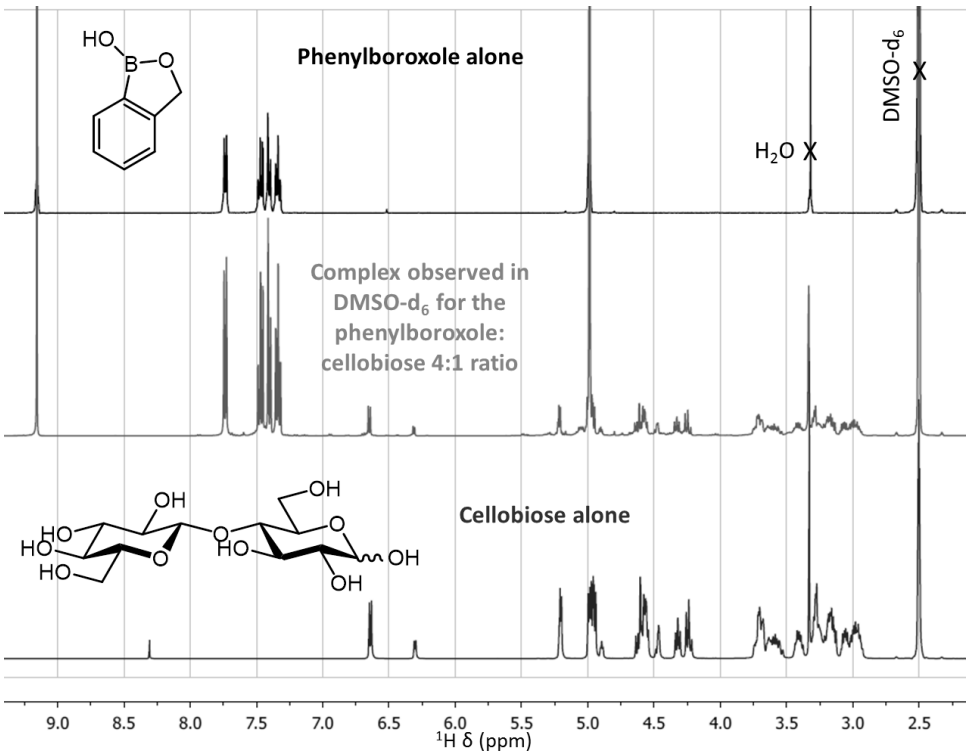

^{1}H NMR spectra of phenylboroxole alone, 4:1 phenylboroxole:cellobiose ratio and cellobiose alone in DMSO-d_6

Appendix II.IX: Complex PBA:xylose after complexation in chloroform

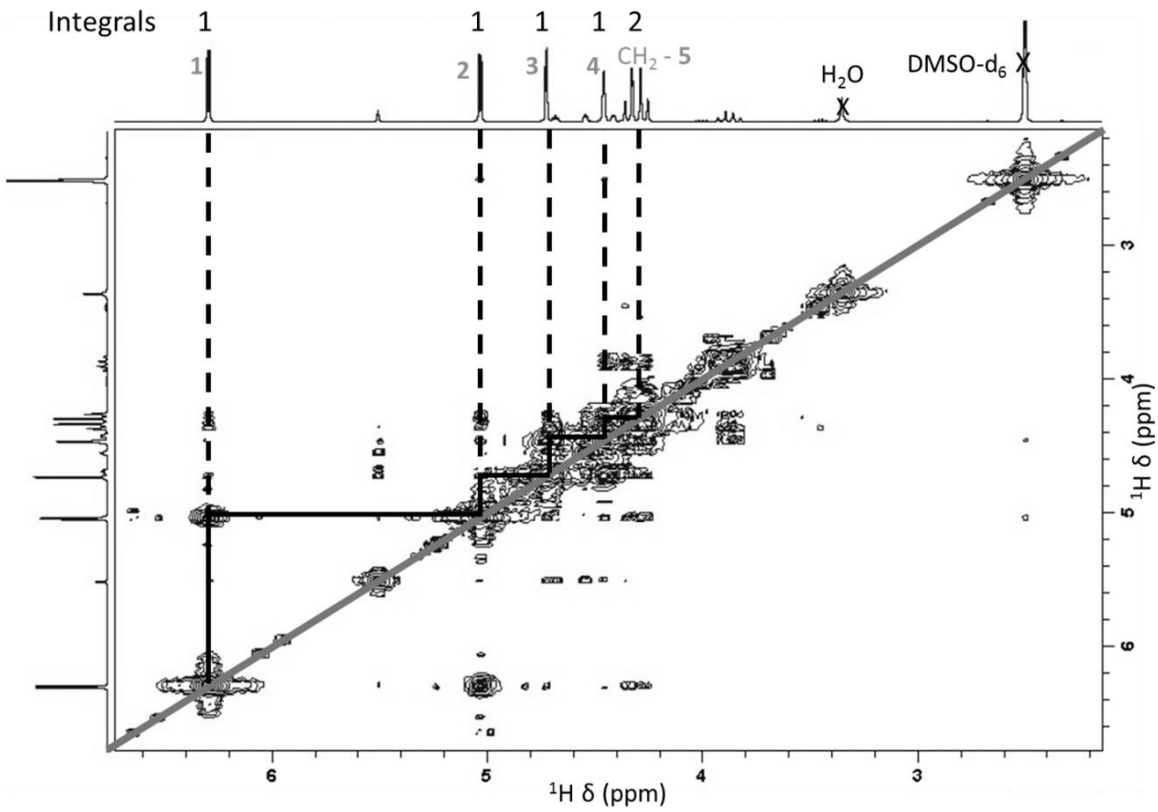

COSY of the complex of PBA and xylose obtained after the complexation in chloroform

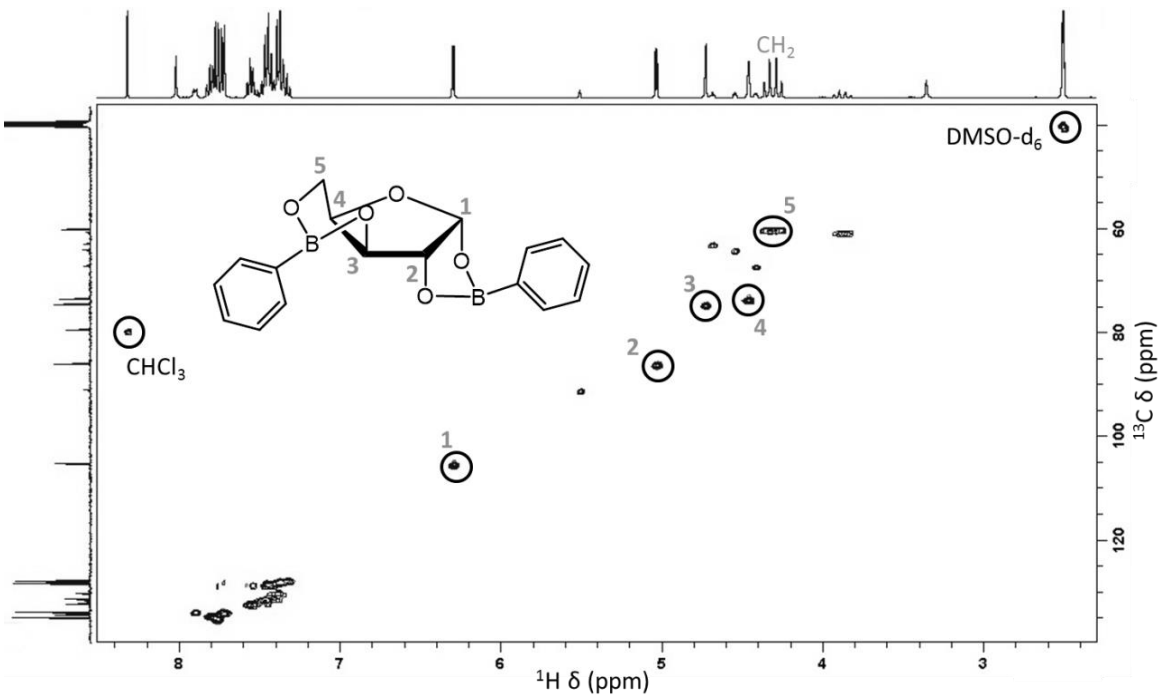

HSQC of the complex of PBA and xylose obtained after the complexation in chloroform

$J_{H\text{-}H}$ coupling constants of the sugar part of the PBA:xylose complex

$J_{1,2}$	$J_{2,3}$	$J_{3,4}$	$J_{4,5a}$	$J_{4,5b}$	$J_{5a,5b}$
4.3 Hz	0.8 Hz	2.6 Hz	Not measured	Not measured	Not measured

Appendix II.X: Complex PBA:mannose after complexation in chloroform

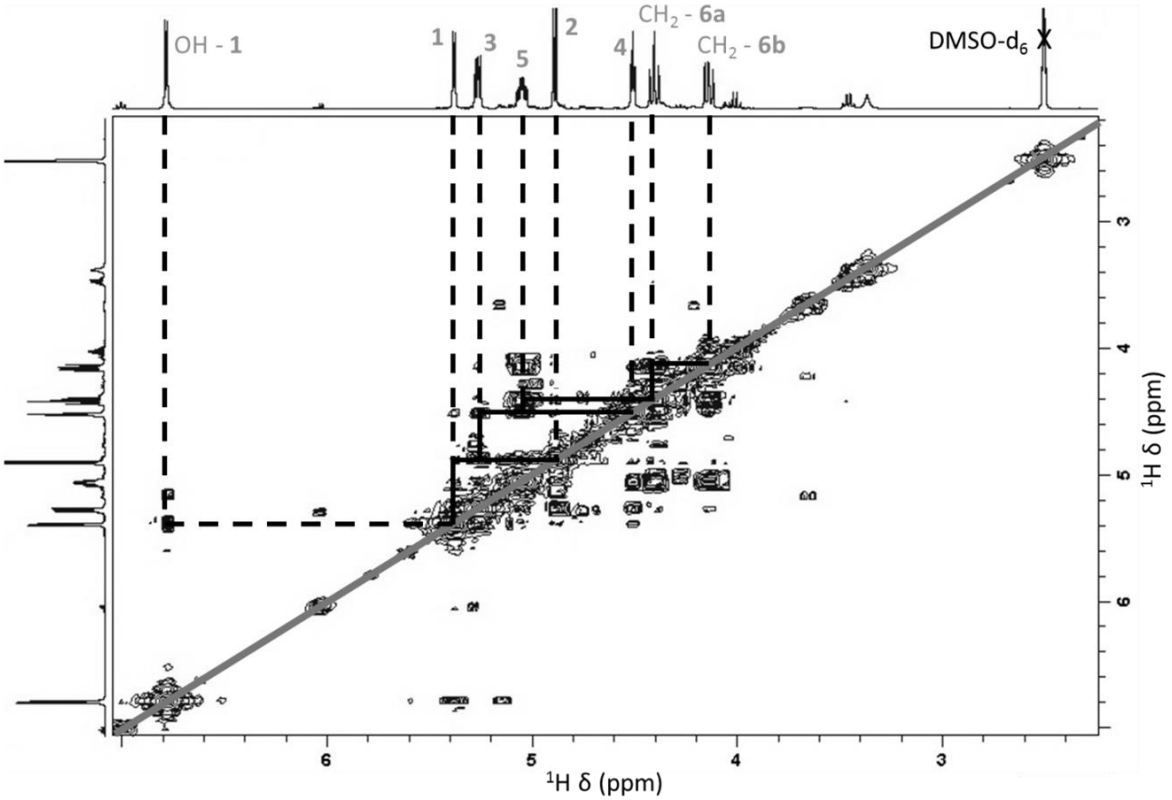

COSY of the complex of PBA and mannose obtained after the complexation in chloroform

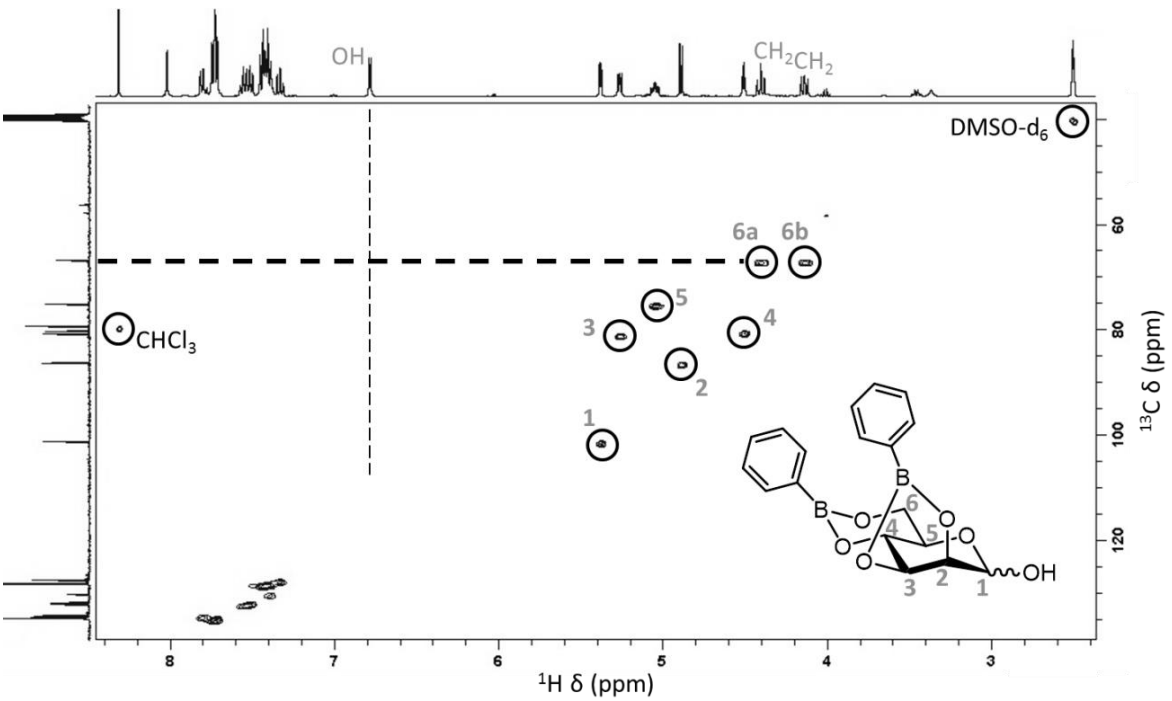

HSQC of the complex of PBA and mannose obtained after the complexation in chloroform

$J_{H\text{-}H}$ coupling constants of the sugar part of the PBA:mannose complex

$J_{1,2}$	$J_{2,3}$	$J_{3,4}$	$J_{4,5}$	$J_{5,6a}$	$J_{5,6b}$	$J_{6a,6b}$
Not measured	6.2 Hz	0.7 Hz	3.7 Hz	10.3 Hz	2.1 Hz	9.1 Hz

Appendix II.XI: Complex PBA:arabinose after complexation in chloroform

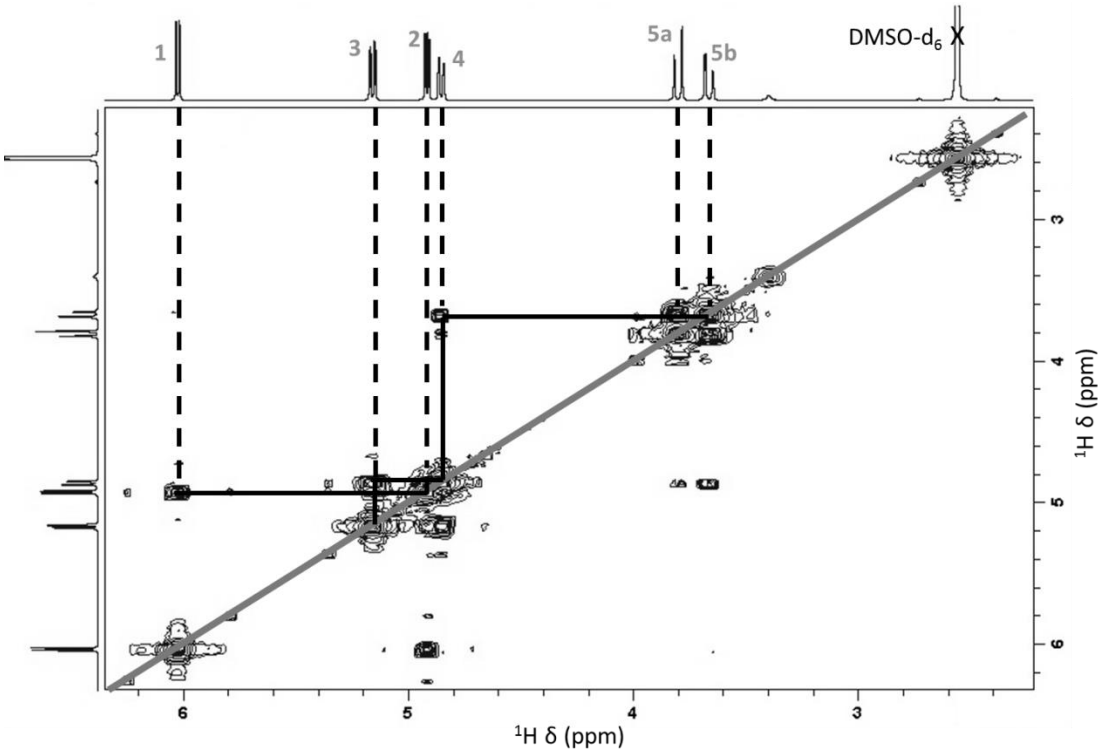

COSY of the complex of PBA and arabinose obtained after the complexation in chloroform

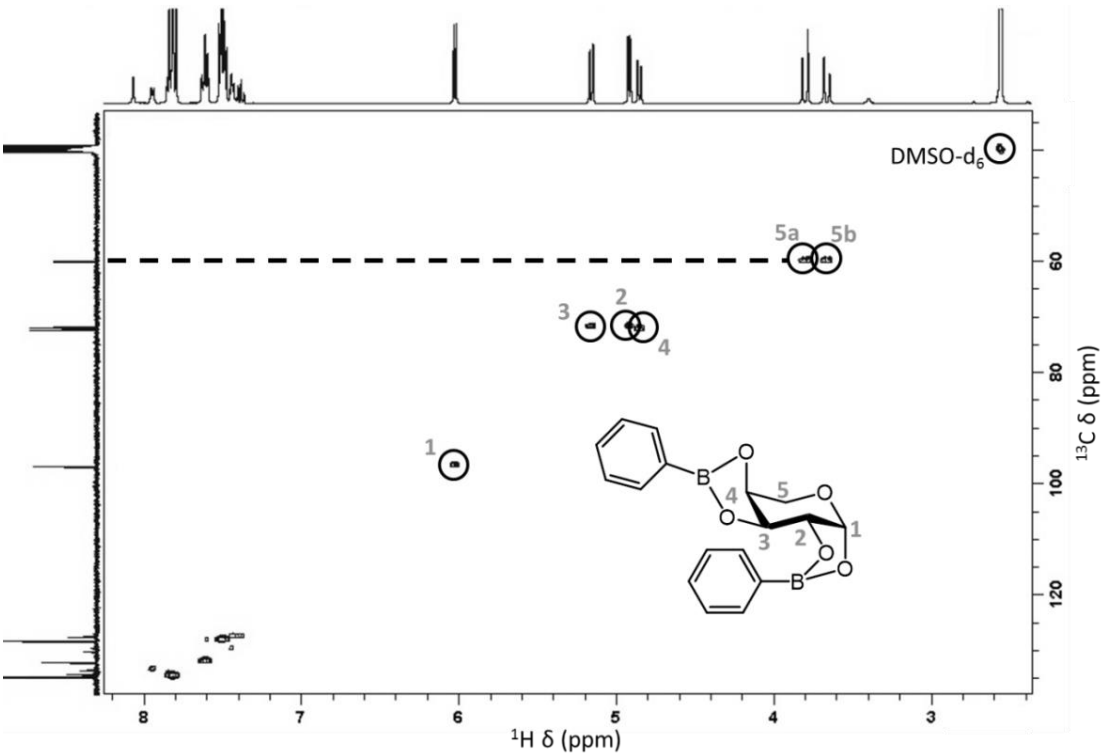

HSQC of the complex of PBA and arabinose obtained after the complexation in chloroform

$J_{H\text{-}H}$ coupling constants of the sugar part of the PBA:arabinose complex

$J_{1,2}$	$J_{2,3}$	$J_{3,4}$	$J_{4,5a}$	$J_{4,5b}$	$J_{5a,5b}$
6.1 Hz	2.5 Hz	8.7 Hz	0.9 Hz	2.2 Hz	13.9 Hz

Appendix II.XII: Complexes observed by complexing PBA on galactose in DMSO-d_6

Structure t1/1

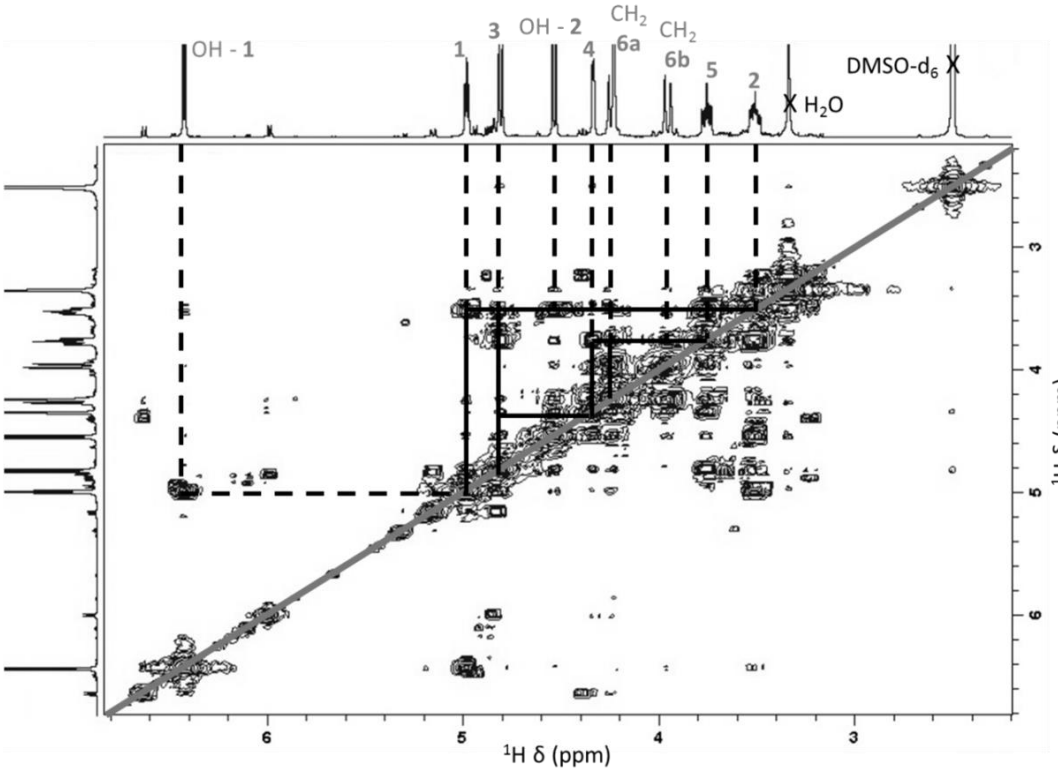

COSY in DMSO-d_6 of the PBA:galactose 1:1 ratio after 6h15 in DMSO-d_6

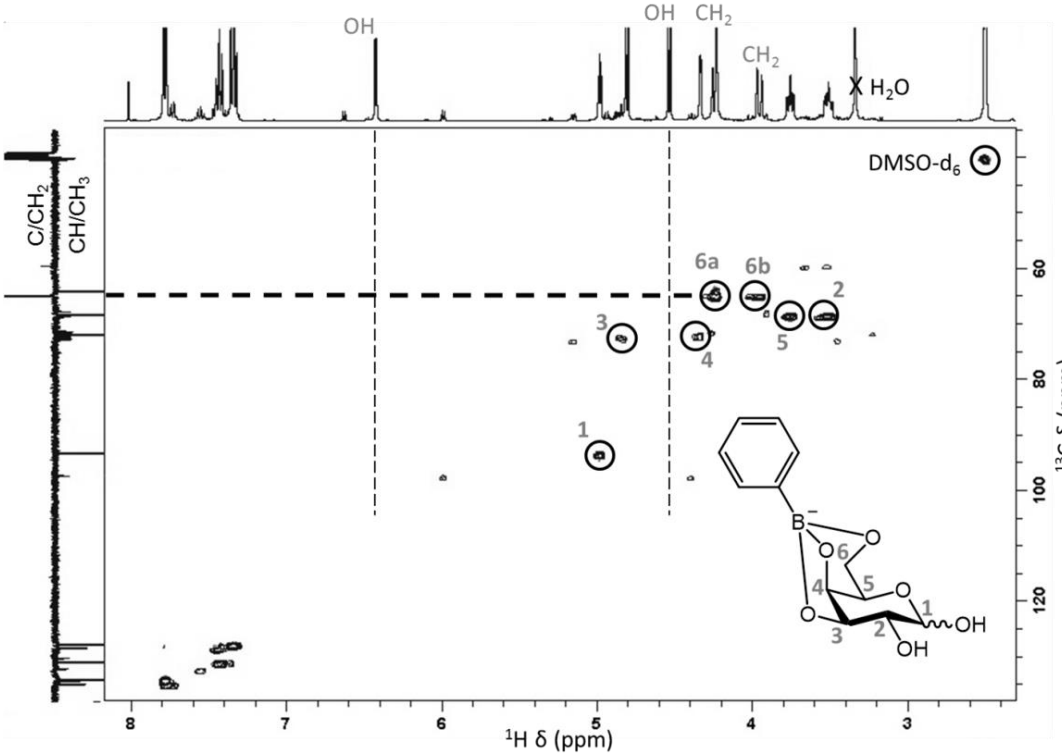

HSQC in DMSO-d_6 of the PBA:galactose 1:1 ratio after 6h15 in DMSO-d_6

The anomeric proton ^{1}H chemical shift increment was 0.07 ppm and the anomeric carbon ^{13}C chemical shift was 93.1 ppm. The proton coupling constants were not calculated.

Appendix II.XII (following): Complexes observed by complexing PBA on galactose in DMSO

Structure 2/1

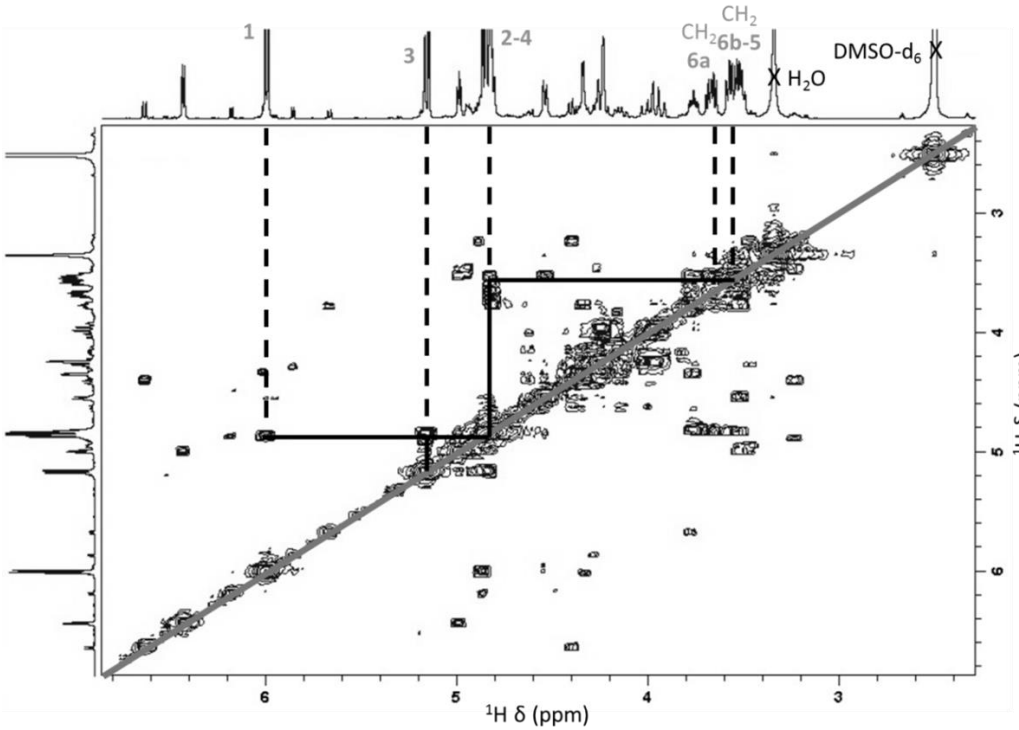

COSY in DMSO-d_6 of the PBA:galactose 2:1 ratio after 9h15 in DMSO-d_6

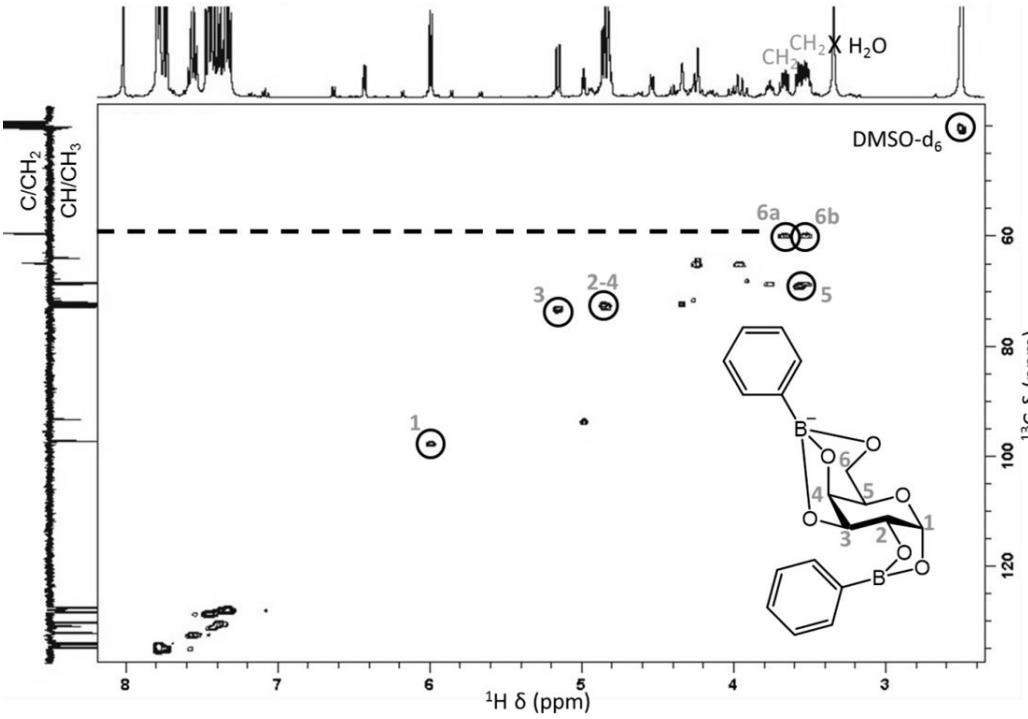

HSQC in DMSO-d_6 of the PBA:galactose 2:1 ratio after 9h15 in DMSO-d_6

The anomeric proton ^{1}H chemical shift increment was 1.09 ppm and the anomeric carbon ^{13}C chemical shift was 97.1 ppm. The proton coupling constants were not calculated. Even though both criteria were not consistent, considering the structure of the other complexes found, the pyranose form was more probable.

Appendix II.XII (following): Complexes observed by complexing PBA on galactose in DMSO

Structure b1/1

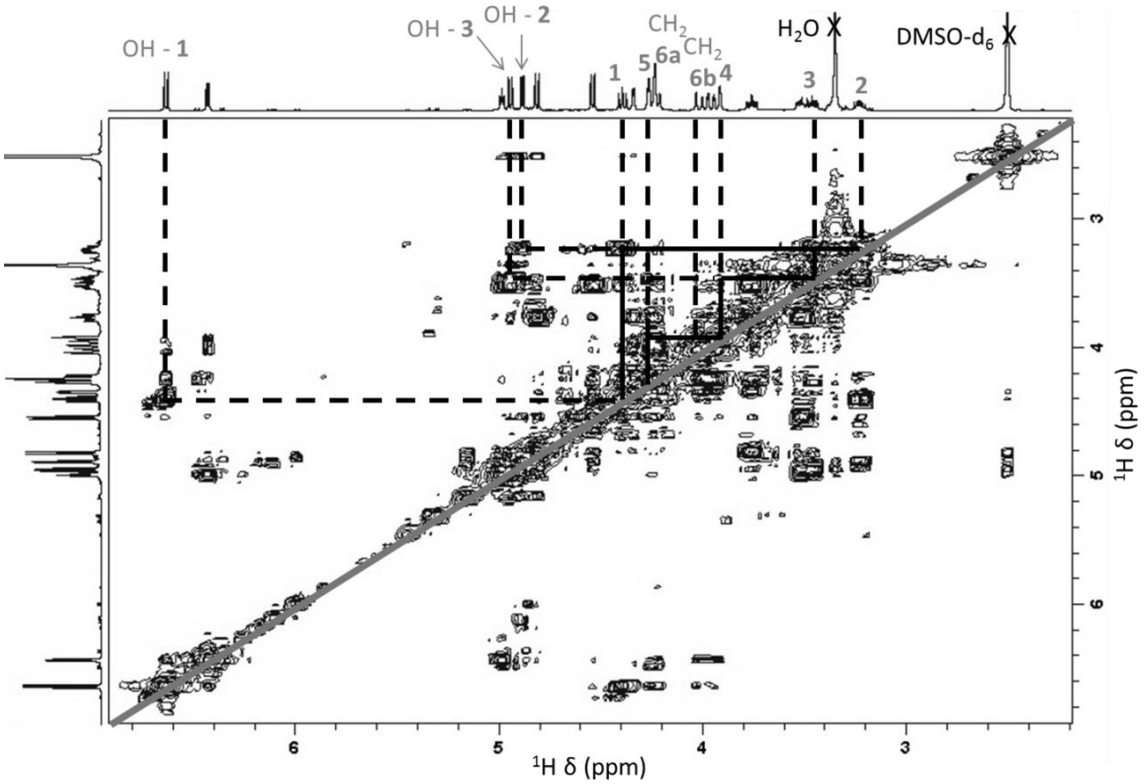

COSY in DMSO-d_6 of the PBA:galactose 1:1 ratio after 7 days in DMSO-d_6

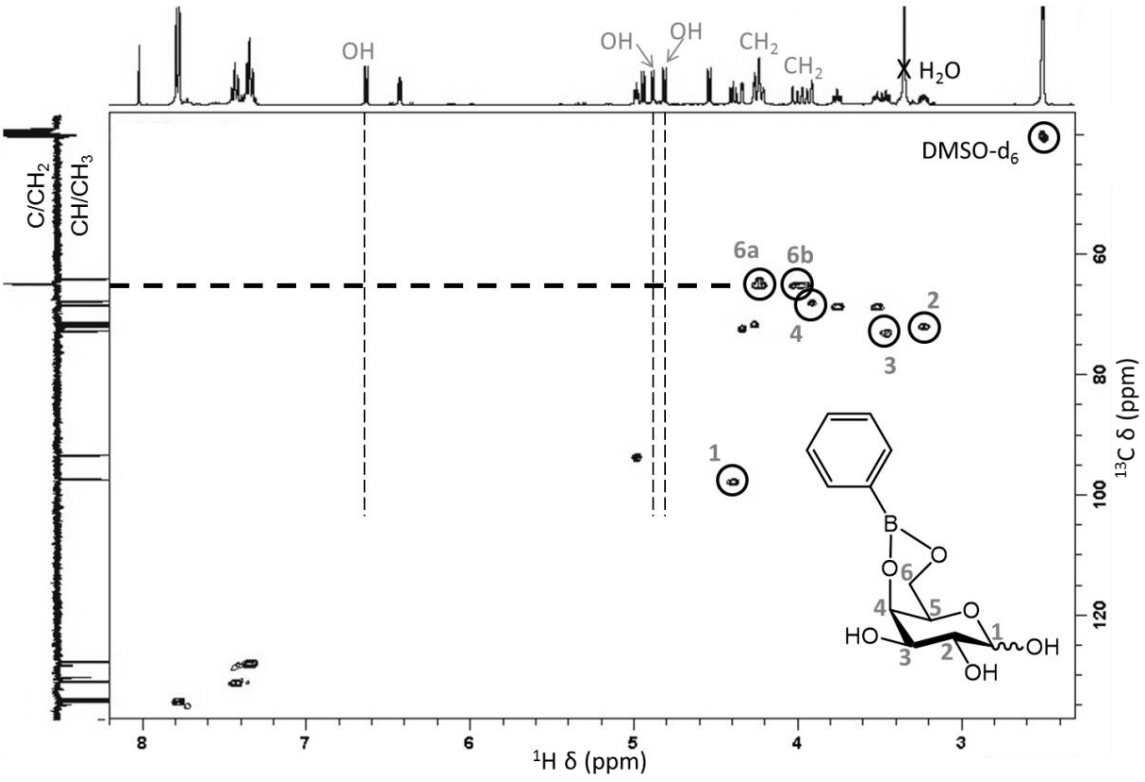

HSQC in DMSO-d_6 of the PBA:galactose 1:1 ratio after 7 days in DMSO-d_6

The anomeric proton ^{1}H chemical shift increment was -0.52 ppm and the anomeric carbon ^{13}C chemical shift was 97.2 ppm. The proton coupling constants were not calculated.

Appendix II.XIII: Summary of the assignments of the ^{1}H NMR spectra of the different complexes studied in this chapter

^{1}H δ (ppm) [a]	Complexation in	Boronic acid position	H-1	H-2	H-3	H-4	H-5	H-5b	H-6a	H-6b	OH [b]	CH_3-1
α-methylglucoside	DMSO-d_6	4,6	4.69	3.37	3.54	3.64	3.75	-	4.15	3.92	(2) 5.04 (3) 5.28	3.32
	Chloroform	2,3 & 4,6	4.67	3.66	3.57	3.38	3.76	-	4.17	3.93	-	3.33
β- methylglucoside	DMSO-d_6	4,6	4.30	3.13	3.39	3.61	3.61	-	4.18	3.92	(2) 5.36 (3) 5.40	3.42
	Chloroform	2,3 & 4,6	4.30	3.13	3.39	3.61	3.61	-	4.18	3.92	-	3.42
Glucose	DMSO-d_6 and chloroform	α-furanose 1,2 & 3,5	6.28	5.05	4.70	4.40	4.33	-	3.66	3.66	(6) 5.16	-
Xylose	DMSO-d_6 and chloroform	α-furanose 1,2 & 3,5	6.30	5.02	4.72	4.45	4.28	4.28	-	-	-	-
Mannose	Chloroform	Pyranose 2,3 & 4,6	5.38	4.89	5.26	4.50	5.05	-	4.40	4.14	(1) 6.79	-
Galactose	DMSO-d_6	Pyranose 3,4,6	4.98	3.51	3.76	4.81	4.34	-	4.23	3.97	(1) 6.41 (2) 4.54	-
		Pyranose 4,6	4.39	3.22	3.48	3.91	4.23	-	4.00	4.00	(1) 6.63 (2) 4.87 (3) 4.93	-
		Pyranose 1,2 & 3,4,6	6.00	4.85	5.15	4.85	3.53	-	3.68	3.53	-	-
Arabinose	DMSO-d_6 and chloroform	Pyranose 1,2 & 3,4	5.97	4.85	5.11	4.80	3.76	3.62	-	-	-	-

[a] Chemical shifts in DMSO-d_6 with the DMSO peak as reference at 2.50 ppm – The second significant figure is only given as an indication,
[b] The number between brackets corresponds to the position of the hydroxyl group

Appendix II.XIV: Summary of the assignments of the ^{13}C NMR spectra of the different complexes studied in this chapter

^{13}C δ (ppm) [a]	Complexation in	Boronic acid position	C-1	C-2	C-3	C-4	C-5	C-6	CH_3-1
α-methylglucoside	DMSO-d_6	4,6	100.6	72.1	71.5	75.2	64.2	64.0	54.9
	Chloroform	2,3 & 4,6	100.6	75.3	71.5	72.1	64.3	64.0	54.9
β- methylglucoside	DMSO-d_6	4,6	104.5	73.8	74.6 [b]	74.4 [b,c]	67.6 [c]	63.7	56.4
	Chloroform	2,3 & 4,6	104.5	73.8	74.6 [b]	74.4 [b,c]	67.6 [c]	63.7	56.4
Glucose	DMSO-d_6 and chloroform	α-furanose 1,2 & 3,5	104.1	85.8	73.6	74.7	70.9	61.8	-
Xylose	DMSO-d_6 and chloroform	α-furanose 1,2 & 3,5	104.9	85.7	74.2	73.2	59.8	-	-
Mannose	Chloroform	Pyranose 2,3 & 4,6	101.0	86.1	80.6	80.1	74.9	66.6	-
Galactose	DMSO-d_6	Pyranose 3,4,6	93.1	68.2	68.2	71.7	71.7	63.8	-
		Pyranose 4,6	97.2	71.4	72.4	67.6	71.1	64.6	-
		Pyranose 1,2 & 3,4,6	97.1	72.2 [d]	72.6	72.0 [d]	64.8	59.3	-
Arabinose	DMSO-d_6 and chloroform	Pyranose 1,2 & 3,4	96.7	71.7 [e]	71.6 [e]	72.2	59.8	-	-

[a] Chemical shifts in DMSO-d_6 with the DMSO peak as reference at 39.52 ppm, [b, c, d, e] The values can be interchanged

References

[1] E. Frankland, B. Duppa, *Proc. R. Soc. London* **1859**, *10*, 568–570.

[2] E. Frankland, *J. Chem. Soc.* **1862**, *15*, 363–381.

[3] D. G. Hall, in *Boronic Acids*, Wiley-VCH Verlag GmbH & Co. KGaA, **2011**, pp. 1–133.

[4] G. Springsteen, B. Wang, *Tetrahedron* **2002**, *58*, 5291–5300.

[5] J. D. Larkin, K. L. Bhat, G. D. Markham, B. R. Brooks, H. F. Schaefer, C. W. Bock, *J. Phys. Chem. A* **2006**, *110*, 10633–10642.

[6] S. J. Rettig, J. Trotter, *Can. J. Chem.* **1977**, *55*, 3071–3075.

[7] M. Sana, G. Leroy, C. Wilante, *Organometallics* **1991**, *10*, 264–270.

[8] N. Miyaura, A. Suzuki, *Chem. Rev.* **1995**, *95*, 2457–2483.

[9] A. J. J. Lennox, G. C. Lloyd-Jones, *Chem. Soc. Rev.* **2014**, *43*, 412–443.

[10] J. Yan, G. Springsteen, S. Deeter, B. Wang, *Tetrahedron* **2004**, *60*, 11205–11209.

[11] C. Lü, H. Li, H. Wang, Z. Liu, *Anal. Chem.* **2013**, *85*, 2361–2369.

[12] P. C. Trippier, C. McGuigan, *Med. Chem. Commun.* **2010**, *1*, 183–198.

[13] W. Seaman, J. R. Johnson, *J. Am. Chem. Soc.* **1931**, *53*, 711–723.

[14] B. C. Crane, N. P. Barwell, P. Gopal, M. Gopichand, T. Higgs, T. D. James, C. M. Jones, A. Mackenzie, K. P. Mulavisala, W. Paterson, *J. Diabetes Sci. Technol.* **2015**, *9*, 751–761.

[15] H. Liu, Y. Li, K. Sun, J. Fan, P. Zhang, J. Meng, S. Wang, L. Jiang, *J. Am. Chem. Soc.* **2013**, *135*, 7603–7609.

[16] A. Paramore, S. Frantz, *Nat. Rev. Drug Discovery* **2003**, *2*, 611–612.

[17] D. Li, Y. Chen, Z. Liu, *Chem. Soc. Rev.* **2015**, *44*, 8097–8123.

[18] E. Seymour, J. M. J. Fréchet, *Tetrahedron Lett.* **1976**, *17*, 1149–1152.

[19] P. J. Duggan, E. M. Tyndall, *J. Chem. Soc., Perkin Trans. 1* **2002**, 1325–1339.

[20] C. D. Roy, H. C. Brown, *Tetrahedron Lett.* **2007**, *48*, 1959–1961.

[21] E. G. Shcherbakova, T. Minami, V. Brega, T. D. James, P. Anzenbacher, *Angew. Chem. Int. Ed.* **2015**, *54*, 7130–7133.

[22] W. Niu, C. O'Sullivan, B. M. Rambo, M. D. Smith, J. J. Lavigne, *Chem. Commun.* **2005**, 4342–4344.

[23] R. Nishiyabu, Y. Kubo, T. D. James, J. S. Fossey, *Chem. Commun.* **2012**, *47*, 1106–1123.

[24] J. A. Riggs, R. K. Litchfield, B. D. Smith, *J. Org. Chem.* **1996**, *61*, 1148–1150.

[25] M. Li, W. Zhu, F. Marken, T. D. James, *Chem. Commun.* **2015**, *51*, 14562–14573.

[26] A. L. Korich, P. M. Iovine, *Dalton Trans.* **2010**, *39*, 1423–1431.

[27] H. R. Snyder, J. A. Kuck, J. R. Johnson, *J. Am. Chem. Soc.* **1938**, *60*, 105–111.

[28] E. F. Archibong, A. J. Thakkar, *Mol. Phys.* **1994**, *81*, 557–567.

[29] M. Forsyth, J. Sun, F. Zhou, D. R. MacFarlane, *Electrochim. Acta* **2003**, *48*, 2129–2136.

[30] M. Mastalerz, *Angew. Chem. Int. Ed.* **2008**, *47*, 445–447.

[31] A. B. Morgan, J. L. Jurs, J. M. Tour, *J. Appl. Polym. Sci.* **2000**, *76*, 1257–1268.

[32] G. Alcaraz, L. Euzenat, O. Mongin, C. Katan, I. Ledoux, J. Zyss, M. Blanchard-Desce, M. Vaultier, *Chem. Commun.* **2003**, 2766–2767.

[33] M. Dowlut, D. G. Hall, *J. Am. Chem. Soc.* **2006**, *128*, 4226–4227.

[34] K. Benner, P. Klüfers, O. Labisch, *Carbohydr. Res.* **2007**, *342*, 2801–2806.

[35] R. van den Berg, J. A. Peters, H. van Bekkum, *Carbohydr. Res.* **1994**, *253*, 1–12.

[36] R. Smoum, A. Rubinstein, M. Srebnik, *Magn. Reson. Chem.* **2003**, *41*, 1015–1020.

[37] M. Meiland, T. Heinze, W. Guenther, T. Liebert, *Tetrahedron Lett.* **2009**, *50*, 469–472.

[38] M. Bérubé, M. Dowlut, D. G. Hall, *J. Org. Chem.* **2008**, *73*, 6471–6479.

[39] M. P. Nicholls, P. K. C. Paul, *Org. Biomol. Chem.* **2004**, *2*, 1434–1441.

[40] J. C. Norrild, H. Eggert, *J. Am. Chem. Soc.* **1995**, *117*, 1479–1484.

[41] S. Shinkai, K. Tsukagoshi, Y. Ishikawa, T. Kunitake, *J. Chem. Soc., Chem. Commun.* **1991**, 1039–1041.

[42] M. Bielecki, H. Eggert, J. C. Norrild, *J. Chem. Soc., Perkin Trans. 2* **1999**, 449–455.

[43] B. Ma, H. F. Schaefer III, N. L. Allinger, *J. Am. Chem. Soc.* **1998**, *120*, 3411–3422.

[44] S. K. Chandran, A. Nangia, *CrystEngComm* **2006**, *8*, 581–585.

[45] X. Pan, X. Yang, C. R. Lowe, *J. Mol. Recognit.* **2008**, *21*, 205–209.

[46] S. P. Draffin, P. J. Duggan, G. D. Fallon, E. M. Tyndall, *Acta Crystallogr., Sect. E: Struct. Rep.* **2005**, *E61*, o1733–o1735.

[47] H. Kawamoto, S. Saito, S. Saka, *Carbohydr. Res.* **2008**, *343*, 249–255.

[48] M. Meiland, T. Heinze, W. Guenther, T. Liebert, *Carbohydr. Res.* **2010**, *345*, 257–263.

[49] J. B. Binder, A. V. Cefali, J. J. Blank, R. T. Raines, *Energy Environ. Sci.* **2010**, *3*, 765–771.

[50] S. Viel, D. Capitani, L. Mannina, A. Segre, *Biomacromolecules* **2003**, *4*, 1843–1847.

Chapter III. Polymer synthesis

Table of Contents

Chapter Purpose

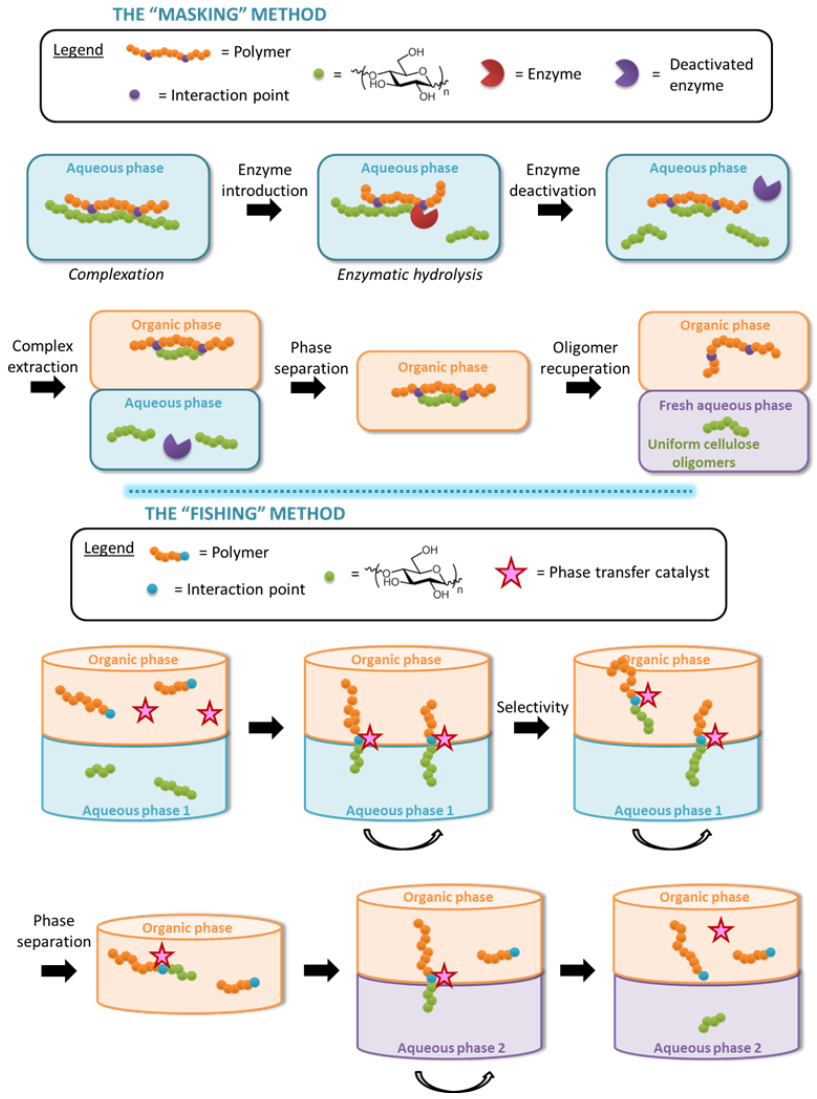

The following polymer structures were determined to be the best suited for the "masking" and the "fishing" methods after the preliminary study of the complexation between phenylboronic acid and different cellulose models. Their preparation will be investigated in this chapter.

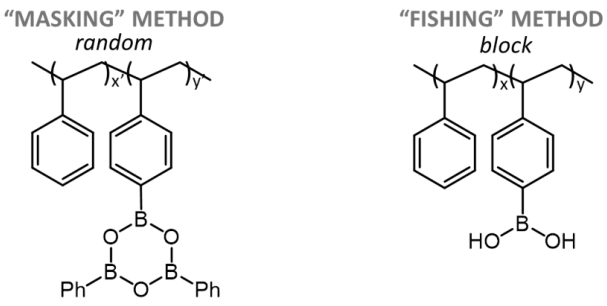

A high control of the molar masses is essential as the dispersity of the cellulose oligomers retrieved after the "fishing" or the "masking" methods depends on it.

III. 1. Bibliography on polymers containing boronic acid entities

III. 1. A) **Synthesis**

Boronic acid polymers are usually prepared by either polymerisation of a boronic acid monomers or a polymer modification reaction[1].

III. 1. A) i) Polymerisation

Boron containing monomers can be polymerised by free radical, metathesis[2] (**Figure III-1a** and **b**) or Ziegler-Natta[3,4] (**Figure III-1c**) polymerisations. These last two types require expensive catalysts and monomers compared to radical polymerisation. They thus will not be discussed further.

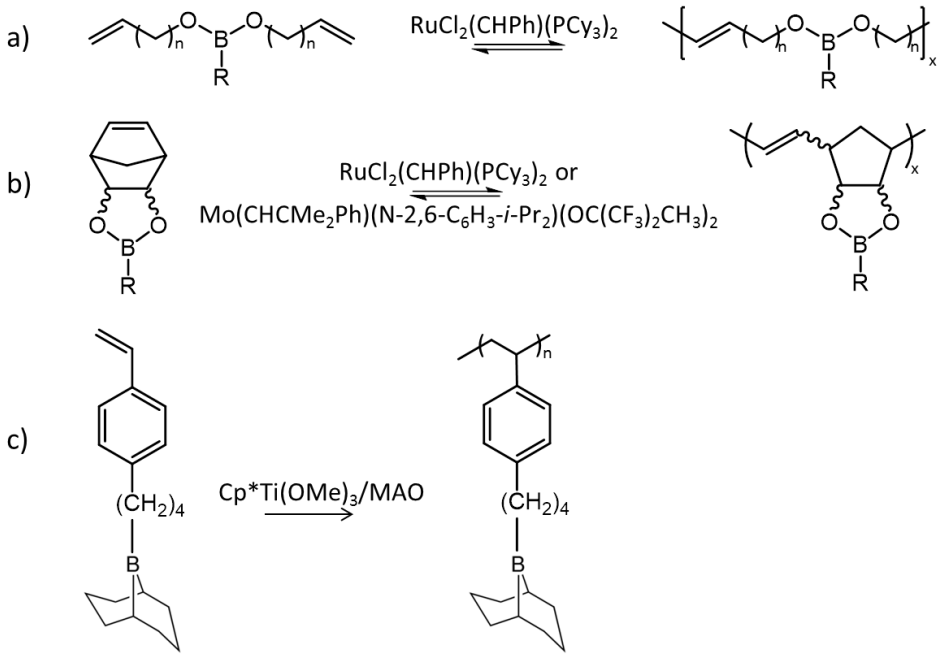

Figure III-1. Examples of a) acyclic diene metathesis[2], b) ring-opening metathesis[2] and c) Ziegler-Natta polymerisation[4] to obtain boron containing polymers

Even though 3-acrylamidophenylboronic acid (APBA, **Figure III-2**) is less commercially available than 4-vinylphenylboronic acid (VBA, **Figure III-2**), its solubility in water and pK_a close to physiological value aroused the interest of many authors in the literature. The boronic acid is often protected, generally by pinacol, before being polymerised (**Figure III-2**) to avoid the formation of anhydrides induced by the solvent and/or the required elevated polymerisation temperatures. However, unprotected boronic acid monomers are able to polymerise in hydrophilic solvents like acetonitrile[5] or ethanol[6], or with a small percentage of water into the reaction medium[7].

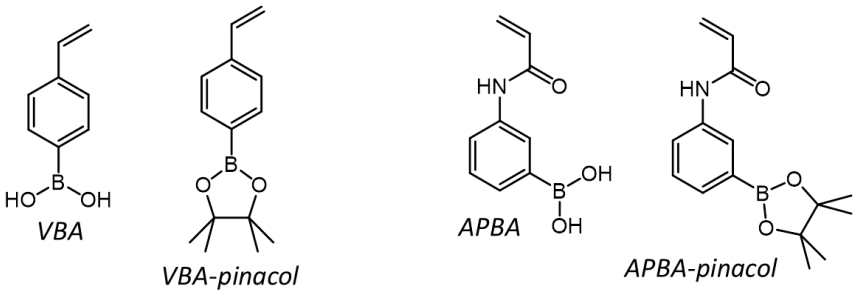

Figure III-2. Structure of some boronic acid containing monomers protected or free

To have a control over a radical polymerisation, the main two techniques employed with boronic acids are reversible addition-fragmentation chain transfer (RAFT)[8] or atom transfer radical polymerization (ATRP)[9,10] (see **Appendix III.I** for the respective mechanisms, p 145).

For RAFT polymerisation, the chain-transfer agent (CTA) mostly used is 2-dodecylsulfanylthiocarbonylsulfanyl-2-methyl-propionic acid (DMP, **Figure III-3a**) with azobisisobutyronitrile (AIBN) as the initiator at 70°C in DMF/H_2O 95/5 v/v for un-protected monomers[11–14] or in DMF[15,16] or anisole[17] with protected monomers. Dibenzyl trithiocarbonate (DBTTC, **Figure III-3b**) or 2-(butylthiocarbonothioylthio) propanoic acid (BTTCP, **Figure III-3c**) and their PEGylated equivalents also presented good results for the homo-polymerisation of VBA in DMF/H_2O 95/5 v/v[18]. Other CTA were also seldom reported like 4-cyanopentanoic acid dithiobenzoate (CPADB, **Figure III-3d**) that was used for APBA with AIBN at 70°C in DMSO/H_2O 95/5 v/v[19] or methyl 3-benzylsulfanylthio carbonylsulfanylpropionate (MBSP, **Figure III-3e**) that was used for the polymerisation of a luminescent boron quinolate monomer[20].

The effectiveness of the CTA is influenced by the monomer(s) being polymerised but also depends strongly on the free radical leaving groups which stabilises or not the intermediate radicals[21,22] (**Appendix III.II**, p 146).

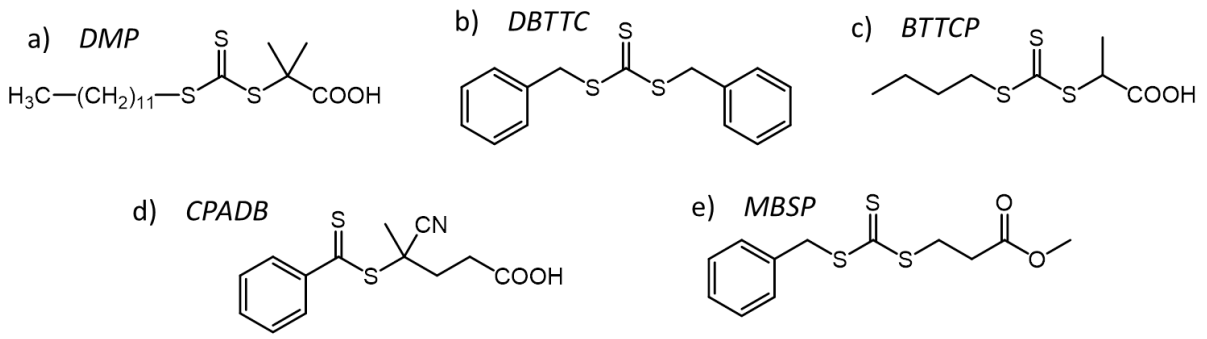

Figure III-3. Structure of several chain transfer agents (CTA): DMP, DBTTC, BTTCP, CPADB and MBSP

For ATRP, only one example was found in the literature concerning the direct polymerisation of a boronic acid containing monomer. In fact, the polymerisation by ATRP of

a boronic acid monomer occurs at a considerably slower rate than for 4-trimethyl silylstyrene for example (**Figure III-4**).

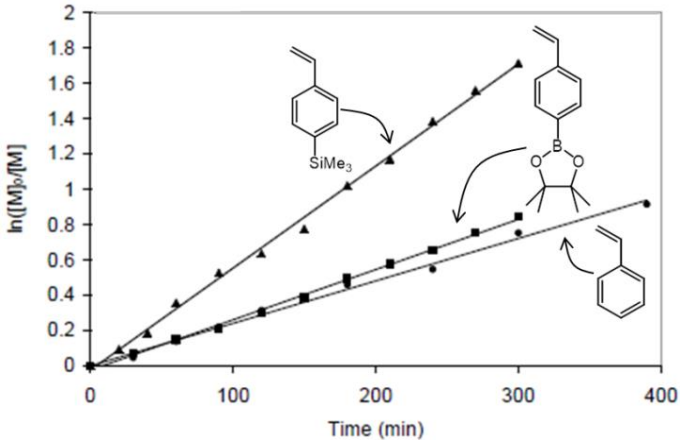

Figure III-4. Kinetic data for ATRP of several monomers in anisole (adapted from Jäkle and coll.[23])

Poly(4-trimethylsilyl styrene) (PTMSS) can be modified afterwards into a boronic acid containing polymer (**Figure III-5**). However, this method is time-consuming compared to RAFT polymerisation and, moreover, BBr_3 is toxic and highly corrosive and needs to be handled very carefully.

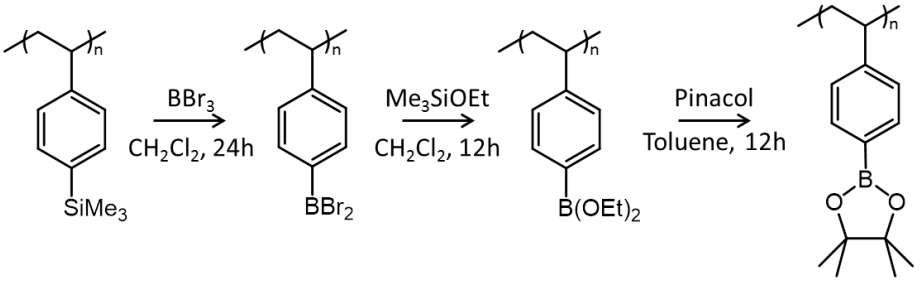

Figure III-5. General method to transform PTMSS into a boronic acid containing polymer (adapted from Jäkle and coll.[24])

To de-protect the monomers, one of the most efficient method is by transesterification either with a polystyrene-boronic acid resin in acetonitrile containing 2% of trifluoroacetic acid under reflux at least 18h[17,25] or with diethanolamine followed by a mild acidic hydrolysis[26].

III. 1. A) ii) Un-functionalised polymer post-modification

The transformation of PTMSS into a boronic acid containing polymer has been explained previously but this post-modification can also be done on un-functionalised polymers as polystyrene. The aromatic ring needs first to be activated with *n*-butyllithium and then functionalised with a borate. An hydrolysis step releases the boronic acid residues (**Figure III-6**) which are expected to be introduced in *para* and in *meta* positions to the

backbone[27]. To obtain solely the *para* position, 4-bromostyrene can be copolymerised with the styrene followed by a bromide-lithium exchange[27,28].

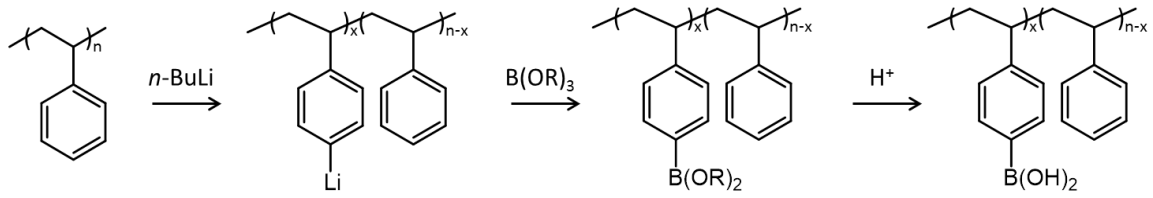

Figure III-6. Example of polystyrene functionalisation with boronic acid[27]

III. 1. B) Applications

All the applications presented in this part were only studied in lab-scale. To our knowledge, boronic acid polymers do not have industrial applications yet.

III. 1. B) i) Glucose detection

The main application of boronic acid containing polymers is glucose detection. For instance, poly(3-acrylamidophenylboronic acid)-*b*-poly(*N*-isopropylacrylamide) (PAPBA-*b*-PNIPAM) was found to be sensitive to pH, temperature and glucose concentration[12] as represented in **Figure III-7**. As seen previously in Chapter II, the influence of the pH occurs around the PAPBA units pK_a (≈ 9). Below the pK_a, the boronic acids are dehydrated and form micelles with a hydrophilic PNIPAM corona and a hydrophobic PAPBA core. When these micelles are exposed to an increase of pH or the addition of polyol such as glucose, they dissociate to form unimers as the PAPBA block becomes soluble in water. These particles can thus be loaded with a dye, or another compound, which release is triggered by pH change or glucose concentration[16]. Then, a temperature increase leads to the PNIPAM block dehydration and interchain aggregation[12]. The transition occurs at the lower critical solution temperature (LCST) that increased from 32°C for PNIPAM alone to 42°C for the block copolymer.

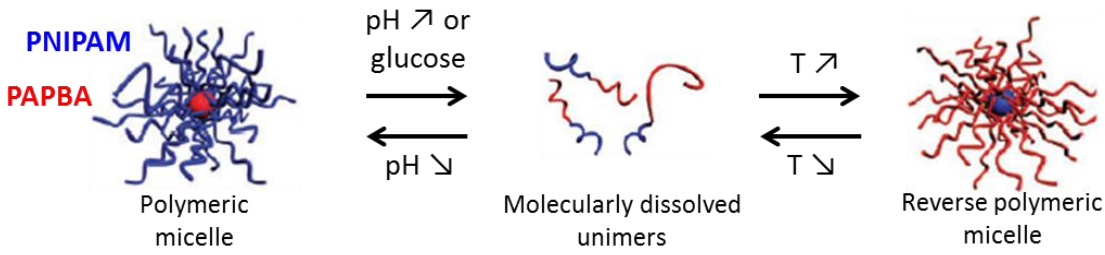

Figure III-7. Block copolymer self-assembly/dissociation in response to changes of pH or temperature (adapted from Sumerlin and coll.[12])

The LCST of a boronic acid containing polymer however depends on the glucose presence[6]. As a matter of fact, a random poly(*N*,*N*-dimethylacrylamide)-PAPBA with

15 mol% of APBA at 0.1 wt% in HEPES buffer had a LCST of around 25°C without glucose and this latter jumped to around 40°C with glucose at 16.7 $g.L^{-1}$.

III. 1. B) ii) Self-assembly and loading

The boronic acid propensity to complex saccharides was also employed to induce self-assembly. APBA was polymerised by RAFT to obtain a block copolymer with a lactose containing monomer (2-lactobionamidoethylmethacrylate, LAMA). Inter and intra-chain interactions led to self-assembled structures in water[19] (**Figure III-8**). These particles had no cytotoxicity on Chinese hamster ovary cells and human colorectal carcinoma. They were loaded with insulin with an encapsulation efficiency between 70% and 86% depending on the length of the PLAMA block. The controlled delivery of the peptide occurred gradually over 12h in phosphate buffered saline (PBS) buffer.

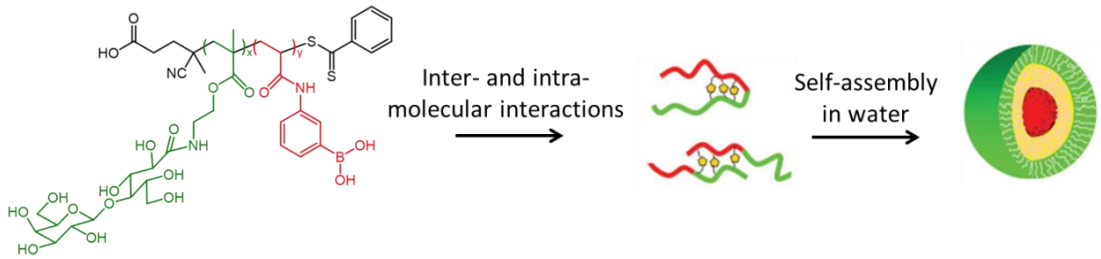

Figure III-8. PAPBA-*b*-PLAMA structure and self-assembly in water (adapted from Li and coll.[19])

In another example[14], PAPBA and poly(N,N-dimethylacrylamide)-*b*-PAPBA (PDMA-*b*-PAPBA) were cross-linked into a dynamic-covalent macromolecular network or multi-arms stars, respectively, after a treatment with multi-functional diols (**Figure III-9**). This cross-linking was driven by boronic esters formation and was thus reversible. The disruption could be induced by the introduction of mono-functional diols but a new addition of a multi-functional diol could rebuild the cross-linking.

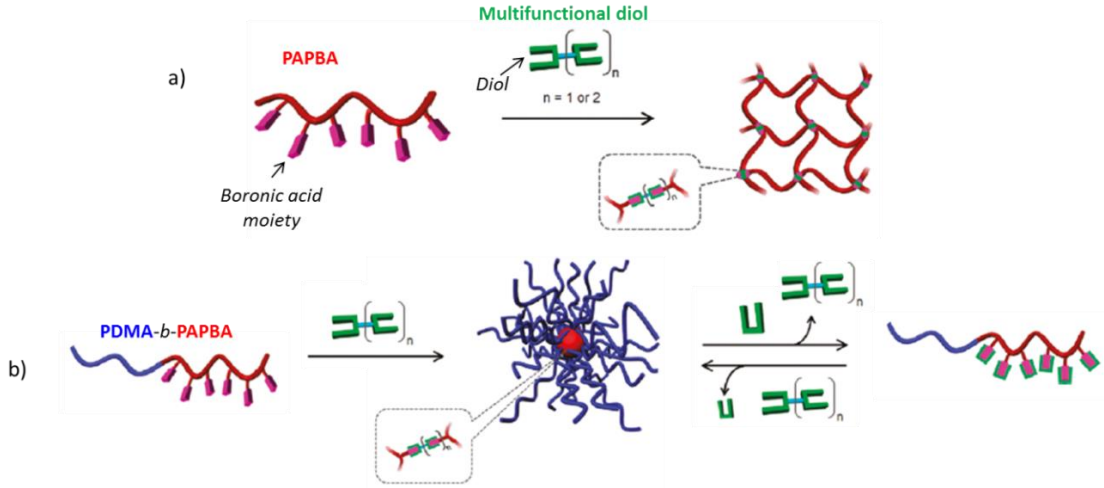

Figure III-9. a) Dynamic-covalent macromolecular network or b) reversible multi-arms stars formation (adapted from Sumerlin and coll.[14])

III. 1. B) iii) Telechelic polymers

Polymers containing only one boronic acid per chain can be produced by introducing the moiety into the RAFT agent[29] or by ATRP with an initiator bearing a trimethylsilyl group that can be subsequently transformed[30]. Three polymer chains can thus organise themselves into a boroxine star upon the addition of amine ligand[29] or water elimination[30] (**Figure III-10**). The glass transition temperature (T_g) of the polymer after boroxine formation had increased from 80°C for the trimethylsilyl equivalent to 101°C which confirms the rearrangement into anhydrides and a more rigid structure[30].

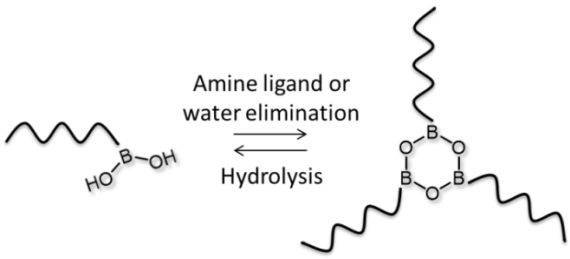

Figure III-10. Schematic rearrangement into a boroxine star formation

Polymers obtained by ATRP having a boronic acid at one extremity can be coupled at the other extremity by atom transfer radical coupling hence possessing a boronic acid moiety at each extremity[30]. Such polymers can also form anhydrides as proven by an increased T_g (112°C compared to the previous 101°C) which confirms the formation of an even more rigid structural framework.

III. 2. Anionic polymerisation

A polymerisation technique leading to small molar masses with a great control over the dispersity is required for the application aimed by this work. Anionic polymerisation is thus the logical choice. Unfortunately, 4-vinylphenylboronic acid (VBA) could not be directly polymerised by this method as it deactivated the polymerisation. Even after protection with pinacol, either the monomer or the remaining free diol induced the same result. Consequently, polystyrenes (PS) with a theoretical polymerisation degree (DP_{th}) of 10 and 50 were obtained by anionic polymerisation of styrene (**Figure III-11**) with *sec*-butyllithium in cyclohexane at 40°C. The polymers were modified afterwards to introduce boronic acid residues as seen previously (**Figure III-6**, p 130).

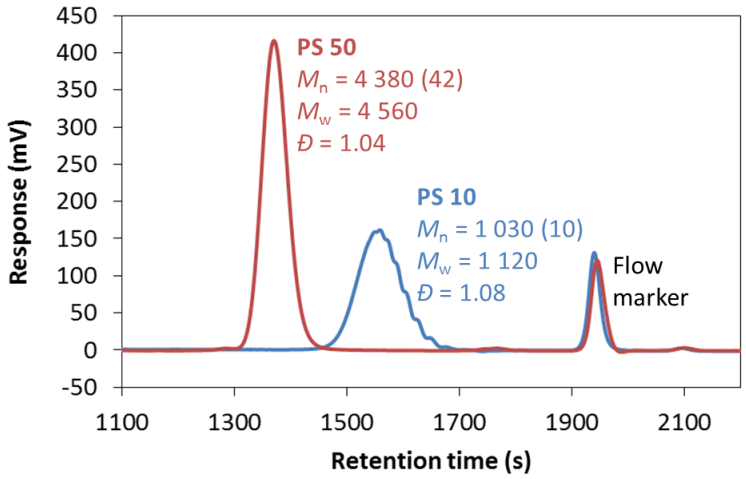

Figure III-11. SEC in THF of two polystyrenes made by anionic polymerisation (M_n and M_w given in g.mol^{-1} and based on polystyrene calibration, value between brackets is the corresponding DP)

In theory, 50% of the phenyl pendant group were modified. Some solubility issue seemed to arise after modification as the SEC signals in THF either decreased instead of increasing or disappeared for the polymer of higher molar mass (**Figure III-12**). Protection with pinacol had a positive effect on the characterisation of PS 10 – $B(OH)_2$ but had no impact on PS 50 – $B(OH)_2$ SEC in THF signal.

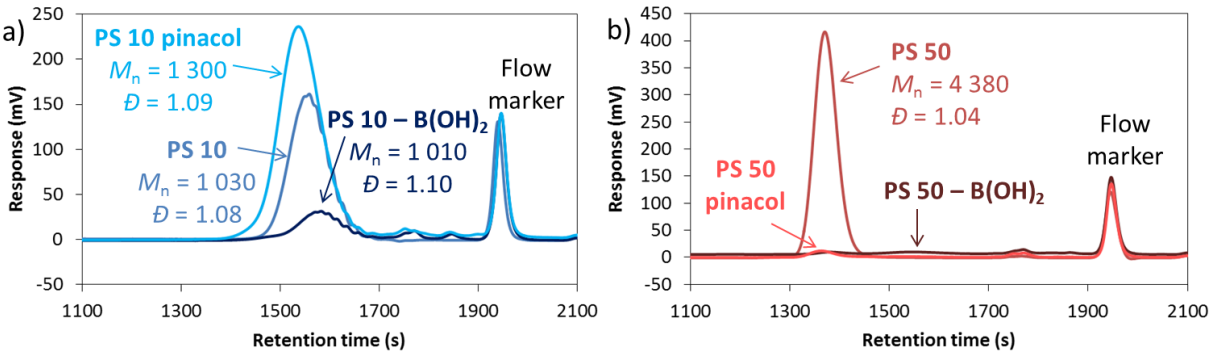

Figure III-12. SEC in THF of a) PS 10 and b) PS 50 of the polystyrene alone (PS), after modification (PS – $B(OH)_2$) and protection with pinacol (PS pinacol) (M_n in g.mol^{-1} based on PS calibration)

The solubility of these polymers in other solvents than THF was also investigated (**Table III-1**) and chloroform appeared to be a good alternative to characterise the polymers modified and protected with pinacol even at high molecular weight. ^{1}H NMR spectra seemed to confirm the good solubility (**Figure III-13**).

Table III-1. Solubility issues depending on the polymer and the solvent

Solvent	PS 10 – $B(OH)_2$ [a]	PS 50 – $B(OH)_2$ [a]	PS 10 pinacol [b]	PS 50 pinacol [b]
Tetrahydrofuran	+	+	-	-
Cyclohexane	--	--	-	-
Dichloromethane	-	--	+	+
Acetone	-	--	-	-
Methanol	+	--	--	--
Chloroform	-	-	+	+

[a] Polystyrene after modification to introduce boronic acid moieties, [b] Polystyrene after modification protected with pinacol – + : Clear solution, - : Blurry solution, -- : Not solubilised

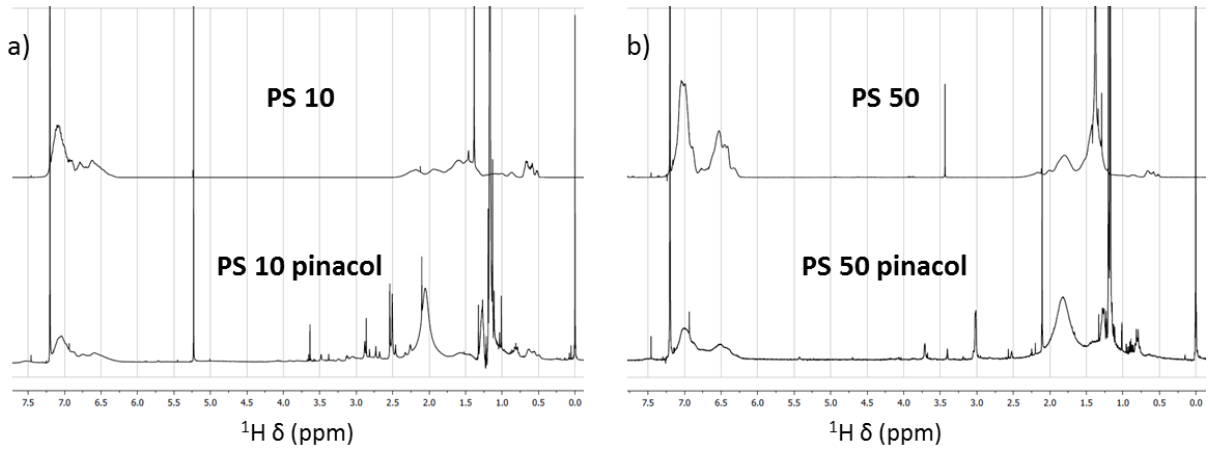

Figure III-13. ^{1}H NMR spectra in $CDCl_3$ of polystyrene alone (above) and after modification and protection with pinacol (below) for a) PS 10 and b) PS 50

SEC in chloroform was then tentatively applied to the polymers after protection with pinacol but, unfortunately, no signals were usable (**Figure III-14**).

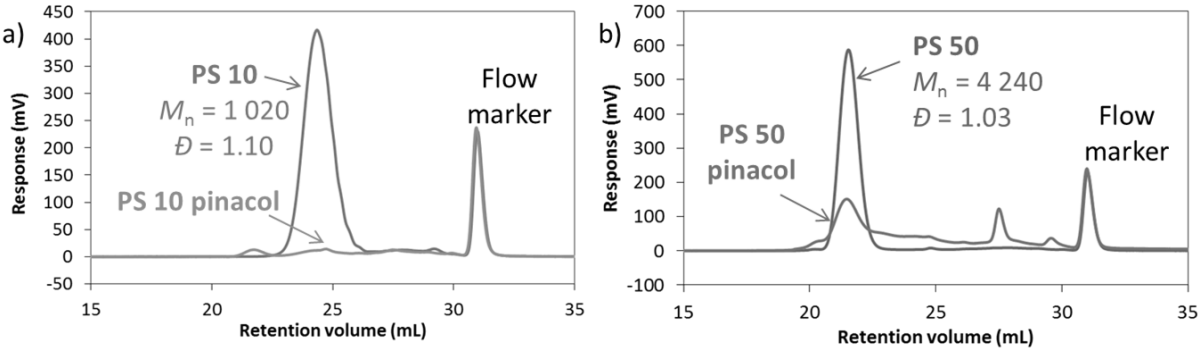

Figure III-14. SEC in chloroform of a) PS 10 and b) PS 50 of the polystyrene alone (PS) and after modification and protection with pinacol (PS pinacol) (M_n based on PS calibration)

The quantity of boronic acid introduced was reduced to 10% but the solubilisation was still an issue. Eventually, another polymerisation technique was chosen.

III. 3. RAFT polymerisation

Due to the bad results achieved with anionic polymerisation, some control over the dispersity of small molar masses had to be surrendered. Based on the literature, the RAFT polymerisation was one of the best and simplest alternatives.

III. 3. A) General parameters determined on polystyrene

DMP, in association with AIBN, was chosen to start the study as it is the most used RAFT agent for the polymerisation of boronic acid containing monomers. The influence of several parameters on the polymerisation kinetics of styrene alone was evaluated (**Table III-2**). The molar masses obtained for Polymer 1 were low compared to the expected ones so the polymerisation was still not finished after 8h whereas, for Polymer 2, the polymerisation was more advanced. Consequently, when a high DP is targeted, the polymerisation time have to be increased to reach a higher conversion. Similarly, a higher AIBN/DMP ratio improved the conversion but the dispersity had also slightly increased (Polymer 3). The solvent (anisole or cyclohexane) had no effect on the polymer characteristics (Polymer 4).

Table III-2. Variation of several parameters of the RAFT polymerisation of polystyrene, values in bold highlight the changes compared to Polymer 1

	Polymer 1	Polymer 2	Polymer 3	Polymer 4
Solvent	Anisole	Anisole	Anisole	**Cyclohexane**
DP_{th}	50	**10**	50	50
AIBN/DMP ratio	0.31	0.46	**1.24**	0.31
Mass yield	44%	83%	95%	41%
M_n (g.mol^{-1}) [a]	2 040	820	3 520	1 970
M_w (g.mol^{-1}) [a]	2 210	950	4 400	2 230
$Đ$ [a]	1.08	1.16	1.25	1.13

Polymerisation of styrene at 4.57 M in different solvent for 8h at 70°C, [a] Determined by SEC in THF based on polystyrene calibration

III. 3. B) Random copolymers

III. 3. B) i) AIBN/DMP ratio

As seen previously, the AIBN/DMP ratio is critical to the control of the polymerisation and consequently was subjected to further investigation. The conversion calculated by NMR

(calculation detailed in **Appendix III.III**, p 147) and the mass yield slightly increased with the AIBN/DMP ratio but the control over the polymerisation decreased as the dispersity increased from 1.1 to 1.6 (**Figure III-15**). Consequently, the best compromise is probably a ratio below 0.8.

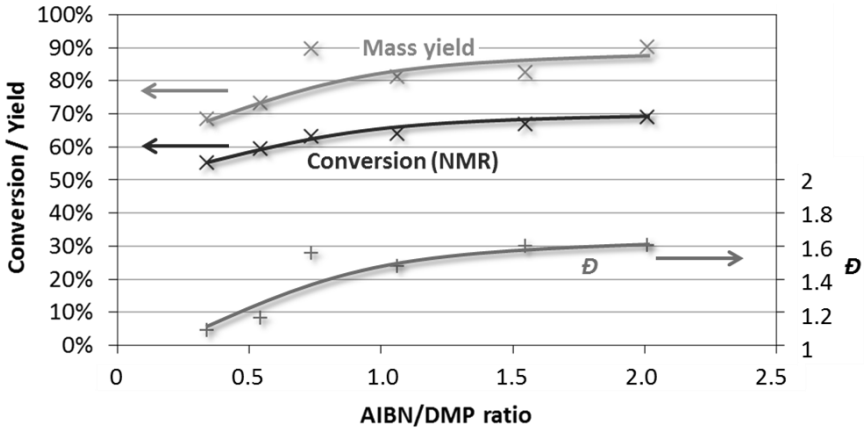

Figure III-15. Effect of the AIBN/DMP ratio on the conversion, mass yield and dispersity (determined by SEC in THF based on polystyrene calibration) – Polymerisation of a random PS-PVBA of DP_{th} 50 with styrene at 2.41 M and VBA at 0.61 M in DMF/H_2O 95/5 v/v at 70°C for 24h

III. 3. B) ii) Determination of the VBA content

Before going further in determining the best polymerisation parameters, a method to determine the actual ratio of VBA in the polymer was elaborated. The guideline was to complex a diol onto the boronic acid groups carried by the polymer that would have specific peaks in ^{1}H NMR, for the complexed and free forms, which do not overlap signals from the polymer.

Three diols (pinacol, 4-methylcatechol and 4-tert-butylcatechol) were considered and only 4-methylcatechol fulfilled the requirements (**Figure III-16a**). The complexation on the polymer was confirmed by DOSY as the specific peak corresponding to the complexed form had the same diffusion coefficient than the polymer (**Figure III-16b**). The method was thus employed and the VBA ratio calculated as detailed in **Appendix III.III** (p 147).

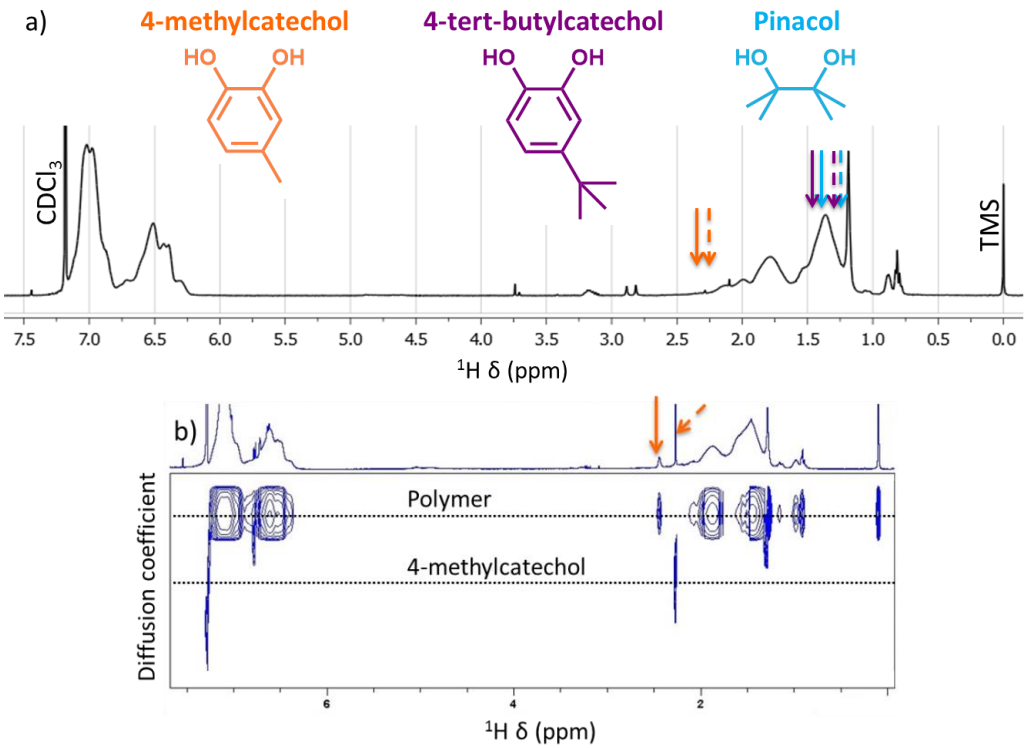

Figure III-16. a) ^{1}H NMR spectrum of a random PS-PVBA copolymer in $CDCl_3$, the arrows correspond to the specific peaks of the diols complexed (full) or free (doted) and b) DOSY of a random PS-PVBA copolymer complexed with 4-methylcatechol

III. 3. B) iii) Selection of the monomer and the solvent

Several options about the monomer (protected or not) and the solvent (anisole or DMF and water) were compared (**Table III-3**).

The yield, conversion, molar masses and VBA content of Polymer 5 (protected VBA polymerised in anisole) are really low compared to the other ones. It could be due to solubility issues which would be difficult to recognise as both monomers and anisole are uncoloured liquids. Moreover, a deprotection step, that may not be complete, is necessary to free the boronic acid moieties from this type of polymer.

As the molar mass obtained was higher than the expected one (*i.e.* 5 600 g.mol^{-1}), the control of Polymer 6 polymerisation was lost. The reason was that the reaction medium viscosity had greatly increased over time. Moreover, anisole was difficult to remove from the polymer which explains the great mass yield observed, higher than the conversion, as the polymer was not completely dry.

As Polymer 7 presented the best results and the higher VBA content, the monomer and solvent chosen for the rest of the report are un-protected VBA in DMF/H_2O 95/5 v/v.

Table III-3. Comparison of several monomer and solvent for the synthesis of random copolymers

	Polymer 5	Polymer 6	Polymer 7
Monomer	VBA pinacol	VBA	VBA
Solvent	Anisole	Anisole	DMF/H_2O 95/5
DP_{th}	47	50	51
Ratio AIBN/DMP	0.78	0.69	0.78
Mass yield	37.4%	95.7%	56.0%
Conversion (NMR) [a]	19.0%	62.6%	57.8%
VBA content [a]	4.9%	17.5%	22.7%
M_n (g.mol^{-1}) [b]	2 990	5 790	4 140
M_w (g.mol^{-1}) [b]	3 400	6 780	4 940
$Đ$ [b]	1.14	1.17	1.19

Polymerisation of random copolymers with styrene at 1.0 M and boronic acid containing monomer at 0.9 M at 70°C for 6h – [a] See ***Appendix III.III*** *(p 147) for the calculation detail, [b] Determined by SEC in THF based on polystyrene calibration – Polymer 6 and Polymer 7 were protected with pinacol before the analysis for comparison with Polymer 5*

III. 3. B) iv) Boronic anhydrides containing polymer

Other solvents were investigated for the synthesis of the random copolymer of styrene and VBA under the anhydride form with phenylboronic acid (PBA). The goal was to polymerise styrene and VBA in the presence of an excess of PBA in an anhydrous solvent to favour the anhydride formation. With the excess of PBA, the probability to form anhydride monomers with only one vinyl group was increased (**Figure III-17**).

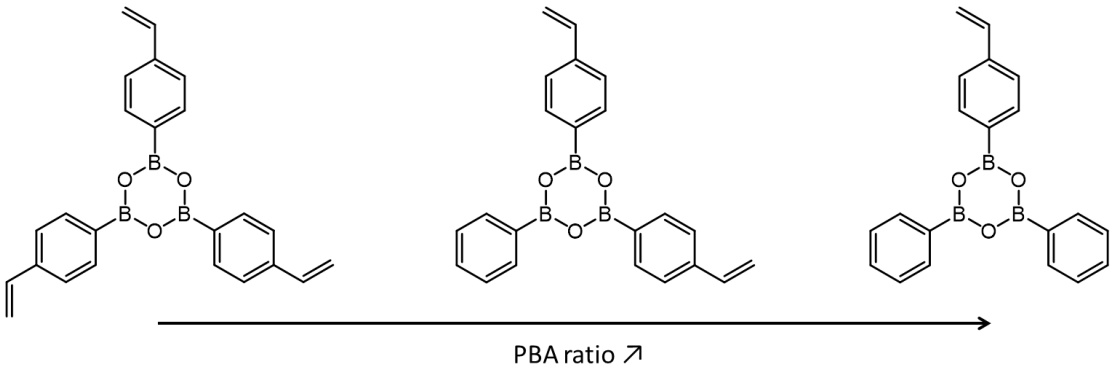

Figure III-17. Formation of the monomer anhydride by increasing the PBA ratio

This approach was assayed with cyclohexane and toluene. With 10 or 4 equivalents of PBA, a complete solubilisation was only reached for a large dilution. Unfortunately, the monomer concentration was then too low for the polymerisation to occur. The complete

solubilisation and the consequent polymerisation were achieved in chloroform but with a really low rate. In fact, the boiling point of chloroform (T_b = 62°C) is low compared to the dissociation temperature of AIBN (usually used at or above 70°C). A new adequate initiator was employed: the 2,2'-azo-bis(4-methoxy-2.4-dimethyl valeronitrile) (V-70, **Figure III-18**) as it has a 10 hour half-life decomposition at 30°C[31].

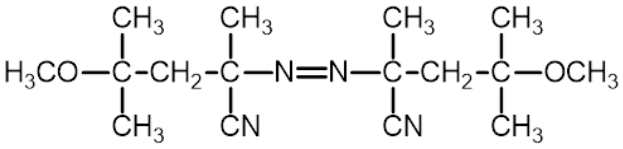

Figure III-18. V-70 (2,2'-azobis(4-methoxy-2.4-dimethyl valeronitrile)) structure

This initiator was thus investigated with styrene but did not present good conversion result after 24h of polymerisation (**Table III-4**). As no purification step was done before using the V-70, the initiator/CTA ratio had to be increased (Polymer 8 and 9) but the conversion was still below 50%. Another RAFT agent, the 3-(benzylthiocarbonothioylthio)propanoic acid (BSPA), was tried but the results were unsatisfactory.

Table III-4. Investigation of V-70 as a polymerisation initiator for polystyrene

	Polymer 8	Polymer 9	Polymer 10
RAFT agent	DMP	DMP	BSPA
DP_{th}	50	54	57
Ratio V-70/CTA	1.5	3.0	3.2
Concentration (M)	2.82	3.88	3.88
Yield (mass)	21.3%	32.5%	9.1%
Conversion (NMR) [a]	25.1%	41.5%	24.2%
M_n (g.mol^{-1}) [b]	1 820	1 920	2 000
M_w (g.mol^{-1}) [b]	1 990	2 230	2 370
$Đ$ [b]	1.09	1.16	1.19

Polymerisation of styrene in chloroform with V-70 as the initiator at 30°C for 24h, [a] See ***Appendix III.III*** *(p 147) for the calculation detail, [b] Determined by SEC in THF based on polystyrene calibration*

Even with these bad results, the synthesis of the boronic anhydrides containing polymer was tested with 5 equivalents of PBA per VBA in chloroform with V-70 at 30°C but after 24h the ^{1}H NMR spectrum presented no characteristic signals for polymers (**Figure III-19**).

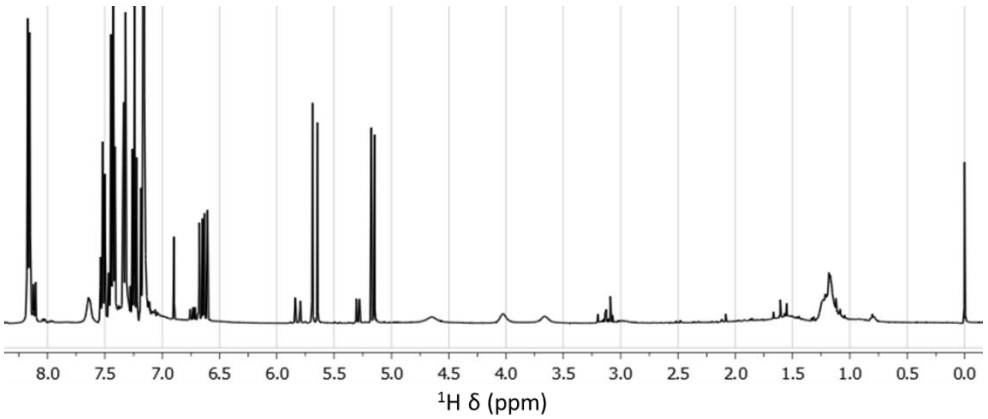

Figure III-19. ^{1}H NMR spectrum in $CDCl_3$ of the reaction media after 24h of polymerisation of styrene and VBA in the presence of PBA in chloroform with DMP and V-70 at 30°C

As the boronic anhydrides containing polymer could not be directly synthesised, another protocol was thus elaborated where the anhydride would be formed after polymerisation of a random copolymer PS-PVBA (**Figure III-20**).

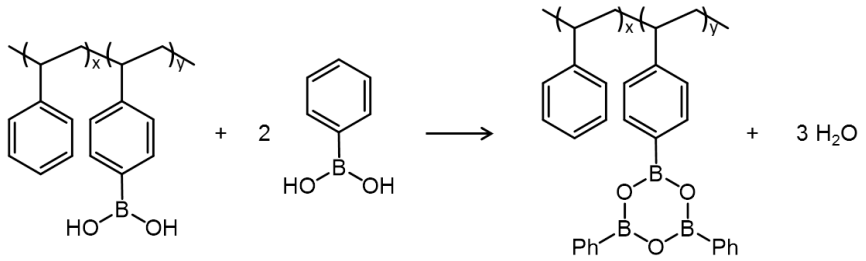

Figure III-20. Formation of the polymer anhydride by complexing PBA on an already synthesised polymer

This protocol was tested with *o*-tolylboronic acid thus the outcome could be confirmed by DOSY analysis as the methyl group would have the same diffusion coefficient as the polymer. Unfortunately, it was not verified as no additional signals had the same diffusion coefficient as the polymer (**Figure III-21**).

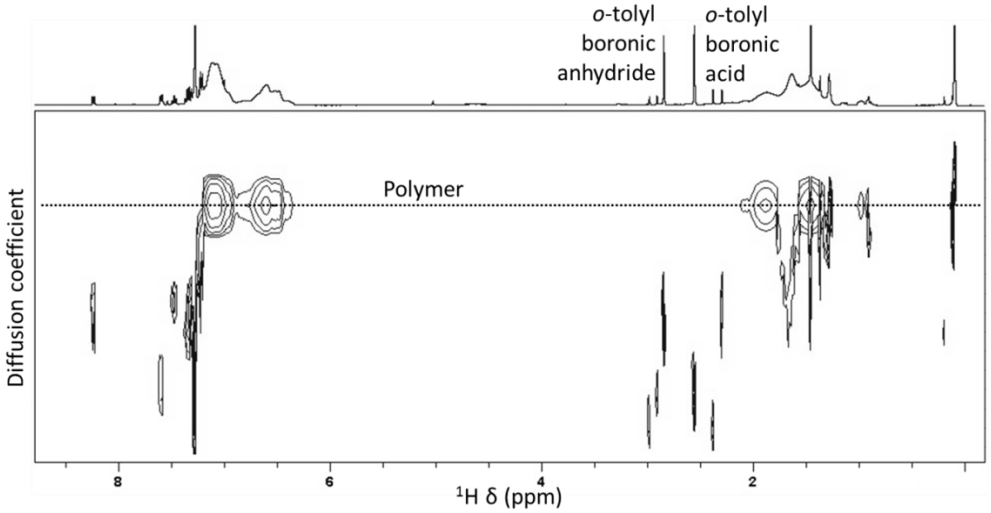

Figure III-21. DOSY in $CDCl_3$ of the polymer anhydride obtained from a random PS-PVBA copolymer

Hence, the attempts to obtain the boronic anhydrides containing polymer were dropped.

III. 3. C) Block copolymers

III. 3. C) i) RAFT agent selection

Changing the RAFT agent was tested to decrease the reaction time as for block copolymers, 24h reaction need to be allowed for each block (**Table III-5**).

BSPA was less efficient than DMP considering all the parameters studied (Polymer 11 and 12). The high dispersity indicated a loss over the polymerisation control. DBTTC (**Figure III-3b**, p 128) did not significantly improve the results obtained with DMP (Polymer 11 and 13). Consequently, DMP was kept as the RAFT agent for the synthesis of the polymers produced for the "fishing" method.

Table III-5. Comparison of several RAFT agents on the synthesis of block copolymers PS-*b*-PVBA

	Polymer 11		Polymer 12		Polymer 13	
RAFT agent	DMP		BSPA		DBTTC	
DP_{th}	50		47		48	
Ratio AIBN/CTA	1.5		1.4		1.5	
	PS block	*Copolymer*	*PS block*	*Copolymer*	*PS block*	*Copolymer*
Conversion (NMR) [a]	93.1%	94.8%	91.7%	92.9%	91.8%	91.3%
Yield (mass)	-	90.1%	-	69.2%	-	92.2%
VBA content [a]	-	1.3%	-	0.2%	-	1.6%
M_n (g.mol^{-1}) [b]	2 680	2 720	1 750	1 770	3 020	2 610
M_w (g.mol^{-1}) [b]	3 620	3 650	2 950	2 980	3 950	3 510
$Đ$ [b]	1.35	1.34	1.69	1.69	1.31	1.35

*Polymerisation of block copolymers with a 94 mol% styrene ratio with AIBN and a monomer concentration of 3.68 M of styrene and 0.24 M of VBA in DMF/H_2O 95/5 v/v at 85°C for 48h, VBA introduction after 24h, [a] See **Appendix III.III** (p 147) for the calculation detail, [b] Determined by SEC in THF based on polystyrene calibration*

III. 3. C) ii) Copolymers for the "fishing" method

Three diblock copolymers and a random one were synthesised to be applied to the "fishing" method. Even though, based on previous information and steric hindrance, block

copolymers are supposed to be more efficient than random ones for the extraction of cellulose oligomers, their efficiency will be tested.

The theoretical total DP of the block copolymers were 50, 75 and 100 with a PS block DP of 45, 69 and 95 respectively. For the random copolymer, the length and monomer ratio was the same as the smaller block with a DP_{th} of 50 and 10 mol% of VBA. Block or random copolymers had the same conversion evolution for similar DP_{th} otherwise the conversion was slightly slower when DP_{th} increased (**Figure III-22**).

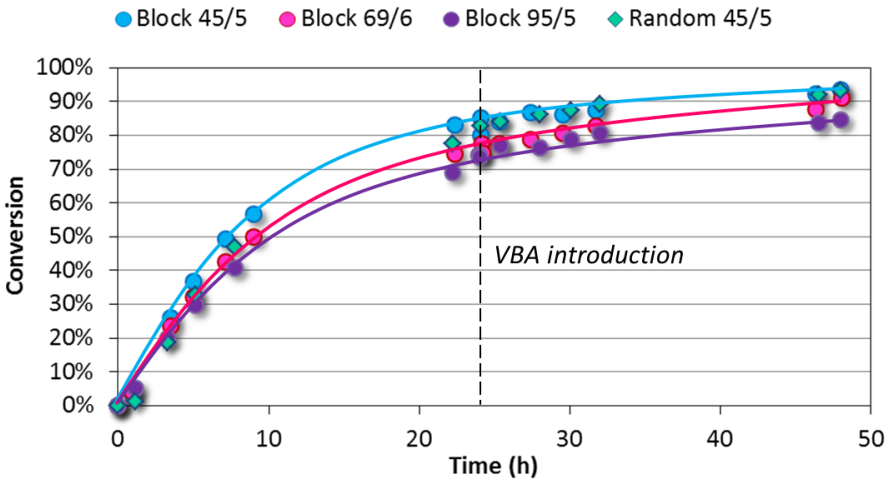

Figure III-22. Evolution of the conversion (NMR) with time (Polymerisations at 1.0 g/mL in DMF/H_2O 95/5 v/v with an AIBN/DMP ratio of 0.50 at 70°C)

The VBA content was measured by the previously described method (**Appendix III.III**, p 147) and the average number of VBA and styrene per chain was then deduced (**Table III-6**). The copolymers obtained were rather composed by a block of PS and a gradient between the two monomers than two pure blocks since the average number of styrene per chain increased after the VBA introduction. The average number of VBA per chain decreased when the PS block DP_{th} increased as the initiator probably started to deactivate before the VBA introduction. The random copolymer however had the higher VBA content.

Table III-6. Characterisation of the different polymers for the "fishing" method

	Block 45/5	Block 69/6	Block 95/5	Random 45/5
Before VBA introduction				
M_n (g.mol^{-1}) [a]	3 090	4 820	6 940	-
M_w (g.mol^{-1}) [a]	3 830	5 740	8 110	-
$Đ$ [a]	1.24	1.19	1.17	-
Average number of styrene per chain [b]	30	46	61	-
After VBA introduction – Final polymer				
Conversion (RMN) [b]	93.6%	90.9%	84.7%	93.2%
Yield (mass)	89.6%	86.6%	81.6%	89.4%
VBA content [b]	6.7%	3.4%	1.5%	11.0%
M_n (g.mol^{-1}) [a]	3 920	6 180	7 060	4 150
M_w (g.mol^{-1}) [a]	4 810	7 260	9 340	4 840
$Đ$ [a]	1.23	1.18	1.32	1.17
Average number of VBA per chain [b]	1.8	1.4	0.7	3.1
Average number of styrene per chain [b]	35	57	67	35

[a] Determined by SEC in THF based on polystyrene calibration, [b] See ***Appendix III.III*** *(p 147) for the calculation detail*

Chapter conclusion

The goal of this study was to synthesise two types of polymer. As their size had to be small and well controlled, the first investigated technique was anionic polymerisation. Unfortunately, boronic acid monomers protected or not deactivated the polymerisation. Polystyrenes synthesised this way were tentatively modified to introduce boronic acid moieties but the polymers obtained could not be characterised because of solubility issues.

Based on the literature, the logical choice for an alternative polymerisation technique was RAFT. Several parameters were investigated to optimise the outcomes and the characterisation. The boronic anhydride containing polymer synthesis was then tried either by polymerising a boronic anhydride containing monomer or by forming the anhydride on an already synthesised polymer. Despite several attempts, both of these methods were unsuccessful.

Four polymers were however synthesised for the “fishing” method, one random and three “blocks” copolymers. The random one will be used for comparison and had the same length and monomer ratio as the smaller block. The three “blocks” had different polystyrene block length and the same theoretical VBA DP. The VBA block was found to be a mixture of styrene and VBA. It was also observed that the longer the styrene block, the smaller the VBA content probably because of radical deactivation during the polymerisation.

Only the “fishing” method will be inquired in the subsequent chapter.

Appendix

Appendix III.I: RAFT and ATRP polymerisation mechanism

RAFT mechanism[32]

Initiation

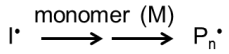

Chain transfer

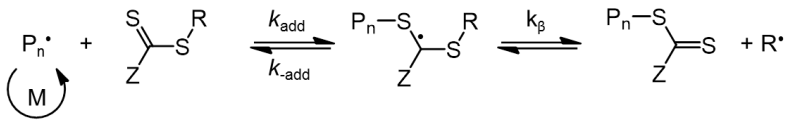

Reinitiation

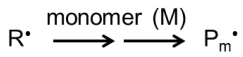

Chain equilibrium / Propagation

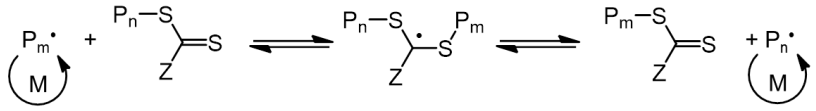

Termination

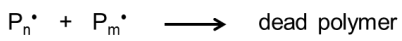

ATRP mechanism[9]

Initiation

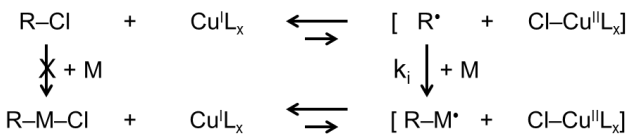

Propagation

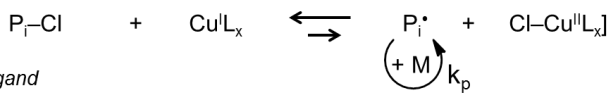

With L a ligand

Termination

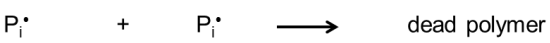

Appendix III.II: Selection of RAFT agent for the polymerisation of various monomers[33]

Dashed lines indicate partial control over polymerisation is achieved (i.e., control over molar mass but poor dispersity control)

MMA: methyl methacrylate, HPMAM: N-(2-hydroxypropyl)methacrylamide, St: styrene, MA: methyl acylate, DMAm: N,N-dimethylacrylamide, VAc: vinyl acetate, NVP: N-vinylpyrrolidone

The partial control is due to low RAFT agent activity for the Z group or to inferior homolytic leaving group ability (MMA, HPMAM) or substantial retardation due to slow reinitiation of polymerisation (VAc, NVP) for the R group

Appendix III.III: Detailed calculation of several parameters

Polystyrene polymerisation conversion

Two or three drops of the reaction media were diluted in $CDCl_3$ and the ^1H NMR spectrum was recorded (see below for an example).

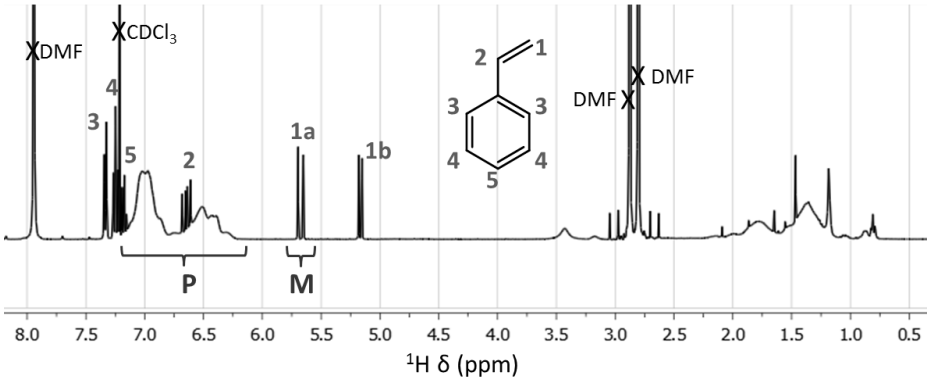

$$\text{Conversion} = 1 - \frac{I_{M(t)}}{I_{M(t)} + I_{P(t)}}$$

With $I_{M(t)}$ the integral value of one proton from the monomer and $I_{P(t)}$ the integral value of one proton from the polymer.

Here,

$$I_{M(t)} = M \qquad I_{P(t)} = \frac{P - 2M}{5}$$

Conversion for copolymers PS-PVBA

Two or three drops of the reaction media were diluted in $CDCl_3$ and the ^1H NMR spectrum was recorded (see below for an example).

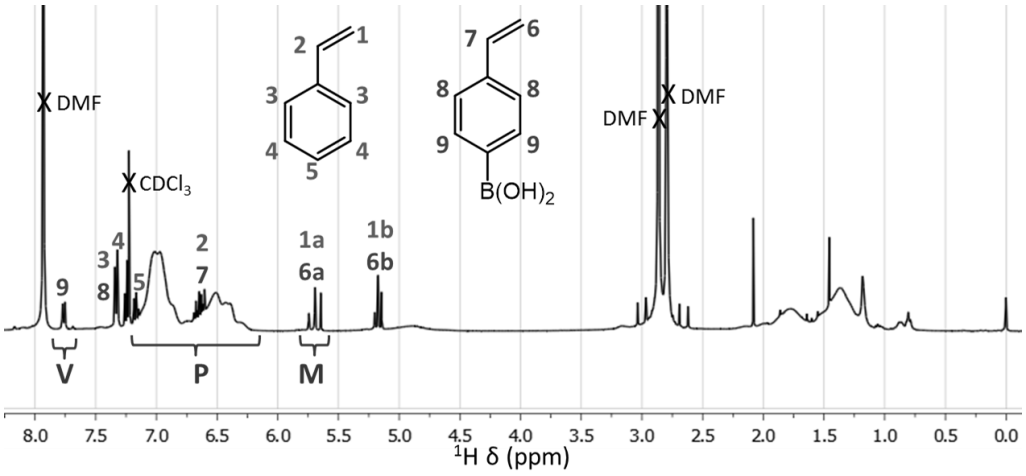

$$\text{Conversion} = 1 - \frac{I_{M(t)}}{I_{M(t)} + I_{P(t)}}$$

With $I_{M(t)}$ the integral value of one proton from the monomer and $I_{P(t)}$ the integral value of one proton from the polymer.

Here,

$$I_{M(t)} = {}^{M}/_{2} \qquad I_{P(t)} = \frac{P - 2M + {}^{V}/_{2}}{9}$$

VBA content

The polymer concerned was solubilised in $CDCl_3$, 4-methylcatechol was added to the solution and the ^{1}H NMR spectrum was recorded (see below for an example).

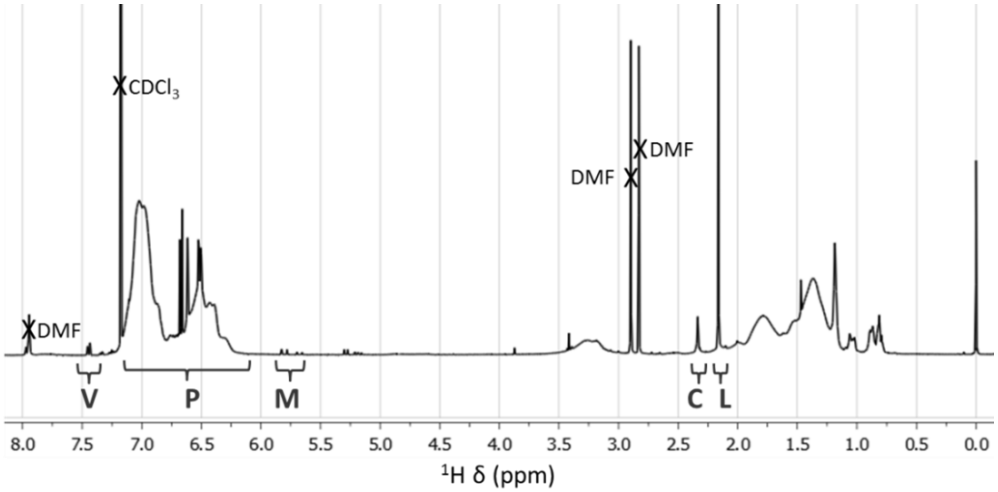

C corresponds to the diol complexed on the polymer and L the free one (**Figure III-16b**, p 137).

$$\text{VBA content} = \frac{\text{Number of boronic acid per chain}}{\text{Total DP of the polymer}}$$

$$\text{VBA content} = \frac{5}{3}\ \frac{C - {}^{3}/_{2}\,V}{P - 2\left(C - {}^{3}/_{2}\,V\right) - 2\,M - L - V}$$

Block polymerisation degree

The average number of VBA or styrene per chain were calculated as follow:

$$DP_{VBA} = \frac{\text{VBA content} \times M_n \text{ measured by SEC}}{M_{VBA}} \qquad DP_{PS} = \frac{M_n \text{ measured by SEC} - (DP_{VBA} \times M_{VBA})}{M_{styrene}}$$

References

[1] F. Jäkle, *J. Inorg. Organomet. Polym. Mater.* **2005**, *15*, 293–307.

[2] P. S. Wolfe, K. B. Wagener, *Macromolecules* **1999**, *32*, 7961–7967.

[3] T. C. Chung, D. Rhubright, *Macromolecules* **1991**, *24*, 970–972.

[4] J. Y. Dong, E. Manias, T. C. Chung, *Macromolecules* **2002**, *35*, 3439–3447.

[5] Y. Qu, J. Liu, K. Yang, Z. Liang, L. Zhang, Y. Zhang, *Chem. Eur. J.* **2012**, *18*, 9056–9062.

[6] K. Kataoka, H. Miyazaki, T. Okano, Y. Sakurai, *Macromolecules* **1994**, *27*, 1061–1062.

[7] G. Vancoillie, S. Pelz, E. Holder, R. Hoogenboom, *Polym. Chem.* **2012**, *3*, 1726–1729.

[8] J. Chiefari, Y. K. Chong, F. Ercole, J. Krstina, J. Jeffery, T. P. T. Le, R. T. A. Mayadunne, G. F. Meijs, C. L. Moad, G. Moad, et al., *Macromolecules* **1998**, *31*, 5559–5562.

[9] J.-S. Wang, K. Matyjaszewski, *J. Am. Chem. Soc.* **1995**, *117*, 5614–5615.

[10] M. Kato, M. Kamigaito, M. Sawamoto, T. Higashimura, *Macromolecules* **1995**, *28*, 1721–1723.

[11] D. Roy, J. N. Cambre, B. S. Sumerlin, *Chem. Commun.* **2008**, 2477–2479.

[12] D. Roy, J. N. Cambre, B. S. Sumerlin, *Chem. Commun.* **2009**, 2106–2108.

[13] J. N. Cambre, D. Roy, B. S. Sumerlin, *Polym. Prepr.* **2011**, *52*, 592–593.

[14] A. P. Bapat, D. Roy, J. G. Ray, D. A. Savin, B. S. Sumerlin, *J. Am. Chem. Soc.* **2011**, *133*, 19832–19838.

[15] D. Roy, B. S. Sumerlin, *ACS Macro Lett.* **2012**, *1*, 529–532.

[16] J. N. Cambre, D. Roy, B. S. Sumerlin, *J. Polym. Sci., Part A: Polym. Chem.* **2012**, *50*, 3373–3382.

[17] J. N. Cambre, D. Roy, S. R. Gondi, B. S. Sumerlin, *J. Am. Chem. Soc.* **2007**, *129*, 10348–10349.

[18] S. Maji, G. Vancoillie, L. Voorhaar, Q. Zhang, R. Hoogenboom, *Macromol. Rapid Commun.* **2014**, *35*, 214–220.

[19] C. Cheng, X. Zhang, Y. Wang, L. Sun, C. Li, *New J. Chem.* **2012**, *36*, 1413–1421.

[20] F. Cheng, F. Jäkle, *Chem. Commun.* **2010**, *46*, 3717–3719.

[21] G. Moad, E. Rizzardo, S. H. Thang, *Aust. J. Chem.* **2005**, *58*, 379–410.

[22] D. J. Keddie, G. Moad, E. Rizzardo, S. H. Thang, *Macromolecules* **2012**, *45*, 5321–5342.

[23] Y. Qin, V. Sukul, D. Pagakos, C. Cui, F. Jäkle, *Macromolecules* **2005**, *38*, 8987–8990.

[24] Y. Qin, G. Cheng, O. Achara, K. Parab, F. Jäkle, *Macromolecules* **2004**, *37*, 7123–7131.

[25] T. E. Pennington, C. Kardiman, C. A. Hutton, *Tetrahedron Lett.* **2004**, *45*, 6657–6660.

[26] J. Sun, M. T. Perfetti, W. L. Santos, *J. Org. Chem.* **2011**, *76*, 3571–3575.

[27] R. J. Kell, P. Hodge, M. Nisar, R. T. Williams, *J. Chem. Soc., Perkin Trans. 1* **2001**, 3403–3408.

[28] I. Königsberg, J. Jagur-Grodzinski, *J. Polym. Sci. Polym. Chem. Ed.* **1983**, *21*, 2649–2663.

[29] P. De, S. R. Gondi, D. Roy, B. S. Sumerlin, *Macromolecules* **2009**, *42*, 5614–5621.

[30] Y. Qin, C. Cui, F. Jäkle, *Macromolecules* **2007**, *40*, 1413–1420.

[31] http://www.wako-chem.co.jp/specialty/oilazo/V-70.htm

[32] G. Moad, J. Chiefari, Y. K. Chong, J. Krstina, R. T. A. Mayadunne, A. Postma, E. Rizzardo, S. H. Thang, *Polym. Int.* **2000**, *49*, 993–1001.

[33] D. J. Keddie, *Chem. Soc. Rev.* **2014**, *43*, 496–505.

Chapter IV. Cellulose depolymerisation and oligomer separation

Table of Contents

Chapter Purpose

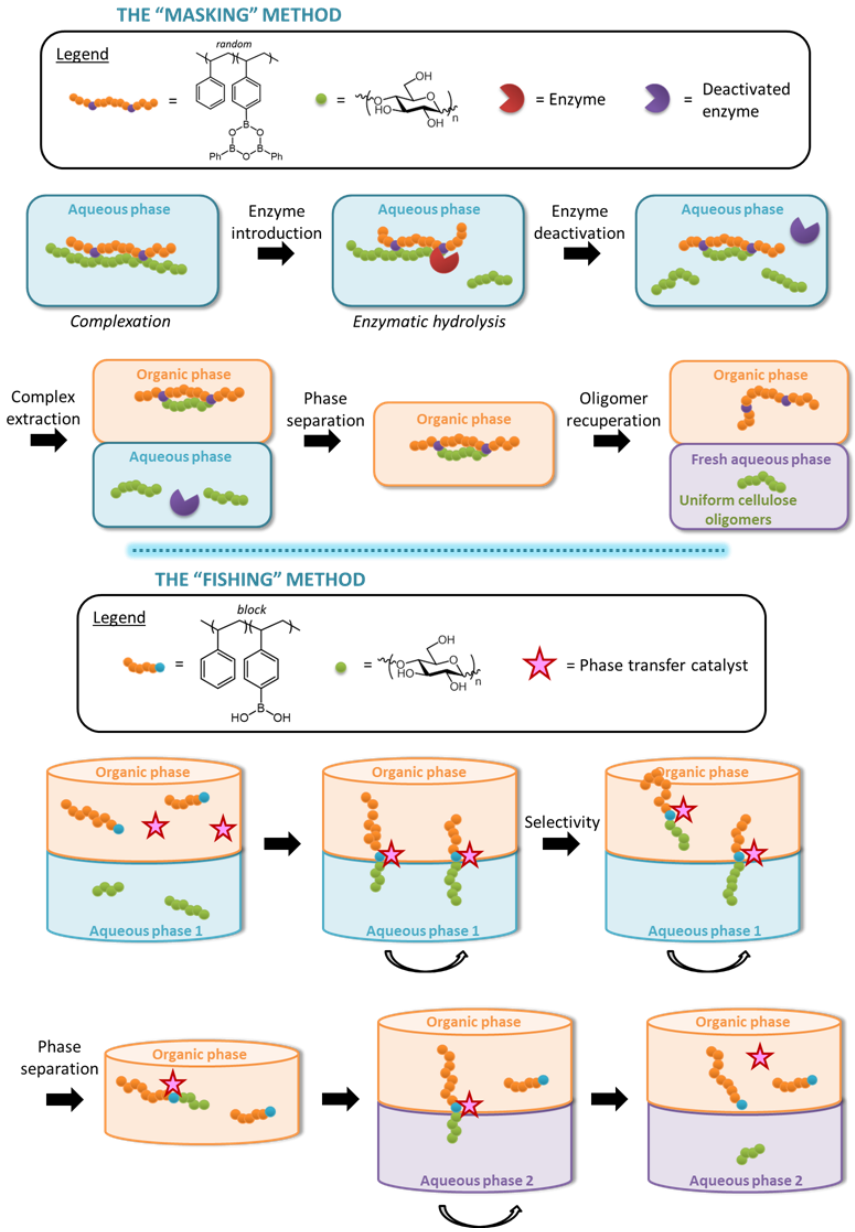

The synthesis of the polymer anhydride necessary to the "masking" method had not been achieved in Chapter III. Consequently, this method was not further investigated. However, four polymers were synthesised for the "fishing" method: three block copolymers of different sizes and a random one.

In this chapter, the production of cellulose oligomers by acidic hydrolysis was optimised and the efficiency of the "fishing" method assessed.

IV. 1. Acidic hydrolysis of cellulose

IV. 1. A) Optimisation of the cellulose acidic hydrolysis protocol

As mentioned in Chapter I, the hydrolysis of cellulose by the phosphoric acid is one of the safest ways to obtain cellulose oligomers with a good yield (**Table I-6**, p 41). The hydrolysis protocol was inspired by already published results[1] and is summarised in **Figure IV-1**. Each step is developed below.

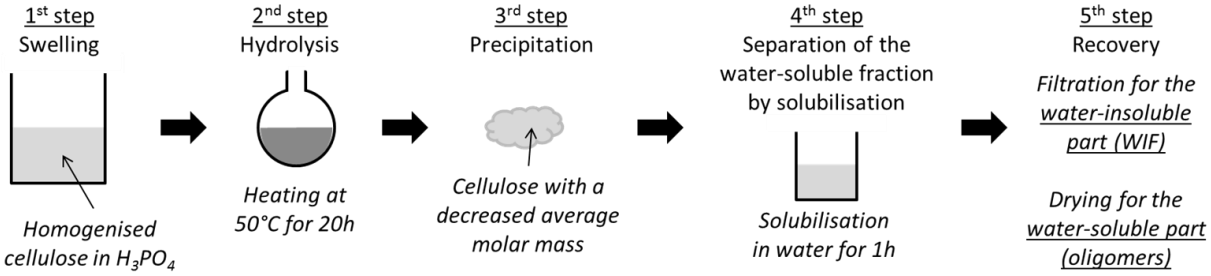

Figure IV-1. Schematic representation of a cellulose acidic hydrolysis protocol

1st step: Swelling

To avoid the formation of big clusters when the cellulose was poured into the aqueous phosphoric acid (85 wt%), the introduction had to be done under mechanical blades stirring. Magnetic stirring or ultrasounds were not sufficient to break the clusters and the resulting solution was too heterogeneous.

Several cellulose concentrations were tested: at 100 $g.L^{-1}$, the heterogeneity and the viscosity of the solution were too high; the clusters formed were not broken during the hydrolysis thus diminishing the final yield. At 80 $g.L^{-1}$ and lower, the viscosity and homogeneity became acceptable. At 50 $g.L^{-1}$, the mass yield in cellulose oligomers was the same as with 80 $g.L^{-1}$ but the final quantity was proportionally smaller. A cellulose concentration of 80 $g.L^{-1}$ was then selected for the rest of the study.

2nd step: Hydrolysis

When the hydrolysis occurred at 55°C for 20h[1], only a small black charred solid was produced, indicating that the cellulose was degraded. The same result was obtained at 50°C for 48h. An hydrolysis at 50°C for 20h gave acceptable results and was used for the rest of the study.

After the hydrolysis, the formation of hydroxymethylfurfural (HMF), a by-product coming from the dehydration of glucose in acidic media[2] (**Appendix I.IX**, p 58), was observed by a colour change from white to brownish. Its content was quantified as it was the only component of the solution that absorbs in UV.

3rd step: Precipitation

THF was chosen as the precipitation solvent because it gave better yield than acetone or isopropanol[1] and no precipitation was observed with ethanol. The solid obtained was thus cellulose with a decreased average molar mass from which the water-soluble oligomers were separated by solubilisation.

4th step: Separation by solubilisation

After removing the water-insoluble fraction (WIF) by filtration, the pH of the solution containing the cellulose oligomers was around 1, confirming the presence of residual phosphoric acid. Its removal was critical to prevent further degradation. An aqueous solution of calcium hydroxide was used to neutralise the solution as calcium cation and phosphate anion form the precipitate $Ca_2(PO_4)_2$ that can be easily removed by filtration.

5th step: Recovery

Two ways were then compared to get the dried oligomers after concentration of the aqueous solution: precipitation in THF or further drying over phosphorus pentoxide in a desiccator under vacuum. The second way was selected because no glucose was detected after the first one, probably because of its solubility in the precipitation solvent. This indicated that some products were probably lost during the first precipitation (3rd step).

This acidic hydrolysis procedure was repeated three times with exactly the same conditions and the repeatability was found to be about ± 5% for the yield of each fraction (**Table IV-1**). The water-soluble oligomers had an average yield of around 23% whereas the WIF corresponded to the majority of the cellulose recovered with an average yield of 45%. Less than 0.5% of the total cellulose was hydrolysed as far as HMF and around one third of the total cellulose was missing after the hydrolysis. This phenomenon was already observed[1] with the same protocol and in the same proportion but no explanation was provided. The THF filtered after the 3rd step (**Figure IV-1**) was brown meaning that it did not only contain the dispersed phosphoric acid but also some other product which could explain the missing mass. Their characterisation was not performed as they were not of interest here, cellulose oligomers being insoluble in THF. The unknown product probably was an HMF polymer[3,4] as the polymerisation is catalysed in acidic condition (**Figure IV-2**).

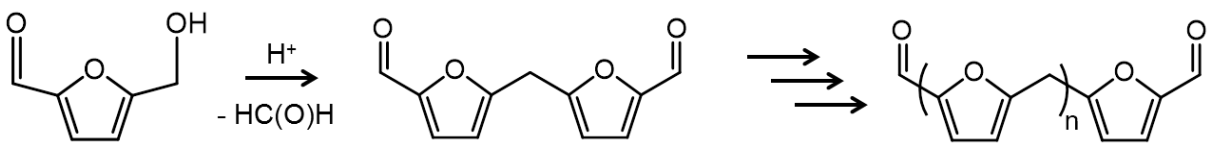

Figure IV-2. HMF polymerisation in acidic conditions (adapted from James *et al.*[5])

Table IV-1. Composition of the product obtained after hydrolysis

	WIF (%)	Water-soluble oligomers (%)	HMF (%)	Difference to 100%
Hydrolysis A	39.6	27.5	0.4	32.5
Hydrolysis B	42.1	25.3	0.3	32.3
Hydrolysis C	53.0	16.8	0.3	29.9
Average	45 ± 6	23 ± 5	0.4 ± 0.1	32 ± 1

IV. 1. B) Optimisation of the hydrolysis products characterisation

As the oligomers were water-soluble, a direct characterisation by SEC with water as the eluent, HPLC or MALDI was possible. On the contrary, the WIF and the initial cellulose needed a functionalisation step to be characterised. The usual one for a SEC analysis is a carbanilation as cellulose tricarbanilate is THF-soluble[6,7]. A signal was observed with the initial cellulose after carbanilation but not with the WIF (**Figure IV-3**). Moreover, this method was not really adequate as the calculation of the corresponding molar mass and DP rests on polystyrene calibration.

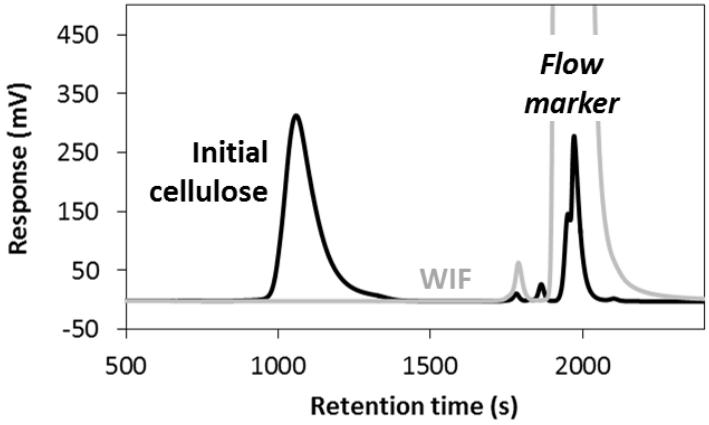

Figure IV-3.SEC in THF of initial cellulose and a WIF after carbanilation (UV data)

In order to detect the WIF, a new characterisation method was considered: SEC with chloroform as the eluent, on cellulose functionalised as acetate. In fact, a good solubility in chloroform is obtained for cellulose acetate with high DS (2.8-3.0[8]). This analysis was performed with a viscosity detector so the molar masses were calculated *via* a universal calibration. This method was found efficient as detailed in §IV. 1. C).

IV. 1. C) Characterisation of the different fractions obtained

The water-soluble oligomers, obtained previously (§IV. 1. A), p 155), were analysed by MALDI and no phosphorylation (+ 79 $g.mol^{-1}$) was noticed (**Figure IV-4**). DP up to 12 were observed as water-soluble.

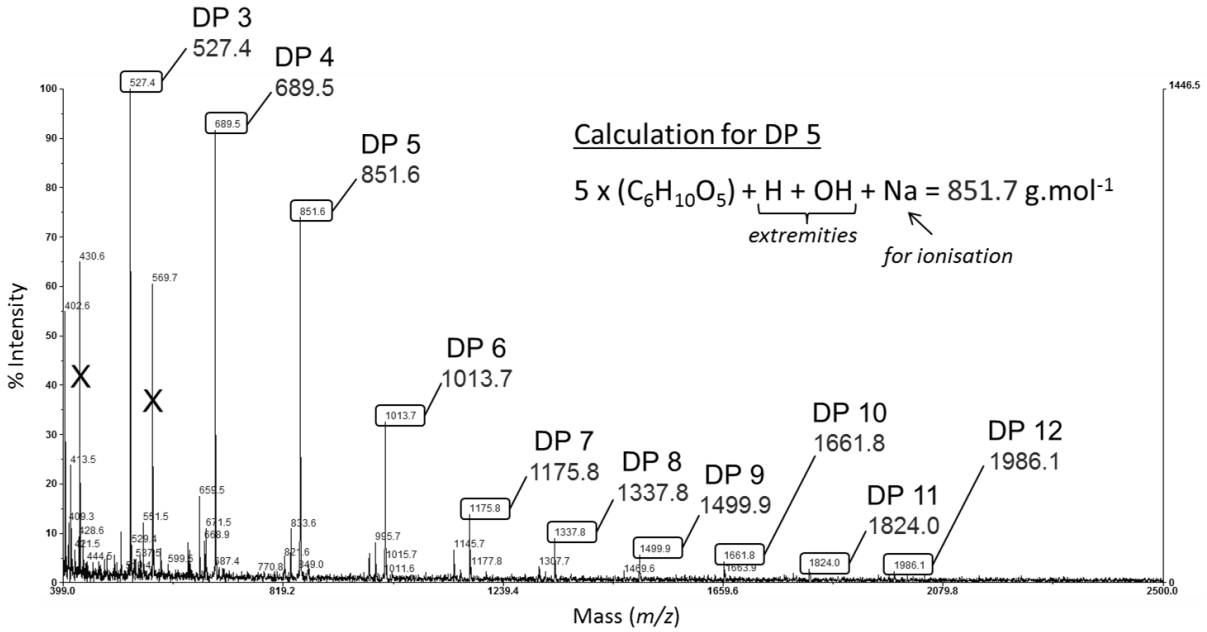

Figure IV-4. Typical MALDI spectra observed for the water-soluble oligomers (the peaks crossed come from the matrix)

Solubility in chloroform was reached for all the acetylated fractions. They thus were analysed by SEC in the same solvent to accurately compare their molar mass distributions. The molar mass of the WIF happened to be really reduced compared to the native cellulose (**Figure IV-5** and **Table IV-2**). The spectra of soluble and insoluble in water fractions overlapped and some cellobiose was found in the WIF (**Figure IV-5**). When the WIF was dispersed in water again, only 1% of the initial solid was extracted. A poor dispersion of the WIF in water seemingly prevented a total recovery of the water-soluble oligomers.

The molar mass distributions obtained were repeatable (**Table IV-2**). For the calculation of the corresponding DP, we considered that no [Bmim]Cl molecule stayed complexed on the compounds after the acetylation.

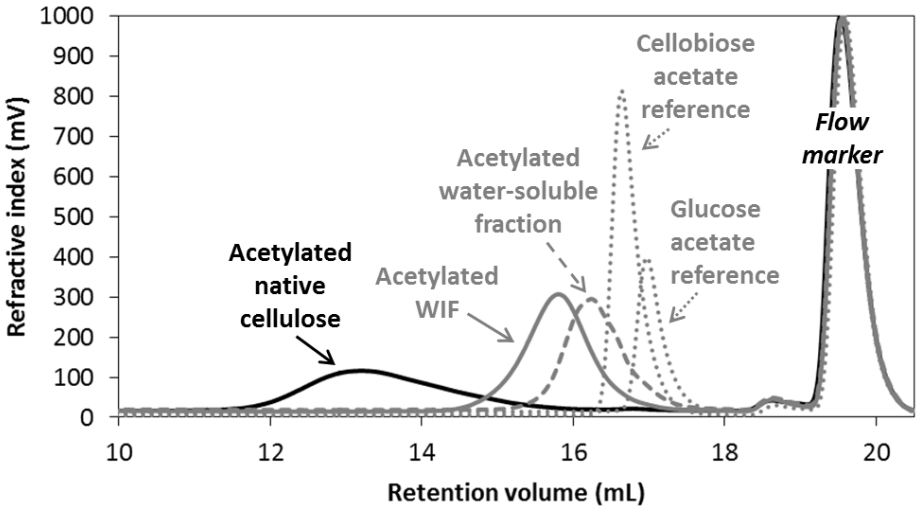

Figure IV-5. SEC in chloroform of several acetylated fractions and references

Table IV-2. Determination of the molar mass and the polymerisation degree (DP) of the acetylated cellulose before and after hydrolysis

	Cellulose before hydrolysis	Hydrolysis A	Hydrolysis B	Hydrolysis C
Acetylated water-insoluble fraction				
M_n (g.mol^{-1}) [a]	12 130 (**43**)	2 160 (**7**)	2 060 (**7**)	2 260 (**8**)
M_w (g.mol^{-1}) [a]	35 210	3 150	3 060	3 150
Đ [a]	2.9	1.5	1.5	1.4
Acetylated water-soluble fraction				
M_n (g.mol^{-1}) [b]	-	1 000 (**3**)	800 (**3**)	1020 (**3**)
M_w (g.mol^{-1}) [b]	-	1 260	1 120	1 340
Đ [b]	-	1.3	1.4	1.3

[a] *Determined with SEC in chloroform using a universal calibration,* [b] *Determined with SEC in chloroform using a polystyrene calibration (calculation based on the viscosity detector not accurate enough). The bold values between braces are the corresponding calculated DP (see* ***Appendix IV.I*** *for the calculation, p 169).*

A more accurate distribution of the different DP present in the water-soluble oligomers was obtained by HPLC and was found to be repeatable at ± 1% (**Table IV-3**). A majority of cellotriose (32.4%) and cellotetraose (26.8%) were present then came cellobiose and glucose at 18.3% and 11.9%, respectively. The solubility in water decreases with an increasing DP. As a result, cellopentaose was present at 9.7% and cellohexaose only at 0.8%. The concentration of DP 7 and above was too low to be detected by HPLC. Their presence in the sample was however confirmed by MALDI (**Figure IV-4**).

The average DP calculated based on this distribution was 3.1, which corresponds to the one determined by SEC in chloroform (**Table IV-2**). This new method is thus relevant to determine the molar mass of cellulose.

Table IV-3. Average ratio and standard deviation of each DP in the water-soluble fraction for the three hydrolyses determined by HPLC

Cellulose oligomer	Ratio (%) [a]	Relative surface
Glucose	17.6 ± 0.6	11.9 ± 1.0
Cellobiose	16.5 ± 0.0	18.3 ±0.0
Cellotriose	19.3 ± 0.1	32.4 ± 0.4
Cellotetraose	28.6 ± 0.2	26.8 ± 0.5
Cellopentaose	15.2 ± 0.4	9.7 ± 0.3
Cellohexaose	2.8 ± 0.0	0.8 ± 0.1

[a] *See* ***Appendix IV.II*** *(p 170) for the calculation*

IV. 2. The "fishing" method

IV. 2. A) Optimisation of the "fishing" method conditions on cellobiose

IV. 2. A) i) Initial conditions

The protocol of the "fishing" method was based on a previously patented[9] and published[10] procedure where xylose, glucose or cellobiose were extracted from an ionic liquid aqueous solution into an organic phase with the use of phenylboronic acid (PBA) or naphthalene-2-boronic acid (N2B). The conditions used are detailed in **Table IV-4**.

Table IV-4. Optimised conditions to extract cellobiose from an aqueous IL solution[10]

Extraction			Sugar recovery
Aqueous phase	Organic phase	Reaction condition	
- Total volume: 5 mL - Various % of [Emim]Ac - 10 mM of sugar *(9.0 mg of glucose or 17.1 mg of cellobiose)* - 0.15 M of $NaHCO_3$ buffer - pH 11 (adjusted with NaOH)	- Total volume: 5 mL - 70 mM of PBA or N2B *(42.7 mg of PBA or 60.2 mg of N2B)* - Solvent: 85/15 v/v *n*-hexane/1-octanol - 150 mM of Aliquat 336™ *(7 vol%)*	Stirring at 1 400 rpm Duration: 2 h Temperature: Room temperature (RT)	Phase separation: centrifugation at 13 000 rpm for 5 minutes Stripping solution: HCl at 0.5 M

This high pH was necessary because the binding constant between a boronic acid and a sugar increases with the pH (§II. 1. B) i), p 74). N2B was more efficient than PBA to extract sugar[10] probably because N2B is around 100 times less soluble in water (at 25°C, 25 $g.L^{-1}$ for PBA[11] *versus* 0.21 $g.L^{-1}$ for N2B[12]). Up to 84% of the initial quantity of cellobiose was extracted with N2B from a 100% [Emim]Ac solution by this method.

IV. 2. A) ii) Adaptation

To adapt this model to the method aimed, several changes were necessary. First, at it was not the purpose here, no ionic liquid were employed

Then, to have 70 mM of boronic acid in a 5 mL volume, more than 13 g of polymer would have been necessary (see **Appendix IV.III** for the calculation, p171). As this concentration would create solubilisation and probably viscosity issues, 2 g of polymer were employed. The value was chosen arbitrarily.

10 mM of cellohexaose in 5 mL represent 49.5 mg. To make sure that the maximal amount of oligomer extractable was reaped, 0.5 g of oligomers were used. The value was also chosen arbitrarily.

IV. 2. A) iii) Influence of several parameters

The conditions of the fishing method were optimised by using the commercial cellobiose.

Solvents of both phases

n-hexane was not used because of its high toxicity and was first replaced by cyclohexane, which presented similar extraction results[13]. Toluene was also tested and seemed to increase the quantity of sugar extracted, probably because of its small solubility in water that may have helped the complexation by enhancing the contact between the two phases. Toluene was used for the rest of the study.

To determine the role of 1-octanol, a "fishing" protocol was performed without it and a very stable gel was obtained after centrifugation (**Figure IV-6a**) most likely caused by the fact that the polymer/sugar complex was amphiphilic. As the sugar was probably trapped in the gel, 1-octanol was thus necessary to the extraction in the organic phase.

As the chain transfer agent used for the polymer synthesis contained a carboxylic acid, the impact of the pH change on the polymer was investigated. Polystyrene synthesised by RAFT with DMP as the chain transfer agent was solubilised in cyclohexane and stirred with a NaOH basified aqueous solution in the usual conditions and an emulsion was formed (**Figure IV-6b**). No emulsion was observed for the same experiment with sodium bicarbonate alone as the base (**Figure IV-6b**). Cellulose oligomers are presumably more pH sensitive than glucose or cellobiose[14]. The pH of the aqueous solution was thus decreased from 11 to 9. Sodium carbonate was chosen as the base because NaOH formed emulsions and it was stronger than sodium bicarbonate.

For the same reasons, the stripping solution HCl concentration was reduced to obtain pH 3 (500 mM reduced to 1 mM).

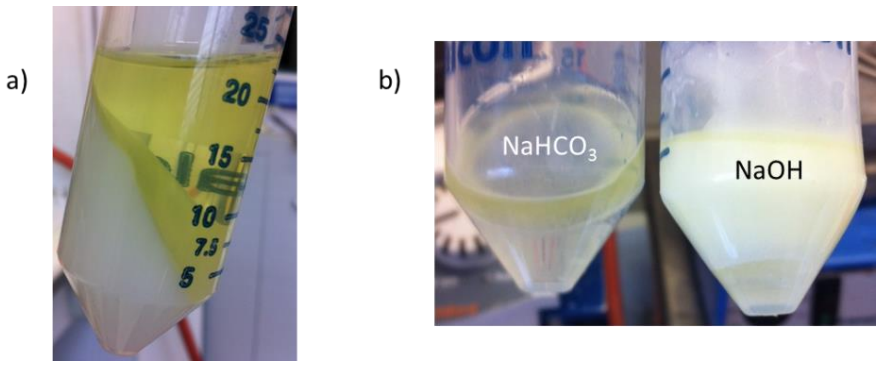

Figure IV-6. a) Picture of a gel formed after an extraction without 1-octanol (tube held vertically) and b) Picture of an emulsion formed by mixing polystyrene is a NaOH (right) or $NaHCO_3$ (left) basified aqueous solution

Phase transfer catalyst

The complex formed with the boronic acid at pH > pK_a is anionic (p$K_{a\ PBA}$ = 8.8[15], p$K_{a\ N2B}$ = 9.5[16]). The phase transfer catalyst Aliquat 336™ is cationic (**Figure IV-7a**), which also helped to stabilise the boronic acid/oligomer complex as illustrated on **Figure IV-7b**.

With the initial conditions (**Table IV-4**, p 160), the polymers of high molecular weight were not well solubilised in the solvent. The solubilisation was found to increase when the ratio of Aliquat was reduced. As a result, the Aliquat 336™ ratio was decreased from 7 vol% to 1 vol%.

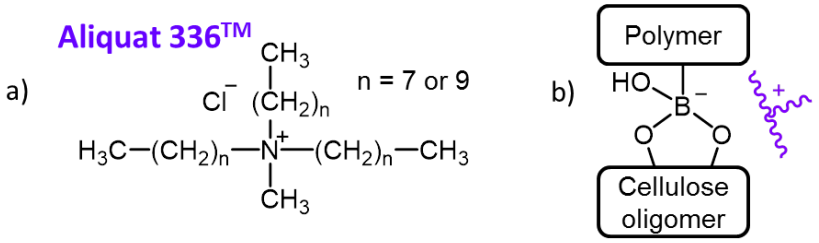

Figure IV-7. a) Structure of the Aliquat 336™, b) Representation of a polymer/cellulose oligomer complex stabilised by the Aliquat 336™ (not to scale)

Stirring and duration

At 1 400 rpm, solution splashed on the round bottom flask walls and product was lost. The stirring speed was thus reduced to 1 000 rpm.

The experiment duration was increased to 4h as the macromolecules used here were heavier than the ones used in the initial conditions. As their diffusion was going to be slower, more time would presumably be necessary for their complexation.

Increasing the time that cellulose oligomer spent in an aqueous solution increased the probability for microbial contamination, consequently and as a precaution, a small quantity of sodium azide was added to the solution (0.3 wt%).

Centrifugation

After a protocol with the chosen conditions so far, the organic phase obtained was blurry and after centrifugation, both phases were clear and a friable film was observed at the interface (**Figure IV-8**). It was recovered and analysed by NMR in D_2O and in THF-d_8 (**Appendix IV.IV**, p 172), the first ^1H NMR spectrum presented characteristic signals of cellobiose whereas the second confirmed the presence of the polymer. These characterisations proved that the recovered film was the polymer/cellobiose complex. As such conditions probably broke some of the cellulose oligomer/polymer complex and made the recovery more difficult, the centrifugation step was replaced by a decantation on standing.

Figure IV-8. Friable interfacial film after centrifugation

Based on all this information, **Table IV-5** summarises the chosen conditions for the rest of the study.

Table IV-5. "Fishing" method conditions

Extraction			Sugar recovery
Aqueous phase	Organic phase	Reaction condition	
- Total volume: 5 mL - 50 mM of Na_2CO_3 *(NaOH forms emulsions)* - pH 9 *(to prevent oligomer degradation)* - 0.5 g of cellulose oligomers *(arbitrary)* - 0.3% of NaN_3	- Total volume: 5 mL - 2 g of polymer *(arbitrary)* - Solvent: 84/15/1 v/v/v toluene/ octanol/Aliquat 336™	Stirring at 1 000 rpm Duration: 4h Temperature: RT	Phase separation: decantation for 2h Stripping solution: HCl at 1 mM (pH 3 *to prevent cellulose degradation*)

IV. 2. B) The "fishing" method on cellulose oligomers

The same batch of cellulose oligomer was used for the four "fishing" experiments with the polymer synthesised for this purpose (§III. 3. C) ii), p 141). Unfortunately, the aqueous phases became a stable gel/emulsion for the four polymers (**Figure IV-9**). The organic phase was still recovered and the supposed oligomers stripped with an acidic solution. The organic phase was not recovered in totality to stay away from the interface and make sure that no aqueous solution was also taken.

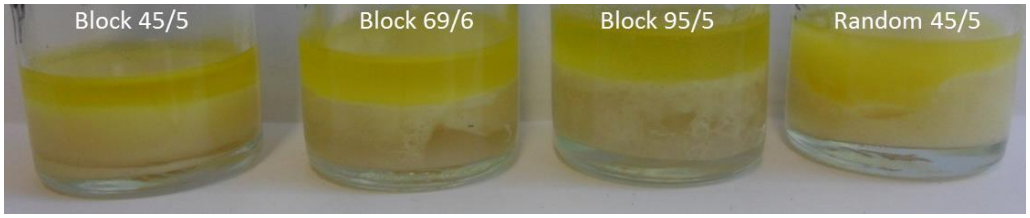

Figure IV-9. Emulsions observed after the "fishing" method on cellulose oligomers (pictures taken after the organic phase recovery)

The acidic solutions were neutralised with NaOH at 0.1 M before being analysed by HPLC (**Figure IV-11a**). No extraction was observed without polymer. With the random polymer, the decantation took a longer time than with the blocks and no oligomers were extracted. Moreover, the limit between the aqueous and organic phases was not well defined (**Figure IV-9**). A network was probably formed, trapping the oligomers in the aqueous phase or, as represented on **Figure IV-10**, an amphiphilic brush copolymer had formed at the interface and could not be solubilised in the organic phase. The composition of the samples extracted with the blocks was deduced from the area ratio of each peak of the HPLC spectra (**Figure IV-11b**). Unexpectedly, no selectivity was detected

Figure IV-10. Reversible amphiphilic brush copolymer formed at the interface during a "fishing" method with a random copolymer – Scheme not to scale

As the HPLC had been calibrated, the quantity of oligomer extracted was calculated (**Table IV-6**). As the molar quantity of boronic acid used corresponded to the maximal quantity of oligomer extracted and considering the approximations done to make the calculations, it seemed that all the oligomers that could be extracted were reaped.

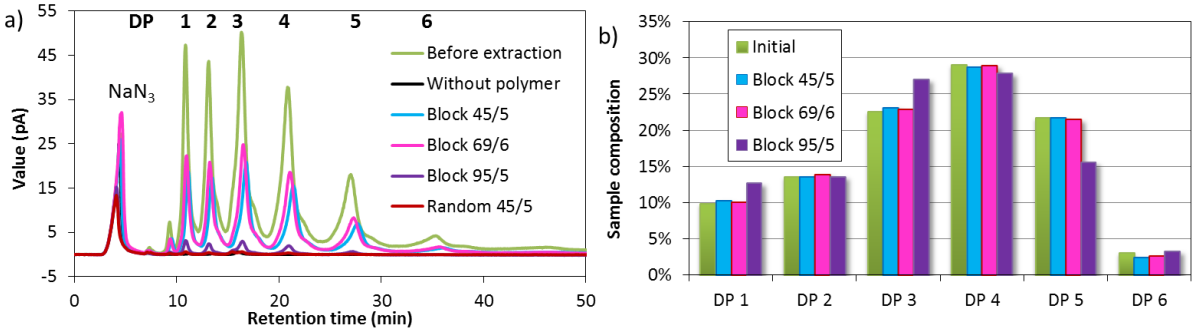

Figure IV-11. a) HPLC and b) composition of the oligomers before and after the "fishing" method depending on the polymer used (see Appendix IV.V (p 173) for calculation)

Table IV-6. Percentage of oligomer extracted depending of the polymer used

	No polymer	Block 45/5	Block 69/6	Block 95/5	Random 45/5
DP styrene/DP VBA measured [a]	-	35/1.8	57/1.4	67/0.7	35/3.1
Quantity of boronic acid in 2 g of polymer [b]	-	34 µmol	11 µmol	4 µmol	53 µmol
Quantity of oligomer extracted [c]	none	42 µmol	47 µmol	4 µmol	none

*[a] See **Table III-6** (p 143), [b] See **Appendix IV.III** (p 171), [c] Determined by HPLC (**Appendix IV.V**, p 173)*

IV. 3. Separation of the cellulose oligomers according to their solubility

IV. 3. A) Preliminary study

As the "fishing" method did not separate the cellulose oligomers, another method was developed involving differential solubilisation in alcohols which are known to solubilise cellulose oligomers depending on their sizes[17,18]. The other common solvents such as acetone or THF were used for precipitation[1], which implies a poor to no solubilisation.

Methanol, ethanol and isopropanol were tested (4h of solubilisation with an oligomer concentration of 0.25 $g.mL^{-1}$). Ethanol and isopropanol had solubilised only a small amount of cellobiose whereas methanol had solubilised a larger DP range (**Figure IV-12a** to **c**). The raw oligomers used here were recovered by precipitation in THF at the 5th step so no glucose was present. Then precipitation was investigated, the oligomers were solubilised in water, introduced in 10 times the volume of the corresponding alcohol and left to stir for 4h. The separation between the two fractions was less clear (**Figure IV-12d** and **e**) or less efficient (**Figure IV-12f**) than the solubilisation in methanol (**Figure IV-12a**).

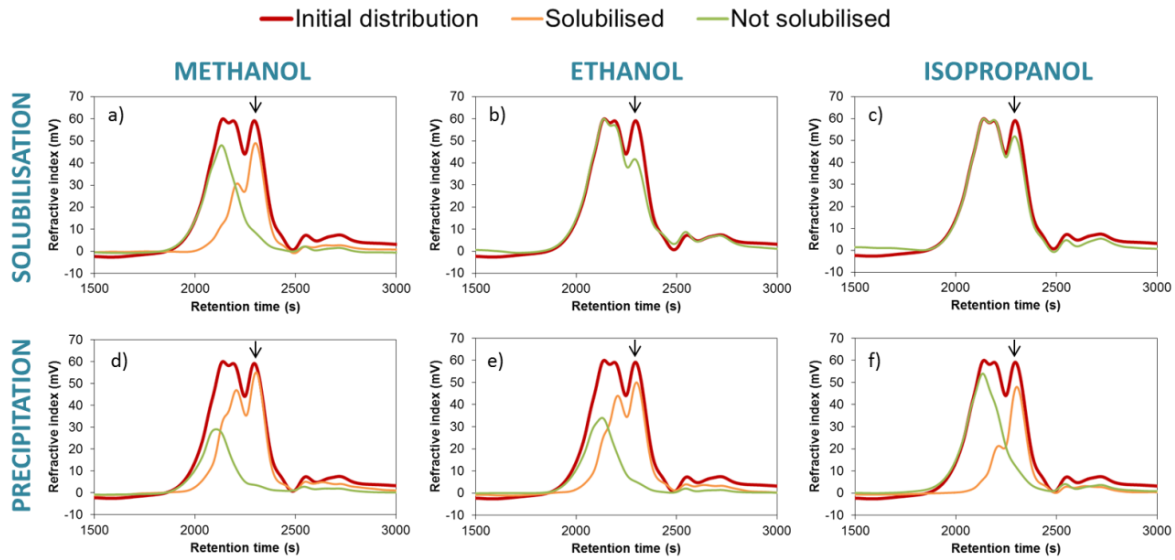

Figure IV-12. SEC of several fractions after solubilisation or precipitation in different alcohols – The block arrow corresponds to the retention time of cellobiose

IV. 3. B) Separation by solubilisation in methanol

As a consequence, methanol (MeOH) alone was chosen to separate the cellulose oligomers by solubilisation. The three water-soluble fractions previously obtained in §IV. 1. A) (p 155) were submitted to this separation for a repeatability study. Almost the same amount of MeOH-soluble fraction was extracted from all the samples (52.5% ± 1%) (**Table IV-7**).

Table IV-7. Composition of the oligomers after solubilisation in methanol – See Appendix IV.II (p 170) for calculation

	MeOH-insoluble fraction (%)	MeOH-soluble oligomers (%)
Hydrolysis A	44.6	52.5
Hydrolysis B	42.8	51.2
Hydrolysis C	45.3	53.7
Average	44.2 ± 1.1	52.5 ± 1.0

Considering the molar mass distributions, an overlap was observed (**Figure IV-13**) as previously with the solubilisation in water. The explanation was also probably the poor dispersion in the solvent. The separation however seemed to occur between DP 3 and 4. The composition of the sample before separation was in agreement with the one determined by HPLC (**Table IV-3**, p 159) and DP up to 12 were observed as it was the case on the MALDI spectra (**Figure IV-4**, p 158).

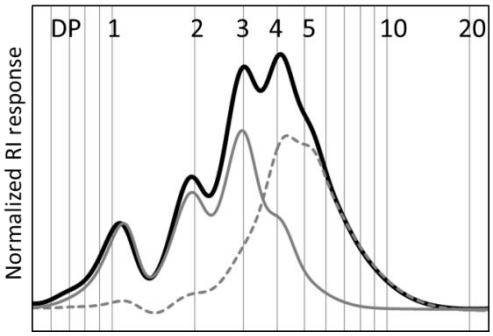

Figure IV-13. SEC with water as the eluent of the different fractions from the hydrolysis A (same behaviour observed for the hydrolysis B and C): before separation (black line), MeOH-soluble fraction (full grey line) and MeOH-insoluble fraction (dotted grey line)

The separation was confirmed to occur between DP 3 and 4 by HPLC (**Figure IV-14**)

In a previous study[18], the cellulose oligomer separation by solubilisation in MeOH was found to occur between DP 4 and 5 (**Table I-9**, p 45).

The MeOH-soluble fraction contains 27% of glucose, 27% of cellobiose and 28% of cellotriose. For cellotetraose, the percentage dropped to 15% as the solubility in MeOH decreased with an increasing DP. The MeOH-insoluble fraction was composed at 42% of cellotetraose, 36% of cellopentaose and 6% of cellotriose. Glucose and cellobiose represented less than 11% of the composition, and cellohexaose 5%.

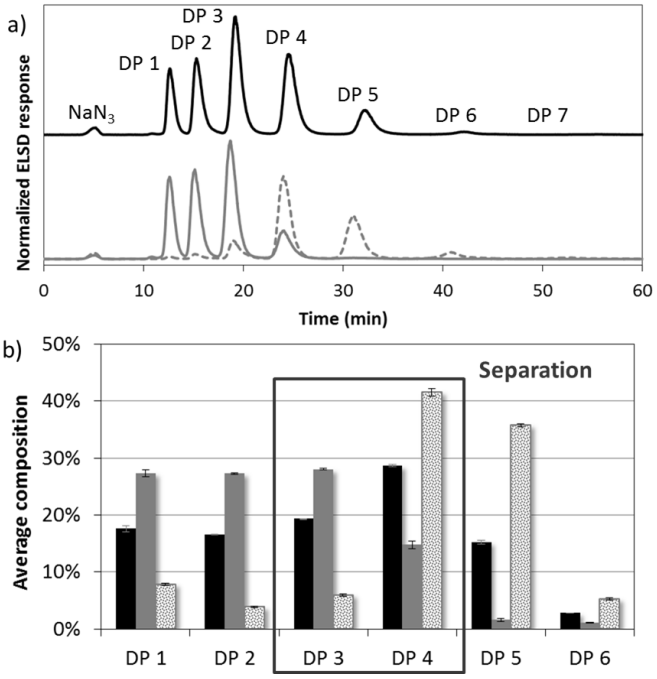

Figure IV-14. a) Normalised HPLC spectra of the different fractions from hydrolysis A (same behaviour observed for the hydrolysis B and C): before separation (black line), MeOH-soluble fraction (full grey line) and MeOH-insoluble fraction (dotted grey line); b) Average of the composition of the different fractions: before separation (black), MeOH-soluble fraction (grey full) and MeOH-insoluble fraction (grey dotted) – Average and standard deviation calculated over the hydrolyses A, B and C – See Appendix IV.II (p 170) for calculation

Chapter conclusion

The goal of this chapter was to determine the efficiency of the “fishing” method. To do so, the acidic hydrolysis of cellulose was performed to produce cellulose oligomers. The samples obtained had a majority of cellotriose and cellotetraose with 19.3% and 28.6% respectively. The oligomer yield was 23% ± 5% (over three hydrolyses).

The oligomers were then submitted to the “fishing” method with four styrene/VBA copolymers. No extraction was observed without any polymer and a network preventing the extraction was probably formed with the random one. The maximal amount of cellulose oligomers that could be extracted seemed to have been reaped. Unexpectedly, no selectivity had been detected.

Another separation method based on differential solubility in alcohol was thus investigated. Methanol was found to be the best candidate. The methanol-soluble fraction contained mainly cellotriose (28%), cellobiose (27%) and glucose (27%) whereas the methanol-insoluble fraction contained 42% of cellotetraose and 36% of cellopentaose.

Appendix

Appendix IV.I: Cellulose acetate DP calculation

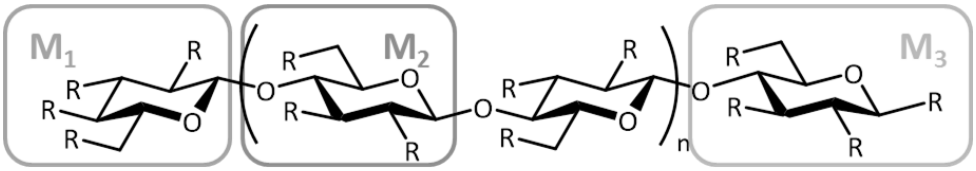

With R = –OH or 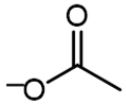

M_1 = C_6H_7O + $^4/_3$ DS x $C_2H_3O_2$ + (4 – $^4/_3$ DS) x OH

M_2 = $C_6H_7O_2$ + DS x $C_2H_3O_2$ + (3 – DS) x OH

M_3 = $C_6H_7O_2$ + $^4/_3$ DS x $C_2H_3O_2$ + (4 – $^4/_3$ DS) x OH

For DP ≥ 2, $M_{SEC} = M_1 + (DP - 2) \times M_2 + M_3$

With M_{SEC} the number average molar mass of the acetylated cellulose measured by SEC in chloroform.

The DP was calculated according to the following equation:

$$DP = 2 + \frac{M_{sec} - M_1 - M_3}{M_2}$$

Appendix IV.II: Cellulose oligomer ratio calculation (Calibration A)

The analyses corresponding to this method were performed using an evaporating light scattering detector (ELSD, Varian 380-LC). The cellulose oligomers concentrations were calculated based on the following calibration (done on the same apparatus). The ratios were then calculated based on the concentrations obtained.

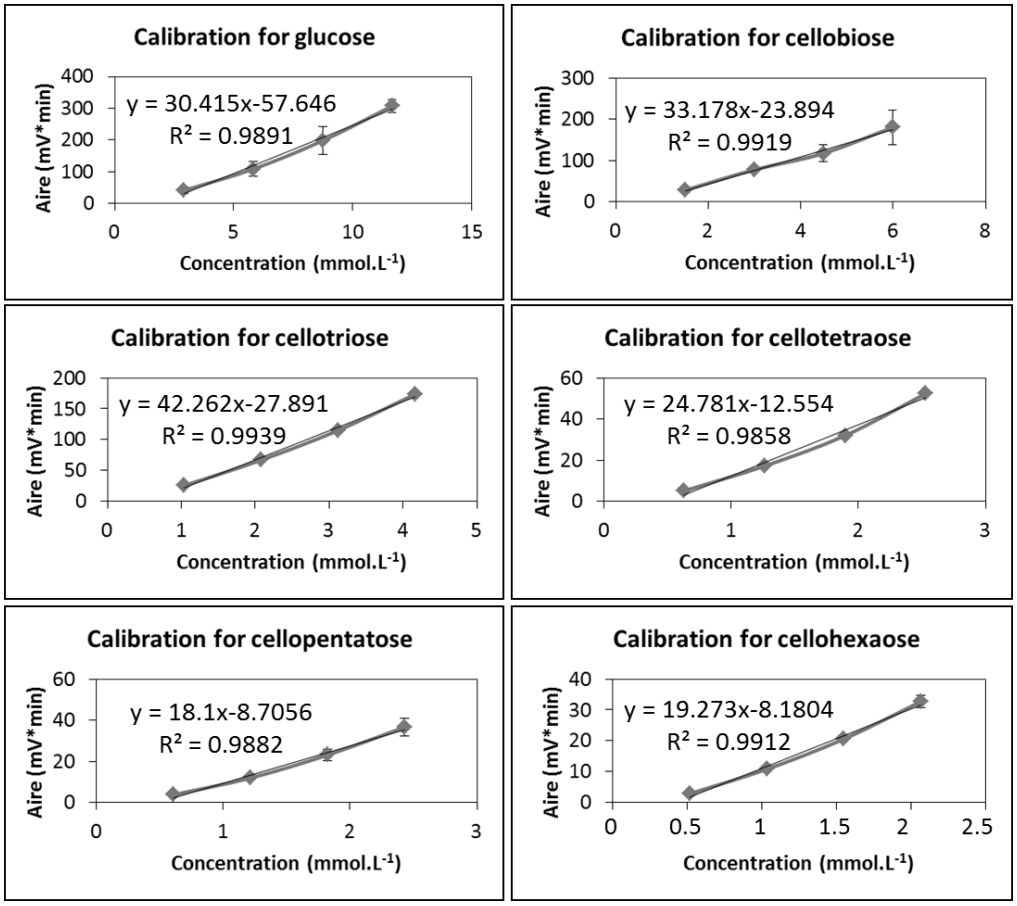

The picture below represents an example of how the areas were measured.

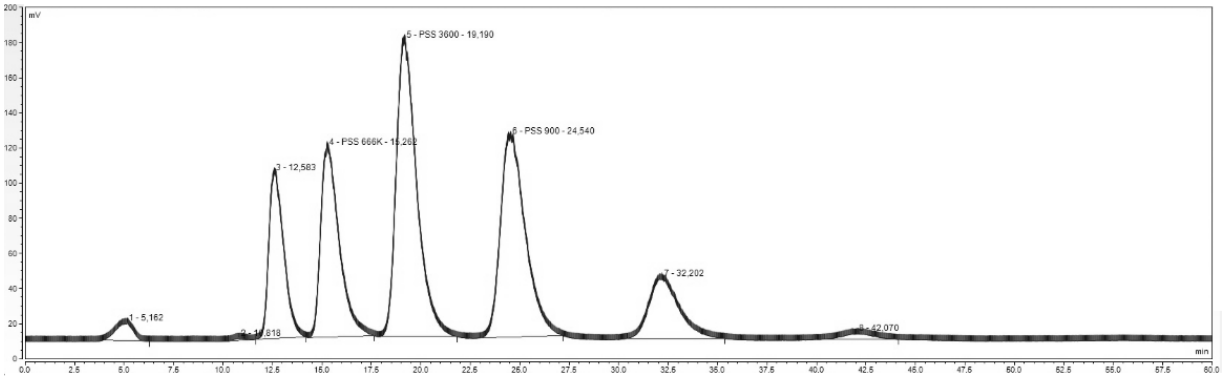

Appendix IV.III: Calculations for the "fishing" method

70 mM of boronic acid in 5 mL of solution corresponds to 0.35 mmol of boronic acid.

The number τ of mmol of boronic acid per gram of polymer is:

$$\tau = \frac{1}{M} \times VBA\ content\ in\ \% \times 1000$$

Then, the quantity m_{polym} of polymer necessary to have 70 mM of boronic acid in a 5 mL volume is:

$$m_{polym} = {}^{0.35}/_{\tau}$$

The calculation was done for the four polymers synthesised for the "fishing" method (see §III. 3. C) ii), p 141) and summarised in the table below.

	Block 45/5	**Block 69/6**	**Block 95/5**	**Random 45/5**
M [a] (g.mol^{-1})	3 920	6 180	7 060	4 150
VBA content [b]	6.7%	3.4%	1.5%	11.0%
τ (µmol.g^{-1})	17	5	2	27
m_{polym} (g)	20.6	64.5	162.5	13.2

[a] M_n determined by SEC in THF based on a polystyrene calibration, [b] Determined by the 4-methylcatechol method (see §III. 3. B) ii), p 136)

Appendix IV.IV: ^{1}H NMR spectra of the interfacial film

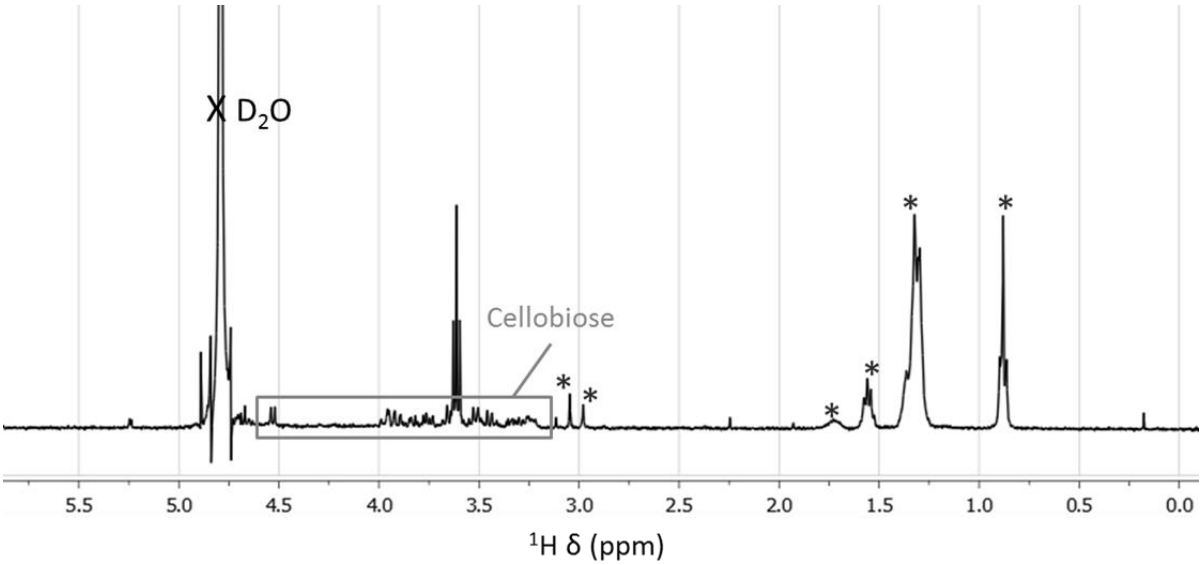

^{1}H NMR spectra of the interfacial film in D_2O (the peaks highlighted with stars correspond to the Aliquat 336^{TM})

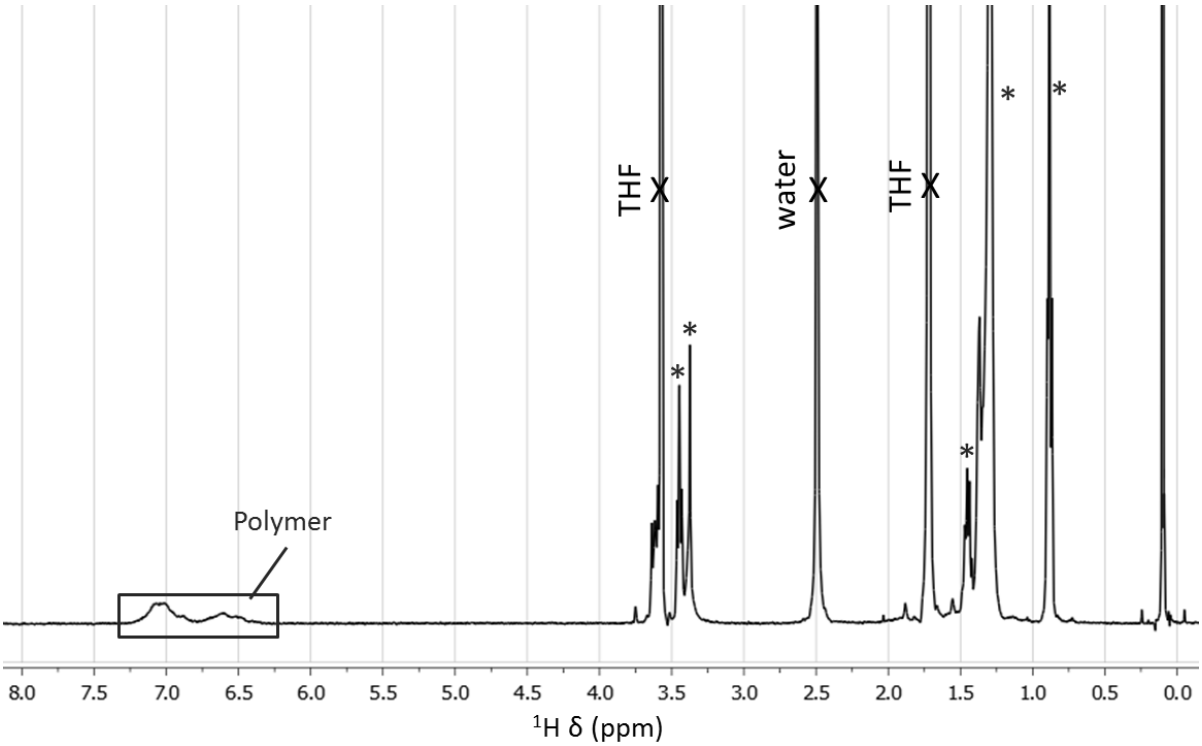

^{1}H NMR spectra of the interfacial film in THF-d_8 (the peaks highlighted with stars correspond to the Aliquat 336^{TM})

Appendix IV.V: Cellulose oligomer ratio calculation (Calibration B)

The analyses corresponding to this method were performed on a Dionex Ultimate 3000 (Thermo Scientifc) equipped with a Corona Veo detector. The cellulose oligomers concentrations were calculated based on the following calibration (done on the same apparatus). The ratios were then calculated based on the concentrations obtained.

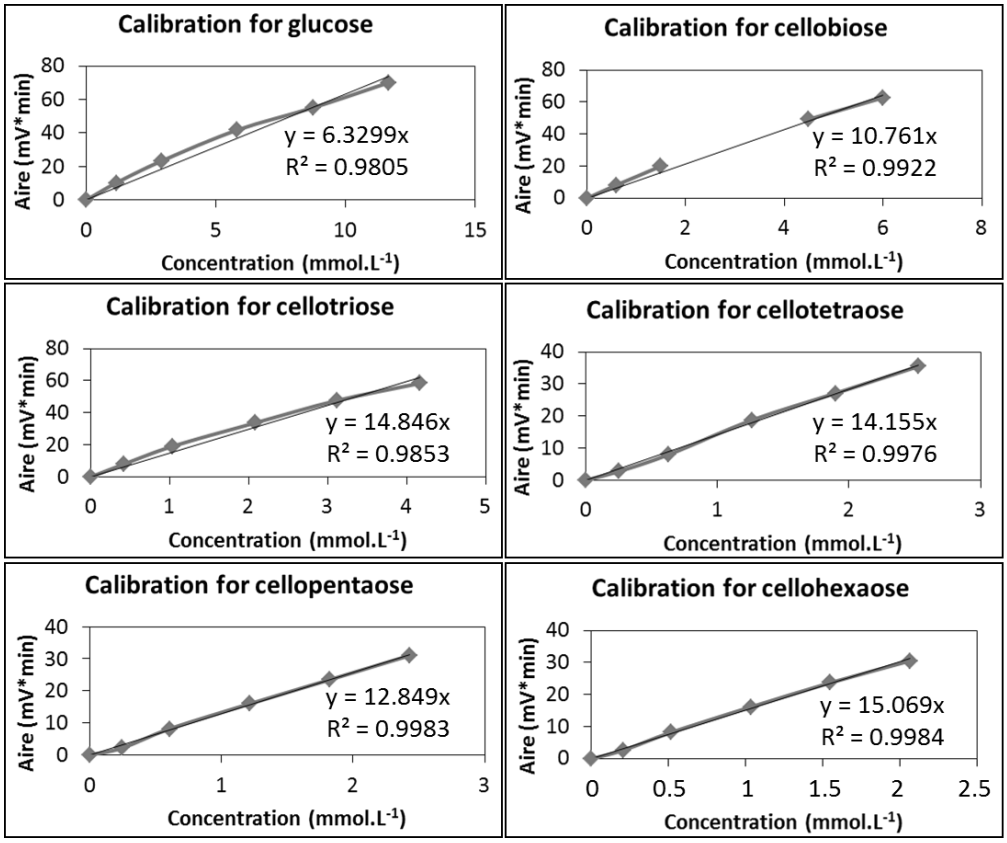

The picture below represents an example of how the areas were measured.

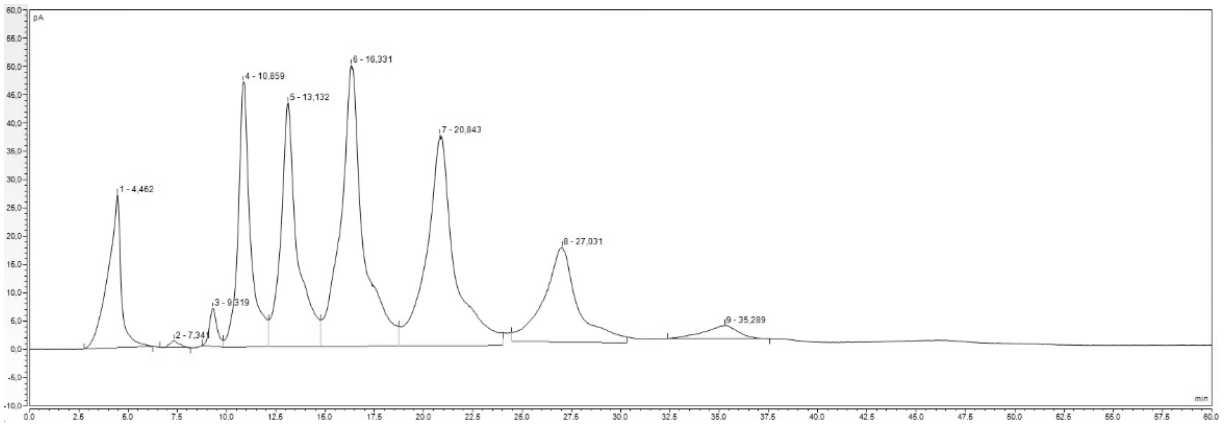

References

[1] T. Liebert, M. Seifert, T. Heinze, *Macromol. Symp.* **2008**, *262*, 140–149.

[2] R. S. Assary, T. Kim, J. J. Low, J. Greeley, L. A. Curtiss, *Phys. Chem. Chem. Phys.* **2012**, *14*, 16603–16611.

[3] B. F. M. Kuster, *Starch* **1990**, *42*, 314–321.

[4] S. M. Shevchenko, K. Chang, J. Robinson, J. N. Saddler, *Bioresour. Technol.* **2000**, *72*, 207–211.

[5] O. O. James, S. Maity, L. A. Usman, K. O. Ajanaku, O. O. Ajani, T. O. Siyanbola, S. Sahu, R. Chaubey, *Energy Environ. Sci.* **2010**, *3*, 1833–1850.

[6] R. Evans, R. H. Wearne, A. F. A. Wallis, *J. Appl. Polym. Sci.* **1989**, *37*, 3291–3303.

[7] H. Pala, M. Mota, F. M. Gama, *Carbohydr. Polym.* **2007**, *68*, 101–108.

[8] T. Heinze, T. Liebert, *Prog. Polym. Sci.* **2001**, *26*, 1689–1762.

[9] T. T. C. Brennan, B. M. Holmes, B. A. Simmons, H. W. Blanch, *Recovery of Sugars from Ionic Liquid Biomass Liquor by Solvent Extraction*, **2010**, WO2011041455 A1.

[10] T. C. R. Brennan, S. Datta, H. W. Blanch, B. A. Simmons, B. M. Holmes, *Bioenergy Res.* **2010**, *3*, 123–133.

[11] R. M. Washburn, E. Levens, C. F. Albright, F. A. Billig, *Org. Synth.* **1959**, *39*, 3–6.

[12] Predicted data generated using the US Environmental Protection Agency's EPISuite™, http://www.chemspider.com/Chemical-Structure.2016127.html

[13] D. Hameister, K. Kragl, *Eng. Life Sci.* **2006**, *6*, 187–192.

[14] C. J. Knill, J. F. Kennedy, *Carbohydr. Polym.* **2003**, *51*, 281–300.

[15] G. Springsteen, B. Wang, *Tetrahedron* **2002**, *58*, 5291–5300.

[16] X. Sun, S.-Y. Xu, S. E. Flower, J. S. Fossey, X. Qian, T. D. James, *Chem. Commun.* **2013**, *49*, 8311–8313.

[17] A. Huebner, M. R. Ladisch, G. T. Tsao, *Biotechnol. Bioeng.* **1978**, *20*, 1669–1677.

[18] N. Claisse, *Préparation et Modification D'oligosaccharides de Cellulose Par Chimie Douce Bio-Inspirée*, Thèse de l'Université de Grenoble, **2012**.

Chapter V.Amphiphilic compounds based on cellulose oligomers

Table of Contents

V. 1. Bibliography

To the best of our knowledge, only a few examples of amphiphilic compounds based on water-soluble cellulose oligomers are found in the literature[1] and most of the time, they are based on the commercial cellobiose[2–4]. Nevertheless, native cellulose and other oligosaccharides were also investigated in this frame. Beforehand, the chemical syntheses and characterisation of such compounds will be explored.

V. 1. A) Generality on amphiphilic compounds based on polysaccharides

V. 1. A) i) Synthesis

Hydrophilic polysaccharides can be modified to become amphiphilic either by grafting (**Figure V-1a**) or by end-to-end coupling with a hydrophobic block (**Figure V-1b**).

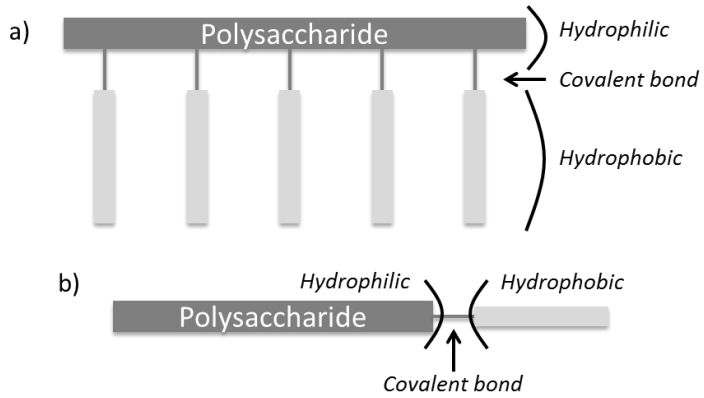

Figure V-1. a) Graft and b) block amphiphilic structures based on polysaccharides

For the synthesis of graft copolymers, the three methods that can be used are summarised in **Figure V-2**[5,6].

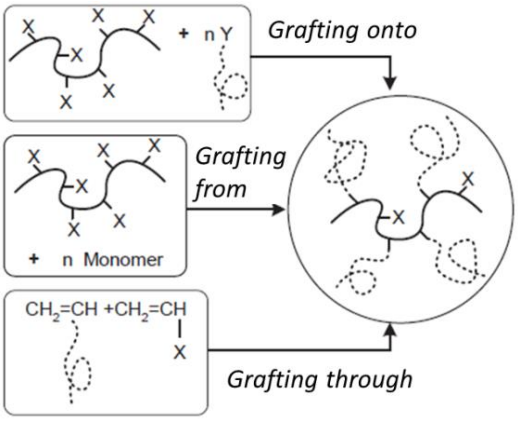

Figure V-2. Methods for the synthesis of graft copolymers (from Huang and coll.[5])

"Grafting onto" involves a coupling reaction between antagonist functions carried by two polymers

"Grafting from" corresponds to the polymerisation of a second monomer from the first polymer, which had been functionalised all along the backbone to initiate RAFT[7,8], ATRP[9,10] or ring opening[11,12] polymerisations, for example

"Grafting through" is the copolymerisation of macromonomers (this technique cannot be applied to cellulose)

To obtain an amphiphilic compound based on block copolymers, the polysaccharide can also serve as a macro-initiator like for the "grafting from" method but with a functionalisation only on the reducing end. The usual way to specifically target this position is by reductive amination[13] with sodium cyanoborohydride[14]. This reaction is based on the "open" form property of saccharides (**Figure V-3**) and thus only the reducing end is affected.

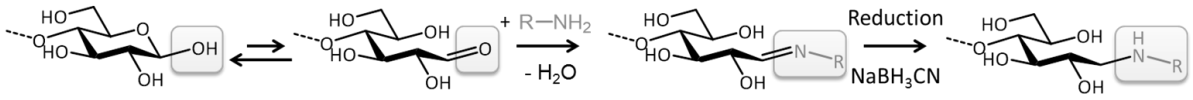

Figure V-3. Reductive amination mechanism – R group possessing a function able to start a polymerisation

Another way to obtain block copolymers from polysaccharides is by end-to-end coupling with another polymer[13], which can be performed by click-chemistry. Click-chemistry reactions were defined, by Sharpless and coll. in 2001[15], as:

- Modular
- Stereospecific
- Wide in scope
- With high yields
- With inoffensive by-products
- Using simple reaction conditions
- With available reagents
- With no or benign solvents

Figure V-4 represents some examples of reaction that fulfil these requirements. Huigsen 1,3-dipolar cycloaddition, also called copper-catalysed azide-alkyne cycloaddition (CuAAC)[16–19], thiol-ene[20]and thiol-yne[21] reactions (**Figure V-4b**, **c** and **d**) are among the most used ones when polysaccharides are involved[22].

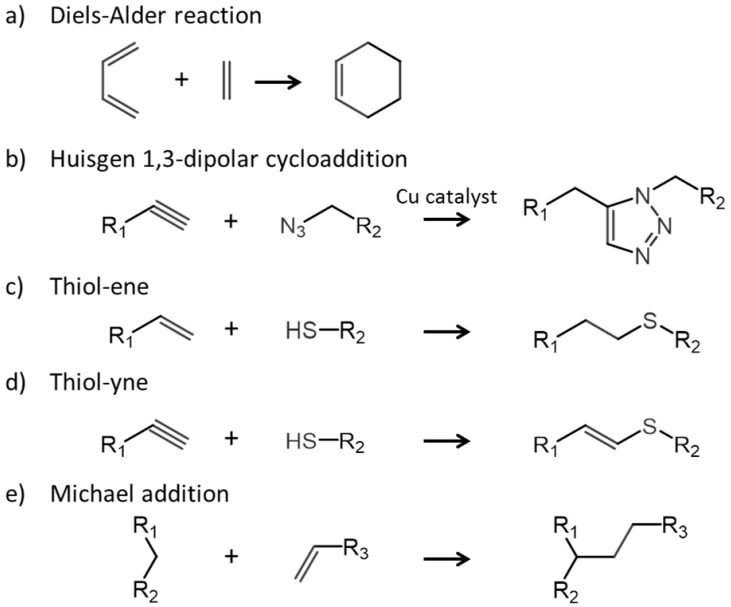

Figure V-4. Some examples of click-chemistry reactions – For reaction e) R_1 and R_2 different from alkyl groups as the hydrogen needs to be activated and R_3 conjugated and electron withdrawing

V. 1. A) ii) Characterisation of the self-assembly

The self-assembly of amphiphilic compounds is driven by an unfavourable mixing enthalpy coupled with a small mixing entropy, macroscopic phase separation being avoided because of the covalent bond connecting the blocks[23]. Three main parameters are used for the characterisation:

- The total degree of polymerisation (N) which influences the entropy of the system
- The Flory-Huggins parameter (χ_{AB}), defined by **Equation I-1**[24], which can be measured, for instance, by spectroscopic ellipsometry[25], atomic force microscopy (AFM)[26] or thermal analysis[27].

$$\chi_{AB} = \frac{z}{k_B T}\left[\varepsilon_{AB} - \frac{1}{2}(\varepsilon_{AA} + \varepsilon_{BB})\right] \qquad \textbf{Equation V-1}$$

With z the number of nearest neighbours per repeat unit in the polymer, $k_B T$ the thermal energy, ε_{AB}, ε_{AA} and ε_{BB} the interaction energies between the corresponding different parts.

- A geometric parameter, the volume fractions of the two parts (f_A and f_B) (**Figure V-5**)

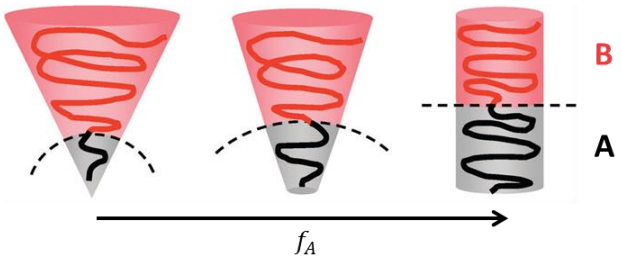

Figure V-5. Representation of the influence of the volume fraction on the morphology of an AB diblock (from Eisenberg[23])

The self-assembly in solution involves six Flory-Huggins parameters[23]: χ_{AB}, χ_{AS}, χ_{AN}, χ_{BS}, χ_{BN} and χ_{SN} with S a good solvent for both blocks and N a non-solvent for one of the blocks. These parameters can be determined by viscosity and cloud point measurements[28] or by solvent vapour swelling[29].

Over 20 morphologies obtained after self-assembly had been identified and some of them are represented on **Figure V-6**[23]. A micelle morphology (**Figure V-6a**) is confirmed when the radius of the core does not exceed the longest hydrophobic chain. Rods are composed of a cylindrical core and a corona surrounding the core (**Figure V-6b**). Their diameter is usually around 30 nm but their length that can exceed tens of micrometers. Bicontinuous rods (**Figure V-6c**) are a three-dimensional networks of interconnected branched rods and are not observed frequently. Lamellae (**Figure V-6d**) are flat or slightly

curved bilayers and are less seen than vesicles (**Figure V-6e**) because of their lower thermodynamic stability. Large compound micelles (**Figure V-6f**) are an aggregation of inverse micelles [hydrophilic core and hydrophobic corona] with the outer surface stabilised by a thin layer of hydrophilic chains. The morphology of self-assembled objects is usually determined by a microscopy technique like transmission electron microscopy (TEM).

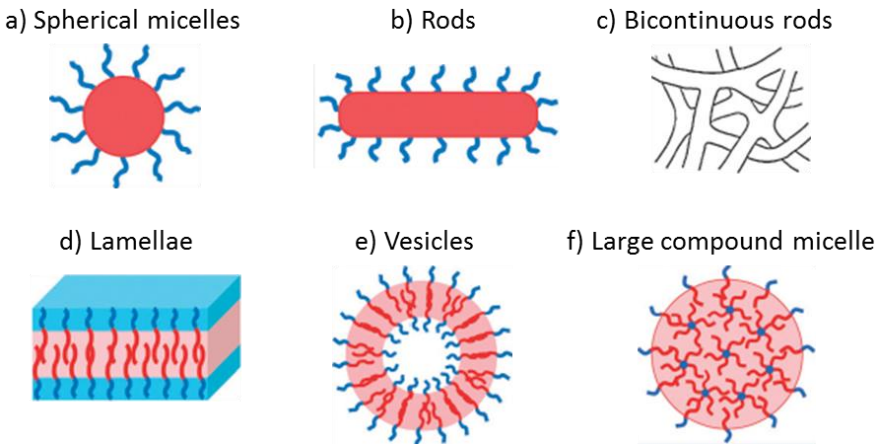

Figure V-6. Examples of morphologies formed by amphiphilic compounds self-assembly (adapted from Mai and Eisenberg[23]) – The blue part is hydrophilic and the red hydrophobic

The surfactant properties of an amphiphilic compounds are characterised by both the critical micelle concentration (CMC) and the hydrophilic-lipophilic balance (HLB).

The CMC is marked out by a drop of the surface tension and the formation of micelles[30] (**Figure V-7**). As the compounds have more interesting propertied above this concentration, the lower the CMC, the smaller the surfactant quantity needed, which is preferred for industrial applications. For example, one of the smallest commercial surfactant CMC is 13-15 $mg.L^{-1}$ for Tween® 80.

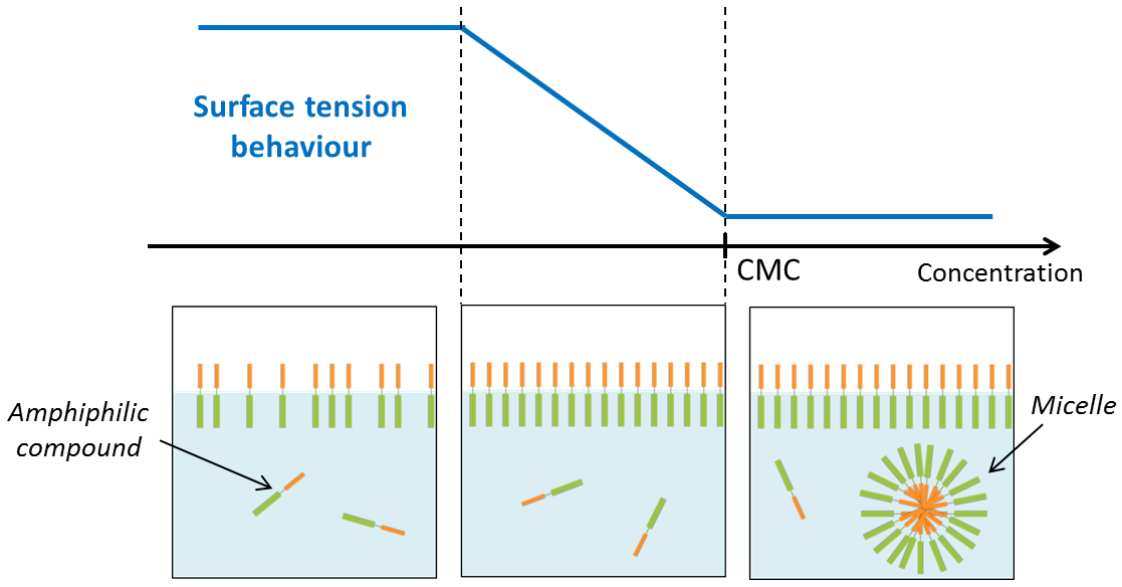

Figure V-7. Critical micelle concentration (CMC) definition (adapted from Saha and coll.[30])

The CMC is usually determined by the pyrene method[31,32]. Pyrene has five predominant peaks in the fluorescence spectrum (**Figure V-8**), the ratio between the first and the third one (I_I/I_{III}) is sensitive to the environment of the molecule[33] and shows a sharp break at the CMC.

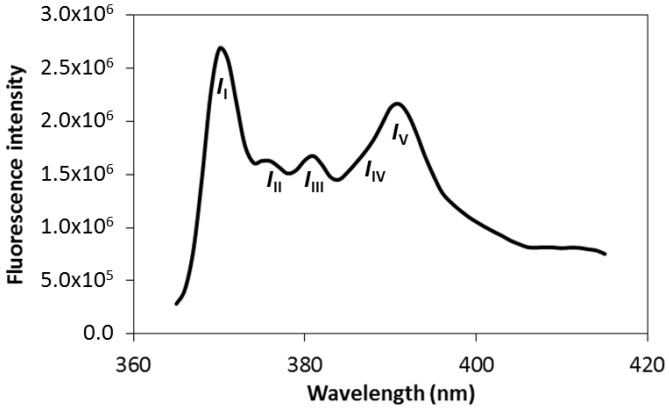

Figure V-8. Fluorescence spectra of pyrene with the definition of the five peaks

The HLB is a value between 0 and 20 that indicates the degree of hydrophilicity or lipophilicity of a surfactant. It is usually calculated by the Griffin's method[34] (**Equation V-2**).

$$HLB = 20 \times \frac{M_{hydrophilic}}{M_{molecule}}$$ **Equation V-2**

The HLB predicts the surfactant properties and applications of a molecule[30,35] as represented in **Figure V-9**.

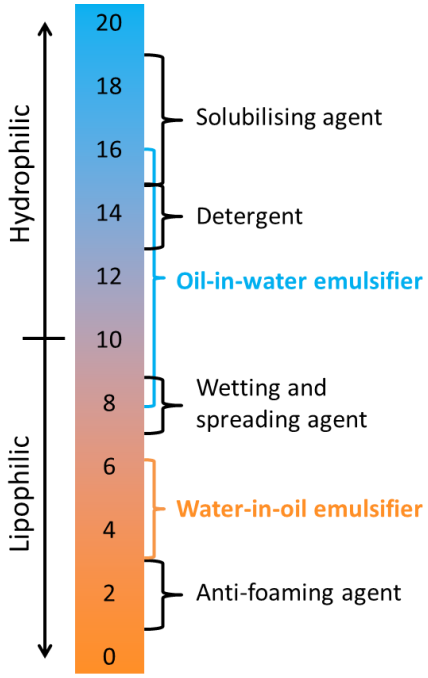

Figure V-9. HLB scale showing surfactant function and properties

V. 1. A) iii) Applications

Amphiphilic compounds based on polysaccharides were applied to a wide range of applications[13]:

- Compatibility agent: Cellulose-*b*-polystyrene was used to enhance the miscibility of cellulose/polystyrene blends in the view of film casting[10]
- Surfactant/Emulsifier: Xylo-oligomers-*b*-polydimethylsiloxane[3] or dextran-*g*-poly(methyl methacrylate)[36] were found to decrease the water-air surface tension and were thus used as non-ionic surfactants
- Cell targeting: The tri-block folic acid-*b*-chitosan oligomers-*b*-polylactic acid was found to target the HeLA cancer cells and was a suitable drug delivery system[37]
- Thermo-responsive materials: The cloud point temperature of several cellulose-*g*-polyacrylamide copolymers was found dependant on the molecular weight but was around 22°C ± 3°C[7]

Some compounds associating a saccharide and an alkyl chain as octyl β-D-glucopyranoside, decyl β-D-maltopyranoside and dodecyl β-D-maltoside are currently commercialised by Sigma-Aldrich, for example, but in small quantity and at high prices.

V. 1. B) Self-assembly of amphiphilic compounds based on cellulose

A really interesting example[38] of "grafting onto" with cellulose (average DP around 200) was obtained with the grafting of stearoyl ester moieties (**Figure V-10a**). The compound, with a substitution degree of 3, was solubilised in dichloromethane and introduced into three volumes of ethyl acetate. The scanning electron microscopy (SEM) of the large particles obtained presented a flower-like structure (**Figure V-10b**). The same structures were obtained with butanol, dioxane and acetone as the non-solvent.

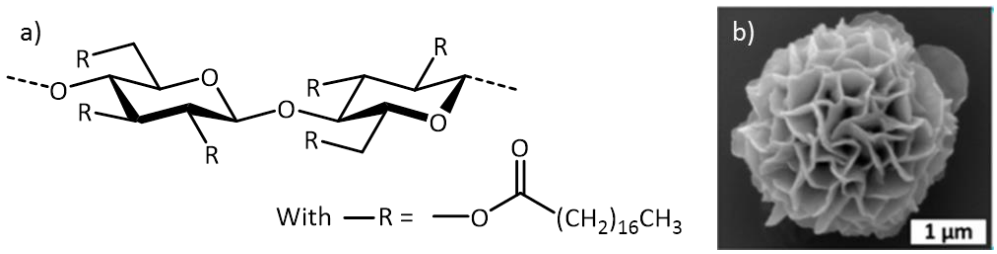

Figure V-10. a) Structure of cellulose-*g*-stearoyl ester, b) SEM of the particles obtained in ethyl acetate (data from Zhang *et al.*[38])

In another example, poly(acrylic acid) had been "grafted from" ethyl cellulose by ATRP[39]. Ethyl cellulose is used so a small substitution degree for poly(acrylic acid) can be obtained (in this work, 0.25). The polymerisation kinetic was of first-order. The particles obtained in water at 1.0 $g.L^{-1}$ had an average diameter of around 100 nm.

As native cellulose is not soluble in common solvents, functionalisation is necessary to obtain block copolymers, thus the cellulose block possibly becomes the hydrophobic one. In this frame, cellulose triacetate had been end-to-end coupled by CuAAC with the amino acid poly(γ-benzyl-L-glutamate) (PBLG)[40]. The goal was to produce a microphase-separated membrane for biological application. A microphase separation of the film and bulk, caused by crystallisation, had been thermally induced and observed by atomic force microscopy (**Figure V-11**).

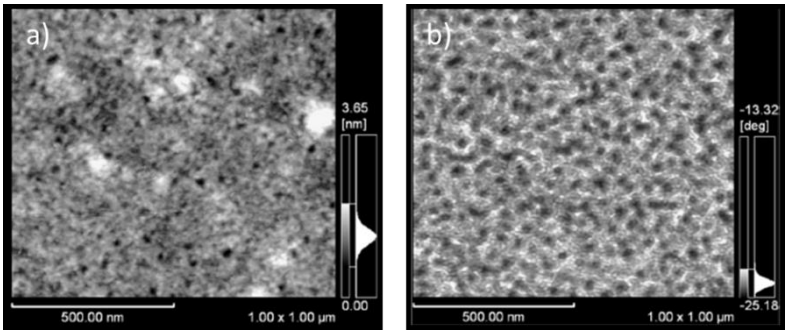

Figure V-11. AFM of a cellulose triacetate-*b*-PBLG thin film, topographic images a) before and b) after annealing at 180°C for 24h (from Kamitakahara *et al.*[40])

V. 1. C) Self-assembly of amphiphilic compounds based on other oligo-saccharides

Malto-oligomers are easily obtained by a ring-opening reaction of commercially available cyclodextrins with iron(III) chloride[41]. Cyclodextrins are cage molecules obtained from the enzymatic degradation of starch by glucoamylase or α-amylase[42]. α, β and γ are the three types of cyclodextrins industrially produced that are composed of 6, 7 or 8 anhydro-glucose units, respectively, linked by α-1,4 bonds (**Figure V-12**).

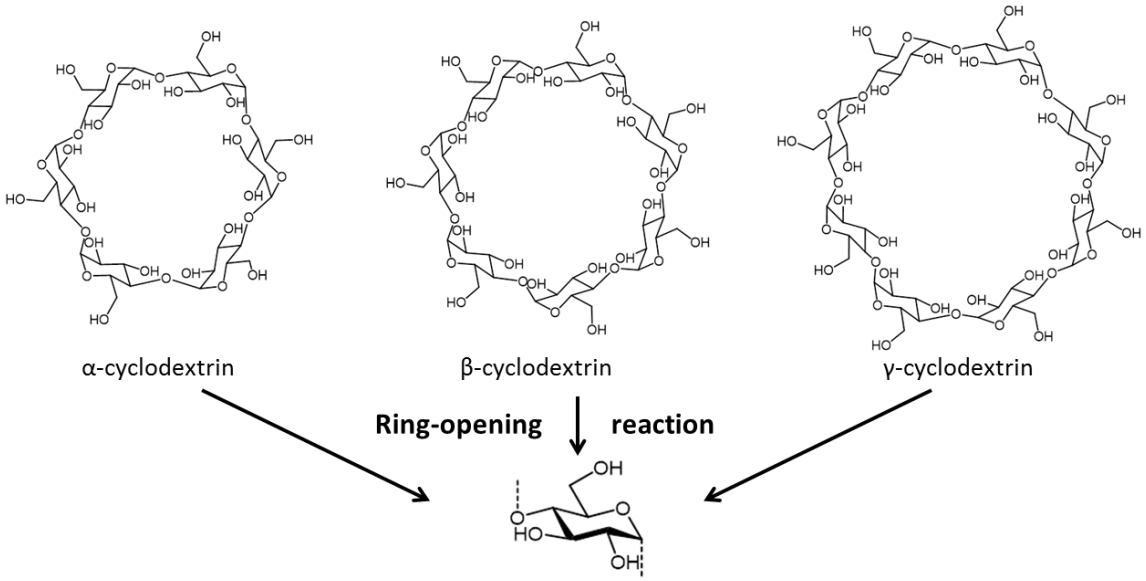

Figure V-12. Cyclodextrins and malto-oligomers structures

Maltoheptaose, obtained from β-cyclodextrins, were coupled by CuAAC with their acetylated analogues to obtain amphiphilic compounds[43]. The same kind of reaction was applied to xylo-oligomers obtained from controlled enzymatic depolymerisation[44] and **Table V-1** compares the properties of the compounds obtained. Spherical micelles were obtained in both cases after self-assembly.

Table V-1. Properties obtained after the end-to-end coupling of oligo-saccharide and their acetylated equivalents

	Maltoheptaose[43]	Xylo-oligomers[44]
DP of the starting oligomers	7	Mixture (7-8-9)
CMC (pyrene method)	100 mg.L^{-1}	40 mg.L^{-1}
Self-assembly in water	Spherical micelles	Spherical micelles
Average diameter	30 nm	25 nm

In our group[45], well defined xylo-oligomers obtained by acidic hydrolysis with a DP of 6 were coupled by CuAAC with two different fatty acids (oleic and ricinoleic, **Figure V-13**).

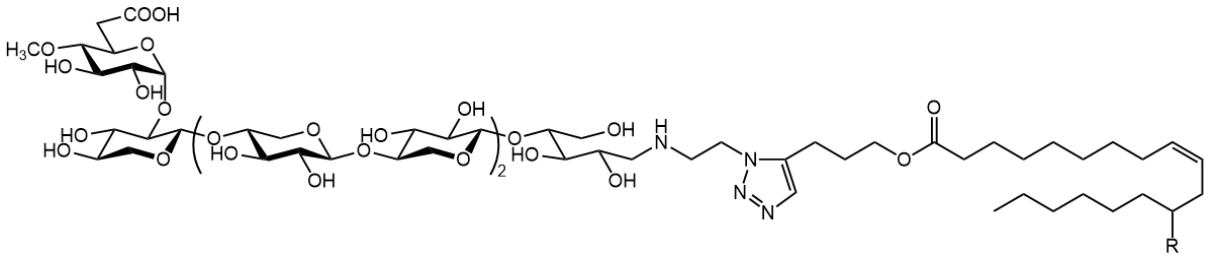

Figure V-13. Structure of the compounds studied in our group, R=H for the oleic acid (XOS-Ol) and R=OH for the ricinoleic acid (XOS-Ric) (from Chemin[45])

Both compounds were soluble in water and chloroform even though the formation of aggregates was observed. Smaller particles were still retrieved after filtration at 0.45 µm. The characteristics of the self-assembly of both compounds are summarised in **Table V-2**.

Table V-2. Characteristics of self-assembly of XOS-Ol and XOS-Ric (from Chemin[45])

		XOS-Ol		XOS-Ric	
		in water	in chloroform	in water	in chloroform
Size of the small particles		50 nm	50 nm	Same as XOS-Ol	
Size of the aggregates	at 10 g.L^{-1}	800 nm	2 500 nm		
	at 1 g.L^{-1}	400 nm	1 500 nm		
	at 0.1 g.L^{-1}	250 nm	700 nm		
CMC (pyrene method)		260 mg.L^{-1}	-	100 mg.L^{-1}	-

V. 2. Synthesis of the amphiphilic compounds based on cellulose oligomers

Based on the literature, the easiest way to obtain the desired amphiphilic compounds would be by copper-catalysed azide-alkyne cycloaddition (**Figure V-14**). The model compound chosen for the hydrophobic part is stearic acid as it is bio-based, commercially available and linear.

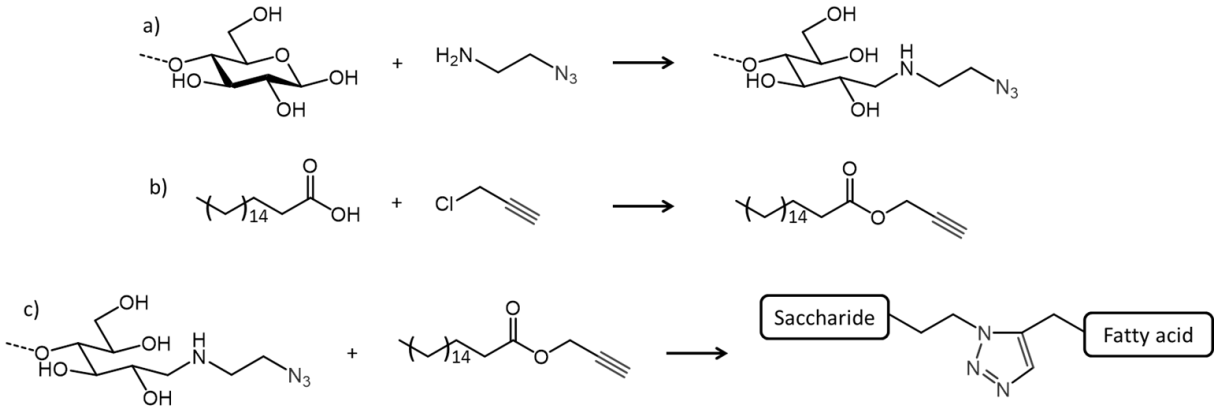

Figure V-14. General reaction scheme to obtain amphiphilic compounds based on cellulose oligomers with a) the azido-functionalisation, b) the alkyne introduction and c) the coupling

The same protocol was performed on cellobiose and the two compounds, CB-SA and CO-SA (**Figure V-15**), were compared on their self-assembly. The composition of the cellulose oligomers used is listed in **Table V-3**.

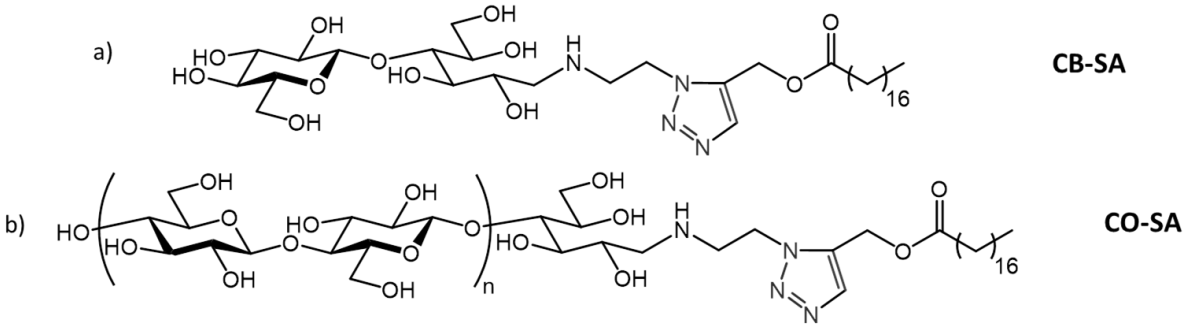

Figure V-15. Structure and notation of the amphiphilic compound based on stearic acid and a) cellobiose (CB-SA) or b) cellulose oligomers (CO-SA)

Table V-3. Composition of the cellulose oligomer used – Determined by HPLC

Glucose	Cellobiose	DP 3	DP 4	DP 5	DP 6	DP 7
1.9%	4.1%	15.8%	38.1%	30.2%	8.2%	1.6%

V. 2. A) Azido-functionalisation

The azide group was introduced on the saccharides *via* a reductive amination reaction with 2-azidoethylamine (**Figure V-14a**). The reaction was performed in water/methanol 1/1 v/v in a microwave at 80°C for 2h[44]. The characterisation of the cellobiose azide is reported on **Appendix V.I** (p 197).

For the cellulose oligomers, the reaction was achieved as confirmed by MALDI spectroscopy (**Figure V-16**) but some partial acetylation was also observed probably due to the presence of acetic acid for the pH adjustment before the microwave heating.

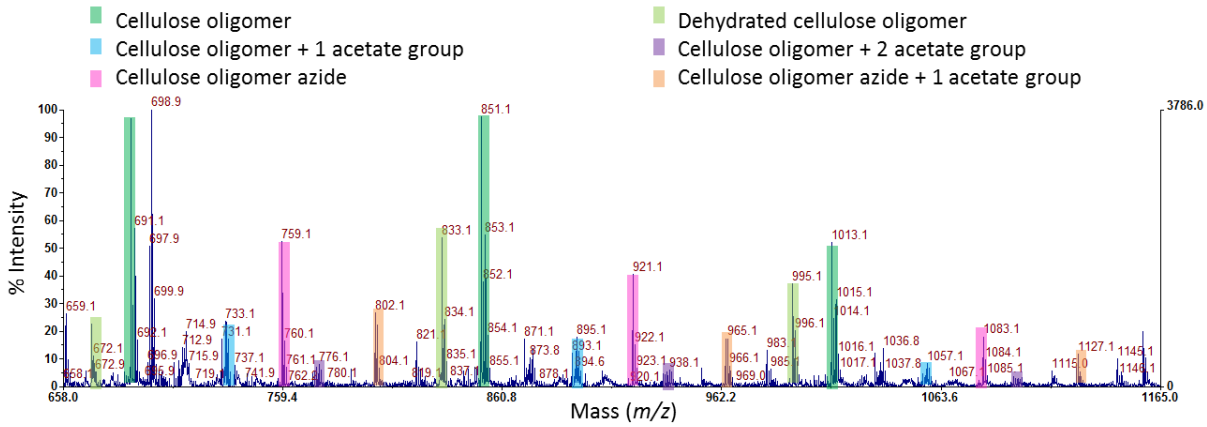

Figure V-16. MALDI spectra of the cellulose oligomers azide

The total conversion was confirmed by NMR and DOSY with the shift of the anomeric proton and only one diffusion coefficient observed (**Figure**). The presence of un-functionalised cellulose oligomers detected by MALDI could be due to some defunctionalisation induced by the ionisation necessary to the analysis.

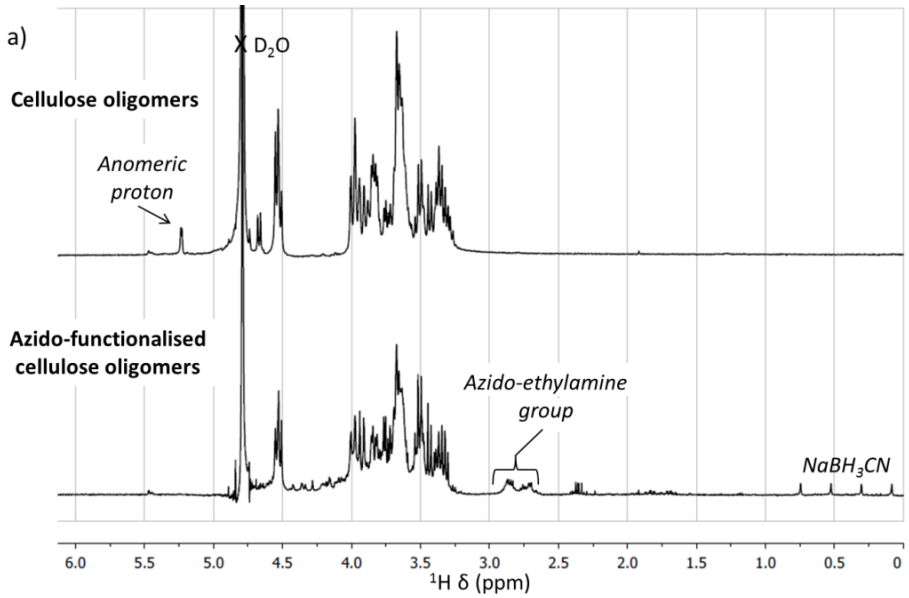

Figure V-17. a) ^{1}H NMR spectra in D_2O of the cellulose oligomers before and after azido-functionalisation

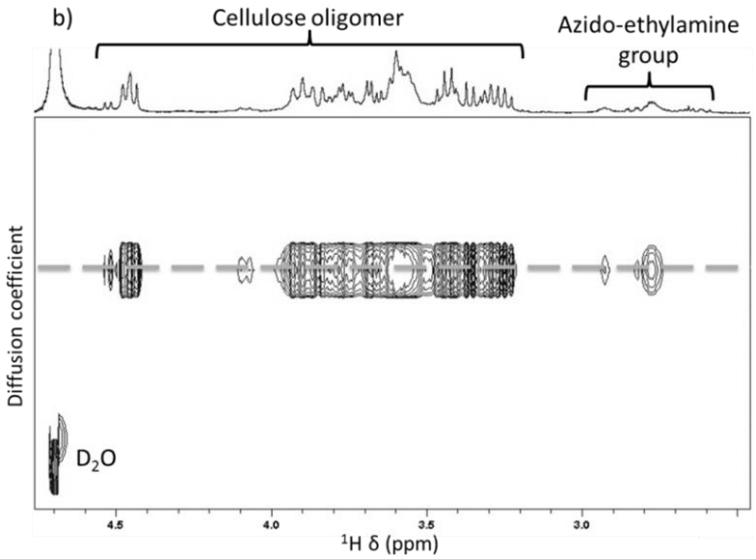

Figure V-17. b) DOSY in D_2O of the azido-functionalised cellulose oligomers

Interestingly, the thermal resistance, observed by thermogravimetric analysis (TGA), of the azido-functionalised saccharides increased compared to the starting material. In fact, the residue at 800°C increased by 21% for the cellobiose and by 15% for the cellulose oligomers (**Figure V-18**). This phenomenon was probably caused by some crosslinking as azide groups had already been used for this purpose[46]. Several reactions could occur[47,48] but the one that actually did was not determined.

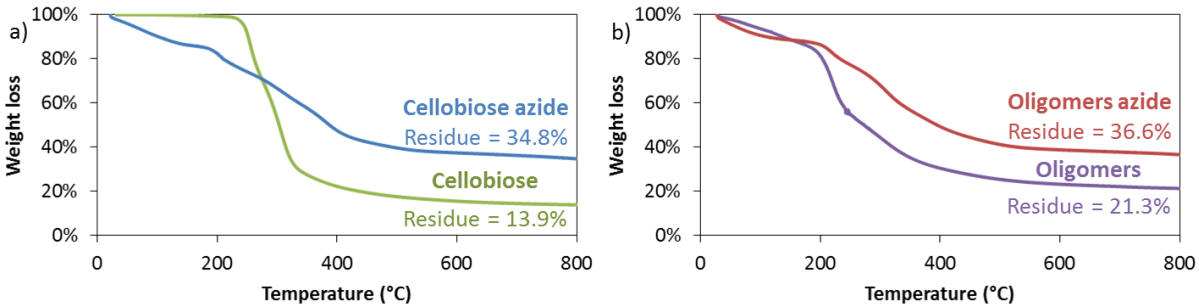

Figure V-18. Comparison of thermal resistance determined by TGA (N_2, 10°C/min) of a) cellobiose and cellobiose azide or b) cellulose oligomers and cellulose oligomers azide

V. 2. B) Stearic alkyne

The reaction between stearic acid and propargyl chloride (**Figure V-14b**, p 185) was performed in DMF in the presence of potassium carbonate at 50°C for 72h. Ethyl acetate (EA) was used to extract the compound from the reaction medium. The formation of the compound was confirmed by ^{1}H NMR (**Figure V-19**), which also allowed calculating the conversion.

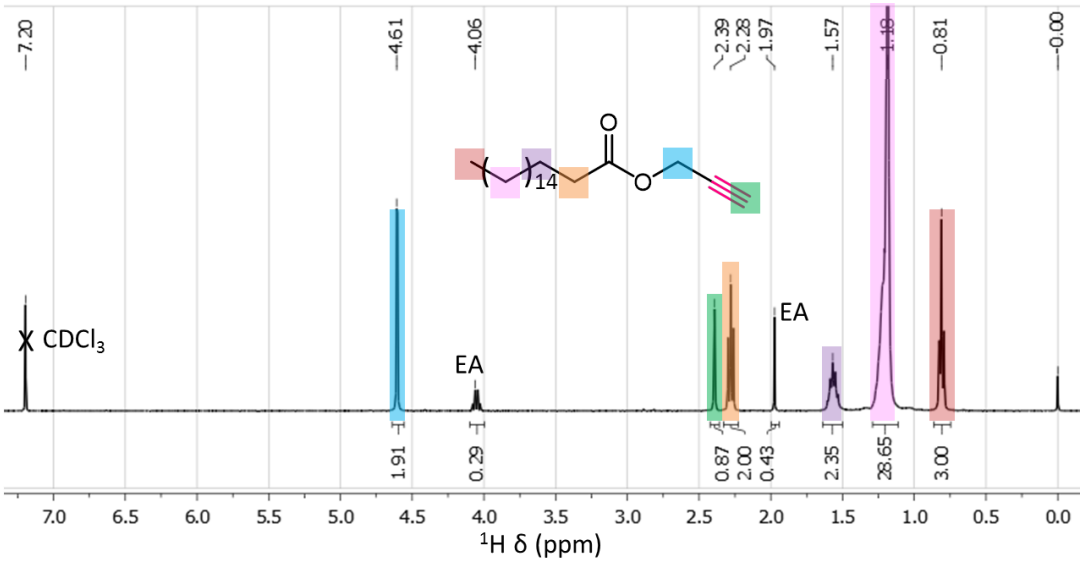

Figure V-19. ^{1}H NMR spectra of stearic alkyne in $CDCl_3$

The reaction was also confirmed by a change in the thermal behaviour observed by TGA and differential scanning calorimetry (DSC). The temperature of degradation at 5% ($T_{d\ 5\%}$), crystallisation (T_c) and melting (T_m) had all decreased by around 30°C after esterification (**Figure V-20**). The enthalpy values, however, were similar meaning that the esterification had almost no impact on the crystallisation state (**Figure V-20b**).

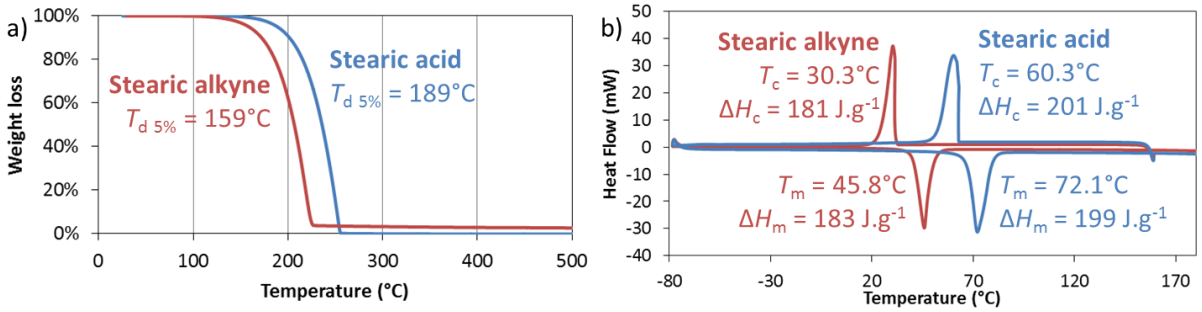

Figure V-20. Comparison of thermal properties of stearic acid and alkyne by a) TGA (N_2, 10°C.min^{-1}) or b) DSC (N_2, 20°C.min^{-1})

V. 2. C) Coupling reaction

The coupling between the azide and the alkyne (**Figure V-14c**, p 185) took place in DMSO with copper sulphate and sodium ascorbate as catalysts at 50°C for three days. After the reaction, no dialysis was performed to remove the catalyst as the compounds sizes were smaller or close to the smallest pores sizes of available dialysis bags and too much product would have been lost.

The characterisation of the cellobiose based amphiphilic compound (CB-SA) is reported on **Appendix V.II** (p 198). For the compound based on cellulose oligomers (CO-SA), the azide band totally disappeared in FT-IR (**Figure V-21f**).

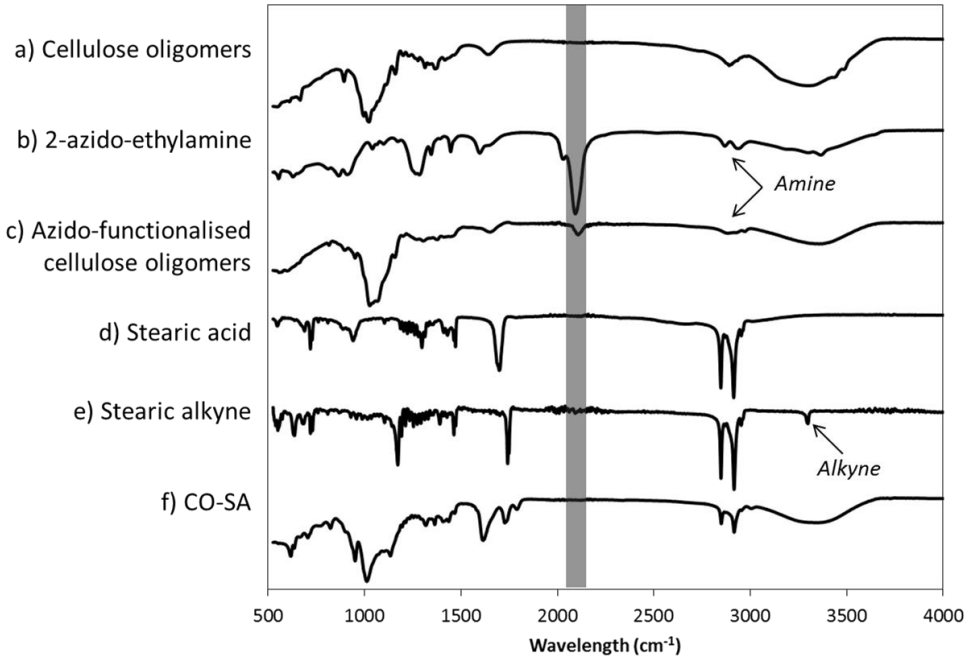

Figure V-21. FT-IR of several compounds – The grey band corresponds to the azide group

The reaction was confirmed by ^{1}H NMR in DMSO-d_6 with the appearance of the triazole peak (**Figure V-22a**). The NMR DOSY also confirmed the reaction as the signals corresponding to the saccharide and the fatty acid parts had the same diffusion coefficient (**Figure V-22b**).

The reaction could not be confirmed by MALDI as the molar masses of the compounds obtained and the oligomers azide were too close, modulo two glucose units:

Cellulose oligomer + azido-ethylamine $= M_{olig} + 68$

Cellulose oligomer + stearic block $= M_{olig} + 390$

$= M_{olig} + 2 \times 162$ *(glucose)* $+ 66$ *(≈ azido-ethylamine)*

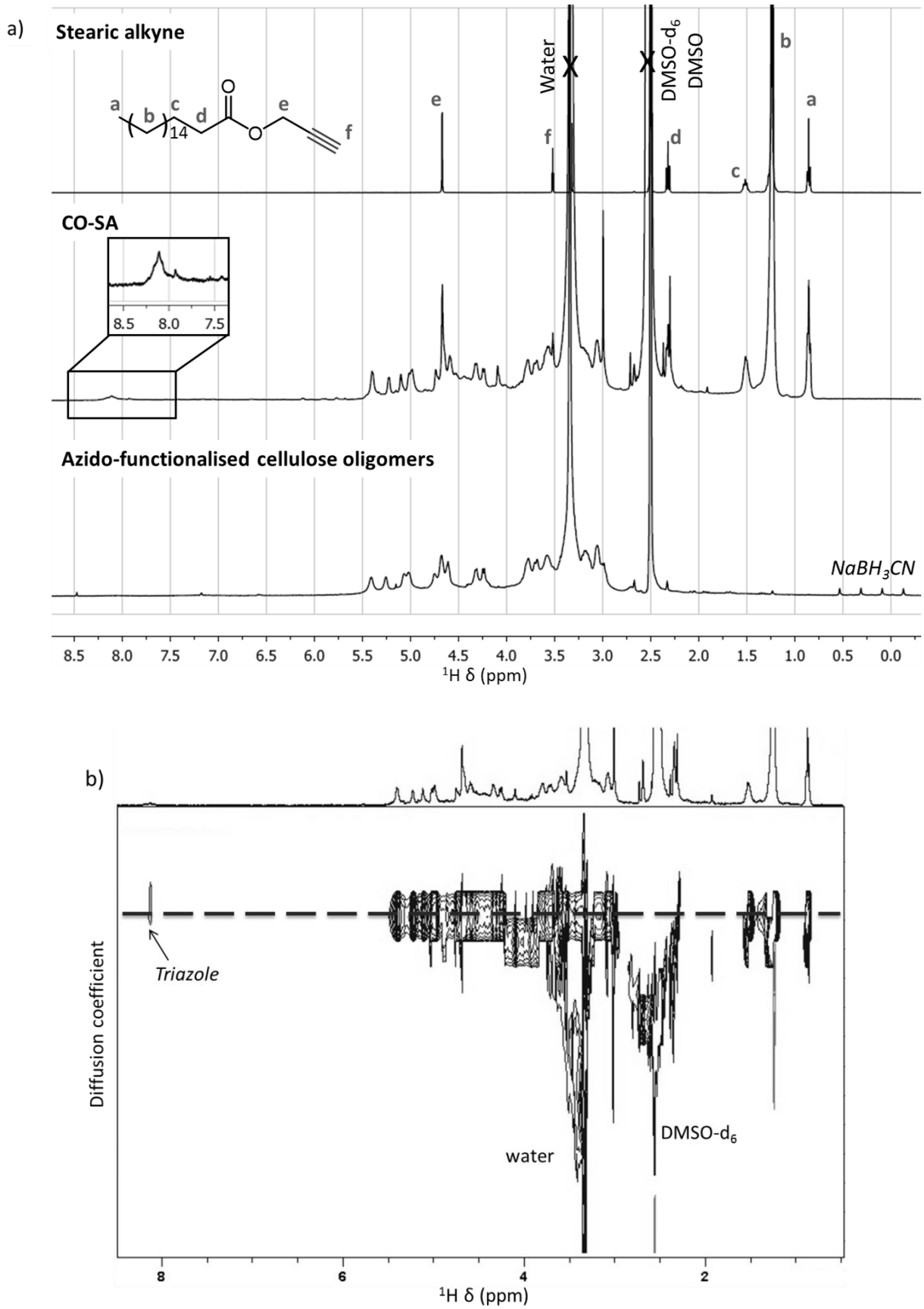

Figure V-22. a) ^{1}H NMR spectra of several compounds in DMSO-d_6 – The portion zoomed on the CO-SA spectra corresponds to the triazole signal and b) DOSY of CO-SA in DMSO-d_6

V. 3. Characterisation of the amphiphilic compounds

V. 3. A) Thermal characteristics

The thermal stability of the amphiphilic compounds was similar to the sugar part but a smaller amount of residue was obtained (**Figure V-23a** and **b**). The last drop at 755°C for CB-SA and 743°C for CO-SA corresponded to the remaining catalyst degradation, which decomposed into copper(II) oxide and sulphur trioxide above 700°C[49]. This drop indicated that the products contained around 8% of catalyst (initial content of copper sulphate: 18 wt%). The presence of residual solvent (**Figure V-23a'** and **b'**) prevented the determination of $T_{d\ 5\%}$.

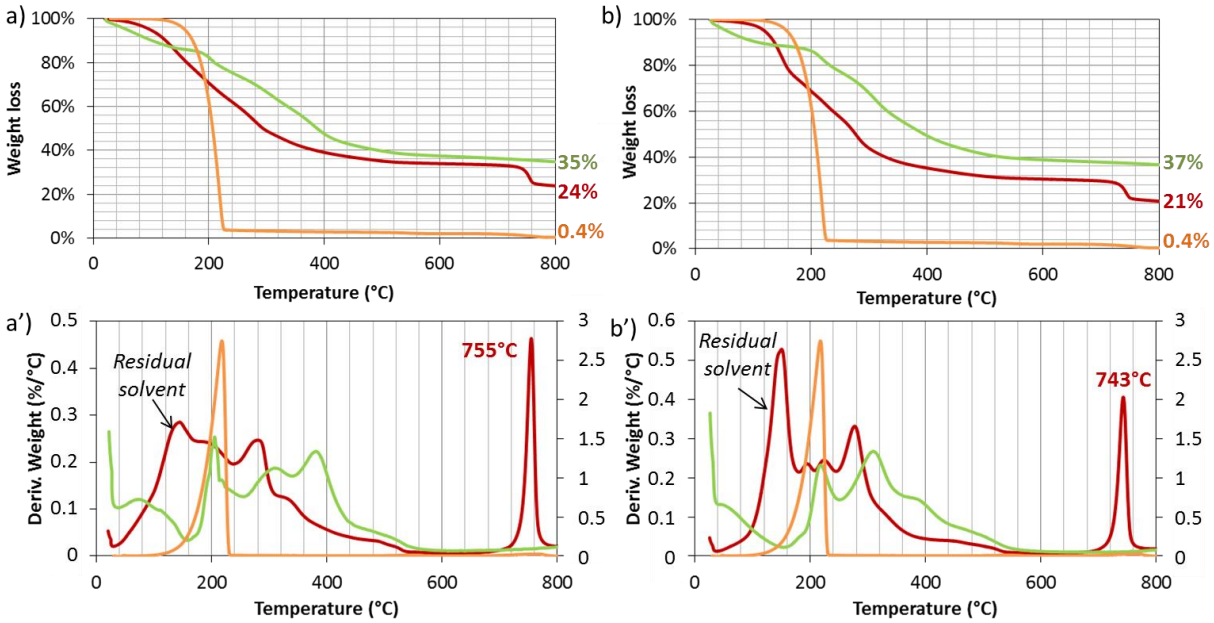

Figure V-23. TGA curves (N_2, 10°C.min^{-1}) in weight loss (a and b) or the first derivative (a' and b') of the cellobiose based compounds (a and a') or the cellulose oligomers based compounds (b and b') – The corresponding azido-functionalised compound (green) and amphiphilic compound (red) are represented as well as the stearic alkyne (orange)

A glass transition temperature (T_g) was observed for the cellulose oligomers but not for cellobiose (**Figure V-24a** and **b**). The T_g disappeared after the coupling and only a melting temperature was observed probably corresponding to the fatty acid part (**Figure V-24f**). The great decrease of the melting enthalpy for the two amphiphilic compounds compared to the stearic alkyne indicated that a great disorder was induced by the sugar block, which had partially prevented the crystallisation of the fatty acid block (**Figure V-24d** to **f**).

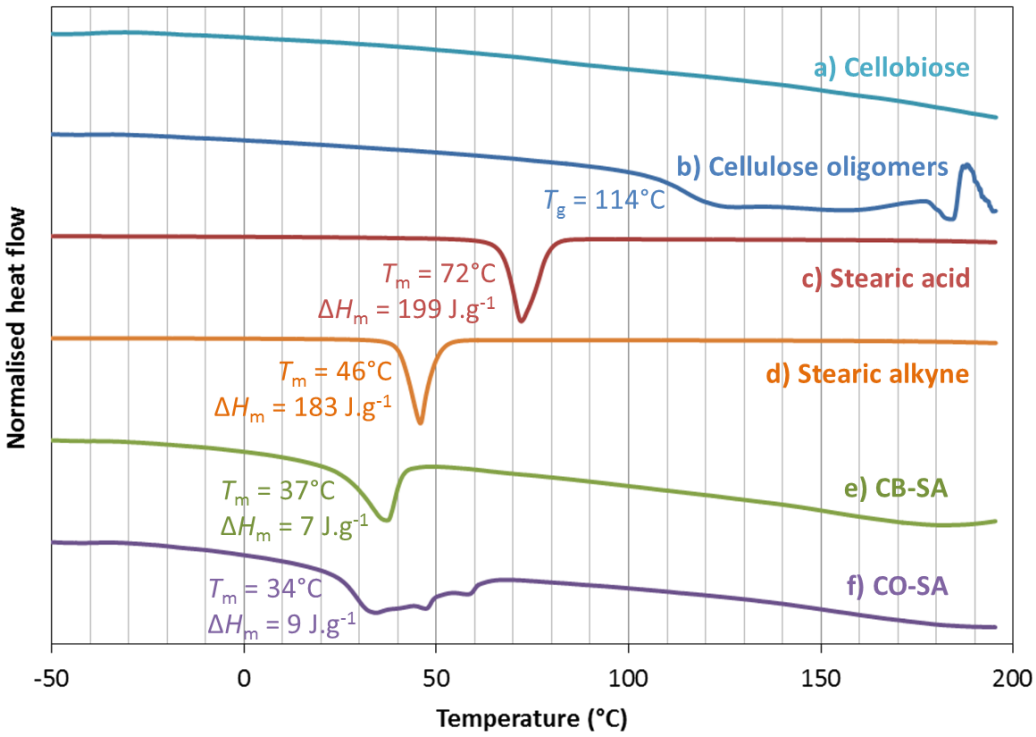

Figure V-24. DSC graphs (N_2, 20°C.min^{-1}) of several compounds

V. 3. B) Self-assembly

First, to determine in which solvent the self-assembly would be investigated, a solubilisation study was performed. CB-SA was not soluble in any solvent tested except for DMSO whereas CO-SA was soluble in DMSO and water (**Figure V-25**). As DMSO was a good solvent for both blocks, no self-assembly was induced. However, water was a non-solvent for the stearic acid, self-assembly was thus probably induced in this solvent.

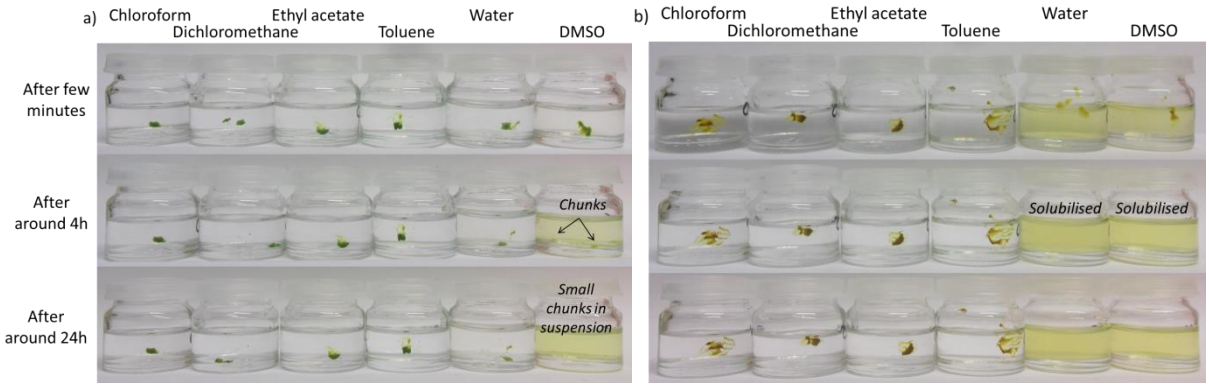

Figure V-25. Solubilisation of a) CB-SA and b) CO-SA in several solvents over time – Concentration: 1 g.L^{-1}, from left to right: chloroform, dichloromethane, ethyl acetate, toluene, water and DMSO

The difference of micellisation between the two compounds came from an unfavourable size ratio of the corresponding blocks. In fact, the stearic acid is twice the size of cellobiose whereas stearic acid and cellulose oligomers have similar sizes for DP > 4

(**Table V-4**). This size difference probably caused some destabilisation for CB-SA resulting in aggregation.

Considering the HLBs, the compounds studied were mainly hydrophilic and should be oil-in-water emulsifiers (**Figure V-9**, p 181). This was likely the reason of their inexistent solubilisation in hydrophobic solvents.

Consequently, only the self-assembly in water of CO-SA was studied in the rest of the study.

Table V-4. Size ratio and HLB of the amphiphilic compounds depending on the cellulose oligomer

Cellulose oligomer	Oligomer length (Å)[50]	Stearic acid length (Å) [a]	Size ratio	HLB [b]
Cellobiose	14.6	27.7	0.5	9.3
Cellotriose	20.2		0.7	11.3
Cellotetraose	26.2		0.9	12.6
Cellopentaose	31.8		1.1	13.6
Cellohexaose	37.6		1.4	14.4

*[a] Calculated as 18 times a C–C bond length, [b] Calculated based on **Equation V-2** (p 181)*

The CMC of CO-SA was determined by the pyrene method and was found to be around 100 mg.L^{-1} (**Figure V-26**). Xylo-oligomers-*b*-ricinoleic acid[45] had the same CMC (**Table V-2**, p 184). Compared to some commercial amphiphilic compounds based on saccharides (**Appendix V.III**, p 200), the value obtained here is in a good range.

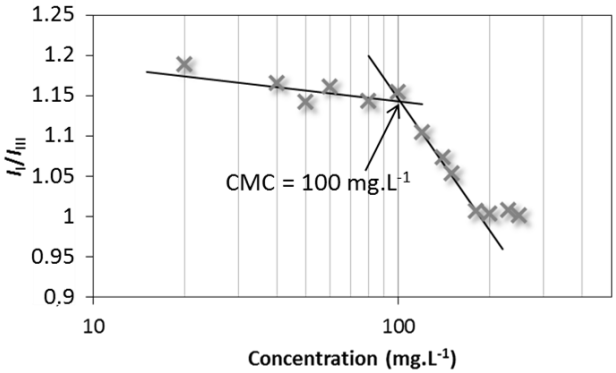

Figure V-26. CMC determination for CO-SA

The particle size distribution measured by dynamic light scattering (DLS) did not depend on the solution concentration and appeared to be stable over time (**Figure V-27**).

The particle size at 200 mg.L^{-1} was 143 nm with a PDI of 0.21 meaning that they were quite homogeneous but too large to be micelles considering that the radius of the core probably exceeded the hydrophobic chain size (30 Å). Interestingly, the dispersity of the

particle size was homogeneous even though the cellulose oligomers DP varied from 3 to 6. This indicated that each cellulose oligomer DP was homogenously distributed over all the particles.

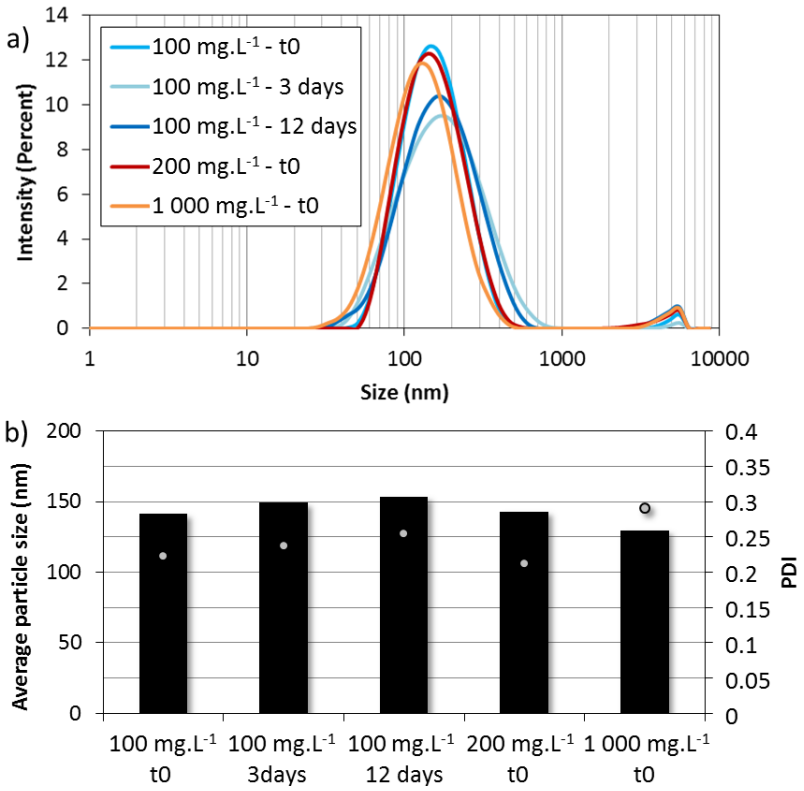

Figure V-27. a) DLS spectra and b) average particle size (column) and PDI (circles) of several solutions of CO-SA measured at different time – The samples were not filtrated before analysis

To determine the morphology of the obtained objects, TEM pictures of a solution of CO-SA at 200 mg.L^{-1} in water, which was higher but close to the CMC, were taken (**Figure V-28**). The average particle size observed by TEM was really smaller than the one determined by DLS (≈ 50 nm *versus* 140 nm). The reason was that for DLS the particles were in solution whereas for TEM, they were "dried" which induced shrinkage. This shrinkage may also explain the not exactly round shape of the particles.

The objects obtained are most probably vesicles

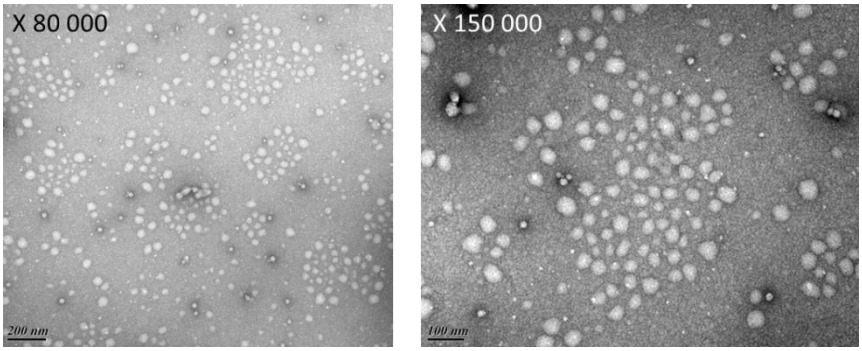

Figure V-28. TEM pictures of CO-SA in water at 200 mg.L^{-1}

The DLS study was also performed on CB-SA. Although some small particles seemed to be formed at first at 100 mg.L^{-1}, they quickly aggregated (**Figure V-29**). After filtration, no particles were seen meaning that all the small particles had aggregated and none of them stayed in solution. After 3 days at 100 mg.L^{-1}, the average object size was 450 nm with a PDI of 0.19.

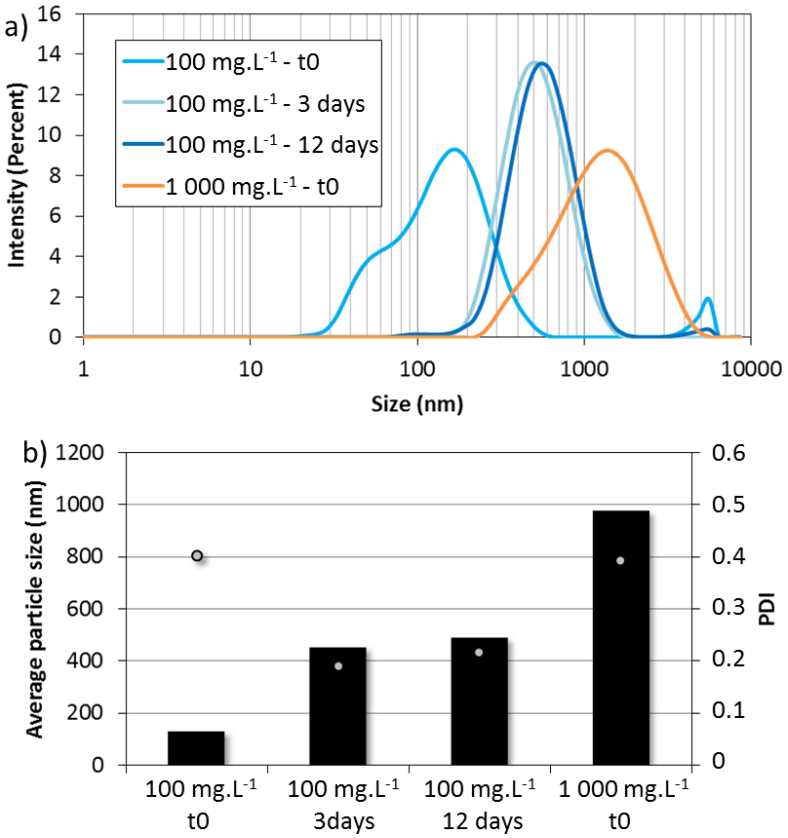

Figure V-29. a) DLS spectra and b) average particle size (column) and PDI (circles) of several solutions of CB-SA measured at different time – The samples were not filtrated before analysis

Chapter conclusion

Cellobiose and water-soluble/methanol-insoluble cellulose oligomers were successfully coupled with a stearic acid to form amphiphilic compounds by copper-catalysed azide-alkyne cycloaddition.

Considering their HLB, they tended to be hydrophilic compounds. In fact, none of them showed any sign of solubilisation with any of the hydrophobic solvents tested.

The cellobiose based compound (CB-SA) also aggregated in water. The phenomenon was observed by DLS. After 3 days at 100 $mg.L^{-1}$ in water, the objects had an average diameter of 450 nm with a PDI of 0.19.

The solubilisation of the compounds based on cellulose oligomers (CO-SA) in water resulted in a clear solution. The CMC of this compound was found to be around 100 $mg.L^{-1}$ which was in a good range for such type of compounds. At 200 $mg.L^{-1}$ in water, the particles had an average diameter of 140 nm with a PDI of 0.21. The TEM pictures taken at this concentration represented quite round particles. The objects were thus probably vesicles considering their large sizes in solution.

As the particles sizes distribution was homogeneous (small PDI), the different cellulose oligomers DP seem well distributed over the particles.

Appendix

Appendix V.I: Characterisation of the azido-functionalised cellobiose

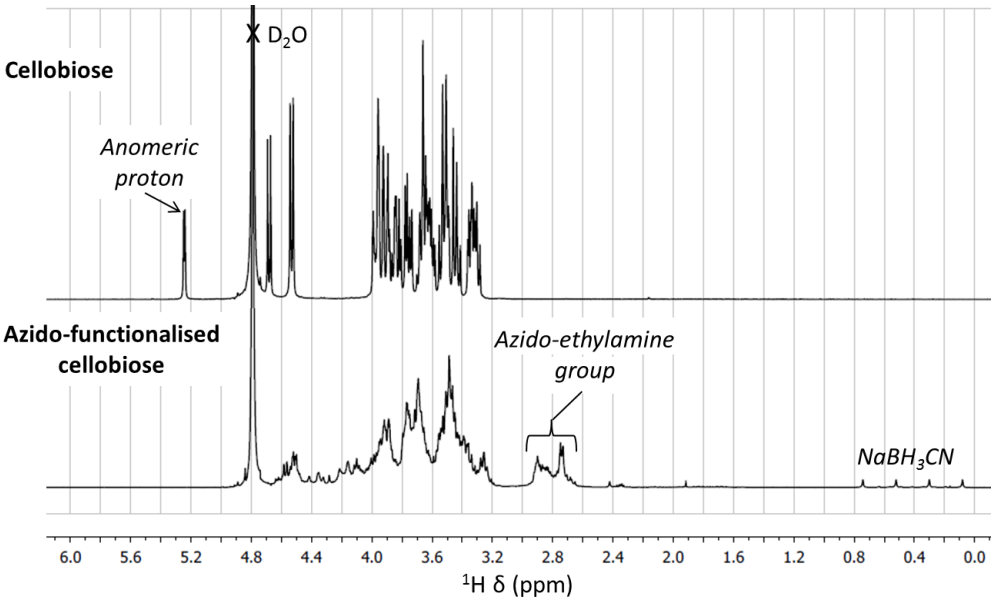

^{1}H NMR spectra in D_2O comparison of the cellobiose before and after azido-functionalisation

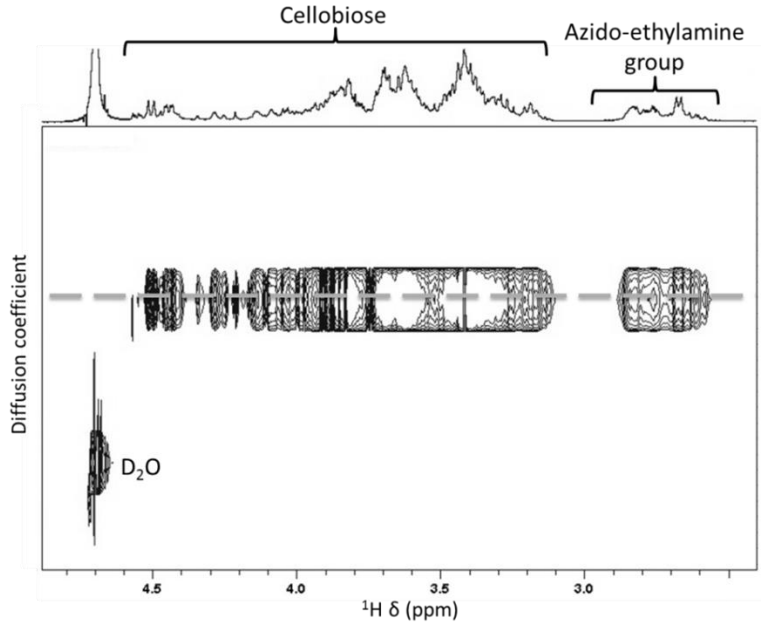

DOSY NMR spectra in D_2O of the cellobiose after azido-functionalisation

Appendix V.II: Characterisation of amphiphilic compound based on cellobiose (CB-SA)

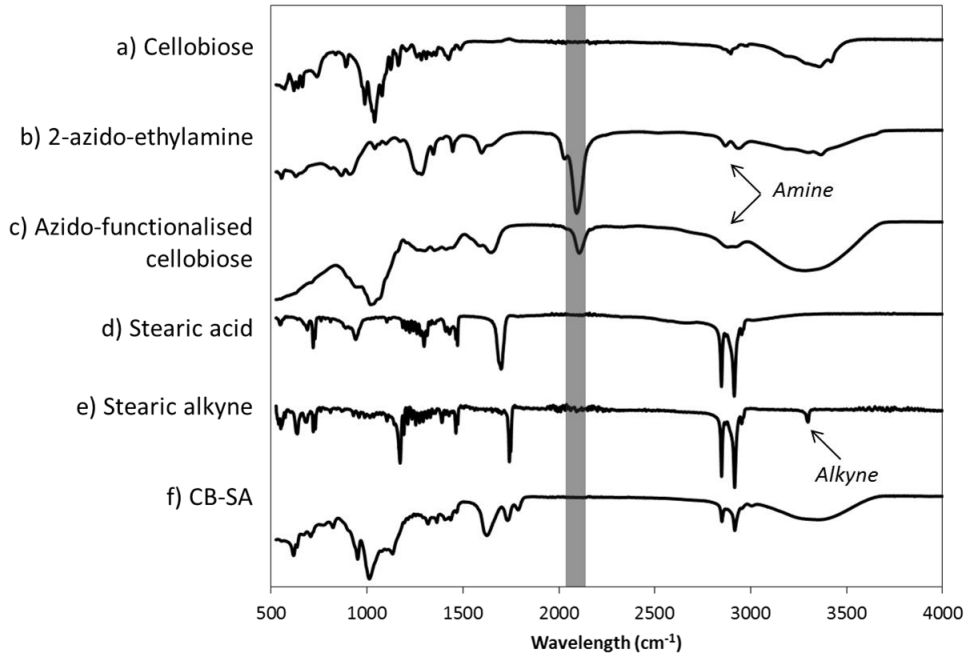

FT-IR of several compounds – The grey band corresponds to the azide group

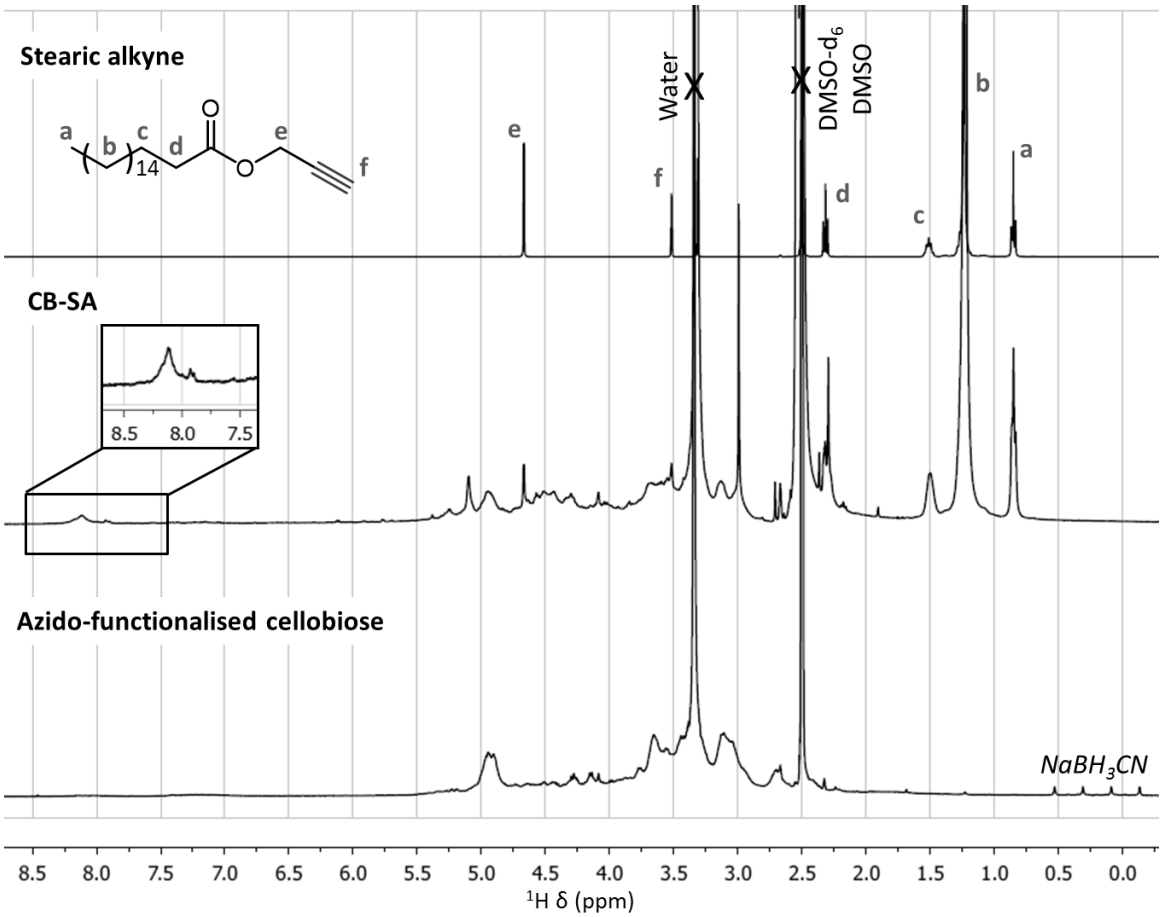

^{1}H NMR spectra of several compounds in DMSO-d_6 – The portion zoomed on the CB-SA spectra corresponds to the triazole signal

Appendix V.II (following): Characterisation of amphiphilic compound based on cellobiose (CB-SA)

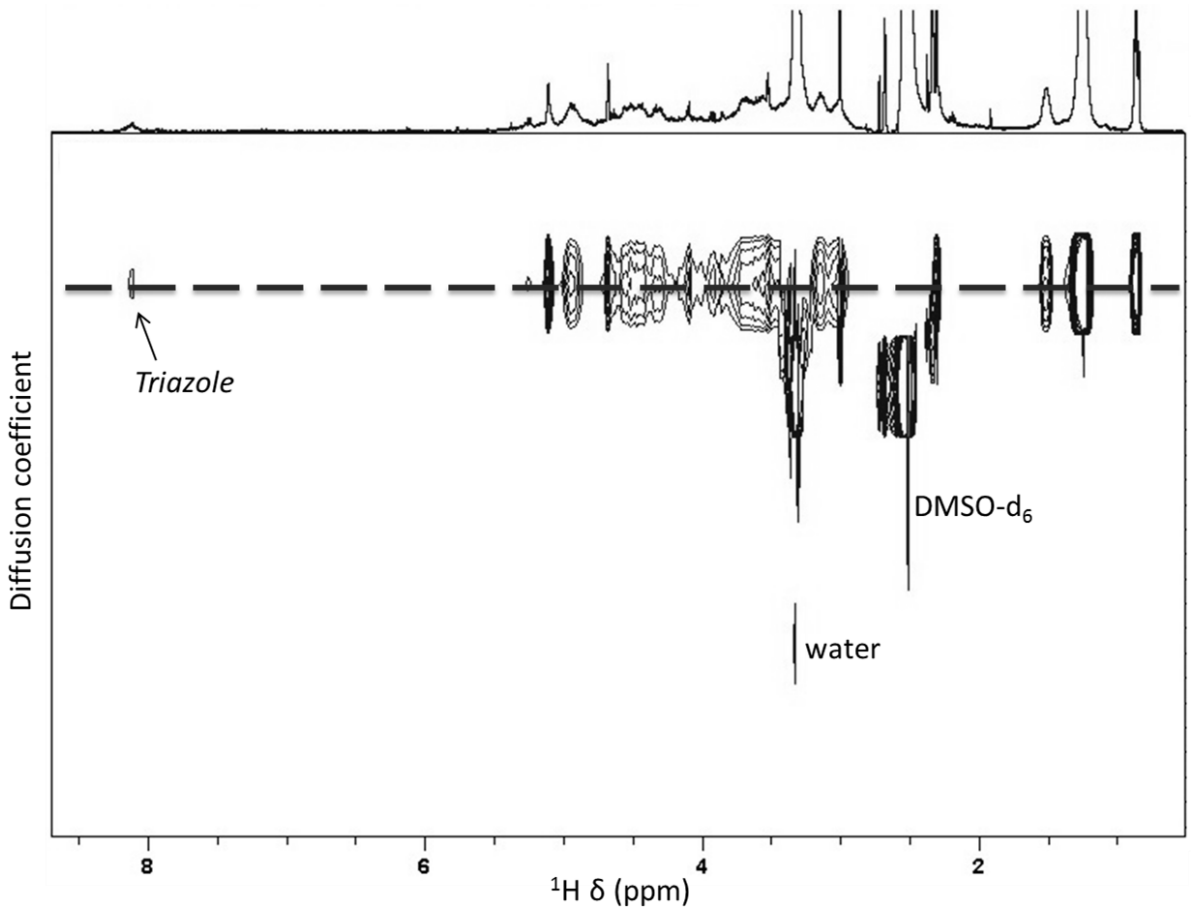

DOSY NMR spectra of CB-SA in DMSO-d_6

Appendix V.III: Characteristics of some commercial amphiphilic compounds based on saccharides

Alkyglucosides	Structure		M (g.mol^{-1})	CMC (mM)	CMC (mg.L^{-1})	CAS number
n-Dodecyl-β-D-glucopyranoside		n = 11	349	0.19	66	59122-55-3
n-Decyl-β-D-glucopyranoside		n = 9	320	2.2	704	58846-77-8
n-Nonyl-β-D-glucopyranoside		n = 8	306	18-20	5 515	69984-73-2
n-Octyl-β-D-glucopyranoside		n = 7	292	25-30	7 305-8 766	29836-26-8

Alkymaltosides	Structure		M (g.mol^{-1})	CMC (mM)	CMC (mg.L^{-1})	CAS number
n-Dodecyl-β-D-maltoside		n = 11	511	0.15-0.19	77-97	69227-93-6
n-Decyl-β-D-maltoside		n = 9	483	1.8	869	82494-09-5
n-Nonyl-β-D-maltoside		n = 8	468	6.0	2 810	106402-05-5
n-Octyl-β-D-maltoside		n = 7	455	23.8	10 817	82494-08-4

References

[1] H. Kamitakahara, F. Nakatsubo, D. Klemm, *Cellulose* **2007**, *14*, 513–528.

[2] S. Berson, D. Viet, S. Halila, H. Driguez, E. Fleury, T. Hamaide, *Macromol. Chem. Phys.* **2008**, *209*, 1814–1825.

[3] S. Halila, M. Manguian, S. Fort, S. Cottaz, T. Hamaide, E. Fleury, H. Driguez, *Macromol. Chem. Phys.* **2008**, *209*, 1282–1290.

[4] H. Kamitakahara, F. Nakatsubo, *Cellulose* **2005**, *12*, 209–219.

[5] H. Kang, R. Liu, Y. Huang, *Polymer* **2015**, *70*, A1–A16.

[6] D. Roy, M. Semsarilar, J. T. Guthrie, S. Perrier, *Chem. Soc. Rev.* **2009**, *38*, 2046–2064.

[7] A. Hufendiek, V. Trouillet, M. A. R. Meier, C. Barner-Kowollik, *Biomacromolecules* **2014**, *15*, 2563–2572.

[8] Y. Liu, X. Jin, X. Zhang, M. Han, S. Ji, *Carbohydr. Polym.* **2015**, *117*, 312–318.

[9] X. Sui, J. Yuan, M. Zhou, J. Zhang, H. Yang, W. Yuan, Y. Wei, C. Pan, *Biomacromolecules* **2008**, *9*, 2615–2620.

[10] S. Yagi, N. Kasuya, K. Fukuda, *Polym. J.* **2010**, *42*, 342–348.

[11] Y. Habibi, A.-L. Goffin, N. Schiltz, E. Duquesne, P. Dubois, A. Dufresne, *J. Mater. Chem.* **2008**, *18*, 5002–5010.

[12] Y. Guo, X. Wang, Z. Shen, X. Shu, R. Sun, *Carbohydr. Polym.* **2013**, *92*, 77–83.

[13] C. Schatz, S. Lecommandoux, *Macromol. Rapid Commun.* **2010**, *31*, 1664–1684.

[14] R. F. Borch, M. D. Bernstein, H. D. Durst, *J. Am. Chem. Soc.* **1971**, *93*, 2897–2904.

[15] H. C. Kolb, M. G. Finn, K. B. Sharpless, *Angew. Chem. Int. Ed.* **2001**, *40*, 2004–2021.

[16] S. Dedola, S. A. Nepogodiev, R. A. Field, *Org. Biomol. Chem.* **2007**, *5*, 1006–1017.

[17] V. V Rostovtsev, L. G. Green, V. V Fokin, K. B. Sharpless, *Angew. Chem. Int. Ed.* **2002**, *41*, 2596–2599.

[18] V. D. Bock, H. Hiemstra, J. H. van Maarseveen, *Eur. J. Org. Chem.* **2006**, 51–68.

[19] M. Meldal, C. W. Tornøe, *Chem. Rev.* **2008**, *108*, 2952–3015.

[20] C. E. Hoyle, C. N. Bowman, *Angew. Chem. Int. Ed.* **2010**, *49*, 1540–1573.

[21] A. B. Lowe, *Polymer* **2014**, *55*, 5517–5549.

[22] X. Meng, K. J. Edgar, *Prog. Polym. Sci.* **2015**, ASAP.

[23] Y. Mai, A. Eisenberg, *Chem. Soc. Rev.* **2012**, *41*, 5969–5985.

[24] F. S. Bates, G. H. Fredrickson, *Phys. Today* **1999**, *52*, 32–38.

[25] H. Elbs, G. Krausch, *Polymer* **2004**, *45*, 7935–7942.

[26] E. A. Men'shikov, A. V Bol'shakova, I. V Yaminskii, *Prot. Met. Phys. Chem. Surfaces* **2009**, *45*, 295–299.

[27] H. S. Lee, W. N. Kim, C. M. Burns, *J. Appl. Polym. Sci.* **1997**, *64*, 1301–1308.

[28] L. Xu, F. Qiu, *Polymer* **2014**, *55*, 6795–6802.

[29] J. A. Emerson, D. T. W. Toolan, J. R. Howse, E. M. Furst, T. H. Epps, *Macromolecules*

2013, *46*, 6533–6540.

[30] S. De, S. Malik, A. Ghosh, R. Saha, B. SAHA, *RSC Adv.* **2015**, *5*, 65757–65767.

[31] J. Aguiar, P. Carpena, J. A. Molina-Bolívar, C. Carnero Ruiz, *J. Colloid Interface Sci.* **2003**, *258*, 116–122.

[32] G. Basu Ray, I. Chakraborty, S. P. Moulik, *J. Colloid Interface Sci.* **2006**, *294*, 248–254.

[33] K. Kalyanasundaram, J. K. Thomas, *J. Am. Chem. Soc.* **1977**, *99*, 2039–2044.

[34] W. C. Griffin, *J. Soc. Cosmet. Chem.* **1954**, *5*, 249–256.

[35] W. C. Griffin, *J. Soc. Cosmet. Chem.* **1949**, *1*, 311–326.

[36] L. Dupayage, C. Nouvel, J.-L. Six, *J. Polym. Sci., Part A: Polym. Chem.* **2011**, *49*, 35–46.

[37] Q. Yang, C. He, Y. Xu, B. Liu, Z. Shao, Z. Zhu, Y. Hou, B. Gong, Y.-M. Shen, *Polym. Chem.* **2015**, *6*, 1454–1464.

[38] K. Zhang, A. Geissler, X. Chen, S. Rosenfeldt, Y. Yang, S. Förster, F. Müller-Plathe, *ACS Macro Lett.* **2015**, *4*, 214–219.

[39] H. Kang, W. Liu, B. He, D. Shen, L. Ma, Y. Huang, *Polymer* **2006**, *47*, 7927–7934.

[40] H. Kamitakahara, A. Baba, A. Yoshinaga, R. Suhara, T. Takano, *Cellulose* **2014**, *21*, 3323–3338.

[41] E. Farkas, L. Jánossy, J. Harangi, L. Kandra, A. Lipták, *Carbohydr. Res.* **1997**, *303*, 407–415.

[42] G. Crini, *Chem. Rev.* **2014**, *114*, 10940–10975.

[43] S. de Medeiros Modolon, I. Otsuka, S. Fort, E. Minatti, R. Borsali, S. Halila, *Biomacromolecules* **2012**, *13*, 1129–1135.

[44] C. Gauche, V. Soldi, S. Fort, R. Borsali, S. Halila, *Carbohydr. Polym.* **2013**, *98*, 1272–1280.

[45] M. Chemin, Valorisation Des Xylanes Du Bois : Vers La Synthèse de Copolymères Amphiphiles Bio-Sourcés, Bordeaux, **2014**.

[46] M. Zhou, F. G. Brunetti, E. Martin, S. Becker, I. Doi, R. N. Santoso, M. S. Lam, *Azide-Based Crosslinking Agents*, **2014**, WO2015004563 A1.

[47] S. Bräse, C. Gil, K. Knepper, V. Zimmermann, *Angew. Chemie - Int. Ed.* **2005**, *44*, 5188–5240.

[48] A. L. Logothetis, *J. Am. Chem. Soc.* **1965**, *87*, 749–754.

[49] A. M. Gadalla, *Int. J. Chem. Kinet.* **1984**, *16*, 655–668.

[50] A. Huebner, M. R. Ladisch, G. T. Tsao, *Biotechnol. Bioeng.* **1978**, *20*, 1669–1677.

Chapter VI. General conclusions and perspectives

Table of Contents

VI. 1. General conclusions

The goal of this work was to produce low dispersed cellulose oligomers with an easily accessible production and separation process. The second objective was to synthesise amphiphilic compounds based on these oligomers and to study their self-assembly.

Cellulose oligomers were obtained by acidic hydrolysis. After hydrolysis, the cellulose had a reduced average molar mass and the oligomers were separated by solubilisation in water. The molar mass distribution of the water-soluble and insoluble fractions presented an overlap but no more oligomers could be extracted from the water-insoluble fraction probably because of a poor dispersion. The actual composition of the cellulose oligomers was calculated by HPLC. Cellotriose and cellotetraose were the main components with 19% and 29%, respectively (average over three experiments). Glucose (17%) and cellobiose (16%) were present in smaller amount. DP 7 and above were not detected by HPLC but their presence was confirmed by MALDI and SEC in water as the eluent. DP up to 12 were detected.

The separation method investigated was based on differential solubilisation. Several alcohols were tested and methanol was found to be the most efficient. The methanol-soluble fraction contained 27% of glucose, 27% of cellobiose and 28% of cellotriose whereas the methanol-insoluble fraction was concentrated in higher sizes with 42% of cellotetraose, 36% of cellopentaose. Cellotriose (6%), cellobiose (4%) and glucose (8%) were also present but in really small amounts.

The methanol-insoluble fraction was then used for the formation of amphiphilic compounds. The cellulose oligomers of higher DP and cellobiose for comparison were functionalised at the reducing extremity with an azide group, which was coupled with a stearic acid, alkyne-functionalised, by copper-catalysed azide-alkyne cycloaddition. Stearic acid was chosen as the hydrophobic block for its linearity, bio-based character and large availability. The self-assembly of these compounds was then investigated. The cellobiose based compound aggregated in all the solvents tested. Only DMSO, a good solvent for both blocks, could solubilise it but no self-assembly was induced. For the oligomer based compound, self-assembly in water without aggregation was detected. Their CMC was calculated at around 100 $mg.L^{-1}$ which is a good range compared to similar compounds found commercially. The TEM pictures at 200 $mg.L^{-1}$ showed more or less spherical particles but their shape may have been altered by shrinkage. The average diameter at 200 $mg.L^{-1}$ was

measured by DLS to be 140 nm with a PDI of 0.21. This size distribution hardly changed over 12 days. The particles presented a great homogeneity meaning that the different cellulose oligomers DP were well distributed over the particles. Because of their large sizes in solution, the particles were probably vesicles.

Two new and innovative strategies were also probed to improve the cellulose oligomers separation (**Figure VI-1**).

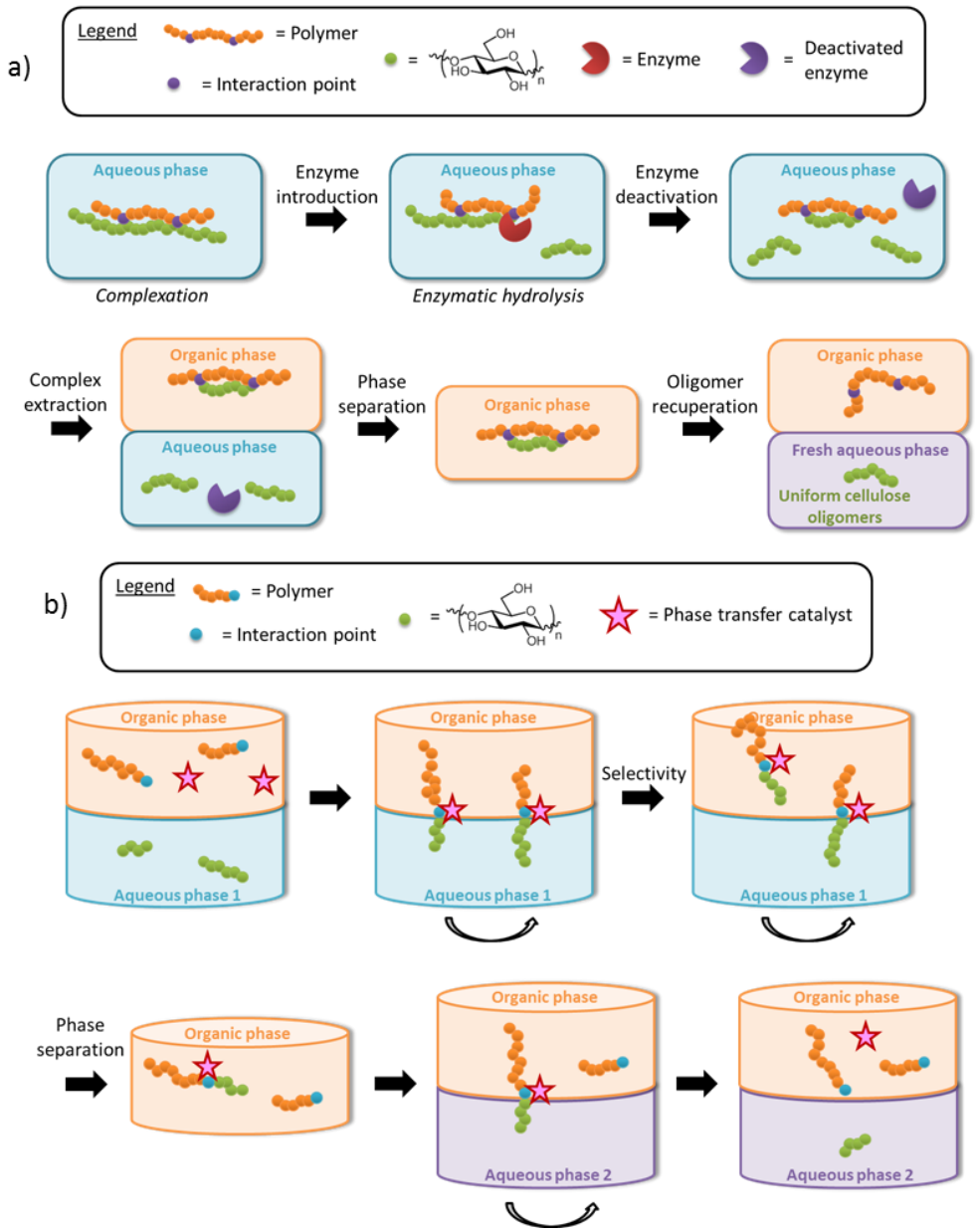

Figure VI-1. Representation of a) the "masking" method and b) the "fishing" method

Boronic acids were chosen to act as interaction points. A preliminary study on models was performed to determine the polymer structure the best suited for each strategy. Phenylboronic acid (PBA) was found to be placed on the α-furanose form of glucose on the

1,2 and 3,5 positions (**Figure VI-2a**). As the 1- and 4-positions are not available along the cellulose backbone, only an interaction at the cellulose oligomer end would be possible in this case. Fortunately, phenylboronic anhydride was able to complex the 2- and 3-positions of the β-methylglucoside (**Figure VI-2b**) allowing a possible complexation along the cellulose backbone.

Other mono-saccharides were also analysed in this complexation study in the view of extending the methods application to other polysaccharides.

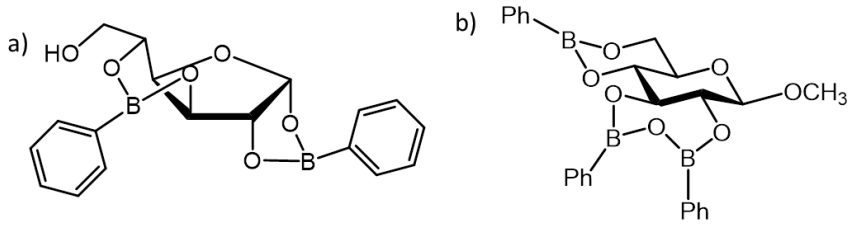

Figure VI-2. Structure of the complex of a) phenylboronic acid on glucose and b) phenylboronic anhydride on β-methylglucoside

As a consequence, a random copolymer of styrene and 4-vinylphenylboronic acid (VBA) under the anhydride form with phenylboronic acid (PBA) (**Figure VI-3a**) was chosen for the "masking" method and a block copolymer of styrene and 4-vinylphenylboronic acid (**Figure VI-3b**) were used for the "fishing" method.

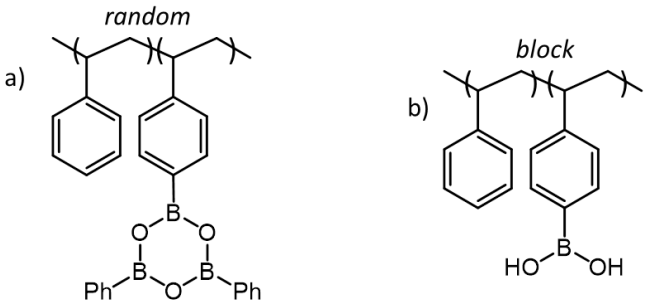

Figure VI-3. Structure of a) a random copolymer of styrene and VBA under the anhydride form with PBA and b) a block copolymer of styrene and VBA

As the boronic anhydride containing polymer was never synthesised before to the best of our knowledge, two different strategies were considered:

- VBA was tried to be polymerised with styrene in an excess of PBA in an hydrophobic solvent that favoured the anhydride form. Unfortunately, no polymer was obtained after several polymerisation attempts because of poor monomer solubility or an inefficient initiator.
- The boronic anhydride was then tried to be formed on an already synthesised random copolymer but again all the attempts failed

Eventually, the trials to synthesise the boronic anhydride containing polymer were dropped.

On the other hand, three block and one random copolymers of styrene and VBA were synthesised and characterised to be used for the "fishing" method. The VBA block had theoretically the same size for the three blocks copolymers, only the styrene block length changed. Nevertheless, it was found that the longer the styrene block, the shorter the VBA block, probably because of a loss of active radicals during the reaction. Moreover, the VBA block was actually a random one as the average number of styrene per chain had increased after the VBA introduction. The random copolymer had the same length and monomer ratio as the smallest block copolymer.

The "fishing" method process and initial conditions were inspired by a previously published method where glucose and cellobiose were extracted from an aqueous phase *via* phenylboronic acid[1,2]. This method was adapted to the requirements involved by the use of cellulose oligomers and boronic acid containing polymers.

The four previously synthesised copolymers were then tested on their capacity to extract cellulose oligomers from an aqueous phase. No oligomers were solubilised in the organic phase without copolymers. The three block copolymers reaped all the oligomers that could be extracted. Unexpectedly, their composition was the same as before the extraction whatever the copolymer used, indicating that no selectivity had occurred. The polymers were seemingly already too long to be selective.

As expected, the random copolymer was not able to extract cellulose oligomers in the organic phase probably because of a network formation trapping the oligomers in the aqueous phase.

VI. 2. Perspectives

VI. 2. A) Cellulose oligomer synthesis

To make a step toward a greener process, the cellulose oligomers could be produced by enzymatic hydrolysis. The cellulose has first to be pre-treated with choline acetate, for instance, as it is a green and enzyme-compatible ionic liquid that reduces cellulose crystallinity and increases accessibility[3]. A multi-stage hydrolysis is then one of the most efficient ways to produce oligomers, according to the literature[4].

VI. 2. B) The “fishing” method

Other parameters need to be investigated to determine whether selectivity of the “fishing” method is achievable. Perhaps, the copolymers used were already too long. The better way to reduce the copolymer molar mass, while keeping a small dispersity, is by anionic polymerisation of styrene and 4-bromostyrene. The bromide groups just have to be subsequently transformed into boronic acid groups.

The selectivity could already be checked by using naphthalene-2-boronic acids as if this compound does not induce selectivity, polymers never will.

The “fishing” method as it is could also be tested on the water-insoluble fraction.

VI. 2. C) The “masking” method

Even though the anhydride containing polymer was not obtained in this work, the “masking” method could be tried with block copolymers that protect cellulose portions by steric hindrance or by possible “wrapping”. The “wrapping” could be increased by changing the styrene block into another one that favours hydrogen bonding for example. Enzymatic hydrolysis in the presence of Block 45/5 and Random 45/5 (see §III. 3. C) ii), p 141) were tried (**Appendix VI.I**, p **Error! Bookmark not defined.**). As the evolution of the HPLC profiles seemed to be the same with or without the presence of polymers, the boronic acid containing polymer did not deactivate the enzymes.

VI. 2. D) Cellulose oligomer separation by solubilisation

The cellulose oligomer separation by solubilisation may also be improved by the use of solvent mixtures. Selective precipitation could also be investigated by solubilising the oligomers in water, gradually adding a non-solvent and recovering the precipitate from time to time.

VI. 2. E) Amphiphilic compounds

It would be interesting to determine the impact of the hydrophobic block nature (presence of an hydroxyl group or an instauration inducing a non-linear fatty acid) or size on the surfactant characteristics. For a same hydrophobic block structure, the longer the length, the smaller the CMC, the smaller the HLB.

The amphiphilic compound synthesis could also be changed to decrease the final copper content. If the stearic acid is first coupled with the azidoethylamine, the final product

is then solubilised in an organic solvent while the copper catalyst stays in the aqueous phase. The reductive amination is then performed on such compound (**Figure VI-4**).

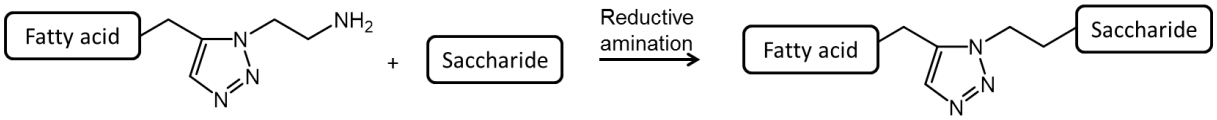

Figure VI-4. Alternative protocol to obtain a final product without copper catalyst

In addition, another type of reaction, as thiolene for example, could be employed to prevent the use of azide and simplify the purification as the reaction is catalysed by UV.

The compounds obtained could also be characterised further for encapsulation efficiency, for instance, to target cosmetic or drug delivery applications.

Appendix

Appendix VI.I: Enzymatic hydrolysis profiles of [Emim]Ac pre-treated cellulose in the presence or not of boronic acid containing polymers

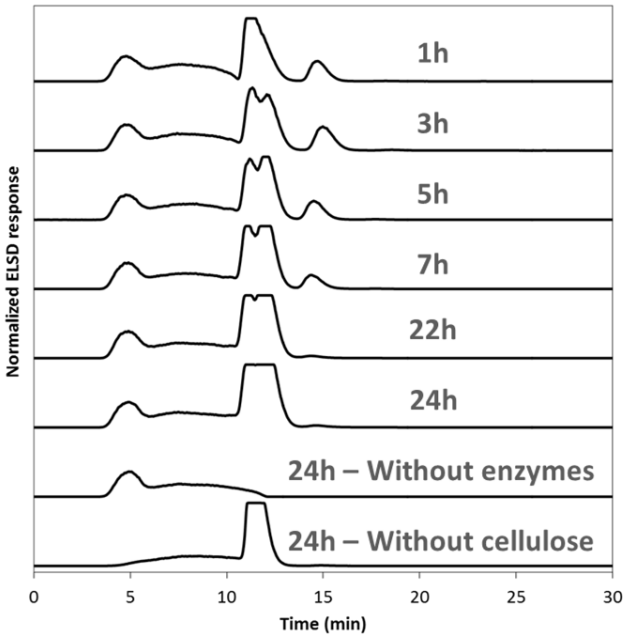

HPLC of samples taken at different time during an [Emim]Ac pre-treated cellulose enzymatic hydrolysis without polymer

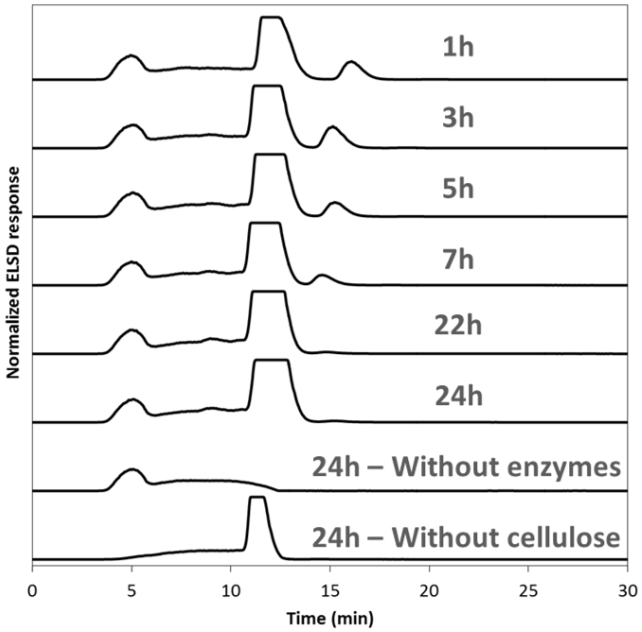

HPLC of samples taken at different time during an [Emim]Ac pre-treated cellulose enzymatic hydrolysis with Block 45/5 (see §III. 3. C) ii), p 141)

Appendix VI.I (following): Enzymatic hydrolysis profiles of [Emim]Ac pre-treated cellulose in the presence or not of boronic acid containing polymers

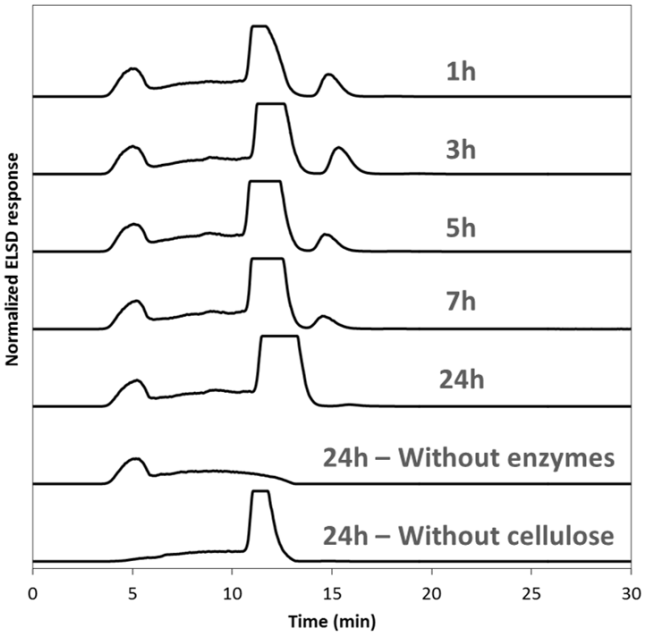

HPLC of samples taken at different time during an [Emim]Ac pre-treated cellulose enzymatic hydrolysis with Random 45/5 (see §III. 3. C) ii), p 141)

References

[1] T. C. R. Brennan, S. Datta, H. W. Blanch, B. A. Simmons, B. M. Holmes, *Bioenergy Res.* **2010**, *3*, 123–133.

[2] T. T. C. Brennan, B. M. Holmes, B. A. Simmons, H. W. Blanch, *Recovery of Sugars from Ionic Liquid Biomass Liquor by Solvent Extraction*, **2010**, WO2011041455 A1.

[3] Q. Zhang, M. Benoit, K. De Oliveira Vigier, J. Barrault, F. Jérôme, *Chem. – A Eur. J.* **2012**, *18*, 1043–1046.

[4] Q. Chu, X. Li, Y. Xu, Z. Wang, J. Huang, S. Yu, Q. Yong, *Process Biochem.* **2014**, *49*, 1217–1222.

Chapter VII. Materials and methods

Table of Contents

VII. 1. Materials and protocols

VII. 1. A) Products and materials

VII. 1. A) i) General

All the solvents used were purchased from **Aldrich** and used as received. Deionized water was obtained from a Millipore Direct 8 system. All the deuterated solvents (DMSO-d_6, $CDCl_3$, D_2O, toluene-d_8, THF-d_8, MeOD) were purchased from **Euriso-top**.

Hydrochloric acid at 37% and sodium hydroxide pellets were purchased from **Aldrich**.

The centrifuge used was an Eppendorf Centrifuge 5804 R.

VII. 1. A) ii) Chapter II

Phenylboronic acid was purchased from **ABCR**. α-methylglucoside was purchased from **Janssen**. β-methylglucoside and NaOD at 40 wt% in D_2O were purchased from **Aldrich**. Glucose was purchased from **Euromedex**. Xylose, mannose, galactose and arabinose were purchased from **Fluka**. Cellobiose was purchased from **Alfa Aeasar**. Phenylboroxole was purchased from **TCI**.

VII. 1. A) iii) Chapter III

4-bromostyrene, 4-vinylphenylboronic acid, tetramethylethylenediamine, anhydrous pinacol, anisole, 1-dodecanethiol, 2-bromo-2-methylpropionic acid and o-tolylboronic acid were purchased from **Alfa Aesar**. Azobisisobutyronitrile (AIBN) and trimethyl borate were purchased from **Acros Organics**. Phenylboronic acid, 4-methylcatechol and potassium phosphate tribasic were purchased from **ABCR**. 4-tert-butylcatechol was purchased from **Fluka**. Styrene, sec-butyllithium at 1.4 M in cyclohexane, n-butyllithium at 1.6 M in hexane, magnesium turnings, triisopropyl borate, carbon disulphide, 1-mercaptopropionic acid, benzyl bromide, sodium sulphide (60 wt%), tetrabutylammonium bromide, benzyl chloride and 1,2,4-trichlorobenzene (SEC flow marker) were purchased from **Aldrich**. 2,2'-azobis(4-methoxy-2.4-dimethyl valeronitrile) (V-70) was kindly supplied by **Wako Pure Chemicals Industries**.

AIBN was recrystallized twice from methanol before use. V-70 was kept at -20°C and used without purification.

The THF used for the Grignard reaction was dried over sodium benzophenone. The styrene used for the anionic polymerisation was dried over calcium hydride. The cyclohexane for the anionic polymerisation was dried over polystyryllithium (obtained from *sec*-butyllithium and styrene). All these solvents were cryo-distilled just before use.

Tetramethylethylenediamine was dried over molecular sieve.

VII. 1. A) iv) Chapter IV

Microcrystalline cellulose, phosphoric acid (85 wt%), hydroxymethylfurfural (for the UV calibration), 1-butyl-3-methylimidazolium chloride ([Bmim]Cl), phenyl isocyanate, acetic anhydride, 1-octanol and Aliquat 336™ were purchased from **Aldrich**. Calcium hydroxide, sodium carbonate and sodium azide were purchased from **Alfa Aesar**. Phosphorus pentoxide was purchased from **Acros Organics**. For the SEC in water and HPLC calibrations, pure cellulose oligomers with a DP from 1 to 7 were purchased from **Elicityl**. For the SEC in chloroform references, glucose pentaacetate was purchased from **Fluka** and cellobiose octaacetate from **Janssen**.

The mechanical stirring for the swelling phase was performed with an IKA® RW 20 digital with five rectangular blades (**Figure VII-1**).

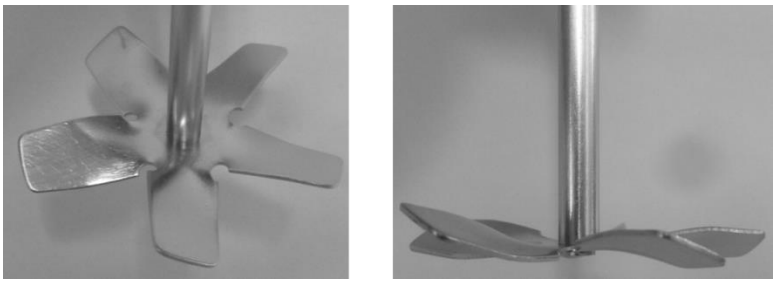

Figure VII-1. Blades used for the swelling phase of the cellulose acidic hydrolysis

VII. 1. A) v) Chapter V

2-bromoethylamine hydrobromide was purchased from **Fluka**. Sodium azide, cellobiose and sodium ascorbate were purchased from **Alfa Aesar**. Acetic acid, stearic acid and pyrene were purchased from **Aldrich**. Sodium cyanoborohydride and potassium carbonate were purchased from **Fisher**. Propargyl chloride was purchased from **TCI**. Copper (II) sulfate pentahydrate was purchased from **Prolabo**. Uranyl acetate (contrast agent for TEM) was purchased from **TAAB**.

The microwave used for the reductive amination was a Milestone Ethos.

VII. 1. A) vi) Chapter VI

Microcrystalline cellulose (batch MKBB9775) and acetic acid were purchased from **Aldrich**. Choline chloride, anion exchange resin Amberlite IRA 400 (OH), sodium azide, citric acid, trisodium citrate dehydrate and sodium acetate were purchased from **Alfa Aesar**. 1-ethyl-3-methyl-imidazolium acetate ([Emim]Ac) and potassium phosphate tribasic were purchased from **ABCR**. The enzymes used (Celluclat 1.5L, batch CCN03138) were purchased from **Novozymes**.

The acetate buffer was prepared by mixing 7.4 mL of acetic acid at 0.2 M, 17.6 mL of sodium acetate at 0.2 M and 80 mL of deionised water. The final pH was 5.0.

The citrate buffer was prepared by solubilising 40 mL of citric acid at 0.1 M and 60 mL of trisodium citrate dehydrate at 0.1 M. The final pH was 4.8.

The enzymatic hydrolysis was performed in an incubator Thermo Scientific Heraeus.

VII. 1. B) Protocols used for Chapter II

VII. 1. B) i) Complexation in DMSO-d_6 or D_2O

To complex phenylboronic acid or phenylboroxole on sugar in DMSO-d_6 or D_2O, the calculated amount of both entities was weighted, in large enough quantity for the balance error to be negligible. Then the solvent was added to reach usual NMR concentration (20-30 $mg.mL^{-1}$). If time evolution was studied, the solvent introduction was the starting point. After solubilisation, 0.5 mL of the solution was introduced in an NMR tube.

In **Figure II-39h** and **i** (p 99)**,** the cellobiose and phenylboronic acid in solution in DMSO-d_6 were heated in a vial at 80°C in an oil bath for the corresponding amount of time before being introduced in the NMR tube.

VII. 1. B) ii) Complexation in toluene

To complex phenylboronic acid on α-methylglucoside in toluene, the protocol found in the literature[1] was adapted as follow.

Molecular sieve was activated in a round bottom flask before adding phenylboronic acid (0.40 g, 3.3 mmol) and 10 mL of toluene. The solution was heated at 100°C for 30 minutes to form boronic anhydrides. Then α-methylglucoside (0.22 g, 1.1 mmol) was added and the solution was kept at 100°C for 5h30. The solvent was then evaporated to obtain the aimed complex.

VII. 1. B) iii) Complexation in chloroform

Phenylboronic acid and the studied sugar in the determined ratio were dispersed in chloroform overnight. Then the solution was filtrated to remove the un-solubilised sugar and the solvent was left to evaporate. Once the complex was dried, it was solubilised in DMSO-d_6 for analysis.

VII. 1. C) Protocols used for Chapter III

VII. 1. C) i) 4-vinylphenylboronic acid (VBA) synthesis

The VBA was synthesised by the following protocol[2,3] for the first trials with anionic polymerisation. For the RAFT, commercial VBA was used.

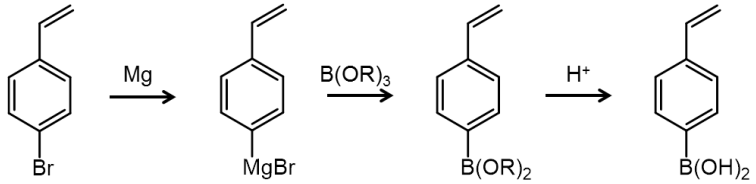

Dried magnesium (1.06 g, 43.5 mmol) and freshly cryo-distilled THF (30 mL) were introduced into a dry three necked round bottom flask under inert atmosphere. The solution was heated to 40°C before adding a few drops of 4-bromostyrene. Once the solution turned green indicating that the Grignard reagent had been formed, the remaining 4-bromostyrene (4 mL, 30.6 mmol) were slowly introduced to the mixture. After the complete introduction, the temperature was dropped to -80°C with a mixture of acetone and dry ice. Trimethyl borate (8 mL, 71.8 mmol) solubilised into 20 mL of dry THF was slowly introduced. The low temperature prevented the formation of the by-products diarylborane and triarylborane[4]. After complete introduction, the solution was allowed to warm up to room temperature overnight. 100 mL of hydrochloric acid at 4 M was added to the solution to hydrolyse the borate. The solution was then extracted twice with 100 mL of diethyl ether. The organic phases were combined and concentrated and the product was obtained by recrystallization from water. 2.11 g of white crystals were obtained (yield 46.7%).

^{1}H NMR (δ ppm, DMSO-d_6): 5.30 (1H, d, C*H*$_2$=CH–Ph), 5.90 (1H, d, C*H*$_2$=CH–Ph), 5.90 (1H, CH$_2$=C*H*–Ph), 7.43 (2H, d, *m*-Ph–B(OH)$_2$), 7.77 (2H, d, *o*-Ph–B(OH)$_2$), 8.01 (2H, s, Ph–B(O*H*)$_2$).

VII. 1. C) ii) VBA protection by pinacol

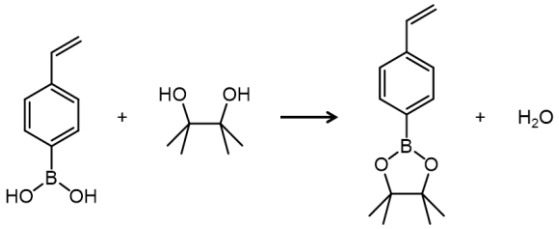

VBA and pinacol were introduced in a dry round bottom flask containing activated molecular sieve and dichloromethane. The solution was stirred overnight at room temperature and then filtrated over celite to remove the molecular sieve as well as most of the un-reacted pinacol. A colourless liquid was obtained after drying (yield 72.7%).

^{1}H NMR (δ ppm, $CDCl_3$): 1.26 (12H, 4 CH_3), 5.21 (1H, C*H*$_2$=CH–Ph), 5.75 (1H, C*H*$_2$=CH–Ph), 6.65 (1H, CH$_2$=C*H*–Ph), 7.33 (2H, d, *m*-Ph–BPin), 7.70 (2H, d, *o*-Ph–BPin).

VII. 1. C) iii) Synthesis of polystyrene by anionic polymerisation

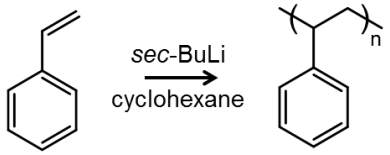

The values given here were used for the synthesis of a polystyrene with a DP 10 (M_{th} = 1 050 g.mol^{-1}). Freshly cryo-distilled cyclohexane (50 mL) was introduced into a dry round bottom flask. The "zero point" was reached by introducing one drop of styrene and as much *sec*-butyllithium (at 1.4 M in cyclohexane) as needed for a yellow colour to start appearing. Once this point was reached, the temperature was decreased to -10°C before adding the remaining *sec*-butyllithium (total volume: 3.4 mL). The remaining styrene (total volume: 5.5 mL) was also added dropwise. The initiation was left to occur for 20 minutes at -10°C then the temperature was increased to 40°C for 1h for the propagation step. After that, the polymerisation was deactivated by the addition of methanol in the amount necessary for the solution to become colourless. The polymer was precipitated in cold methanol and dried. 4.61 g of a white solid were obtained (yield: 87%).

The polymerisation was confirmed by proton NMR in $CDCl_3$ with a typical double hill in the range of 6.0 to 7.5 ppm.

SEC in THF (polystyrene calibration): M_n = 1 030 g.mol^{-1}, M_w = 1 120 g.mol^{-1}, $Đ$ = 1.08.

For DP 50 (M_{th} = 5 100 g.mol^{-1}), 0.7 mL of *sec*-butyllithium at 1.4 M in cyclohexane were used for the same amount of styrene (yield: 92%).

SEC in THF (polystyrene calibration): M_n = 4 380 g.mol^{-1}, M_w = 4 560 g.mol^{-1}, $Đ$ = 1.04

VII. 1. C) iv) Introduction of boronic acid moieties on a polystyrene

This protocol was based on published literature[5] and the values given here were used to obtain 50% functionalisation.

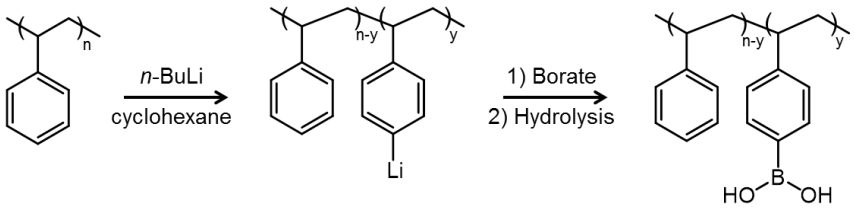

The previously synthesised polystyrene with a DP 10 (2 g) was solubilised in freshly cryo-distilled cyclohexane (20 mL). *n*-butyllithium (7.5 mL) and the co-initiator tetramethylethylenediamine (1.3 mL) were added to the solution before heating at 65°C for 3h. After that, the solvent was removed under vacuum and replaced by freshly cryo-distilled THF (20 mL). The boration occured with the introduction of triisopropyl borate (2.2 mL) at room temperature overnight. A solution containing 67 vol% of dioxane, 25 vol% of water and 8 vol% of commercial hydrochloric acid at 37% (12 mL) was used to hydrolyse the borate at 60°C for 2h. The solvents were then tried to be removed by evaporation and 4.09 g of polymer were obtained.

With the DP 50, 6.0 mL of *n*-butyllithium and 2.8 mL of tetramethylethylenediamine were used for the same amount of polystyrene. The rest of the quantities were the same and 4.04 g of polymer was obtained.

The yield for both of these reactions seemed to be over a 100% because some residual solvent was probably still present. It could not be removed as these polymers were insoluble in all the solvents tested.

VII. 1. C) v) Polymer protection by pinacol

The same protocol used with VBA was employed, see §VII. 1. C) ii).

VII. 1. C) vi) RAFT chain transfer agent synthesis

DMP (2-(dodecylthiocarbonothioylthio)-2-methylpropionic acid)

The synthesis of DMP was adapted from the literature[6] as follow.

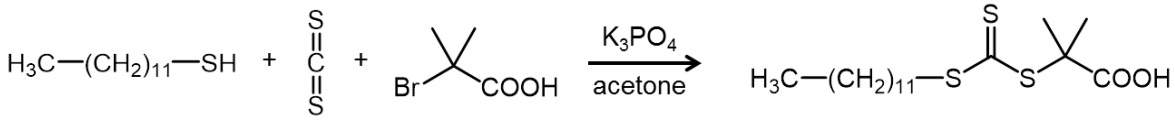

In a suspension of K_3PO_4 (3.87 g, 18.2 mmol) in 60 mL of acetone was added 1-dodecanethiol (4.4 mL, 18.4 mmol). The solution was stirred at room temperature for 10 minutes before adding carbon disulphide (3.0 mL, 49.6 mmol). The solution turned yellow and was stirred like this for 10 additional minutes. To finish, 2-bromo-2-methylpropionic acid (2.31 g, 13.8 mmol) was added. The solution was stirred at room temperature overnight (≈ 16h). A KBr precipitate was observed. Then the reaction was quenched by the addition of 280 mL of hydrochloric acid at 1 M, the acetone was evaporated and the product extracted twice with 300 mL of dichloromethane even though the aqueous phase had lost its colour after the first extraction. The organic phases were combined, concentrated to reach around 150 mL and washed with 150 mL of water and 150 mL of brine. It was then dried over $MgSO_4$ before being evaporated. The oil obtained was dispersed in heptane and left at -20°C for few hours for re-crystallisation. 3.73 g of a yellow solid was obtained (yield: 74.0%).

^{1}H NMR (δ ppm, $CDCl_3$): 0.81 (3H, S–CH_2–$(CH_2)_{10}$–CH_3), 1.32-1.19 (20H, S–CH_2–$(CH_2)_{10}$–CH_3), 1.66 (6H, S–C(CH_3)$_2$–COOH), 3.21 (2H, S–CH_2–$(CH_2)_{10}$–CH_3).

^{13}C NMR (δ ppm, $CDCl_3$): 14.3 (S–CH_2–$(CH_2)_{10}$–CH_3), 22.8 (S–CH_2–$(CH_2)_{10}$–CH_3), 25.4 (S–C(CH_3)$_2$–COOH), 28.0, 29.1, 29.3, 29.5, 29.6, 29.7, 29.8, 32.1 (S–CH_2–$(CH_2)_{10}$–CH_3), 37.2 (S–CH_2–$(CH_2)_{10}$–CH_3), 55.7 (S–C(CH_3)$_2$–COOH), 178.1 (S–C(CH_3)$_2$–COOH).

BSPA (3-(benzylthiocarbonothioylthio)propanoic acid)

The synthesis of BSPA was adapted from the literature[6] as follow.

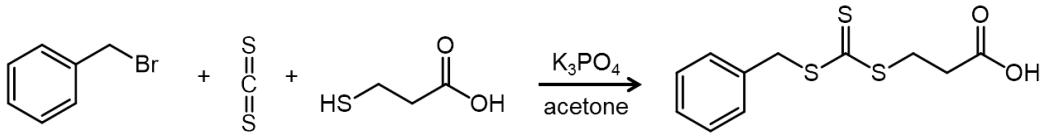

In a suspension of K_3PO_4 (3.92 g, 18.5 mmol) in 40 mL of acetone was added 1-mercapto propionic acid (1.6 mL, 18.4 mmol). The solution was stirred at room temperature for 10 minutes before adding carbon disulphide (3.4 mL, 56.3 mmol). The solution turned yellow and was stirred for 10 additional minutes. To finish benzyl bromide (2.2 mL, 18.5 mmol) was added. A KBr precipitate was observed. The solution was stirred at room temperature for 20 minutes before evaporating the solvent. The product was dispersed in 195 mL of brine and extracted twice with 200 mL of dichloromethane. The organic phases were combined and washed with brine before being concentrated. 5.04 g of a yellow solid were obtained (yield > 99%).

^{1}H NMR (δ ppm, $CDCl_3$): 2.76 (2H, S–CH_2–CH_2–COOH), 3.55 (2H, S–CH_2–CH_2–COOH), 4.54 (2H, Ph–CH_2–S), 7.15-7.32 (5H, *Ph*–CH_2–S).

^{13}C NMR (δ ppm, $CDCl_3$): 31.1 (S–CH_2–*C*H_2–COOH), 33.1 (S–*C*H_2–CH_2–COOH), 41.7 (Ph–*C*H_2–S), 128.0, 128.9, 129.4, 134.9 (*Ph*–CH_2–S), 177.4 (S–CH_2–CH_2–*C*OOH).

DBTTC (Dibenzyl trithiocarbonate)

The synthesis of DBTTC was adapted from the literature[7] as follow.

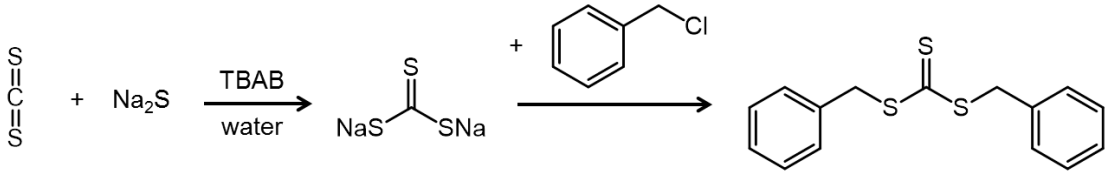

Sodium trithiocarbonate was first obtained by reacting sodium sulfide (60 wt%, 1.74 g, 22.3 mmol) with carbon disulfide (1.5 mL, 24.8 mmol) at room temperature for 2h in 3.6 mL of water containing tetrabutylammonium bromide (0.2 g, 0.7 mmol).

In a second step, benzyl chloride (4.9 mL, 42.6 mmol) was added dropwise to the solution for 10 min. The reaction was performed at room temperature for 3h, followed by a period of 1h at 70°C. Once the reaction medium was back to room temperature, an additional charge of tetrabutylammonium bromide (0.21 g, 0.66 mmol) dissolved in 0.4 mL of water was added. The solution was then stirred overnight (≈15h) to complete the reaction. After separation of the organic (orange) and aqueous (yellow) phases, DBTTC was obtained by extraction in chloroform. 5.01 g of an orange oil was obtained (yield: 77.5%).

^{1}H NMR (δ ppm, $CDCl_3$): 4.64-4.70 (4H, S–CH_2–Ph x2), 7.33-7.46 (10H, S–CH_2–*Ph* x2).

^{13}C NMR (δ ppm, $CDCl_3$): 41.6 (S–*C*H_2–Ph x2), 127.8, 128.7, 129.3, 134.9 (S–CH_2–*Ph* x2).

VII. 1. C) vii) RAFT polymerisation: general procedure

The required amount of monomer(s), initiator, CTA and solvent were introduced into a Schlenk. The oxygen was removed from the reaction media by three vacuum/argon cycles. The temperature was then increased to the required value for the required amount of time. Then the polymer was precipitated in methanol and dried.

Before the SEC analysis of the PS-PVBA copolymers, the polymer was further dried overnight at 80°C in an oven.

VII. 1. C) viii) Synthesis of the random copolymer PS-boronic anhydride

The required amount of polymer and o-tolylboronic acid were solubilised in ethyl acetate. The solution was then heated overnight in an oven at 80°C for the solvent to be removed and to favour the anhydride formation.

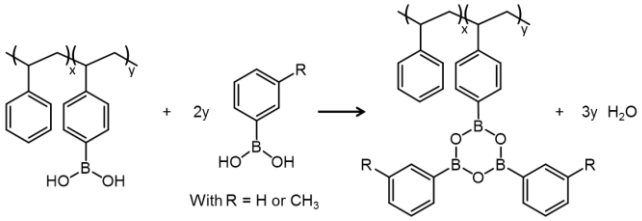

VII. 1. D) **Protocols used for Chapter IV**

VII. 1. D) i) Acidic hydrolysis of cellulose

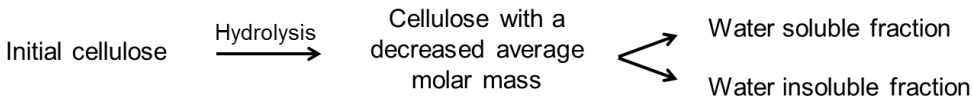

As previously described[8] and if not specified otherwise, cellulose (5 g) was added into phosphoric acid at 85 wt% (60 mL) under mechanical blade stirring at 250 rpm. The cellulose was left to swell at room temperature for 30 minutes. Before starting the hydrolysis, oxygen was removed by three vacuum/argon cycles and then the solution was heated at 50°C for 20h. The solution obtained was dark brown and 0.1 mL of the solution was extracted to measure the HMF quantity. The cellulose was then precipitated in 600 mL of THF and filtered off. To separate the water-soluble fraction, the obtained brownish solid was introduced into 50 mL of deionized water under stirring for 1h. The mixture was then centrifuged; the remaining solid obtained was the water-insoluble fraction (WIF). The solution containing the water-soluble fraction (oligomers) was neutralised with aqueous calcium hydroxide at 0.1 $g.mL^{-1}$ and then filtered to remove the formed precipitate. The solution was concentrated by evaporation and both fractions were dried over phosphorus pentoxide in a desiccator under vacuum until no mass decrease was detected.

The percentages of water-soluble or insoluble fractions were calculated as follow.

$$\tau_{olig} = \frac{Mass\ of\ the\ dried\ oligomers}{Mass\ of\ cellulose\ hydrolysed} \qquad \tau_{WIF} = \frac{Mass\ of\ the\ dried\ WIF}{Mass\ of\ cellulose\ hydrolysed}$$

VII. 1. D) ii) Cellulose carbanilate

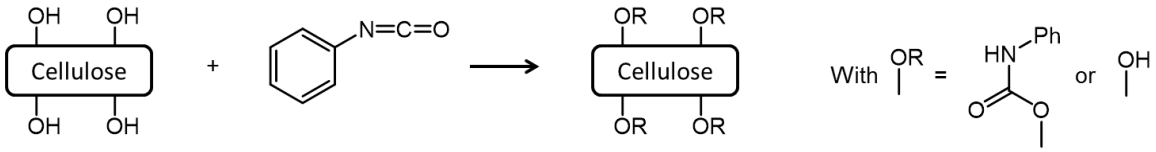

Based on a previously published procedure[9], cellulose (0.5 g) was solubilised in [Bmim]Cl (4.5 g) at 80°C. Once the solution was homogenised, phenyl isocyanate (3.5 mL) was added to the solution and a small emission of CO_2 was observed (reaction with water that produces CO_2 and phenyl amine, the water came from the hygroscopic character of [Bmim]Cl). The solution was left to react for 2h at 80°C then 2 mL of methanol was added to quench the reaction. The product was then precipitated in methanol and dried to obtain 0.9 g of a white solid.

The reaction was achieved when the final product was THF-soluble. The yield was not calculated as the reaction with methanol produced a known by-product, the methyl phenyl carbamate, which could not be removed from the carbanilated cellulose.

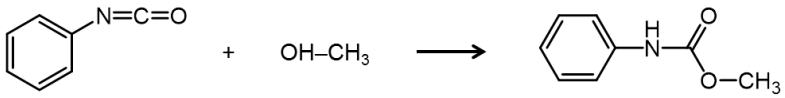

^{1}H NMR (δ ppm, $CDCl_3$): 3.78 (3H, –C(O)–O–C*H*$_3$), 6.61 (N*H*), 7.07 (1H, *p-Ph*), 7.31 (2H, *m-Ph*), 7.37 (2H, *o-Ph*).

VII. 1. D) iii) Cellulose acetate

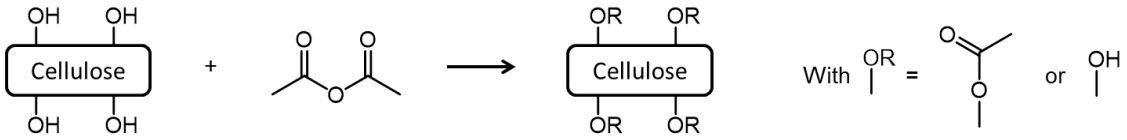

Cellulose (0.2 g) was solubilised in [Bmim]Cl (2 g) at 90°C. After solubilisation, the temperature was decreased to 80°C and acetic anhydride (2 mL) was added to the solution. The reaction occurred at 80°C for 4h. The cellulose acetate was then precipitated in 50 mL of water and dried over phosphorus pentoxide in a desiccator under vacuum until no mass decrease was detected.

For all the functionalised samples, the substitution degree (DS) was approximated to 2.8-3.0 as they were entirely soluble in chloroform after acetylation[10].

VII. 1. D) iv) "Fishing" method

If not stated otherwise, the polymer (2 g) was solubilised in toluene (4.2 mL) containing octanol (0.75 mL) and Aliquat 336™ (0.06 mL). Separately, cellulose oligomers (0.5 g) were solubilised in 5 mL of deionized water. The pH was adjusted to 9 with the

addition of around 250 µL of Na_2CO_3 at 1 M and 0.08 mL of sodium azide at 2 wt% was added to prevent microbial contamination. Both of the solutions were then introduced into a 50 mL round bottom flask and stirred at 1 000 rpm for 4h. The stirring was stopped, the solution was introduced in a narrow vial and left to decant. The blurry organic phase was retrieved with a syringe away from the interface and introduced in a new 50 mL round bottom flask containing 5 mL of HCl at 1 mM (pH 3). Both solutions were stirred at 400 rpm for 30 minutes and decanted in less than 10 minutes. The aqueous phase was retrieved, neutralised with NaOH at 0.1 M and 50 µL of sodium azide at 2 wt% was added. The solution was then analysed by HPLC.

VII. 1. D) v) Separation by solubilisation

Unless stated otherwise, the water soluble oligomers were introduced in methanol (MeOH) at 20 $g.L^{-1}$ and stirred for 24h at room temperature. Then the soluble and insoluble fractions were separated by centrifugation, the solvent was evaporated and the samples were finished to dry over phosphorus pentoxide in a desiccator under vacuum until no mass decrease was detected.

The percentages of MeOH-soluble or insoluble fractions were calculated as follow:

$$\tau_{MeOH-sol} = \frac{Mass\ of\ the\ dried\ MeOH-soluble\ fraction}{Mass\ of\ initial\ cellulose\ oligomers}$$

$$\tau_{MeOH-insol} = \frac{Mass\ of\ the\ dried\ MeOH-insoluble\ fraction}{Mass\ of\ initial\ cellulose\ oligomers}$$

VII. 1. E) **Protocols used for Chapter V**

VII. 1. E) i) Azido-ethylamine synthesis

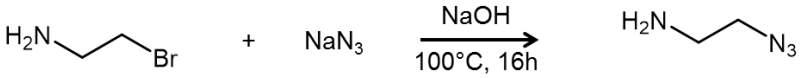

Based on a previously published procedure[11], 2-bromoethylamine hydrobromide (10.2 g, 50 mmol) was dissolved in 40 mL of water. Separately, sodium azide (9.75 g, 150 mmol, 3 eq) was dissolved in 20 mL of water. Both homogeneous solutions were then mixed and stirred under reflux for 16h. The temperature was then reduced and kept below 5°C with an ice bath. Sodium hydroxide (12 g) was added to the solution and left to react for several minutes. The product was extracted twice with 100 mL of diethyl ether, a yellowish oil was obtained (yield: 82.1%).

^{1}H NMR (δ ppm, $CDCl_3$): 1.17 (NH_2), 2.81 (2H, NH_2–CH_2), 3.31 (2H, CH_2–N_3) [2-bromoethylamine hydrobromide is not soluble in $CDCl_3$].

VII. 1. E) ii) Azide group introduction

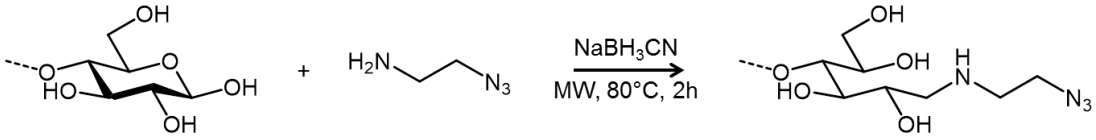

Based on a previously published procedure[12], cellobiose (1.0 g, 2.9 mmol) was dissolved in 30 mL of distilled water/methanol 1/1 v/v and acidified to pH 5-6 using acetic acid at 0.2 M. Azido-ethylamine (0.50 g, 5.8 mmol, 2 eq) and sodium cyanoborohydride (0.37 g, 5.8 mmol, 2 eq) were added to the mixture and the solution was heated at 40°C under stirring until complete solubilisation. The reaction took place in a microwave (MW) oven (560 W) at 80°C for 2h. The solution was precipitated in 200 mL of isopropanol and the solid was separated by centrifugation at 8000 rpm for 10 min at 4°C. The residual isopropanol was eliminated by dissolving again the product in water. After drying, a white powder was obtained (yield: 70.8%, conversion ^{1}H NMR: 100%). See Appendix V.I (p 197) for the characterisation.

The same protocol was used for water-soluble/methanol-insoluble cellulose oligomers with 0.75 g in 24 mL water/methanol 1/1 v/v, 0.52 g of azido-ethylamine and 0.28 g of sodium cyanoborohydride (yield: 87%, conversion ^{1}H NMR: 100%). See §V. 2. A), (p 186) for the characterisation.

VII. 1. E) iii) Stearic alkyne synthesis

The stearic alkyne synthesis was adapted from the literature[13] as follow.

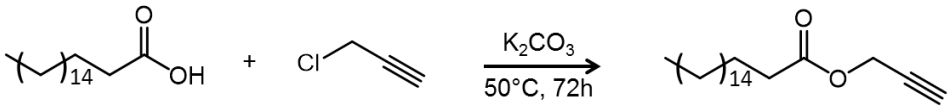

Stearic acid (3.6 g, 13 mmol), propargyl chloride (2 mL, 27 mmol, 2 eq) and potassium carbonate (4 g, 29 mmol) were dissolved in 40 mL of DMF. The reaction took place at 50°C for 72h. The product was extracted with 200 mL of ethyl acetate and the organic phase was washed twice with a 1 M of HCl (200 mL), brine (200 mL) and aqueous $NaHCO_3$ (200 mL). After drying, a white powder was obtained (yield: 98.5%, conversion: 95.5%).

^{1}H NMR (δ ppm, $CDCl_3$): 0.81 (3H, $(CH_2)_{16}$–C*H*$_3$), 1.18 (28H, CH_2–CH_2–(C*H*$_2$)$_{14}$–CH_3), 1.57 (2H, CH_2–C*H*$_2$–$(CH_2)_{14}$–CH_3), 2.28 (2H, C*H*$_2$–CH_2–$(CH_2)_{14}$–CH_3), 2.39 (1H, C*H*≡C–CH_2), 4.61 (2H, CH≡C–C*H*$_2$).

VII. 1. E) iv) Azide-alkyne coupling reaction

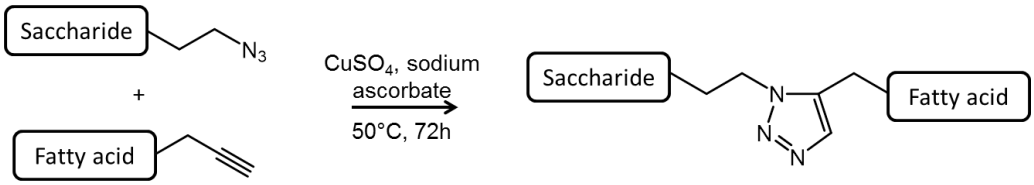

Cellobiose-azide (0.51 g, 1.2 mmol) and stearic alkyne (0.39 g, 1.2 mmol, 1 eq) were dissolved completely in 18 mL of DMSO. Copper (II) sulphate pentahydrate (0.31 g, 1.2 mmol, 1 eq) and sodium ascorbate (0.48 g, 2.4 mmol, 2 eq) were also added and the coupling reaction took place at 50°C for 72h. The solution was then precipitated in 250 mL of isopropanol. The solid obtained was separated by centrifugation at 8000 rpm for 10 min and washed several times with water. After solvent evaporation, the product was dried over P_2O_5 for 72h (1.37 g of product obtained, yield not calculated due to residual catalyst and solvent).

The product formation was confirmed by the disappearance of the azide peak in FT-IR and the appearance of the triazole signal in ^{1}H NMR in DMSO-d_6 (8.5 - 7.5 ppm).

The same protocol was used for water-soluble/methanol-insoluble cellulose oligomers azide with 0.40 g of the corresponding azide, 0.32 g of stearic alkyne in 15 mL of DMSO with 0.24 g of $CuSO_4 \cdot 5H_2O$ and 0.38 g of sodium ascorbate. 1.22 g of product obtained (yield not calculated due to residual catalyst and solvent).

VII. 1. F) Protocols investigated for Chapter VI

VII. 1. F) i) Choline acetate

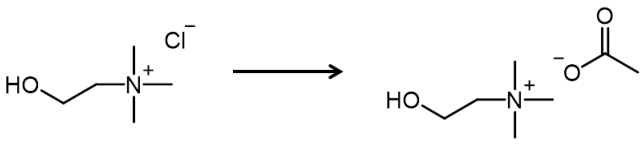

Choline chloride was solubilised in water and flushed through an anion exchange resin (Amberlite IRA 400 (OH)) to form the choline hydroxide. The pH of the solution was reduced with acetic acid until pH 4.9 where a pH plateau was detected. To finish, the water was evaporated.

^{1}H NMR (δ ppm, D_2O): 1.96 (3H, C*H*$_3$-acetate), 3.21 (9H, C*H*$_3$-choline), 3.52 (2H, N-C*H*$_2$-CH$_2$-OH), 4.06 (2H, N-CH$_2$-C*H*$_2$-OH).

VII. 1. F) ii) Cellulose pre-treatment with [Emim]Ac

Cellulose (0.64 g) was introduced into [Emim]Ac (6.4 g) and heated at 120°C for 2h. The solution became red. The temperature was decreased to 70°C and 25 mL of a solution at 40 wt% of potassium phosphate tribasic was introduced. The precipitated cellulose was

filtrated and washed several times with acetate buffer until the coloration had disappeared. The cellulose morphology change was visible with a naked eye (**Figure VII-2**).

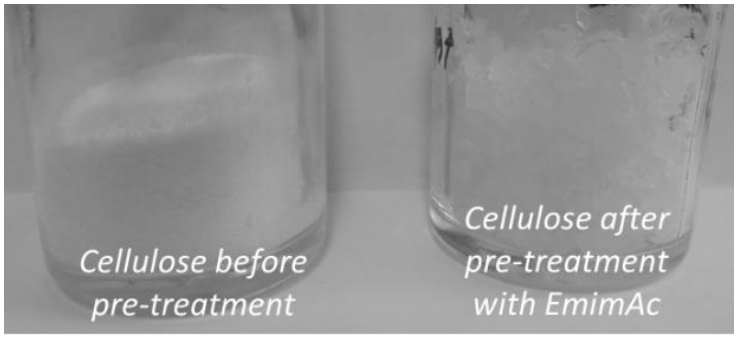

Figure VII-2. Comparison of cellulose after and before pre-treatment with [Emim]Ac

VII. 1. F) iii) Cellulose enzymatic hydrolysis

The protocol was based on the corresponding Laboratory Analytical Procedure[14]. As kinetics were performed, it was chosen to prepare as many vials as points needed in order to not disturb the reaction medium by taking aliquot. In each of them was introduced [Emim]Ac pre-treated cellulose (0.3 g), citrate buffer (5 mL), a solution at 2 wt% of sodium azide (50 µL), deionized water (5 mL) and, if needed, polymer (0.2 g). The solutions are heated at 50°C before the enzymes introduction (50 µL) and kept at this temperature. At chosen times, a vial was removed, introduced in water at 100°C to deactivate the enzymes and centrifuged at 4 000 rpm for 10 minutes. The supernatant was then analysed by HPLC.

VII. 2. Characterisation

VII. 2. A) **Spectroscopy**

VII. 2. A) i) Nuclear magnetic resonance (NMR)

The NMR analyses were performed on a Bruker Avance I NMR spectrometer operating at 400.2 MHz for ^{1}H and 100.6 MHz for ^{13}C. If not stated otherwise, the parameters used for each analysis is listed in **Table VII-1**. The coupling constants were calculated based on JRES experiments displaying a 2D spectra of ^{1}H *versus* the multiplicity.

Table VII-1. Parameters used for several NMR analyses

Analysis	Bruker topspin software program	Number of scans
^{1}H NMR	*Proton*	16
^{13}C NMR	*Carbon1024*	1024
COSY	*COSYGPSWZG*	8
HSQC	*HSQCGPSWZG*	8
JMOD	*C13APT*	512

Around 8 mg of samples were solubilised in 0.4 mL of deuterated solvents. The solvent peak was used as reference to determine the chemical shifts (**Table VII-2**).

Table VII-2. Peaks of reference for several deuterated solvents[15]

Deuterated solvent	^{1}H δ (ppm)	^{13}C δ (ppm)
DMSO-d_6	2.50 (centre)	39.52 (centre)
D_2O	4.79	-
$CDCl_3$	TMS at 0	77.16 (centre)
THF-d_8	3.58 and 1.72	-

All DOSY (Diffusion Ordered Spectroscopy)[16,17] measurements were performed at 298K on a Bruker Avance III HD 400 spectrometer operating at 400.33 MHz and equipped with a 5 mm Bruker multinuclear z-gradient direct cryoprobe-head capable of producing gradients in the z direction with strength 53.5 G.cm^{-1}. For each sample, 2 mg was dissolved in 0.4 ml of deuterated solvent for internal lock and spinning (only when $CDCl_3$ is used as the solvent) was used to minimise convection effects. The DOSY spectra were acquired with the *ledbpgp2s* pulse program from Bruker topspin software. The duration of the pulse gradients and the diffusion time were adjusted in order to obtain full attenuation of the signals at 95 % of maximum gradient strength (**Table VII-3**). The gradients strength was linearly incremented in TD steps (**Table VII-3**) from 5% to 95% of the maximum gradient strength. The data were processed using 8192 points in the F2 dimension and 128 points in the F1 dimension with the Bruker topspin software. Field gradient calibration was accomplished at 25°C using the self-diffusion coefficient of H_2O+D_2O at 19.0 x 10^{-10} m^2.s^{-1} [18,19].

Table VII-3. Coefficient used for the DOSY analyses

	Duration of the gradient pulses (µs)	Diffusion time (ms)	TD	Delay between echoes (s)
Chapter II	2 000	150	32	3
Chapter III	1 200	100	16	3
Chapter V	1 800	100	16	3

VII. 2. A) ii) Ultraviolet (UV) spectroscopy

HMF concentration was estimated by measuring the absorbance at 286 nm (**Figure VII-3a**) with an UV spectrometer (model Lambda 18, Perkin Elmer). A calibration curve was set up using HMF solutions of concentrations going from 0.098 to 0.0049 mmol.L^{-1} (**Figure VII-3b**).

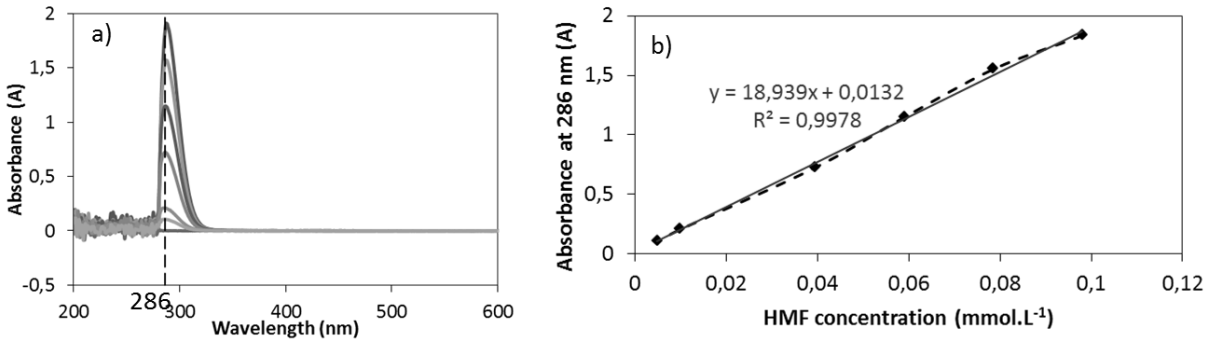

Figure VII-3. a) UV spectra and b) calibration curve used to determine the HMF concentration

To determine the concentration of HMF in solution after the cellulose acidic hydrolysis, 0.1 mL of solution was taken right after the reaction and diluted 40 times with distilled water to reach a concentration within the calibration range. The solution obtained was placed in a 3 mL quartz cell for the spectrometric analysis.

VII. 2. A) iii) Fourier transformation infra-red (FT-IR) spectroscopy

The FT-IR spectra were recorded on a Nicolet iS10 (Thermo Scientific) system. The diamond Smart Orbit went from 30 000 to 200 cm^{-1}. The spectra were recorded with 16 scans in transmission.

VII. 2. A) iv) Matrix-assisted laser desorption/ionisation (MALDI)

MALDI analyses were performed in the CESAMO (ISM, Bordeaux University), on a Voyager mass spectrometer (Applied Biosystems). The instrument was equipped with a pulsed N_2 laser (337 nm) and a time-delayed extracted ion source. Spectra were recorded in the positive-ion mode using the reflectron and with an accelerating voltage of 20 kV. Products and matrix were dissolved in water. The matrix 2,5-dihydroxybenzoic acid (Fluka

Chemika, >98.5%) solution was prepared at 10 $g.L^{-1}$. The solutions were combined in a 10:1 volume ratio of matrix to product. 1–2 µL of the obtained solution was deposited onto the product target and vacuum-dried.

VII. 2. B) **Chromatography**

VII. 2. B) i) Size exclusion chromatography (SEC)

With THF as the eluent

The apparatus (PL-GPC 50, Polymer laboratories – Varian) was equipped with four columns TSK gel HXL-L (guard column, 6.0 mm ID x 4.0 cm L) G4000HXL (7.8 mm ID x 30.0 cm L) G3000HXL (7.8 mm ID x 30.0 cm L) G2000HXL (7.8 mm ID x 30.0 cm L) from Tosoh Bioscience as well as an UV (K-2501, Knauer) and a RI detector included in the apparatus (polystyrene calibration). The eluent flow was fixed at 1 $mL.min^{-1}$.

The samples were solubilised at around 3-5 $g.L^{-1}$ in THF containing 0.2 vol% of 1,2,4-trichlorobenzene as a flow marker. Only the UV data were used but the RI and UV spectra were similar.

With chloroform as the eluent

The molar mass of the acetylated cellulose was determined by SEC in chloroform (Viscotek TDA Model 305 from Malvern Instruments) using two columns PLgel 5µm MIXED-C 300 x 7.5 mm with a flow rate of 1 $mL.min^{-1}$. The molar masses presented were calculated using several detectors included in the apparatus as RI (polystyrene calibration) and viscosity (universal calibration).

The samples were solubilised in chloroform containing 1,2,4-trichlorobenzene as the flow marker at a concentration accurately measured varying from 3 to 5 $mg.mL^{-1}$.

With water as the eluent

The apparatus (Jasco PU-980) was equipped with two TSK gel columns G3000PW G2000PW with a RI detector (Wyatt Optilab Rex). The columns were calibrated using cellulose oligomers standards. The eluent was an aqueous buffer at pH 7 containing 0.2 M of sodium nitrate and 0.01 M of disodium phosphate with 0.03% of sodium azide to prevent microbial contamination. The eluent low rate was 0.5 $mL.min^{-1}$.

The samples were dissolved in the eluent at a concentration of 6 $g.L^{-1}$.

Based on the SEC of cellulose oligomers references, **Figure VII-4** was used as the calibration curve to obtain the SEC spectra as a function of the DP.

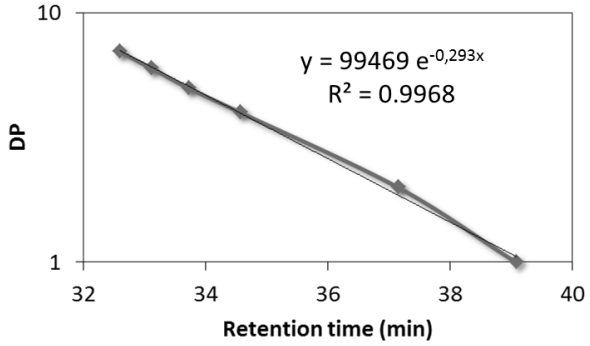

Figure VII-4. SEC in water calibration curve

VII. 2. B) ii) High performance liquid chromatography (HPLC)

For Calibration A (**Appendix IV.II**, p 170), the apparatus used was a HPLC with an evaporating light scattering detector (ELSD, Varian 380-LC) and a Prevail carbohydrate ES 5µ column. The evaporator and nebuliser temperatures were set at 90°C and 25°C, respectively. 10 µL of the samples were injected. The eluent was a solution of 65/35 v/v acetonitrile/water with a flow rate of 0.5 $mL.min^{-1}$. The samples were dissolved at 10 $g.L^{-1}$ in water with 0.03% of NaN_3 to prevent microbial contamination. The peaks were identified thanks to cellulose oligomers standards.

For Calibration B (**Appendix IV.V**, p 173), a Dionex Ultimate 3000 (Thermo Scientifc) equipped with a Corona Veo detector was used with the same column and conditions as previously.

The commercial cellotetraose, cellopentaose and cellohexaose, used for both calibrations, were only pure at 97.3%, 97.5% and 85.3% according to the supplier. These values were used to adjust the concentration.

VII. 2. C) Thermal analysis

VII. 2. C) i) Thermogravimetric analysis (TGA)

The TGA were performed on a TGA-Q50 V6.7 Build 203 (TA Instrument) apparatus. The sample was heated from 30°C to 800°C at 10°C per minutes under a nitrogen flow of 90 mL per minutes.

VII. 2. C) ii) Differential scanning calorimetry (DSC)

The DSC analyses were obtained from a DSC-Q100 V9.9 Build 303 (TA Instruments) apparatus. The sample was placed in an aluminium hermetic pan and submitted to a first increase from 10°C to 160°C then the temperature was decreased to -80°C and heated again to 200°C. For the amphiphilic compounds, the first increase of temperature went up to

200°C to remove the residual DMSO that may still be present. The heating rate was 20°C per minutes and the samples were under a nitrogen flow of 50 mL per minutes.

The data shown corresponded to the second heating; the cooling was sometimes also represented.

VII. 2. D) Dynamic light scattering (DLS)

The DLS analyses were performed on a Malvern Nano ZS ZetaSizer equipped with a HeNe standard laser at 632.8 nm. The measurements were done at 25°C and at a 90° angle. The particle size and distribution were determined by the cumulant method (second order).

VII. 2. E) Transmission electron microscopy (TEM)

TEM pictures were taken at the BIC (Bordeaux Imaging Centre), on a microscope Hitachi H7650.

The TEM grids were prepared by deposing a drop of the solution and letting it adsorb for 90 seconds. The excess of solvent was carefully removed with a tissue while trying to not displace all the particles on one side. A contrast agent was then deposited to be able to observe the organic materials. As previously, uranyl acetate at 1 wt% in water was deposited on the grid.

VII. 2. F) Fluorescence

The pyrene fluorescence data were recorded from a Fluoromax-4 (Horiba Scientific) fluorimeter. The solutions were excited at 334 nm and the emission spectra were recorded from 365 to 420 nm. The excitation slit was 8 nm and the emission slit 2 nm[20]. I_I and I_{III} peaks respectively corresponded to the wavelengths 373 nm and 384 nm[20,21].

The stock solution of pyrene was prepared by dissolving 12 mg of pyrene in 1 L of ethanol (left to stir for 24h). 1 mL of this solution was dispersed in 1 L of water; a solution at 0.06 µM was then obtained. A stock solution of the sample dissolved in the pyrene solution was prepared and diluted, as needed, with the pyrene solution. The fluorescence spectra were recorded 24h after the solutions were prepared.

References

[1] M. Meiland, T. Heinze, W. Guenther, T. Liebert, *Tetrahedron Lett.* **2009**, *50*, 469–472.

[2] J. Leebrick, H. Ramsden, *J. Org. Chem.* **1958**, *23*, 935–936.

[3] R. L. Letsinger, S. B. Hamilton, *J. Am. Chem. Soc.* **1959**, *81*, 3009–3012.

[4] D. G. Hall, in *Boronic Acids*, Wiley-VCH Verlag GmbH & Co. KGaA, **2011**, pp. 1–133.

[5] R. J. Kell, P. Hodge, M. Nisar, R. T. Williams, *J. Chem. Soc., Perkin Trans. 1* **2001**, 3403–3408.

[6] J. Skey, R. K. O'Reilly, *Chem. Commun.* **2008**, 4183–4185.

[7] J. Warnant, J. Garnier, A. van Herk, P.-E. Dufils, J. Vinas, P. Lacroix-Desmazes, *Polym. Chem.* **2013**, *4*, 5656–5663.

[8] T. Liebert, M. Seifert, T. Heinze, *Macromol. Symp.* **2008**, *262*, 140–149.

[9] S. Barthel, T. Heinze, *Green Chem.* **2006**, *8*, 301–306.

[10] T. Heinze, T. Liebert, *Prog. Polym. Sci.* **2001**, *26*, 1689–1762.

[11] N.-T. Huynh, Y.-S. Jeon, M. Zrinyi, J.-H. Kim, *Polym. Int.* **2013**, *62*, 266–272.

[12] C. Gauche, V. Soldi, S. Fort, R. Borsali, S. Halila, *Carbohydr. Polym.* **2013**, *98*, 1272–1280.

[13] L. Zhang, X. Jia, J. Dong, D. Chen, J. Liu, L. Zhang, X. Wen, *Chem. Biol. Drug Des.* **2014**, *83*, 297–305.

[14] Laboratory Analytical Procedure NREL/TP-510-42629, M. Selig, N. Weiss, Y. Ji, *Enzymatic Saccharification of Lignocellulosic Biomass*, **2008**.

[15] G. R. Fulmer, A. J. M. Miller, N. H. Sherden, H. E. Gottlieb, A. Nudelman, B. M. Stoltz, J. E. Bercaw, K. I. Goldberg, *Organometallics* **2010**, *29*, 2176–2179.

[16] C. S. Johnson, *Prog. Nucl. Magn. Reson. Spectrosc.* **1999**, *34*, 203–256.

[17] P. Stilbs, *Anal. Chem.* **1981**, *53*, 2135–2137.

[18] M. Holz, H. Weingärtner, *J. Magn. Reson.* **1991**, *92*, 115–125.

[19] L. G. Longsworth, *J. Phys. Chem.* **1960**, *64*, 1914–1917.

[20] A. Dominguez, A. Fernandez, N. Gonzalez, E. Iglesias, L. Montenegro, *J. Chem. Educ.* **1997**, *74*, 1227–1231.

[21] J. Aguiar, P. Carpena, J. A. Molina-Bolívar, C. Carnero Ruiz, *J. Colloid Interface Sci.* **2003**, *258*, 116–122.